ELECTRONICALLY SCANNABLE NARROW BEAM PLASMA ANTENNA SYSTEM

THE THESIS SUBMITTED
IN PARTIAL FULFILMENT
OF THE REQUIREMENTS
FOR THE DEGREE -

DOCTOR OF PHILOSOPHY

by

DHANI RAM

PLASMA RESEARCH DIVISION,
DEPARTMENT OF PHYSICS,
BIRLA INSTITUTE OF TECHNOLOGY & SCIENCE
PILANI (RAJASTHAN) INDIA

DEC. 1972

TO MY FATHER

CERTIFICATE

The study and work on "Electronically Scannable Narrow Beam Plasma Antenna System", carried out and presented here in by Mr. Dhani Ram embodies original investigation and was carried out under my supervision and guidance since September 1969. It is recommended that the thesis be accepted for the award of degree of Doctor of Philosphy in Plasma Research Division, Department of Physics, Faculty of Science, Birla Institute of Technology and Science, Pilani, Rajasthan.

J. S. Verma

(J. S. Verma)
Associate Professor,
Head, Dept. of Physics.

ACKNOWLEDGEMENT

The author is very much indebted to his supervisor Dr. J. S. Verma, Professor and Head, Dept. of Physics, B.I.T.S., Pilani (Raj.) for his excellent guidance, interest and continuous encouragement.

The author is thankful to Dr. Amarjit Singh , Director, Central Electronics Engineering Research Institute, Pilani and Dr. K. C. Gupta, Assistant Professor, Dept. of Electrical Engineering, I.I.T. Kanpur for their important discussions and suggestions from time to time.

The author greatfully acknowledges the help given by Mr. B. K. Kaushik, N.K. Joshi and V. Sharma for the compiling work of this thesis. The author is thankful to his friends for making his stay at Pilani a rememberable happy experience.

Special thanks are due to the Dept. of Information Processing Centre for providing computation facilities. Thanks are due to Mr. S. K. Sinha, Dept. of Physics for the typing work. Thanks are due to Mr. K. N. Sharma for doing the drawing work.

The author is greatful to Dr. C. R. Mitra, Director, B.I.T.S. and Dr. A. K. Datta Gupta, Dean Faculty of Science, B.I.T.S., Pilani (Raj.) for providing available facilities and constant encouragement during this research work. In the last the author wishes to express his thanks to C.S.I.R. for awarding Junior Research Fellowship (from Sept. 1969 to March 1972) and Senior Research Fellowship (from March 1972 onwards) for the research work reported here.

(DHANI RAM).

CAPTIONS TO THE FIGURES

Fig. 2.1 Figure of the Geometry analysed.

Fig. 2.2 Radiation pattern of magnetic ring source in plasma column having central conductor along its axis.

Fig. 2.3 Detailed structure of the radiation peaks in the radiation pattern of magnetic ring source in plasma column having central conductor along its axis.

Fig. 2.4 Graph between $H_{\phi p}$ (Amplitude of the radiation peak) and $K_o b$.

Fig. 2.5 Graph between $H_{\phi p}$ (Amplitude of the radiation peak) and $K_o a$.

Fig. 2.6 Graph between $H_{\phi p}$ (Amplitude of the radiation peak) and $K_o a_1$.

Fig. 2.7 Figure of the geometry analysed .

Fig. 2.8 Radiation pattern of electric ring source in plasma column having central conductor along its axis.

Fig. 2.9 Detailed structure of the radiation peaks in the radiation pattern of electric ring source in plasma column having central conductor along its axis.

LIST OF SYMBOLS

e	charge of the electron.
m	mass of the electron.
U	velocity of sound.
v	average electron velocity.
w	source frequency.
w_p	electron plasma frequency.
n_o	electron density.
*	sign of multiplication.
HPWB	Half Power Beam Width.
$J_1(\ )$	Bessel function of first kind and first order.
$J_o(\ )$	Bessel function of first kind and zeroth order.
$Y_1(\ )$	Bessel function of second kind and first order.
$Y_o(\ )$	Bessel function of second kind and zeroth order.
$I_1(\ )$	modified Bessel function of first kind and first order.
$I_o(\ )$	modified Bessel function of first kind and zeroth order.
$K_1(\ )$	modified Bessel function of second kind and first order.
$K_o(\ )$	modified Bessel function of second kind and zeroth order.
$H_1(\ )$	Hankel function of first kind and first order.
$H_o(\ )$	Hankel function of first kind and zeroth order.
k_o	propagation constant in free space.
a_1	radius of the central conductor.

***

TABLE OF CONTENTS

CHAPTER 1.

I N T R O D U C T I O N

Plasma study has received a great deal of attention in the last two decades. The problem of complete blackout suffered by the space vehicle while its re-entrance into the earth's atmosphere, wave phenomenon like Whistlers, Luxembrough effect, and some other inospheric guiding properties encouraged the scientists to do research in the field of electromagnetic wave propagation in the plasma medium. The indication of the presence of multiple narrow radiation peaks in the computation of the radiation pattern of an antenna on models of re-entry vehicles[1-2], the excitation of complex waves on plasma geometries[3], and the excitation of leaky waves on cylindrical plasma geometries[4-5] have motivated the research work reported here.

Much work has been done in the field of electromagnetic radiation from sources immersed in plasma. A good review of this study has been given by Bachynki[6]. These studies are mainly concerned with the characteristic performance of antennas in plasma environments. Relatively less work has been done in the field of waveguiding properties of plasma geometries.

Seshadri and his co-workers have discussed the excitation of surface waves on different types of plasma columns (isotropic plasma column[7], warm plasma column[8], axially magnetised plasma column[9]) by electric dipole in the plasma. This phenomenon is mainly found in the opaque region ($w < w_p$). Tamir[10] also discussed the excitation of surface waves and complex waves on infinite grounded plasma slab excited by infinite magnetic line source.

In 1962 Tamir[3] did a remarkable work in the field of waveguiding properties of plasma surfaces. In case of grounded infinite plasma slab excited by an infinite magnetic line source, they have predicted the presence of forward and backward surface waves and complex waves on the plasma surface. In the transparent region ($w > w_p$), they predicted the presence of leaky waves on plasma surface. They calculated the radiation field of an infinite magnetic line source in grounded plasma slab by three different methods ((1) by the usual method of calculating the far field, the saddle point integration method, (2) by near field consideration of the proper excited leaky wave (3) by geometrical optical considerations) and showed that in the transparent region ($w > w_p$) all these methods predict the presence of radiation peaks before the critical angle ($\sin^2\theta_c = \epsilon_p$).

Harris[11] (in 1968), in case of ungrounded infinite plasma slab excited by an infinite magnetic line source, indicated the presence of well enhanced radiation peaks beyond the critical angle. He pointed out that the air gap between grounded plane and plasma slab is mainly responsible for the formation of radiation peaks beyond the critical angle. He attributed these radiation peaks to the excitation of leaky waves on plasma surface.

Characteristics of leaky waves have been discussed by many authors[12-18]. An excellent summary and bibliography is given by F. J. Zucker[19]. Leaky waves are fast waves supported by the interface of two media. As they progress, they continuously radiate energy.

Meltz and Shore[20] discussed the excitation of leaky waves on an-isotropic plasma slab excited by a magnetic line source and a magnetic ring source of electromagnetic waves. They showed that the radiation pattern calculated by the usual method of saddle point integration and by using Kirchoff-Huygens principle coincides well near the radiation peaks. However, the physical realisation of an infinite plasma slab and an infinite magnetic line source is not very convenient.

Much work has been done in the field of excitation of leaky waves on various surfaces like inductive grid structure[21] reactance surface and the sheath helix[22], rectangular waveguide[14] and circular waveguide[15]. Samaddar and Yildiz[5] hinted the excitation of leaky waves on plasma column by magnetic ring source in the plasma. They did not go deep into the phenomenon. Gupta[23] studied the radiation pattern of magnetic ring source in plasma column and predicted the emergence of radiation peaks and expected these radiation peaks to be due to the excitation of leaky waves on plasma column. Dimensions of the plasma geometry required for his case are quite large. To have a plasma geometry of large dimensions is in itself a big problem. So the attention was focused in the direction of searching for a practically feasible plasma geometry excited by a suitable source of electromagnetic waves to get well enhanced and sharp radiation peaks. The work reported in this thesis suggests various practically feasible plasma geometries excited by some practically convenient sources of electromagnetic waves. The designs are expected to support leaky waves and to account for the formation of well enhanced and sharp radiation peaks in the radiation patterns. The directions of these radiation peaks can be changed by changing the plasma density. Number of radiation peaks can be controlled by suitably adjusting the values of different parameters. Based upon these results, it is suggested to develop an electronically scannable narrow beam plasma antenna system. Plasma is assumed to be an isotropic, incompressible and lossless dielectric medium having ϵ_p as a relative dielectric constant given by the relation $\epsilon_p = 1 - \frac{w_p^2}{w^2}$ where w is the source frequency and w_p is the electron plasma frequency. The work reported here is concerned with the transparent region ($w > w_p$) .

The radiation pattern of a magnetic ring source in a plasma column having central conductor along its axis has been discussed in chapter 2. In this case the radiation peaks near and before the critical angle are formed. The importance of the central conductor has been emphasized in the work. It is an important addition, and is mainly reponsible for the formation of the radiation peaks before the critical angle. In this study it is found that the radius of the magnetic ring source does not change the direction of the radiation peak formed near and before the critical angle. Radiation pattern of an electric ring source in a plasma column having central conductor along its axis has also been discussed. The cases of more practically feasible sources of electromagnetic waves such as open ended co-axial line excited in TEM mode, open ended circular waveguide excited in circular symmetric modes (TM_{01} and TE_{01} mode) have also been discussed.

Chapter 3 is concerned with the radiation patterns of circular symmetric sources (Magnetic ring source, Electric ring source, open ended co-axial line excited in TEM mode, open ended circular waveguide excited in circular symmetric modes (TM_{01} mode and TE_{01} mode)) in an air core having central conductor and surrounded by an annular plasma column. This study of the radiation patterns of different sources in an air core having central conductor along its axis and surrounded by an annular plasma layer predictsthe formation of well enhanced and sharp radiation peaks beyond the critical angle. It is pointed out that the air core having central conductor along its axis is an important addition and is mainly responsible for the formation of well enhanced radiation peaks beyond the critical angle.

Radiation patternsof circular symmetric sources (magnetic ring source, electric ring source, open ended co-axial line excited in TEM mode, open ended circular waveguide excited in circular symmetric modes (TM_{01} and TE_{01} mode)) in plasma column having central conductor and surrounded by two more annular plasma layers have been discussed in chapter 4. In these cases also sharp radiation peaks beyond the critical angle of the layer having least relative dielectric constant are formed. The importance of the innermost plasma column having central conductor along its axis has been stressed.

Chapter 5 is concerned with the radiation pattern of magnetic ring source in compressible plasma column having central conductor along its axis. It is pointed out that the compressibility of the plasma is responsible for the excitation of acoustic waves in the plasma. In this case it is shown that it is possible to separate plasma modes and electromagnetic modes in the plasma region. Compressibility of the plasma affects the radiation pattern of the magnetic ring source in a complicated way.

Chapter 6 contains the summary, concluding remarks and suggestions for the further work.

CHAPTER 2.

EXCITATION OF ISOTROPIC INCOMPRESSIBLE PLASMA COLUMN HAVING CENTRAL CONDUCTOR ALONG ITS AXIS.

2.1 Excitation by Magnetic Ring Source.

- 2.1.1 Introduction
- 2.1.2 Analysis
- 2.1.3 Characteristics of the Radiation Pattern
- 2.1.4 Discussion

2.2 Excitation by Electric Ring Source.

- 2.2.1 Introduction
- 2.2.2 Analysis
- 2.2.3 Characteristics of the Radiation Pattern
- 2.2.4 Discussion

2.3 Excitation by Open Ended Co-axial Line Excited in TEM Mode.

- 2.3.1 Introduction
- 2.3.2 Analysis
- 2.3.3 Characteristics of the Radiation Pattern

2.4 Excitation by Waveguide Excited in Circular Symmetric Mode (TM_{01} and TE_{01} mode).

- 2.4.1 Introduction
- 2.4.2 Analysis
- 2.4.3 Characteristics of the Radiation Pattern.

CHAPTER 2.

EXCITATION OF ISOTROPIC INCOMPRESSIBLE PLASMA COLUMN HAVING CENTRAL CONDUCTOR ALONG ITS AXIS.

2.1 Excitation by Magnetic Ring Source:

2.1.1 INTRODUCTION:- Tamir and Oliner[3] (1962) in case of an infinite grounded plasma slab excited by an infinite magnetic line source predicted the presence of sharp narrow radiation peaks near and before the critical angle. They concluded that these radiation peaks in the radiation pattern of an infinite magnetic line source in the infinite grounded plasma slab are due to the excitation of leaky waves on the plasma surface.

These predictions encouraged to look for the similar phenomenon in case of more practically feasible cylindrical plasma geometry (plasma column having central conductor along its axis) excited by suitable electromagnetic source (magnetic ring source in the plasma column).

The present study is concerned with the radiation pattern of the magnetic ring source in the plasma column having a conductor along the axis. Source form of the Maxwell's equations is used resulting into an inhomogeneous wave equation. Subjected to proper boundary conditions, the solution of the resulting inhomogeneous equation is obtained by the usual technique of method of integral transforms. This yields the solution for the field in the form of a definite integral. Radiation field is obtained from the asymptotic evaluation of the integral by means of saddle point integration. It is found that a well enhanced radiation peak is formed near the critical angle and its direction can be scanned by varying the plasma density. Diameter of the ring source has no effect on the direction of radiation peak but affects its amplitude.

2.1.2 ANALYSIS:- The geometry of the configuration analysed is shown in fig.2.1. An infinitely long plasma column of radius b and having a conductor along the axis is oriented with its axis along the Z axis of the cylindrical coordinate (r, Ø, Z) system. The source of electromagnetic radiation is a ring of magnetic current of radius a ($a < b$) concentric with the plasma column and situated at Z = 0 plane. This source of electromagnetic radiation is mathematically represented by

$$\bar{M} = \bar{\phi}\ \delta (r - a)\ \delta (Z) \qquad (2.1)$$

where δ represents Kronecker's delta function, $\bar{\phi}$ is a unit vector in the Ø direction. Here circular symmetric mode is considered. Source form of the Maxwell's equations governing electromagnetic field written in the differential form for e^{-jwt} time dependence can be written as

$$\nabla \times \bar{E} = jw\mu \bar{H} - \bar{M} \tag{2.2}$$

$$\nabla \times \bar{H} = -jw\epsilon \bar{E} \tag{2.3}$$

Taking curl of equation (2.3) and substituting the value of $\nabla \times \bar{E}$ from equation (2.2) we get

$$\nabla \times \nabla \times \bar{H} - w^2 \mu\epsilon \bar{H} = j w\epsilon \bar{M} \tag{2.4}$$

Now considering circular symmetric mode we have

$$\left[\nabla \times \nabla \times \bar{H}\right]_\phi - w^2 \mu \epsilon H_\phi = j w\epsilon \delta (r - a) \delta (Z) \tag{2.5}$$

Expanding it in the cylindrical coordinates we have,

$$\frac{d^2 H_\phi}{d r^2} + \frac{1}{r} \frac{dH_\phi}{d r} + \left(K^2 - \frac{1}{r^2} \right) H_\phi + \frac{d^2 H_\phi}{d Z^2}$$

$$= -j w\epsilon \delta(r - a) \delta (Z) \tag{2.6}$$

where $K^2 = w^2 \mu\epsilon$

The equation (2.6) is solved with the help of integral transforms. Let the Fourier transform of H_ϕ (r, Z) be defined as,

$$h(r, \xi) = \int_{-\infty}^{\infty} H_\phi (r, Z) e^{-j \xi Z} dZ$$

and inverse transform be given by,

$$H_\phi (r, Z) = \frac{1}{2\pi} \int_{-\infty}^{\infty} h (r, \xi) e^{j \xi Z} d\xi$$

Multiplying each term of equation (2.6) by $e^{-j \xi Z}$ and integrating over the infinite range with respect to Z we get,

$$\frac{d^2h}{d\,r^2} + \frac{1}{r}\,\frac{dh}{dr} + \left(K^2 - \xi^2 - \frac{1}{r^2} \right)h = jw\epsilon\,\delta(r-a) \qquad (2.7)$$

The source variation $\delta(\,Z\,)$ vanishes because

$$\int_{-\infty}^{\infty} \delta(\,Z\,)\, e^{-j\xi Z}\, dZ = 1$$

Equation (2.7) is considered to be an ordinary differential equation with ξ as a parameter constant. Boundary conditions on h follow from the boundary conditions on its inverse Fourier transform. Taking into account the proper boundary conditions on h and its derivative with respect to r the solution for h is obtained in the free space. Its inverse Fourier transform gives the radiation field in free space.

COMPUTATION OF BOUNDARY VALUE PROBLEM:

Consider the inhomogeneous differential equation (2.7). The delta function is related by the relation,

$$\delta(\,r-a\,) = 1 \qquad \text{for } r = a$$

$$\delta(\,r-a\,) = 0 \qquad \text{for } r \neq a$$

For all values of r other than r = a the equation (2.7) reduces to a homogeneous differential equation

$$\frac{d^2h}{d\,r^2} + \frac{1}{r}\,\frac{d\,h}{d\,r} + \left(K^2 - \xi^2 - \frac{1}{r^2} \right) h = 0 \qquad (2.8)$$

The delta function $\delta(r - a)$ imposes boundary conditions on h which must be satisfied at $r = a$. Multiplying equation(2.7) by dr, integrating over the interval 2Δ from $r = a - \Delta$ to $r = a + \Delta$, assuming the continuation of h around $r = a$ and taking limit as $\Delta \to 0$ we have,

$$\left.\frac{dh}{dr}\right|_{a+\Delta} - \left.\frac{dh}{dr}\right|_{a-\Delta} = -j w \epsilon_p \tag{2.9}$$

The remaining boundary conditions on $h(r, \xi)$ follow from the boundary conditions imposed on $H_\phi(r, Z)$ and $E_Z(r, Z)$ by the Maxwell's equations. As shown in fig. (2.1) the region between $r = a_1$ to $r = a$ is denoted as region I, between $r = a$ to $r = b$ region II and the region for $r > b$ as region III. The solution of equation (2.8) in the region I is given as

$$h = A_1 J_1(v_1 r) + B_1 Y_1(v_1 r)$$

where $v_1^2 = K_1^2 - \xi^2$ and $K_1^2 = w^2 \mu \epsilon_p$

In the region II as,

$$h = A_2 J_1(v_1 r) + B_2 Y_1(v_1 r)$$

In the region III, also taking into account the radiation condition on H_ϕ we have the solution of equation (2.8) as

$$h = A_3 H_1(v_o r)$$

where $v_o^2 = K_o^2 - \xi^2$, $K_o^2 = w^2 \mu \epsilon_o$

H_1 is the Hankel function and ϵ_0 is the dielectric constant of the free space.

The continuation of H_ϕ at any r for all the values of Z implies that

$$h(r, \xi) = \int_{-\infty}^{\infty} H_\phi(r, Z)\, e^{-j \xi Z}\, dZ$$

must also be continuous. From the Maxwell's equations we have

$$\bar{E} = \left(\frac{1}{-jw\epsilon} \right) \nabla \times \bar{H}$$

$$E_Z = -\frac{1}{jw\epsilon} \left(\frac{dH_\phi}{dr} + \frac{1}{r} H_\phi \right)$$

The continuation of E_Z (r, Z) at any r for all the values of Z also implies that

$$-\frac{1}{jw\epsilon} \left(\frac{dh}{dr} + \frac{h}{r} \right)$$

be continuous. Where ϵ is the dielectric constant of that medium.

1) At ($r = a_1$) the conductor surface the tangential electric vector namely E_Z(r, Z) is continuous. So we have

$$-\frac{1}{jw\epsilon_p} \left| \frac{dh}{dr} + \frac{h}{r} \right|_{r = a_1 + \Delta} = 0$$

$$\left| \frac{dh}{dr} + \frac{h}{r} \right|_{r = a_1 + \Delta} = 0$$

2) At (r = a) the location of magnetic ring source, continuation of H_ϕ and equation (2.9) gives

$$h\Big|_{a-\Delta} = h\Big|_{a+\Delta}$$

$$\frac{dh}{dr}\Big|_{a+\Delta} - \frac{dh}{dr}\Big|_{a-\Delta} = -jw\epsilon_r$$

3) At (r = b) the boundary of the plasma column, continuation of E_z and H_ϕ gives

$$h\Big|_{b-\Delta} = h\Big|_{b+\Delta}$$

$$\frac{\epsilon_p}{\epsilon_o}\frac{dh}{dr}\Big|_{b+\Delta} - \frac{dh}{dr}\Big|_{b-\Delta} + \left(\frac{\epsilon_p}{\epsilon_o} - 1\right)\frac{h}{r}\Big|_{b+\Delta} = 0$$

Applying all these boundary conditions on the solution for different regions we have,

$$A_1J_o(v_1 a_1)+B_1Y_o(v_1 a_1) = 0$$

$$A_1\left\{(v_1 a)J_o(v_1 a)-J_1(v_1 a)\right\} +B_1\left\{(v_1 a)Y_o(v_1 a)-Y_1(v_1a)\right\}$$
$$-A_2\left\{(v_1 a)J_o(v_1a)-J_1(v_1a)\right\} -B_2\left\{(v_1a)Y_o(v_1a)-Y_1(v_1a)\right\} =jw\epsilon_p a$$

$$A_1J_1(v_1a)+B_1Y_1(v_1a)-A_2J_1(v_1a)-B_2Y_1(v_1a) = 0$$

$$A_2J_1(v_1b) +B_2Y_1(v_1b) - A_3H_1(v_ob) = 0$$

$$A_2 \left\{ (v_1 b)\, J_o(v_1 b) - J_1(v_1 b) \right\} + B_2 \left\{ (v_1 b)\, Y_o(v_1 b) - Y_1(v_1 b) \right\} -$$

$$- A_3 \left\{ \frac{\epsilon_p}{\epsilon_o} (v_o b)\, H_o(v_o b) - H_1(v_o b) \right\} = 0$$

Here we have five equations and five constants. Solving these equations the expression for A_3 will be,

$$A_3 = \frac{j w \epsilon_p \epsilon_o a \left\{ J_o(v_1 a_1) Y_1(v_1 a) - Y_o(v_1 a_1) J_1(v_1 a) \right\}}{H_1(v_o b)(v_1 b) \left\{ Y_o(v_1 a_1) J_o(v_1 b) - J_o(v_1 a_1) Y_o(v_1 b) \right\} - H_o(v_1 b) \left\{ \frac{\epsilon_p}{\epsilon_o}(v_o b) Y_o(v_1 a_1) J_1(v_1 b) - J_o(v_1 a_1) * Y_1(v_1 b) \right\}} \quad (2.10)$$

Therefore, the solution in the free space is

$$h = A_3 H_1(v_o r) \quad (2.11)$$

and taking the inverse Fourier transform,

$$H_\phi(r, Z) = \frac{1}{2\pi} \int_{-\infty}^{\infty} A_3 H_1(v_o r)\, e^{j \xi Z}\, d\xi \quad (2.12)$$

CALCULATION OF THE RADIATION FIELD:

The variables v_1 and v_o which appear in the integrand of equation (2.12) are multiple-valued functions in the neighbourhood of $v_1 = 0$ and $v_o = 0$ respectively. It can be shown, by expanding the integrand about $v_1 = 0$ that it is an even function of V_1. But at $v_o = 0$ the Hankel function which appears in the integrand has logarithmic singularity, hence $v_o = 0$ gives branch points of the integrand.

Consider the integral of equation (2.12) as contour integral in ξ plane, the method of saddle point integration is applied to evaluate the integral (2.12). Introduce the transformation,

$$\xi = K_o \operatorname{Sin} \psi$$

$$\text{where } \psi = \tau + j\lambda$$

This transformation transforms the region of integration in ξ plane into a strip in the ψ plane, which is bounded by two curved lines corresponding to the branch cuts $\xi = \pm K_o$ in the ψ plane. The branch cuts in ψ plane are given by,

$$\operatorname{Sin} \tau \quad \operatorname{Cosh} \lambda = \pm 1$$

This transformation yields,

$$v_o = K_o \operatorname{Cos} \psi$$

$$v_1 = K_o \sqrt{\epsilon_p - \operatorname{Sin}^2 \psi}$$

The equation (2.12) transforms to

$$H_\phi(r, Z) = \frac{1}{2\pi} \int_C A_3(\psi) H_1^{\cdot\cdot}(K_o r \operatorname{Cos}\psi) e^{+jK_o \operatorname{Sin}\psi z} K_o \operatorname{Cos}\psi \, d\psi \quad (2.13$$

Shifting from cylindrical coordinate system (r, ϕ, Z) to spherical coordinate system (R, θ, ϕ)(Fig. 2.1) with the help of the transformation

$$r = R \cos \theta$$

$$Z = R \sin \theta$$

equation (2.13) transforms to

$$H_{\phi}(R,\theta) = \frac{1}{2\pi} \int_{c} A_3(\psi) H_1(RK_o \cos\theta \cos\psi) \exp\{(jRK_o \sin\theta \, * \, * \sin\psi)\} K_o \cos\psi \, d\psi \qquad (2.14)$$

Taking approximate value of Hankel function of the integrand of equation (2.14) for large value of R, namely

$$H_1(RK_o \cos\theta \cos\psi) \exp(jRK_o \sin\theta \sin\psi) \quad e^{-j(\frac{3\pi}{4})} \, * \, * \left(\frac{2}{K_o R \cos\theta \cos\psi} \right)^{\frac{1}{2}} \exp \; jK_o R \cos(\psi - \theta)$$

we have

$$H_{\phi}(R,\theta) \; \frac{1}{\pi} \int_{c} A_3 \, e^{-j(\frac{3\pi}{4})} \left(\frac{K_o}{2\pi R \cos\theta} \right)^{\frac{1}{2}} * \, * (\cos\psi)^{\frac{1}{2}} \, e^{jK_oR \cos(\psi - \theta)} \, d\psi \quad \text{for } K_oR \gg 1 \qquad (2.15)$$

The saddle point of this integral is given by

$$\frac{d}{d\psi} \cos(\psi - \theta) = 0$$

which gives $\psi = \theta$ as saddle point.

The steepest descent path (S.D.P.) is given by the constant phase of the exponential factor of the integrand of equation (2.15) and is to pass through the saddle point. So we have,

Im j Cos (Ψ - θ) = constant and is to pass through Ψ = θ which gives

$$\cos(\tau - \theta)\cosh\lambda = 1$$

$$\sin(\tau + \frac{\pi}{2} - \theta)\cosh\lambda = 1$$

Applying the standard method (given in appendix A) of saddle point integration, the lowest order approximation of the integral is given as

$$H_\phi(R, \theta) = \frac{-jw\epsilon_r}{\pi} F(\theta) \frac{e^{jK_oR}}{R} \tag{2.16}$$

$$F(\theta) = \frac{a\left\{J_o(v_1a_1)Y_1(v_1a) - Y_o(v_1a_1)J_1(v_1a)\right\}}{H_1(v_ob)(v_1b)\left\{Y_o(v_1a_1)J_o(v_1b) - J_o(v_1a_1)Y_o(v_1b)\right\} - H_o(v_ob)\left\{\frac{\epsilon_r}{\epsilon_o}(v_ob)Y_o(v_1a_1)J_1(v_1b) - J_o(v_1a_1)Y_1(v_1b)\right\}}$$

$$v_o = K_o \cos\theta$$

$$v_1 = K_o\sqrt{\epsilon_r - \sin^2\theta}$$

H_ϕ (R, θ) gives the radiation field in free space.

2.1.3 CHARACTERISTICS OF THE RADIATION FIELD:

The radiation pattern given by equation (2.16) (Variation of F (θ) with θ) has been computed with the help of computer IBM-1130 for K_ob = 6π , K_oa_1 = .09,

$K_o a = 1$, $\epsilon_p = .5$ and $\epsilon_p = .9$. In both the cases, well enhanced radiation peak is formed near and before the critical angle ($\sin^2 \theta_c = \epsilon_p$). The detailed structure of these peaks is shown in fig. 2.3. The half power beam width for $\epsilon_p = .5$ is $.044^\circ$ and for $\epsilon_p = .9$ is $.086^\circ$. The effect of different parameters on the shape of the radiation pattern is discussed below.

Effect of the diameter of the magnetic ring source:-

It is found that the direction of the radiation peak is independent of the diameter of the magnetic ring source of electromagnetic waves but the amplitude of the radiation peak depends upon it. It is found that with the increase in the diameter of the magnetic ring source, the radiation peak amplitude decreases. This behaviour is shown in fig. 2.5.

Effect of the diameter of central conductor:-

The diameter of central conductor has little effect on the amplitude of the radiation peak but affects its direction . It is shown in fig. 2.6.

Effect of the diameter of plasma column:-

Diameter of the plasma column affects the direction as well as the amplitude of the radiation peak. With the increase in the diameter of the plasma column, the radiation peak becomes stronger and move closer to the critical angle. It is shown in fig. 2.4.

Effect of the plasma density:-

Here the plasma is considered to be an isotropic, incompressible, lossless dielectric medium characterised by the relative dielectric constant $\epsilon_p = 1 - \frac{w_p^2}{w^2}$. The direction of the radiation peak mainly depends upon ϵ_p, and for constant source frequency w it depends upon the plasma density ($w_p \propto \sqrt{n_0}$). Radiation peaks for ϵ_p=0.5 and ϵ_p= 0.9 are shown in fig. (2.2).

2.1.4 DISCUSSION:-

The main observation in the present study is that a sharp radiation peak formed near and before the critical angle is consistent with the results of Tamir and Oliner[3] who in the case of an infinite grounded plasma slab excited by the infinite magnetic line source of electromagnetic waves predicted the presence of the radiation peak near and before the critical angle. This radiation peak obtained is expected to be due to the excitation of the leaky wave on the plasma column surface.

In fig. 2.6 it is found that the amplitude of the radiation peak increases with the decrease in the diameter of the central conductor. But the speculation that the absence of the central conductor may give rise to stronger radiation peak is not correct. Also the expression for the radiation pattern of the magnetic ring source in the plasma column in the absence of the central conductor can not be deduced from that of magnetic ring source in the plasma column having central conductor along its axis by merely putting the value of the diameter of the central conductor equal to zero in it.

It is because that the very presence of the central conductor imposes forced boundary conditions on the fields of electromagnetic wave. The expression for the radiation pattern of the magnetic ring source in the plasma column in the absence of the central conductor has been derived by Gupta and Garg[23] (1971). They have shown the presence of radiation peaks in the radiation pattern in their case also. But those radiation peaks found are quite broad and require quite higher value of $K_o b$. Comparing these two cases, we find that the very presence of the central conductor modifies the whole radiation pattern.

2.2 EXCITATION BY ELECTRIC RING SOURCE:

2.2.1 INTRODUCTION:- In section 2.1 the radiation pattern of magnetic ring source in plasma column having central conduc-tor along its axis has been discussed. On the same lines the radiation pattern of electric ring source in plasma column having central conductor along its axis can be studied.

The present study is concerned with the radiation pattern of the electric ring source in the plasma column having a conductor along the axis. Source form of the Maxwell's equations is used resulting into an inhomogeneous wave equation. Subjected to proper boundary conditions, the solution of the resulting inhomogeneous equation is obtained by the usual techqnique of method of integral transforms. This yields the solution for the field in the form of a definite integral. Radiation field is obtained from the asymptotic evaluation of the integral by means of saddle point integration. It is found that well enhanced radiation peaks are formed before the critical angle and their direction can be scanned by varying the plasma density.

2.2.2 ANALYSIS:-

The geometry of the configuration analysed is shown in fig.2.7. An infinitely long plasma column of radius b and having a conductor along the axis is oriented with its axis along the Z axis of the cylindrical coordinate (r, Ø, Z) system. The source of electromagnetic radiation is a ring of electric current of radius a (a $\angle$ b) concentric with the plasma column and situated at Z = 0 plane. This source of electromagnetic radiation is mathematically represented by

$$\bar{M} = \bar{\phi}\,\delta(r - a)\,\delta(Z) \tag{2.17}$$

where δ represents Kronecker's delta function, $\bar{\phi}$ is a unit vector in the ϕ direction. Here circular symmetric mode is considered. Source form of the Maxwell's equations governing electromagnetic field written in the differential form for e^{-jwt} time dependence can be written as

$$\nabla \times \bar{H} = -jw\epsilon\bar{E} + \bar{M} \tag{2.18}$$

$$\nabla \times \bar{E} = jw\mu\,\bar{H} \tag{2.19}$$

Taking curl of equation (2.19) and substituting the value of $\nabla \times \bar{H}$ from equation (2.18) we get,

$$-\nabla \times \nabla \times \bar{E} + w^2\mu\epsilon\,\bar{E} = -jw\mu\,\bar{M} \tag{2.20}$$

Now considering circular symmetric mode we have

$$(\nabla \times \nabla \times \bar{E})_\phi - w^2\mu\epsilon E_\phi = jw\mu\,\delta(r - a)\,\delta(Z) \tag{2.21}$$

Expanding it in the cylindrical coordinates we have,

$$\frac{d^2E_\phi}{d\,r^2} + \frac{1}{r}\frac{dE_\phi}{dr} + \left(K^2 - \frac{1}{r^2}\right)E_\phi + \frac{d^2E_\phi}{d\,Z^2} = -jw\mu\,\delta(r-a)\,\delta(Z) \tag{2.22}$$

The equation (2.22) is solved with help of integral transforms. Let the Fourier transforms of $E_\phi(r, Z)$ be defined as,

$$h(r,\xi) = \int_{-\infty}^{\infty} E_\phi(r, Z)\, e^{-j\xi Z}\, dZ$$

and inverse transform be given by

$$E_{\phi}(r, Z) = \frac{1}{2\pi} \int_{-\infty}^{\infty} h(r, \xi) e^{j\xi Z} d\xi$$

Multiplying each term of equation (2.22) by $e^{-j\xi Z}$ and integrating over the infinite range with respects to Z we get,

$$\frac{d^2h}{dr^2} + \frac{1}{r}\frac{dh}{dr} + \left(K^2 - \xi^2 - \frac{1}{r^2}\right) h = -jw\mu\, \delta(r - a) \qquad (2.23)$$

The source variation $\delta(Z)$ vanishes because

$$\int_{-\infty}^{\infty} \delta(Z)\, e^{-j\xi Z}\, dZ = 1$$

Equation (2.23) is considered to be an ordinary differential equation with ξ as a parameter constant. The boundary conditions on h follow from the boundary conditions on its inverse Fourier transform. Taking into account the proper boundary conditions on h and its derivative with respect to r the solution for h is obtained in the free space. Its inverse Fourier transform gives the radiation field in free space.

COMPUTATION OF BOUNDARY VALUE PROBLEM:

Consider the inhomogeneous differential equation (2.23). The delta function is related by the relation,

$$\delta(r - a) = 1 \qquad \text{for } r = a$$

$$\delta(r - a) = 0 \qquad \text{for } r \neq a$$

For all values of r other than r = a the equation (2.23) reduces to a homogeneous differential equation

$$\frac{d^2 h}{d r^2} + \frac{1}{r} \frac{d h}{d r} + \left(K^2 - \xi^2 - \frac{1}{r^2} \right) h = 0 \quad (2.24)$$

The delta function δ (r - a) imposes boundary conditions on h which must be satisfied at r = a. Multiplying equation (2.23) by dr and integrating over the interval r = a - Δ from to r = a + Δ . Assuming the continuation of h around r = a and taking limit as $\Delta \to 0$ we have,

$$\left.\frac{d h}{d r}\right|_{a+\Delta} - \left.\frac{d h}{d r}\right|_{a-\Delta} = -jw\mu \quad (2.25)$$

The remaining boundary conditions on h (r, ξ) follow from the boundary conditions imposed on E_ϕ (r, Z) by the Maxwell's equations. As shown in fig. (2.7) the region between r = a_1 to r = a is denoted as region I, between r = a to r = b region II and the region for r > b as region III. The solution of equation (2.24) in the region I is given as,

$$h = A_1 J_1(v_1 r) + B_1 Y_1(v_1 r)$$

where $v_1^2 = K_1^2 - \xi^2$ and $K_1^2 = w^2 \mu \epsilon_p$

In the region II as,

$$h = A_2 J_1(v_1 r) + B_2 Y_1(v_1 r)$$

In the region III, also taking into account the radiation condition on E_ϕ (r, Z), we have the solution of equation (2.24) as

$$h = A_3 H_1 (v_o r)$$

where $v_o^2 = K_o^2 - \xi^2$, $K_o^2 = w^2 \mu \epsilon_o$

H_1 is the Hankel function and ϵ_o is the dielectric constant of the free space.

The continuation of E_ϕ at any r for all the values of Z implies that

$$h(r, \xi) = \int_{-\infty}^{\infty} E_\phi (r, Z) e^{-j \xi Z} dZ$$

must also be continuous. From the Maxwell's equations we have,

$$\bar{H} = \frac{1}{j w \mu} (\nabla \times \bar{E}) .$$

$$H_Z = \frac{1}{j w \mu} \left(\frac{d E_\phi}{d r} + \frac{E_\phi}{r} \right) .$$

The continuation of H_Z(r, Z) at any r for all the values of Z implies that

$$\frac{1}{j w \mu} \left(\frac{d E_\phi}{d r} + \frac{E_\phi}{r} \right) .$$

be continuous.

1) At the conductor surface the ($r = a_1$) the tangential electric vector namely E_ϕ (r, Z) is continuous. Therefore,

$$h \Big|_{r = a_1 + \Delta} = 0$$

2) At the location of magnetic ring source of electromagnetic waves (r = a), the continuation of E_ϕ and the equation (2.25) give.

$$h \Big|_{a - \Delta} = h \Big|_{a + \Delta}$$

$$\frac{d\,h}{d\,r}\Big|_{a+\Delta} - \frac{d\,h}{d\,r}\Big|_{a-\Delta} = - j\,w\,\mu$$

3) At the boundary of the plasma column (r = b), the continuation of E_ϕ and H_Z gives

$$h \Big|_{b - \Delta} = h \Big|_{b + \Delta}$$

$$\frac{d\,h}{d\,r} + \frac{h}{r}\Big|_{b-\Delta} = \frac{d\,h}{d\,r} + \frac{h}{r}\Big|_{b+\Delta}$$

Applying all these boundary conditions on the solution for different regions we have,

$$A_1 J_1(v_1 a_1) + B_1 Y_1(v_1 a_1) = 0$$

$$A_1\{(v_1 a) J_o(v_1 a) - J_1(v_1 a) + B_1\{(v_1 a) Y_o(v_1 a) - Y_1(v_1 a)\} -$$

$$-A_2\{(v_1 a) J_o(v_1 a) - J_1(v_1 a)\} - B_2\{(v_1 a) Y_o(v_1 a) - Y_1(v_1 a)\} =$$

$$= j w \mu a$$

$$A_1 J_1(v_1 a) + B_1 Y_1(v_1 a) - A_2 J_1(v_1 a) - B_2 Y_1(v_1 a) = 0$$

$$A_2 J_1(v_1 b) + B_2 Y_1(v_1 b) - A_3 H_1(v_o b) = 0$$

$$A_2\{(v_1 b) J_o(v_1 b) - J_1(v_1 b)\} + B_2\{(v_1 b) Y_o(v_1 b) - Y_1(v_1 b)\} -$$

$$-A_3\{(v_o b) H_o(v_o b) - H_1(v_o b)\} = 0$$

Here we have five equations and five constants. Solving these equations the expression for A_3 will be,

$$A_3 = \frac{j w \mu a \{J_1(v_1 a_1) Y_1(v_1 a) - Y_1(v_1 a_1) J_1(v_1 a)\}}{H_1(v_o b)(v_1 b)\{Y_1(v_1 a_1) J_o(v_1 b) - J_1(v_1 a_1) Y_o(v_1 b)\} - H_o(v_o b)\{(v_o b) Y_1(v_1 a_1) J_1(v_1 b) - J_1(v_1 a_1) Y_1(v_1 b)\}}$$

Therefore, the solution in the free space is,

$$h = A_3 H_1(v_o r) \tag{2.26}$$

taking the inverse fourier transform,

$$E_\phi (r, Z) = \frac{1}{2\pi} \int_{-\infty}^{\infty} A_3 H_1(v_o r) e^{j \xi Z} \, d\xi \tag{2.27}$$

CALCULATION OF THE RADIATION FIELD:-

The variables v_1 and v_o which appear in the integrand of equation (2.27) are multiple valued functions in the neighbourhood of $v_1 = 0$ and $v_o = 0$ respectively. It can be shown, by expanding the integrand about $v_1 = 0$ that the integrand is an even function of ξ. But at $v_o = 0$ the Hankel function which appears in the integrand has logarithmic singularity, hence $v_o = 0$ gives branch points of the integrand.

Consider the integral of equation (2.27) as contour integral in ξ plane, apply the method of saddle point integration to evaluate the integral (2.27), introduce the transformation

$$\xi = K_o \sin \psi$$

where $\psi = \tau + j\lambda$

This transformation transforms the region of integration in ξ plane into a strip in the ψ plane, which is bounded by two curved lines corresponding to the branch cuts $\xi = \pm K_o$ in the ψ plane. The branch cuts in ψ plane are given by,

$$\sin \tau \quad \cosh \lambda \quad = \pm \quad 1$$

This transformation yields,

$$v_o = K_o \cos\psi$$

$$v_1 = K_o \sqrt{\epsilon_p - \sin^2\psi}$$

The equation (2.27) transforms to

$$E_\phi(r, Z) = \frac{1}{2\pi}\int_C A_3(\psi)\, H_1^-(K_o r \cos\psi)\, e^{jK_o \cos\psi\, Z}\, d\psi \quad (2.28)$$

Shifting from cylindrical coordinate system (r, Ø, Z) to spherical coordinate system (R, θ, Ø) with the help of the transformation

$$r = R \cos\theta$$

$$Z = R \sin\theta$$

equation (2.28) transforms to

$$E_\phi(r, \theta) = \frac{1}{2\pi}\int_C A_3(\psi)\, H_1(K_o R \cos\theta \cos\psi)\, e^{jK_o R \sin\theta \cos\psi}\, d\psi \quad (2.29)$$

Taking approximate value of Hankel function of the integrand of equation (2.29) for large value of R

We have

$$E_\phi(R, \theta) = \frac{1}{\pi}\int_C A_3\, e^{-j\left(\frac{3\pi}{4}\right)} \left(\frac{K_o}{2\pi R \cos\theta}\right)^{\frac{1}{2}} * (\cos\psi)^{\frac{1}{2}}\, e^{jK_o R \cos(\psi - \theta)}\, d\psi \quad (2.30)$$

The saddle point of integral of equation (2.30) is given by

$$\frac{d}{d\psi}\cos(\psi - \theta) = 0$$

which gives $\psi = \theta$ as saddle point.

The steepest descent path (S. D. P.) is given by the constant phase of the exponential factor of the integrand of equation (2.30) and is to pass through the saddle point. So we have,

$\text{Im}\ j\ \text{Cos}\ (\psi - \theta) =$ constant and is to pass through $\psi = \theta$ which gives,

$$\text{Cos}\ (\tau - \theta)\ \text{Cosh}\ \lambda = 1$$

$$\text{Sin}\ (\tau + \frac{\pi}{2} - \theta)\ \text{Cosh}\ \lambda = 1$$

Applying the standard method of saddle point integration (see appendix A) the lowest order approximation of the integral is given as,

$$E_\phi\ (R, \theta) = \frac{j\ w\ \mu}{\pi}\ F(\theta)\ \frac{e^{jK_oR}}{R} \qquad (2.31)$$

$$F(\theta) = \frac{a\left\{J_1(v_1\ a_1)Y_1(v_1\ a) - Y_1(v_1\ a_1)\ J_1(v_1\ a)\right\}}{H_1(v_o\ b)(v_1\ b)\left\{Y_1(v_1\ a_1)J_o(v_1\ b) - J_1(v_1\ a_1)Y_o(v_1\ b)\right\} - H_o(v_o\ b)\left\{(v_o\ b)Y_1(v_1 a_1)J_1(v_1\ b) - J_1(v_1\ a_1)Y_1(v_1\ b)\right\}}$$

$$v_o = K_o\ \text{Cos}\ \theta$$

$$v_1 = K_o\ \sqrt{\epsilon_p - \text{Sin}^2\ \theta}$$

$E_\phi\ (R, \theta)$ gives the required radiation field in the free space.

2.2.3 CHARACTERISTICS OF THE RADIATION FIELD:-

The radiation pattern given by equation (2.31) (variation of F (θ) with θ) has been computed with the help of computer IBM-1130 for $K_o b = 6\pi$, $K_o a_1 = .09$, $K_o a = 1$, $\epsilon_p = .5$ and $\epsilon_p = .9$. In both the cases radiation peaks before the critical angle ($\sin^2 \theta_c = \epsilon_p$) are formed. The detailed structure of stronger peaks is shown in fig. 2.9. The effect of different parameters on the shape of the radiation pattern is discussed below.

Effect of the diameter of the electric ring source:-

Diameter of the electric ring source of the electromagnetic waves does not affect the direction of the radiation peak but affects its amplitude. Higher values of the diameter of the electric ring source of electromagnetic waves give rise to stronger radiation peak. This behaviour is shown in fig. (2.11).

Effect of the diameter of the central conductor:-

The diameter of the central conductor affects the direction as well as the amplitude of the radiation peak. Higher values of the central conductor give rise to weaker radiation peaks. It is shown in fig. 2.12.

Effect of the diameter of the plasma column:-

Stronger and sharper radiation peak is formed before and near the critical angle for larger diameter of the plasma column. Number of radiation peaks also increases with the increase in the diameter of the plasma column. The variation of radiation peak amplitude with the diameter of the plasma column for fixed value of source frequency is shown in fig. (2.10).

Effect of plasma density:-

Here the plasma medium is considered to be isotropic, incompressible, lossless characterised by the relative dielectric constant ϵ_p given by $\epsilon_p = 1 - \frac{w_p^2}{w^2}$. The direction of the radiation peak mainly depends upon ϵ_p and for the constant source frequency (it depends upon the plasma density ($w_p^2 \propto n_o$)). The radiation peaks for $\epsilon_p = .5$ and $\epsilon_p = .9$ are shown in fig. (2.8).

2.2.4 DISCUSSION:-

This study of the radiation pattern of electric ring source in the plasma column having central conductor along its axis shows the presence of more then one radiation peak before the critical angle. These radiation peaks are expected to be due to the excitation of leaky waves on the plasma surface. The number of radiation peaks corresponds to the number of leaky waves excited.

In fig. (2.12) it is found that the amplitude of the radiation peak increases with the decrease in the diameter of the central conductor. But the speculation that the absence of the central conductor may give rise to stronger radiation peak is not correct. Also the expression for the radiation pattern of the electric ring source in the plasma column in the absence of the central conductor can not be deduced from that of electric ring source in the plasma column having central conductor along its axis by merely putting the value of the diameter of the central conductor equal to zero in it. It is because, the very presence of the central conductor imposes forced boundary conditions on the fields of electromagnetic wave. The expression for the radiation pattern of the electric ring source in the plasma column in the absence of the central conductor has been derived by Gupta and Garg[23] (1971). They have shown the presence of radiation peaks in the radiation pattern of the electric ring source in the plasma column. But those radiation peaks found are quite broad and require quite higher value of $K_o b$. Comparing these two cases (plasma column with and without the central conductor), we find that the very presence of the central conductor modifies the whole radiation pattern to give stronger and sharper radiation peak near and before the critical angle.

2.3 EXCITATION BY OPEN ENDED CO-AXIAL LINE:

2.3.1 INTRODUCTION:-

In the previous study of the radiation pattern of magnetic ring source in plasma column having central conductor along its axis it is found that the diameter of the magnetic ring source has little effect on the direction of the radiation peak but affects its amplitude. In the same study the source of excitation is a magnetic ring source of field distribution given by Kronecker's delta function. The physical realization of such an ideal magnetic ring source is not very convenient. This study of the radiation pattern of an open ended co-axial line excited in TEM mode in plasma column having central conductor along its axis is an attempt in the direction of studying the case of more practically feasible source of electromagnetic waves.

The present study is concerned with the radiation pattern of an open ended co-axial transmission line excited in the TEM mode in a plasma column having a central conductor along the axis. The field distribution at the open end cross-section of the co-axial line is assumed to be equivalent to the vector sum of magnetic current rings of various radii ranging from the outer radius of the inner conductor to the inner radius of the outer conductor of the co-axial line. The radiation field is obtained as a vector sum of field components due to individual rings of magnetic current.

This type of geometry gives rise to a well enhanced radiation peak near and before the critical angle. Its amplitude depends upon the diameter of the plasma column, the outer diameter of the inner conductor and the inner diameter of the outer conductor of the co-axial line. The direction of the radiation peak depends upon the plasma density. There is a small change in the amplitude and HPBW of the peak with change in the plasma density.

2.3.2 ANALYSIS:-

An infinitely long plasma column of radius b having a central conductor of radius a_1 along its axis is oriented with its axis along the z axis of the cylindrical coordinate (r, Ø, Z) system(fig. 2.13). The source of electro-magnetic radiation is an open ended co-axial line, with open end at the Z = 0 plane.

The expression for the radiation pattern of magnetic ring source in plasma column having central conductor along its axis as derived in section 2.1 (equation 2.16) is

$$H_{\phi}(R, \theta) = \frac{-j\, w \epsilon_p}{\pi} F(\theta) \frac{e^{jK_oR}}{R}$$

$$F(\theta) = F_1(\theta)\, F_2(\theta)$$

$$F_1(\theta) = a \left\{ J_o(v_1 a_1)\, Y_1(v_1 a) - Y_o(v_1 a_1) J_1(v_1 a) \right\}$$

$$F_2(\theta) = \frac{1}{H_1(v_o b)(v_1 b)\left\{ Y_o(v_1 a_1) J_o(v_1 b) - J_o(v_1 a_1) Y_1(v_1 b)\right\} - H_o(v_o b)\left\{\epsilon_p (v_o b) Y_o(v_1 a_1) J_1(v_1 b) - J_o(v_1 a_1) Y_1(v_1 b)\right\}}$$

The field distribution at the open end of the co-axial line (at the Z = 0 plane) is assumed to be equivalent to the vector sum of magnetic current rings with various radii ranging from the outer radius of the inner conductor (a_1) to the inner radius of the outer conductor (a_3) of the co-axial line at the Z = 0 plane. The magnitude of the magnetic current in each ring is assumed to be proportional to the value of H_{ϕ} at that particular location in the co-axial line. For a co-axial line excited in the TEM mode H_{ϕ} is taken to be given by the relation $H_{\phi} = \frac{I_o}{2\pi a}$ where I_o is the total current. The total radiation field is obtained as a vector sum of field components due to the individual rings of magnetic current. So in the case of the co-axial line excitation F (θ) is modified to

$$F(\theta) = \int_{a_1}^{a_3} \frac{I_o}{2\pi a} F_1(\theta) F_2(\theta)\, da$$

$$= \frac{F_2(\theta)}{2\pi} I_o \int_{a_1}^{a_3} \frac{1}{a}\, a \left\{ J_o(v_1 a_1) Y_1(v_1 a) - Y_o(v_1 a_1) J_1(v_1 a) \right\} da$$

$$= \frac{F_2(\theta)}{2\pi} I_o \frac{1}{v_1} \left\{ J_o(v_1 a_3) Y_o(v_1 a_1) - J_o(v_1 a_1) Y_o(v_1 a_3) \right\}$$

2.3.3 CHARACTERISTICS OF THE RADIATION FIELD:-

The radiation patterns (variation of F (θ) with θ) have been computed with the help of an IBM-1130 computer, for $K_ob = 19$, $K_oa_1 = 0.09$, $K_oa_3 = 0.9$, $\epsilon_p = .3$ and $\epsilon_p = .7$ (see fig. 2.14). In both the cases a well enhanced radiation peak is formed near and before the critical angle ($\sin^2\theta_c = \epsilon_p$). The detailed structure of these peaks is shown in fig. (2.15). The half power beam width for $\epsilon_p = 0.3$ is 0.07^o and for $\epsilon_p = 0.7$ is 0.048^o. The effect of different parameters on the shape of the radiation pattern is discussed below:

Effect of K_ob:-

The radiation peak becomes sharper, stronger and moves closer to the critical angle as the value of K_ob is increased. That means that for a fixed value of K_o the increase in the diameter of the plasma column gives rise to a sharper and stronger radiation peak near and before the critical angle. The variation of peak amplitude with K_ob is shown in fig. 2.16.

Effect of K_oa_3:-

K_oa_3 does not affect the direction of the radiation peak of the radiation pattern but affects its amplitude. For excitation of the TEM mode in a co-axial line K_oa_3 should be < 1. The variation of peak amplitude with K_oa_3 is shown in fig. 2.17.

Effect of K_oa_1:-

It affects the amplitude and sharpness of the radiation peak and to a small extent affects its direction too. A smaller value of K_oa_1 gives rise to a sharper and stronger radiation peak. The variation of peak amplitude with K_oa_1 is shown in fig. 2.18.

Effect of Plasma Density:-

The direction of the radiation peak depends upon the plasma density. The location of the radiation peak for two different value of ϵ_p, which for a constant source frequency corresponds to different plasma densities, is shown in fig. 2.14. It is found that the half power beam width increases and the amplitude decreases with the decrease in plasma density i.e. with increase in ϵ_p.

2.4 EXCITATION BY WAVEGUIDE EXCITED IN CIRCULAR SYMMETRIC MODES (TM_{01} AND TE_{01} MODE) :

2.4.1 INTRODUCTION:

In the case of magnetic ring source excitation as well as electric ring source excitation of the plasma column having central conductor along its axis it is found that the diameter of the ring source has little effect on the direction of the radiation peaks but effects their amplitude. In this case ring source of electromagnetic waves is mathematically represented by Kronecker's delta functions. The physical realization of such an ideal ring source is not very convenient. In case of co-axial line excitation (section 2.3) of plasma column having central conductor along its axis, it is found that the peak amplitude increases with the increase in the inner radius of the outer conductor of the co-axial line at the open end. But for the TEM mode excitation in co-axial line $K_0 a_3 < 1$ (K_0 is the free space propagation constant and a_3 is the inner radius of the outer conductor of the co-axial line at the open end). This fact inspired the author to look for the wave-guide excitation which provides larger values of K_oa_3 ($2.4 \angle K_oa_3 \angle 3.5$ in case of circular wave-guide excited in TM_{o1} mode and $3.83 \angle K_oa_3 \angle 5.13$ in case of circular wave-guide excited in TE_{o1} mode). Here a_3 is the inner radius of the circular wave guide at the open end. This study of the radiation pattern of open ended circular cylindrical waveguide (excited in circular symmetric TM_{o1} and TE_{o1} mode) in the plasma column having central conductor along its axis is an attempt in the direction of studying the case of more practically feasible source of electromagnetic wave.

The field distribution at the open end cross-section of the circular wave-guide excited in TM_{o1} and TE_{o1} mode is assumed to be equivalent to the vector sum of current rings of various radii ranging from the outer radius of the central conductor to the inner radius of the circular wave-guide at the open end. The radiation pattern is obtained as a vector sum of field components due to individual rings of current.

In both the cases (wave-guide excited in TM_{o1} and TE_{o1} mode), this type of geometry gives rise to a well enhanced radiation peak before the critical angle. The amplitude of the radiation peak depends upon the diameter of plasma column, the diameter of the central conductor and the diameter of wave-guide at the open end. In case of the wave-guide excited in TE_{o1} mode the number of radidation peaks formed is more than that of the wave-guide excited in TM_{01} mode. The direction of the radiation peak depends upon the plasma density.

2.4.2 ANALYSIS:-

An infinitely long plasma column of radius b having a central conductor of radius a_1, along its axis is oriented with its axis along the Z axis of the cylindrical coordinate (r, ϕ , Z) system (fig. 2.19). The source of electromagnetic radiation is an open ended wave-guide (excited in TM_{01} and TE_{01} mode) with open end at Z = 0 plane.

Waveguide excitation(wave guide excited in TM_{01} mode):-

Equation (2.16) gives the expression for the radiation pattern of magnetic ring source in plasma column having central conductor along its axis. This after some modification can be put in the form

$$H_\phi(R, \theta) = \frac{-jw\,\epsilon_p}{\pi} F(\theta) \quad \frac{e^{jK_0R}}{R}$$

$$F(\theta) = F_1(\theta)\, F_2(\theta)$$

$$F_1(\theta) = a\left\{ J_o(v_1 a_1) Y_1(v_1 a) - Y_o(v_1 a_1) J_1(v_1 a) \right\}$$

$$F_2(\theta) = \frac{1}{H_1(v_o b)(v_1 b)\left\{ Y_o(v_1 a_1) J_o(v_1 b) - J_o(v_1 a_1) Y_o(v_1 b)\right\} - H_o(v_o b)\left\{ \frac{\epsilon_p}{\epsilon_o}(v_o b) Y_o(v_1 a_1) J_1(v_1 b) - J_o(v_1 a_1) Y_1(v_1 b)\right\}}$$

Consider the case when plasma filled wave-guide carries a circular symmetric TM_{01} mode. The field in the excitation aperture (i. e. interface between the plasma filled wave-guide and the plasma column) is assumed to be same as that of the incident wave in a plasma filled wave-guide. Under these conditions the field distribution at the open end of the wave-guide can be considered to be equivalent to the vector sum of magnetic current rings with various radii ranging from the outer radius of the central conductor to the inner radius of the circular wave-guide. The magnitude of the magnetic current in each ring is assumed to be proportional to the value of H_ϕ at that particular location in the wave-guide. In the wave-guide for circular symmetric TM_{01} mode, H_ϕ is proportional to $J_1(hr)$ where h, in the case of circular symmetric TM mode, is given by the root of $J_o(h a_3)=0$ where a_3 is the inner radius of the plasma filled wave-guide. So in the case of wave-guide TM_{01} mode excitation $F(\theta)$ is modified to

$$F(\theta) = \int_{a_1}^{a_3} F(\theta)_{\text{magnetic ring}} \, J_1(h a)\, da = F_2(\theta) \int_{a_1}^{a_3} F_1(\theta)\, J_1(h a)\, da$$

$$= F_2(\theta) \int_{a_1}^{a_3} a \left\{ J_o(v_1 a_1) Y_1(v_1 a) - Y_o(v_1 a_1) J_1(v_1 a) \right\} J_1(ha)\, da$$

$$= \frac{F_2(\theta)}{v_1^2 - h^2} \Big[(v_1 a_3) J_1(h a_3) \left\{ Y_o(v_1 a_1) J_o(v_1 a_3) - J_o(v_1 a_1) Y_o(v_1 a_3) \right\} + \frac{2}{\pi} J_o(h a_1) \frac{h}{v_1} \Big]$$

for $h \neq v_1$

$$= 0.5F_2(\theta)\Big[a_3^2\, J_1(ha_3)\left\{J_o(ha_1)Y_1(ha_3)-Y_o(ha_1)J_1(ha_3)\right\} -$$

$$-\frac{1}{h^2}\left(\frac{2}{\pi}\right) J_o(ha_1) + \left(\frac{a_1}{h}\right)\left(\frac{2}{\pi}\right) J_1(ha_1) -$$

$$-\frac{a_3}{h}\, J_o(ha_1)Y_o(ha_3)J_1(ha_3)\Big] \quad \text{for } h = v_1$$

Waveguide excitation (Waveguide excited in TE_{01} mode):

In section 3.2 equation 2.31 gives the expression for the radiation pattern of electric ring source in plasma column having central conductor. This after some modification can be put as

$$E_\phi(R, \theta) = \frac{j\, w\, \mu}{\pi}\; F'(\theta)\; \frac{e^{iK_oR}}{R}$$

where

$$F'(\theta) = F_1'(\theta)\; F_2'(\theta)$$

$$F_1'(\theta) = a\left\{J_1(v_1a_1)Y_1(v_1a)-Y_1(v_1a_1)J_1(v_1a)\right\}$$

$$F_2'(\theta) = \frac{1}{H_1(v_ob)(v_1b)\left\{Y_1(v_1a_1)J_o(v_1b)-J_1(v_1a_1)Y_o(v_1b)\right\} - H_o(v_ob)\left\{(v_ob)Y_1(v_1a_1)J_1(v_1b)-J_1(v_1a_1)Y_1(v_1b)\right\}}$$

Consider the case when the plasma filled wave-guide carries a circular symmetric TE_{01} mode. The field in the excitation aperture (i.e. interface between the plasma filled wave-guide and the plasma column) is assumed to be same as that of the incident wave in plasma filled wave-guide. The field distribution at the excitation aperture (open end cross-section of circular wave-guide) can be considered to be equivalent to the vector sum of electric current rings with various radii ranging from the outer radius of the central conductor to the inner radius of the circular wave-guide at the open end cross-section of the circular wave-guide. The magnitude of electric current in each ring is considered to be proportional to the value of E_ϕ at that particular location in the wave-guide. For circular symmetric TE_{01} mode, E_ϕ is proportional to $J_1(hr)$, where h, in case of circular symmetric TE_{01} mode, is given by the first root of $J_0'(ha_3) = 0$, a_3 is the inner radius of the circular wave-guide at the open end. In the case of wave-guide TE_{01} mode excitation $F'(\theta)$ is modified to

$$F'(\theta) = \int_{a_1}^{a_3} F'(\theta)_{\text{Electric ring}} J_1(ha)da = F_2'(\theta)\int_{a_1}^{a_3} F_1'(\theta)J_1(ha)da$$

$$= F_2'(\theta)\int_{a_1}^{a_3} a\left\{J_1(v_1a_1)Y_1(v_1a) - Y_1(v_1a_1)J_1(v_1a)\right\}J_1(ha)da$$

$$= \frac{F_2'(\theta)}{v_1^2-h^2}\left[(a_3h)J_0(ha_3)\left\{J_1(v_1a_1)Y_1(v_1a_3) - J_1(v_1a_3)Y_1(v_1a_1)\right\} + \left(\frac{2}{\pi}\right) J_1(ha_1)\right]$$

for $h \neq v_1$

$$= \frac{F_2'(\theta)}{2}\left[a_3^2 J_o(ha_3)\left\{ Y_o(ha_3)J_1(ha_1)-Y_1(ha_1)J_0(ha_3)\right\} + \right.$$

$$+ \frac{2}{\pi} J_1(ha_1) \quad \frac{a_1}{h} \quad - \left(\frac{2}{\pi}\right) \quad \frac{a_1}{h} J_0(ha_1) -$$

$$\left. - \frac{a_3}{h} J_1(ha_1)Y_1(ha_3)J_o(ha_3) \right] \qquad \text{for } h = v_1$$

2.4.3 CHARACTERISTICS OF THE RADIATION FIELD:

The radiation pattern (variation of $F'(\theta)$ with θ) has been computed with the help of IBM-1130 computer for the wave-guide excited in TM_{01} with the parametric value $K_ob = 6\pi$, $K_oa_1 = .09$, $K_oa_3 = 2.4$, $\epsilon_p = .1$, $\epsilon_p = .5$ and for the wave-guide excited in TE_{01} mode with parametric value $K_ob = 6\pi$, $K_oa_1 = .09$, $K_oa_3 = 3.83$, $\epsilon_p = .1$, $\epsilon_p = .5$ (see fig. 2.20). In all these cases a well enhanced radiation peak is formed near and before the critical angle ($\sin^2\theta_c = \epsilon_p$). After the critical angle the amplitudo of the radiation field falls off rapidly. The detailed structure of these peaks is shown in fig. 2.21a and fig. 2.21b . The effect of different parameters on the radiation field is discussed below.

Effect of K_ob:

In case of wave-guide excited in TM_{01} mode the radiation peak becomes sharper, stronger and moves closer to the critical angle as the value of K_ob is increased. But in case of wave-guide excited in TE_{01} mode we find the opposite effect i.e. the increase in K_ob results in to the formation of broader and weaker radiation peak before the critical angle. This is shown in fig. 2.22.

Effect of K_oa_3:

In both the cases (wave-guide excited in TM_{01} and TE_{01} mode) K_oa_3 does not affect the direction of the radiation peak of the radiation pattern but affects its amplitude. Consideration for proper excitation of TM_{01} and TE_{01} mode in circular wave-guide limits the value K_oa_3. In circular cylindrical wave-guide for TM_{01} mode the passband extends from $K_oa_3 = 2.4$ to $K_oa_3 = 3.5$ and for TE_{01} mode the passband extends from $K_oa_3 = 3.83$ to $K_oa_3 = 5.13$. The variation of peak amplitude with K_oa_3 (K_oa_3 varied only in the passband) is shown in fig. 2.23a and 2.23b.

Effect of K_oa_1:

In both the cases (wave-guide excited in TM_{01} and TE_{01} mode) K_oa_1 affects the amplitude and sharpness of the radiation peak and to a small extent it also affects its direction. Smaller value of K_oa_1 gives rise to a sharper and stronger radiation peak. The variation of peak amplitude with K_oa_1 is shown in fig. 2.24a and fig. 2.24b.

Effect of plasma density:

The direction of the radiation peak depends upon the plasma density. The location of radiation peak for different values of ϵ_p which for constant source frequency, corresponds to different plasma densities are shown in fig. 2.20. In the case of wave-guide TM_{01} mode excitation half power beam width of the radiation peak for $\epsilon_p = .1$ is 0.65° for $\epsilon_p = .5$ is 0.04475°. In the case of wave-guide TE_{01} mode excitation half power beam width for $\epsilon_p = .1$ is 1.18° and for $\epsilon_p = 0.5$ is $.77^\circ$. It is found that in both the cases (wave-guide excited in TM_{01} and TE_{01} mode) the amplitude of the radiation peak decreases with the decrease in plasma density. In both the cases (wave-guide excited in TM_{01} mode and wave-guide excited in TE_{01} mode) the half power beam width decreases with the decrease in plasma density.

***

CHAPTER 3.

EXCITATION OF ISOTROPIC INCOMPRESSIBLE ANNULAR PLASMA COLUMN SURROUNDING AN AIR CORE HAVING CENTRAL CONDUCTOR ALONG ITS AXIS.

CHAPTER 3.

EXCITATION OF ISOTROPIC INCOMPRESSIBLE ANNULAR PLASMA COLUMN SURROUNDING AN AIR CORE HAVING CENTRAL CONDUCTOR ALONG ITS AXIS.

3.1 EXCITATION BY MAGNETIC RING SOURCE:

3.1.1 INTRODUCTION:

Harris[11] (1968) studied the radiation pattern of an infinite magnetic line source in air gap between grounded plane and plasma slab. In this case he predicted the presence of well enhanced and sharp narrow radiation peaks beyond the critical angle. It is an interesting result. He explained that the emergence of sharp narrow radiation peaks is mainly due to the air gap between plasma slab and grounded plane. This phenomenon (the emergence of sharp narrow radiation peaks beyond the critical angle) was not found in the case of grounded plasma slab excited by magnetic line source studied by Tamir[3] (1962). Harris[11] (1968) attributed these radiation peaks(formed beyond the critical angle in case of ungrounded plasma slab excited by infinite magnetic line source) to the excitation of leaky waves on the plasma surface. This study encourged to look for the similar phenomenon (the emergence of well enhanced radiation peaks beyond the critical angle) in case of more practically feasible cylindrical plasma geometry (Annular plasma column surrounding an air core having central conductor along its axis) excited by the corresponding circular symmetric ring source (Magnetic ring source in air core).

3.1.1 ANALYSIS:

The geometry of the configuration analysed is shown in fig. 3.1. An infinitely long air column of radius a_2 having an infinitely long conductor of radius a_1 along its longitudinal axis and surrounded by an annular plasma column of inner radius a_2 and outer radius b is oriented with its axis along the Z axis of the (r, Ø, Z) cylindrical coordinate system. The source of electromagnetic radiation is a ring of magnetic current of radius a ($a \angle a_2$) concentric with the air column and situated at Z = 0 plane. This source of electromagnetic radiation is mathematically represented by

$$\bar{M} = \bar{\phi}\, \delta(r - a)\ \delta(Z)$$

where δ represents Kronecker's delta function, $\bar{\phi}$ is a unit vector in the Ø direction. Here the circular symmetric mode is considered. The source form of Maxwell's equations governing the electromagnetic field written in differential form for an e^{-jwt} time dependence can be written as,

$$\nabla \times \bar{E} = j\, w\, \mu\, \bar{H} - \bar{M}$$

$$\nabla \times \bar{H} = -\, j\, w\, \epsilon\, \bar{E}$$

Taking curl of second equation and substituting value of $\nabla \times \bar{E}$

from first equation,

$$\nabla \times \nabla \times \bar{H} - w^2 \mu \epsilon \bar{H} = j w \epsilon \bar{M}$$

Considering circular symmetric mode , we have,

$$(\nabla \times \nabla \times \bar{H})_{\phi} - w^2 \mu \epsilon H_{\phi} = jw\epsilon \, \delta(r - a) \, \delta(Z)$$

Expanding it in cylindrical coordinates we have,

$$\frac{d^2 H_\phi}{d r^2} + \frac{1}{r} \frac{dH_\phi}{d r} + (K^2 - \frac{1}{r^2}) H_\phi + \frac{d^2 H_\phi}{d Z^2} = -jw\epsilon \, \delta(r-a) \, \delta(Z) \qquad (3.1)$$

where $K^2 = w^2 \mu \epsilon$

In order to solve equation (3.1) we apply the method of integral transforms . Let the Fourier transform of $H_\phi(r, Z)$ be defined as

$$h(r, \xi) = \int_{-\infty}^{\infty} H_\phi(r, Z) \, e^{-j \xi Z} \, dZ$$

and inverse transform be given by

$$H_\phi(r, Z) = \frac{1}{2\pi} \int_{-\infty}^{\infty} h(r, \xi) \, e^{j \xi Z} \, d\xi$$

Now multiplying each term of equation (3.1) by $e^{-j \xi Z}$ and integrating over the infinite range with respect to Z we get,

$$\frac{d^2 h}{d r^2} + \frac{1}{r} \frac{dh}{dr} + (K^2 - \xi^2 - \frac{1}{r^2}) h = -jw\epsilon \, \delta(r - a) \qquad (3.2)$$

Equation (3.2) is considered to be ordinary differential equation with ξ as a parameter constant. Boundary conditions on h follow from the boundary conditions on its inverse Fourier transform. As a result of proper boundary conditions the solution for h in free space is found out and then its inverse Fourier transform gives us the field in free space. The details are worked out in the following sections.

Computation of Boundary Value Problem :

Consider the inhomogeneous differential equation (3.2). The delta function is related by the relation,

$$\delta(r-a) = 1 \quad \text{for } r = a$$

$$\delta(r-a) = 0 \quad \text{for } r \neq a$$

So for all values of r other than r = a equation (3.2) reduces to homogeneous differential equation

$$\frac{d^2h}{dr^2} + \frac{1}{r}\frac{dh}{dr} + \left(K^2 - \xi^2 - \frac{1}{r^2}\right) h = 0$$

Delta function $\delta(r-a)$ implies boundary conditions on h which must be satisfied at r = a. Multiplying equation (3.2) by dr and integrating over the interval 2Δ from $r = a - \Delta$ to $r = a + \Delta$ and assuming the continuation of h around r = a and taking limit as $\Delta \to 0$ we have

$$\left.\frac{dh}{dr}\right|_{a+\Delta} - \left.\frac{dh}{dr}\right|_{a-\Delta} = -j\,w\,\epsilon_1 \qquad (3.4)$$

Where ϵ_1 is dielectric constant of the medium.
The remaining boundary conditions on $h(r, \xi)$ correspond to the boundary conditions imposed on $H_\phi(r, Z)$ and $E_Z(r, Z)$

by Maxwell's equation. As shown in fig. 3.1 region between $r = a_1$ to $r = a$ is denoted as region I, between $r = a$ to $r = a_2$ as region II, between $r = a_2$ to $r = b$ as region III and the region for which $r > b$ as region IV.

Now solution of equation (3.3) in region I is given as

$$h = A_1 J_1(v_1 r) + B_1 Y_1(v_1 r)$$

where $v_1^2 = K_1^2 - \xi^2$ and $K_1^2 = w^2 \mu \epsilon_1$

In region II is given as

$$h = A_2 J_1(v_1 r) + B_2 Y_1(v_1 r)$$

In region III is given as

$$h = A_3 I_1(v_2 r) + B_3 K_1(v_2 r)$$

where $v_2^2 = \xi^2 - K_2^2$, $K_2^2 = w^2 \mu \epsilon_p$

I_1 and K_1 are modified Bassel functions

In region IV, also taking into account the radiation condition oh H_ϕ we have solution of equation (3.3) as

$$h = A_4 H_1 (v_o r), \text{where } v_o^2 = K_o^2 - \xi^2,\ K_o^2 = w^2 \mu \epsilon_o$$

H_1 is Hankel function

Continuation of H_ϕ at any r for all Z implies that

$$h(r, \xi) = \int_{-\infty}^{\infty} H_\phi (r, Z) e^{-j \xi Z} dZ$$

must also be continuous.

From Maxwell's equations we have

$$\bar{E} = \left(\frac{1}{-jw\epsilon}\right) \nabla \times \bar{H}$$

$$E_Z(r, Z) = -\frac{1}{jw\epsilon}\left(\frac{d H_\phi}{d r} + \frac{1}{r} H_\phi\right)$$

so the continuity of $E_Z(r, Z)$ at any r for all Z implies that

$$-\frac{1}{jw\epsilon}\left(\frac{d h}{d r} + \frac{h}{r}\right)$$ be continuous

where ϵ is the dielectric constant of that medium.

(1) Now at ($r = a_1$) conductor surface tangential electric vector namely $E_Z(r, Z)$ is continuous, so we have,

$$-\frac{1}{jw\epsilon_1}\left.\left(\frac{d h}{d r} + \frac{h}{r}\right)\right|_{r = a_1+\Delta} = 0$$

$$\left.\left(\frac{d h}{d r} + \frac{h}{r}\right)\right|_{r = a_1+\Delta} = 0$$

(2) At ($r = a$) the location of magnetic ring source of electromagnetic waves we have, from equation (3.4) and continuation of H_ϕ

$$h\Big|_{a-\Delta} = h\Big|_{a+\Delta}$$

$$\left.\frac{d h}{d r}\right|_{a+\Delta} - \left.\frac{d h}{d r}\right|_{a-\Delta} = -j w\epsilon$$

(3) At $r = a_2$ continuation of E_z and H_ϕ gives

$$h\Big|_{a_2-\Delta} = h\Big|_{a_2+\Delta}$$

$$\frac{dh}{dr}\Big|_{a_2+\Delta} - \frac{dh}{dr}\Big|_{a_1-\Delta} + \left(\frac{\epsilon_1}{\epsilon_p} - 1\right)\frac{h}{r}\Big|_{a_2+\Delta} = 0$$

(4) At $r = b$ continuation of E_z and H_ϕ gives

$$h\Big|_{b-\Delta} = h\Big|_{b+\Delta}$$

$$\frac{dh}{dr}\Big|_{b+\Delta} - \frac{dh}{dr}\Big|_{b-\Delta} + \left(\frac{\epsilon_p}{\epsilon_0} - 1\right)\frac{h}{r}\Big|_{b+\Delta} = 0$$

Applying all these boundary conditions on the solution in different regions we have

$$A_1(v_1a_1)\,J_o(v_1a_1) + B_1(v_1a_1)\,Y_o(v_1a_1) = 0$$

$$A_1J_1(v_1a) + B_1Y_1(v_1a) - A_2J_1(v_1a) - B_2Y_1(v_1a) = 0$$

$$A_1\left\{(v_1a)\,J_o(v_1a) - J_1(v_1a)\right\} + B_1\left\{(v_1a)\,Y_o(v_1a) - Y_1(v_1a)\right\} -$$

$$-A_2\left\{(v_1a)J_o(v_1a) - J_1(v_1a)\right\} - B_2\left\{(v_1a)Y_o(v_1a) - Y_1(v_1a)\right\} = jw\epsilon_1 a$$

$$A_2J_1(v_1a_2) + B_2Y_1(v_1a_2) - A_3I_1(v_2a_2) - B_3K_1(v_2a_2) = 0$$

$$A_2\left\{(v_1a_2)J_o(v_1a_2) - J_1(v_1a_2)\right\} + B_2\left\{(v_1a_2)Y_o(v_1a_2) - Y_1(v_1a_2)\right\}$$

$$-A_3\left\{\frac{\epsilon_1}{\epsilon_p}(v_2a_2)I_o(v_2a_2) - I_1(v_2a_2)\right\} + B_3\left\{\frac{\epsilon_1}{\epsilon_p}(v_2a_2)K_o(v_2a_2) + K_1(v_2a_2)\right\} = 0$$

$$A_3 I_1(v_2 b) + B_3 K_1(v_2 b) - A_4 H_1(v_o b) = 0$$

$$A_3 \left\{ (v_2 b) I_o(v_2 b) - I_1(v_2 b) \right\} + B_3 \left\{ -(v_2 b) K_o(v_2 b) - K_1(v_2 b) \right\} -$$

$$-A_4 \left\{ \frac{\epsilon_p}{\epsilon_o}(v_o b)\, H_o^1 (v_o b) - H_1 (v_o b) \right\} = 0$$

Here we have 7 constants and 7 equations. Our main aim here is to find out A_4 which, in turn, by inverting the Fourier transform in free space will give us radiation pattern in free space. By solving these equations we have,

$$A_4 = jw\, \epsilon_1\, F(v_o, v_1, v_2)$$

$$F(v_o, v_1, v_2) = \frac{\left[a(v_2 b) \left\{ I_1(v_2 b) K_o(v_2 b) + I_o(v_2 b) K_1(v_2 b) \right\} * \left\{ J_o(v_1 a_2) Y_1(v_1 a) - Y_o(v_1 a_1) J_1(v_1 a) \right\} \right]}{a_{67} \left\{ a_{12}(a_{76} X_1 - a_{75} X_2) - a_{11}(a_{76} X_3 - a_{75} X_4) \right\} - a_{77} \left\{ a_{12}(a_{66} X_1 - a_{65} X_2) - a_{11}(a_{66} X_3 - a_{65} X_4) \right\}}$$

$X_1 = a_{55}\, a_{43} - a_{45}\, a_{53}$, $X_2 = a_{56}\, a_{43} - a_{46}\, a_{53}$,

$X_3 = a_{55}\, a_{44} - a_{45}\, a_{54}$, $X_4 = a_{56}\, a_{44} - a_{46}\, a_{54}$,

$a_{11} = J_o(v_1 a_1)$, $a_{12} = Y_o(v_1 a_1)$, $a_{43} = J_1(v_1 a_2)$, $a_{44} = Y_1(v_1 a_2)$,

$a_{45} = I_1(v_2 a_2)$, $a_{53} = (v_1 a_2) J_o(v_1 a_2) - J_1(v_1 a_2)$,

$a_{54} = (v_1 a_2) Y_o(v_1 a_2) - Y_1(v_1 a_2)$, $a_{55} = -\left\{ \frac{\epsilon_1}{\epsilon_p}(v_2 a_2) I_o(v_2 a_2) - I_1(v_2 a_2) \right\}$,

$a_{56} = \frac{\epsilon_1}{\epsilon_p}(v_2 a_2)\, K_o(v_2 a_2) + K_1(v_2 a_2)$, $a_{65} = I_1(v_2 b)$, $a_{66} = K_1(v_2 b)$,

$a_{67} = -H_1(v_o b)$, $a_{75} = (v_2 b)\, I_o(v_2 b) - I_1(v_2 b)$,

$a_{76} = -\left\{ (v_2 b)\, K_o(v_2 b) + K_1(v_2 b) \right\}$, $a_{77} = -\left\{ \frac{\epsilon_p}{\epsilon_o}(v_o b) H_o(v_o b) - H_1(v_o b) \right\}$

So solution in free space is

$$h(r, \xi) = A_4 H_1(v_o r)$$

Inverting it,

$$H_\phi(r, Z) = \frac{1}{2\pi} \int_{-\infty}^{\infty} h(r, \xi)\, e^{j\xi Z}\, d\xi$$

$$= \frac{1}{2\pi} \int_{-\infty}^{\infty} A_4 H_1(v_o r)\, e^{j\xi Z}\, d\xi \qquad (3.5)$$

CALCULATION OF RADIATION FIELD:

Consider integral (3.5) as contour integral in ξ plane. The variables v_1 and v_2 which appear in the integrand of equation (3.5) are multiple valued functions in the neighbourhood of $\xi = \pm K_1$ and $\xi = \pm K_2$ respectively. It can be shown, by expanding the integrand about $v_1 = 0$ and $v_2 = 0$ that the integrand is an even function of v_1 and v_2 respectively. But at $v_o = 0$, the Hankel functions which appear in the integrand have logarithmic singularity, so $\xi = \pm K_o$ are branch points of the integrand.

Let us now apply the method of saddle point integration to evaluate the integral (3.5). Introduce the transformation

$$\xi = K_o \sin\psi$$

where $$\psi = \tau + j\lambda$$

This transformation transforms the region of integration in ξ plane into a strip in the ψ plane, which is bounded by two curved lines corresponding to the branch cuts ($\xi = \pm K_o$) in the ψ plane. Branch cuts in ψ plane are given by

$$\sin\tau \ \cosh\lambda = \pm 1$$

This transformation yields

$$v_o = K_o \cos\psi$$

$$v_1 = K_o \sqrt{\epsilon_1 - \sin^2\psi}$$

$$v_2 = K_o \sqrt{\sin^2\psi - \epsilon_p}$$

Equation (3.5) now transforms to

$$H_\phi(r, Z) = \int_c A_4(\psi)\, H_1(K_o r \cos\psi)\, e^{jK_o \sin(\psi) Z} K_o \cos\psi \, d\psi \qquad (3.6)$$

For large r, replacing the Hankel function in the integrand of equation (3.6) by its asymptotic value and shifting to spherical coordinate system (R, θ, ϕ) as shown in fig. (3.1),

$$H_\phi(R,\theta) = \frac{jw\epsilon_1 a}{\pi} e^{-\frac{j3\pi}{4}} \left(\frac{K_o}{2\pi R \cos\theta}\right)^{\frac{1}{2}} A_4(\psi) *$$

$$* \sqrt{\cos\psi}\ e^{jK_o R \cos(\psi - \theta)}\, d\psi \qquad (3.7)$$

The saddle point of this integral is given by

$$\frac{d}{d\psi} \cos(\psi - \theta) = 0$$

which gives $\psi = \theta$ as a saddle point.

The steepest descent path (S. D. P.) is given by the constant phase of the exponential factor of the integrand and is to pass through saddle point. So we have

Im j Cos ($\psi - \theta$) = constant and is to pass through $\psi = \theta$

which gives

$$\cos(\Upsilon - \theta)\cosh\lambda = 1$$

$$\sin(\Upsilon + \frac{\pi}{2} - \theta)\cosh\lambda = 1$$

Applying the standard method (see appendix A) of saddle point integration, the lowest order approximation of integral is given as

$$H_\phi(R, \theta) = \frac{-jw\epsilon_1}{\pi} \quad F(\theta) \quad \frac{e^{jK_oR}}{R} \tag{3.8}$$

where

$$F(\theta) = F(v_o, v_1, v_2)\Big|_{\psi = \theta}$$

3.1.3 CHARACTERISTICS OF THE RADIATION FIELD:

Radiation patterns (variation of $F(\theta)$ with θ for θ greater than a critical angle given by $\sin^2\theta_c = \epsilon_p$) have been computed (fig. 3.2) for $K_ob = 6\pi$, $K_oa_1 = .09$, $K_oa = .5\pi$, $K_oa_2 = \pi$, $\epsilon_p = .1$ and for $\epsilon_p = .5$. The detailed structure of these two peaks is shown in fig. (3.3). The half power beam width for $\epsilon_p = .1$ is $.00000015^{\circ}$ and for $\epsilon_p = .5$ is $.00000032^{\circ}$. The effects of different parameters on the radiation pattern are discussed below.

Effect of the diameter of the magnetic ring source:

Diameter of the magnetic ring source does not affect the directions of the radiation peaks but affects their amplitudes. This behaviour is shown in fig. 3.5.

Effect of $K_o b$:

Higher values of $K_o b$ gives rise to stronger radiation peaks. To some extent $K_o b$ also affects the direction of the radiation peak. This behaviour is shown in fig. 3.4.

Effect of $K_o a_1$:

$K_o a_1$ affects the amplitude of the radiation peaks. This behaviour is shown in fig. 3.5. To some extent it also affects the direction of the radiation peaks.

Effect of $K_o a_2$:

$K_o a_2$ affects the direction as well as the number of radiation peaks formed. This behaviour is shown in table 3.1.

Effect of plasma density:

As the plasma medium is characterised by the relative dielectric constant $\epsilon_p = \left(1 - \frac{w_p^2}{w^2}\right)$ so as plasma frequency($w_p^2 \propto n_o$, where n_o is plasma density) is increased dielectric constant of the medium decreases. Here only the transparent region ($w > w_p$) is considered i.e. it corresponds to a positive value for ϵ_p . A change in ϵ_p changes the direction of the radiation peak. Radiation peaks corresponding to different value of ϵ_p are shown in fig. 3.3.

3.1.4 DISCUSSION:

In this case of annular plasma column surrounding an air core having central conductor along its axis and excited by the magnetic ring source in air core, well enhanced radiation peaks beyond the critical angle are formed. This is consistant with the results of Harris[11] (1968), who analysed corresponding planar plasma geometry excited by magnetic line source. Here the radiation peaks formed beyond the critical angle are mainly due to the air core present. These are expected to be due to the excitation of leaky waves on plasma surface.

3.2 EXCITATION BY ELECTRIC RING SOURCE:

3.2.1 INTRODUCTION:

In section 3.1 of this chapter, the radiation pattern of magnetic ring source in air core having central conductor along its axis and surrounded by an annular plasma column has been studied. On the similar lines in this section, the analysis of the radiation pattern of the electric ring source in air core having central conductor along its axis and surrounded by an annular plasma column has been presented. In this case also well enhanced radiation peaks beyond the critical angle are found. The directions of these radiation peaks depend upon the inner and outer diameter of the plasma column and outer diameter of the central conductor. The diameter of the electric ring source has no effect on the directions of the radiation peaks but affects their amplitude. Directions of the radiation peaks can be changed by changing the plasma density.

3.2.2 ANALYSIS:

The geometry of the configuration analysed is as shown in fig. 3.7. An infinitely long air column of radius a_2 having infinitely long conductor of radius a_1 along longitudinal axis and surrounded by annular plasma column of inner radius a_2 and outer radius b is oriented with its axis along the Z axis of the cylindrical coordinate system (r, ϕ, Z) . The source of electromagnetic radiation is a ring of electric current of radius a ($a \angle a_2$) concentric with the air column and situated at the Z = 0 plane. This source of electromagnetic radiation is mathematically represented by

$$\bar{M} = \bar{\phi}\,\delta(r - a)\,\delta(Z)$$

where δ represents Kronecker's delta function, $\bar{\phi}$ is a unit vactor in the ϕ direction. Here the circular symmetric mode (TE_{01} mode) is considered. The source form of Maxwell's equations governing electromagnetic field written in differential form for an e^{-jwt} time dependence can be written as,

$$\nabla \times \bar{E} = j\,w\,\mu\,\bar{H}$$

$$\nabla \times \bar{H} = -j\,w\epsilon\,\bar{E} + \bar{M}$$

Taking curl of first equation and substituting value of $\nabla \times \bar{H}$ from second equation we have,

$$-\nabla \times \nabla \times \bar{E} + w^2\,\mu\,\epsilon\,\bar{E} = -jw\mu\,\bar{M}$$

Now considering circular symmetric mode we have,

$$(\nabla \times \nabla \times \bar{E}) - w^2\mu\epsilon E_\phi = jw\mu\,\delta(r - a)\,\delta(Z)$$

Expanding it in cylindrical coordinates we have,

$$\frac{d^2E_\phi}{dr^2} + \frac{1}{r}\,\frac{dE_\phi}{dr} + (K^2 - \frac{1}{r^2})\,E_\phi + \frac{d^2E_\phi}{dZ^2} = -jw\mu\,\delta(r-a)\,\delta(Z) \tag{3.9}$$

In order to solve equation (3.9) we apply the method of integral transforms. Let the Fourier transform of $E_\phi(r,Z)$

be defined as,

$$h\ (r, \xi\ ) = \int_{-\infty}^{\infty} E_{\emptyset}(\ r,\ Z)\ e^{-j\,\xi\,Z}\, dZ$$

and inverse transform be given by,

$$E_{\emptyset}(r,Z) = \frac{1}{2\pi} \int_{-\infty}^{\infty} h(r,\ \xi\ )e^{j\,\xi\,Z}\, d\xi$$

Now multiplying each term of equation (3.9) by $e^{-j\,\xi\,Z}$ and integrating over the infinite range with respect to Z we get,

$$\frac{d^2h}{dr^2} + \frac{1}{r}\ \frac{dh}{dr} + (K^2 - \xi^2 - \frac{1}{r^2})\ h = -jw\mu\ \delta(r-a) \qquad (3.10)$$

Equation (3.10) is considered to be ordinary differential equation with ξ as a parameter constant. Boundary conditions on h follows from the boundary conditions on its inverse Fourier transform. As a result of proper boundary conditions the solution for h in free space is found out and then its inverse Fourier transform gives us the field in free space, the details are worked out in the following sections.

Computation of Boundary value problem:

Consider the inhomogeneous differential equation (3.10). The delta function is related by the relation,

$$\delta(\ r - a\ ) = 1 \quad \text{for } r = a$$

$$\delta(\ r - a\ ) = 0 \quad \text{for } r \neq a$$

So for all values of r other than r = a equation (3.10) reduces to homogeneous differential equation

$$\frac{d^2h}{dr^2} + \frac{1}{r}\ \frac{dh}{dr} + (\ K^2 - \xi^2 - \frac{1}{r^2})\ h = 0 \qquad (3.11)$$

Delta function $\delta(r - a)$ imposes boundary conditions on h which must be staisfied at r = a . Multiplying equation(3.10) by dr and integrating over the interval 2Δ from $r = a - \Delta$ to $r = a + \Delta$ and assuming the continuation of h around r = a and taking limit as $\Delta \to 0$ we have,

$$\left.\frac{dh}{dr}\right|_{a+\Delta} - \left.\frac{dh}{dr}\right|_{a-\Delta} = -jw\mu \qquad (3.12)$$

Where μ is permeability constant of the medium. The remaining boundary conditions on h (r, ξ) correspond to the boundary conditions imposed on E_ϕ (r, Z) and $H_Z(r, Z)$ by Maxwell's equations. As shown in fig. (3.7) region between $r = a_1$ to r = a is denoted as region I, between r = a to $r = a_2$ as region II, between $r = a_2$ to r = b as region III and the region for which r > b as region IV.

Now solution of equation (3.11) in region I is given as

$$h = A_1 J_1(v_1 r) + B_1 Y_1(v_1 r)$$

where $v_1^2 = K_1^2 - \xi^2$ and $K_1^2 = w^2 \mu \epsilon_1$

In region II is given as

$$h = A_2 J_1(v_1 r) + B_2 Y_1(v_1 r)$$

In region III is given as

$$h = A_3 I_1(v_2 r) + B_3 K_1(v_2 r)$$

where $v_2^2 = \xi^2 - K_2^2$, $K_2^2 = w^2 \mu \epsilon_p$

I_1 and K_1 are modified Bessel functions.

In region IV, also taking into account the radiation condition on E_ϕ we have solution of equation (3.11) as

$$h = A_4 H_1(v_o r) \text{ where } v_o^2 = K_o^2 - \xi^2,\ K_o^2 = w^2 \mu \epsilon$$

H_1 is Hankel function.

Continuation of E_ϕ at any r for all Z implies that

$$h(r, \xi) = \int_{-\infty}^{\infty} E_\phi(r, Z)\, e^{-j \xi Z}\, dZ$$

must also be continuous.

From Maxwell's equations we have

$$\bar{H} = \frac{1}{jw\mu}(\nabla \times \bar{E})$$

$$H_Z = \frac{1}{jw\mu}\left(\frac{dE_\phi}{dr} + \frac{E_\phi}{r}\right) \qquad (3.13)$$

so the continuation of $H_Z(r, Z)$ at any r for all Z implies that

$$\frac{1}{jw\mu}\left(\frac{dE_\phi}{dr} + \frac{E_\phi}{r}\right)$$

be continuous

(1) Now at ($r = a_1$) the conductor surface, tangential electric vector namely $E_\phi(r, Z)$ is continuous so we have,

$$h\Big|_{a_1+\Delta} = 0$$

(2) At (r = a) the location of electric ring source of electromagnetic waves we have from equation (3.13) and continuation of E_ϕ

$$h\Big|_{a-\Delta} = h\Big|_{a+\Delta}$$

$$\frac{dh}{dr}\Big|_{a+\Delta} - \frac{dh}{dr}\Big|_{a-\Delta} = -jw\mu$$

(3) At ($r = a_2$) continuation of E_ϕ and H_z gives

$$h\Big|_{a_2-\Delta} = h\Big|_{a_2+\Delta}$$

$$\frac{dh}{dr}\Big|_{a_2-\Delta} = \frac{dh}{dr}\Big|_{a_2+\Delta}$$

(4) At (r = b) continuation of H_z and E_ϕ gives,

$$\frac{dh}{dr}\Big|_{b-\Delta} - \frac{dh}{dr}\Big|_{b+\Delta} = 0$$

$$h\Big|_{b-\Delta} = h\Big|_{b+\Delta}$$

Applying all these boundary conditions on the solution in different regions we have

$$A_1 J_1(v_1 a_1) + B_1 Y_1(v_1 a_1) = 0 \qquad (3.14)$$

$$A_1 J_1(v_1 a)+B_1 Y_1(v_1 a)-A_2 J_1(v_1 a)-B_2 Y_1(v_1 a) = 0 \qquad (3.15)$$

$$A_1 \left\{ (v_1 a)J_o(v_1 a)- J_1(v_1 a)\right\} + B_1\left\{(v_1 a)\, Y_o(v_1 a)-Y_1(v_1 a)\right\} -$$

$$-A_2 \left\{(v_1 a)J_o(v_1 a)-J_1(v_1 a)\right\} -B_2\left\{(v_1 a)Y_o(v_1 a)-Y_1(v_1 a)\right\} =jw/ua \qquad (3.16)$$

$$A_2 J_1(v_1 a_2)+B_2 Y_1(v_1 a_2)-A_3 I_1(v_2 a_2)-B_3 K_1(v_2 a_2) = 0 \qquad (3.17)$$

$$A_2 \left\{(v_1 a_2)J_o(v_1 a_2)-J_1(v_1 a_2)\right\} +B_2 \left\{(v_1 a_2)Y_o(v_1 a_2)-Y_1(v_1 a_2)\right\} -$$

$$-A_3\left\{(v_2 a_2)I_o(v_2 a_2)-I_1(v_2 a_2)\right\} +B_3 \left\{(v_2 a_2)K_o(v_2 a_2)+K_1(v_2 a_2)\right\} =0 \qquad (3.18)$$

$$A_3 I_1(v_2 b) +B_3 K_1(v_2 b)-A_4 H_1(v_o b) = 0 \qquad (3.19)$$

$$A_3 \left\{(v_2 b)I_o(v_2 b)-I_1(v_2 b)\right\} -B_3\left\{ (v_2 b)K_o(v_2 b)-K_1(v_2 b) \right\}-$$

$$-A_4\left\{(v_o b)H_o(v_o b)-H_1(v_o b)\right\} = 0 \qquad (3.20)$$

Here we have 7 constants and 7 equations. Our main aim here is to find out A_4 which, in turn, by inverting the Fourier transform will give us radiation pattern in free space. By solving these equations we have,

$$A_4 = j\, w\, /u\, a\, F'(v_o, v_1, v_2)$$

$$F'(v_o, v_1, v_2) = \frac{\left[a(v_2 b)\left\{ I_1(v_2 b)K_o(v_2 b) + I_o(v_2 b)K_1(v_2 b)\right\} * \left\{ J_1(v_1 a_1)Y_1(v_1 a) - Y_1(v_1 a_1)J_1(v_1 a)\right\} \right]}{a_{67}\left\{ a_{12}(a_{76} X_1 - a_{75} X_2) - a_{11}(a_{76} X_3 - a_{75} X_4)\right\} - a_{77}\left\{ a_{12}(a_{66} X_1 - a_{65} X_2) - a_{11}(a_{66} X_3 - a_{65} X_4)\right\}}$$

$X_1 = a_{55}\, a_{43} - a_{45}\, a_{53}$, $X_2 = a_{56}\, a_{43} - a_{46}\, a_{53}$, $X_3 = a_{55}\, a_{44} - a_{45} a_{54}$,

$X_4 = a_{56}\, a_{44} - a_{46} a_{54}$, $a_{11} = J_1(v_1 a_1)$, $a_{12} = Y_1(v_1 a_1)$, $a_{43} = J_1(v_1 a_2)$,

$a_{44} = Y_1(v_1 a_2)$, $a_{53} = (v_1 a_2)\, J_o(v_1 a_2) - J_1(v_1 a_2)$,

$a_{54} = (v_1 a_2) Y_o(v_1 a_2) - Y_1(v_1 a_2)$, $a_{55} = -\left\{ (v_2 a_2) I_o(v_2 a_2) - I_1(v_2 a_2)\right\}$,

$a_{56} = (v_2 a_2) K_o(v_2 a_2) + K_1(v_2 a_2)$, $a_{65} = I_1(v_2 b)$, $a_{66} = K_1(v_2 b)$,

$a_{67} = -H_1(v_o b)$, $a_{76} = -\left\{ (v_2 b) K_o(v_2 b) + K_1(v_2 b)\right\}$,

$a_{77} = -\left\{ (v_o b)\, H_o(v_o b) - H_1(v_o b)\right\}$

So solution in free space is,

$$h(r, \xi) = A_4 H_1(v_o r)$$

Inverting it we have

$$E_\phi(r, Z) = \frac{1}{2\pi} \int_{-\infty}^{\infty} A_4 H_1(v_o r)\, e^{j \xi Z}\, d\xi \qquad (3.21)$$

CALCULATION OF RADIATION FIELD:

The variables v_1 and v_2 which appear in the integrand of equation (3.21) are multiple-valued functions in the neighbourhood of $\xi = \pm K_1$ and $\xi = \pm K_2$ respectively.

It can be shown by expanding the integrand about $v_1 = 0$ and $v_2 = 0$ that the integrand is an even function of v_1 and v_2 respectively. But at $v_o = 0$, the Hankel functions which appear in the integrand have logarithmic singularity, so $\xi = \pm K_o$ are branch points of the integrand.

Let us now apply the method of saddle point integration to evaluate the integral (3.21). Introduce the transformation

$$\xi = K_o \sin\psi$$

where $\psi = \tau + j\lambda$

This transformation transforms the region of integration in ξ plane into a strip in the ψ plane, which is bounded by two curved lines corresponding to the branch cuts ($\xi = \pm K_o$) in the ψ plane. Branch cuts in ψ plane are given by,

$$\sin\tau \cosh\lambda = \pm 1$$

This transformation yields

$$v_o = K_o \cos\psi$$

$$v_1 = K_o \sqrt{(\epsilon_1 - \sin^2\psi)}$$

$$v_2 = K_o \sqrt{\sin^2\psi - \epsilon_2}$$

Now equation (3.21) transforms to

$$E_{\phi}(r, Z) = \frac{1}{2\pi} \int A_4(\psi) H_1 (K_o r \cos\psi) e^{jK_o \sin\psi Z} *$$

$$* K_o \cos\psi \; d\psi \qquad (3.22)$$

Now for large r replacing Hankel function in the integrand of equation (3.22) by its asymptotic value and shifting to spherical coordinate system (R, θ, ∅) as shown in fig. (3.7), we have

$$E_{\phi}(R, \theta) = \frac{j w \mu a}{\pi} e^{-(\frac{j3\pi}{4})} \left(\frac{K_o}{2\pi R \cos\theta} \right)^{\frac{1}{2}} *$$

$$\int_c A_4(\psi) (\cos\psi)^{\frac{1}{2}} e^{jK_o R \cos(\psi - \theta)} \, d\psi$$

The saddle point of this integral is given by

$$\frac{d}{d\psi} \cos(\psi - \theta) = 0$$

which gives saddle point at $\psi = \theta$.

The steepest descent path (S.D.P.) is given by the constant phase of the exponential factor of the integrand and is to pass through saddle point. So we have

$\text{Im}\, j \cos(\psi - \theta) = \text{Constant}$ and is to pass through $\psi = \theta$ which gives

$$\cos(\tau - \theta) \cosh\lambda = 1$$

$$\sin(\tau + \frac{\pi}{2} - \theta) \cosh\lambda = 1$$

Applying the standard method (see appendix A) of saddle point integration, the lowest order approximation of integral is given as,

$$E_\phi(r, \theta) = \frac{-jw\mu a}{\pi} F(\theta) \frac{e^{jK_oR}}{R} \tag{3.23}$$

where

$$F(\theta) = F(v_o, v_1, v_2)\Big|_{\psi = \theta} \tag{3.24}$$

3.2.3 CHARACTERISTICS OF THE RADIATION FIELD:

Radiation patterns (variation of $F(\theta)$ with θ for θ greater than critical angle given by $\sin^2 \theta_c = \epsilon_p$) have been computed for $K_ob = 6\pi$, $K_oa_1 = .09$, $K_oa = .5\pi$, $K_oa_2 = \pi$ and $\epsilon_p = .1$ and for $\epsilon_p = .5$. In both the cases we get well enhanced and narrow radiation peaks beyond the critical angle . It is shown in fig. 3.8. The detailed structure of these peaks is also shown in fig. 3.9. The half power beam width for $\epsilon_p = .1$ is $.00000038^\circ$ and for $\epsilon_p = .5$ is $.000000335^\circ$. The effect of different parameters on the radiation pattern is discussed below.

Effect of K_ob:

Higher values of K_ob give rise to weaker radiation peaks. This behaviour is shown in fig. 3.10.

Effect of K_oa_2:

Number of radiation peaks formed beyond the critical angle increases with the increase in the value of K_oa_2. This behaviour is shown in Table No. 3.2.

Effect of $K_o a$:

$K_o a$ does not affect the direction of the radiation peaks but affects their amplitude. This behaviour is shown in fig. 3.11.

Effect of $K_o a_1$:

Increase in the value of $K_o a_1$ results into the decrease in the amplitude of the radiation peak . It is shown in fig. 3.12.

Effect of plasma density:

ϵ_p ($\epsilon_p = 1 - \frac{w_p^2}{w^2}$) affects the direction of the radiation peak of the radiation pattern. So for constant source frequency, the direction of the radiation peak can be changed by changing the plasma density ($w_p^2 \propto n_o$). Radiation patterns for two different values of ϵ_p i.e. different values of plasma density are shown in fig. 3.8.

3.2.4 DISCUSSION:

In this section the radiation pattern of electric ring source in air core having central conductor and surrounded by an annular plasma column has been discussed. In this case we get well enhanced radiation peaks beyond the critical angle. These are very sharp peaks. These are expected to be due to the excitation of leaky waves on the plasma surface. In this geometry the air core is an important addition and is responsible for the formation of radiation peaks beyond the critical angle.

3.3 EXCITATION BY OPEN ENDED COAXIAL LINE EXCITED IN TEM MODE.

3.3.1. INTRODUCTION:

In section 3.1 of this chapter the radiation pattern of the magnetic ring source in air core having central conductor along its axis and surrounded by an annular plasma column has been discussed. In that case it is found that the diameter of the magnetic ring source of electromagnetic waves does not affect the directions of the radiation peaks but affects their amplitudes. Moreover, the physical realization of the ideal magnetic ring source with field distribution given by delta function is not very convenient. The study of the radiation pattern of the open ended coaxial line in air core having central conductor along its axis and surrounded by an annular plasma column is an attempt in the direction of studying the case of the more practically feasible source of electromagnetic waves.

The present study is concerned with the radiation pattern of an open ended co-axial line excited in TEM mode in air core having central conductor and surrounded by an annular plasma column. Well enhanced multiple radiation peaks are formed beyond the critical angle. Number of radiation peaks in radiation pattern depends upon the inner and outer diameter of the annular plasma column. Directions of the radiation peaks do not depend upon the inner diameter of the outer conductor of co-axial line at the open end. Central conductor also affects the directions of radiation peaks. The directions of these radiation peaks can be changed by changing the plasma density.

3.3.2 ANALYSIS:

The geometry of the configuration analysed is as shown in fig. (3.13). An infinitely long air core of radius a_2 having infinitely long conductor of radius a_1 along the lognitudinal axis and surrounded by an annular plasma column of inner radius a_2 and the outer radius b is oriented with its axis along the Z axis of the cylindrical coordinate system (r, Ø, Z). The source of electromagnetic radiation is an open ended co-axial line excited in TEM mode with its open end at Z = 0 plane. The expression for radiation pattern of magnetic ring source of radius'a' in air core having central conductor and surrounded by an annular plasma column, (the equation (3.8)) after some simplification can be written as

$$H_{\phi}(R, \theta) = -\frac{jw\epsilon_1}{\pi} F(\theta) \frac{e^{jK_oR}}{R} \tag{3.24}$$

where $F(\theta) = F_1(\theta) F_2(\theta)$

$$F_1(\theta) = \frac{(v_2b)\left\{I_1(v_2b)K_o(v_2b)+I_o(v_2b)K_1(v_2b)\right\}}{a_{67}\left\{a_{12}(a_{76}X_1-a_{75}X_2)-a_{11}(a_{76}X_3-a_{75}X_4)\right\} - a_{77}\, a_{12}(a_{66}X_1-a_{65}X_2)-a_{11}(a_{66}X_3-a_{65}X_4)}$$

$F_2(\theta) = a\ J_o(v_1a_1)\ Y_1(v_1a)-Y_o(v_1a_1)J_1(v_1a)$

$X_1 = a_{55}\, a_{43} - a_{45}\, a_{53}$, $X_2 = a_{56}\, a_{43} - a_{46}\, a_{53}$,

$X_3 = a_{55}\, a_{44} - a_{45}\, a_{54}$, $X_4 = a_{56}\, a_{44} - a_{46}\, a_{54}$,

$a_{11} = J_o(v_1 a_1)$, $a_{12} = Y_o(v_1a_1)$, $a_{43} = J_1(v_1a_2)$,

$a_{44} = Y_1(v_1a_2)$, $a_{53} = (v_1a_2)\, J_o(v_1a_2)-J_1(v_1a_2)$,

$a_{54} = (v_1a_2)\, Y_o(v_1a_2)-Y_1(v_1a_2)$, $a_{55} = -\left\{\frac{\epsilon_o}{\epsilon_p}(v_2a_2)I_o(v_2a_2)-I_1(v_2a_2)\right\}$

$a_{56} = \frac{\epsilon_o}{\epsilon_p}(v_2a_2)\, K_o(v_2a_2)+K_1(v_2a_2)$,

$a_{65} = I_1(v_2b)$, $a_{66} = K_1(v_2b)$, $a_{67} = -H_1(v_ob)$,

$a_{76} = -\left\{(v_2b)K_o(v_2b)+K_1(v_2\, b)\right\}$,

$a_{77} = -\left\{\frac{\epsilon_p}{\epsilon_o}(v_o\, b)\, H_o(v_o\, b) - H_1(v_o\, b)\right\}$,

$v_o = K_o \cos\theta$, $v_1 = K_o\sqrt{\epsilon_p - \sin^2\theta}$, $v_2 = K_o\sqrt{\epsilon_1 - \sin^2\theta}$

$\epsilon_1 = \epsilon_o$

ϵ_0 is relative dielectric const. of free space. K_0 is free space propagation constant. J_n, Y_n, H_n, I_n, K_n, are Bessel functions of first kind, second kind, function of first kind, modified Bessel functions of first kind, second kind and of n th order respectively. F(θ) is a factor which determines the variation of field with θ. $F_2(\theta)$ contains source terms. The field distribution of an open ended co-axial line at Z = 0 can be considered to be equivalent to the vector sum of the magnetic current rings with various radii ranging from the outer radius of the inner conductor to the inner radius of the outer conductor of the co-axial line. The magnitude of the magnetic current in each ring is considered to be proportional to the value of H_ϕ at that particular location in the co-axial line. For the co-axial line excited in TEM mode, H_ϕ is proportional to $I_0/2\pi a$, where I_0 is the current. The total radiation pattern of open ended co-axial line with its open end at Z = 0 plane can be obtained as a vector sum of the field components due to individual rings of magnetic current. F(θ) in this case is modified as

$$F(\theta) = \int_{a_1}^{a_3} F(\theta)_{\text{magnetic ring}} \frac{I_0}{2\pi a} \, da$$

Where a_1 is the outer radius of the inner conductor, a_3 is the inner radius of the outer conductor of the open ended co-axial line at Z = 0 plane.

It reduces to

$$F(\theta) = F_1(\theta) \int_{a_1}^{a_3} F_2(\theta) \frac{I_o}{2\pi a} da$$

$$= F_1(\theta) \int_{a_1}^{a_3} a \left\{ J_o(v_1 a_1) Y_1(v_1 a) - Y_o(v_1 a_1) J_1(v_1 a) \right\} \frac{I_o}{2\pi a} da$$

$$= \frac{F_1(\theta) I_o}{2\pi v_1} \left\{ J_o(v_1 a_3) Y_o(v_1 a_1) - J_o(v_1 a_1) Y_o(v_1 a_3) \right\} \quad (3.25)$$

3.3.3 CHARACTERISTICS OF THE RADIATION FIELD:

Ratiation pattern (variation of $F(\theta)$ with θ) for different parameters has been computed with the help of IBM-1130 computer . This configuration results into multiple narrow radiation peaks beyond the critical angle. Number of radiation peaks depends upon the inner and outer diameter of the annular plasma column. This behaviour is shown in table No. 3.3. Radiation peaks also become sharper with thinner annular plasma column and shifts towards end fire direction. Compromising parametric values ($K_o b = 5$, $K_o a_2 = 2.54$, $K_o a_1 = .09$, $K_o a = .9$, $\epsilon_p = .1$, $\epsilon_p = .5$) are selected to give rise to single narrow beam radiation peak beyond the critical angle. Computed results are graphed in fig. 3.14, Fig. 3.15 gives the detailed structure of these radiation peaks.

Effect of Plasma Density:

Directions of the radiation peaks for constant source frequency depend upon the plasma density. As is clear from fig. 2.14, increase in plasma density results into sharper radiation peaks. Half power beam width for ϵ_p =.1 is .0031° and for ϵ_p = .5 is .15° (shown in fig. 3.15).

Effect of $K_o a$:

Direction of the radiation peak does not depend upon $K_o a$. Fig. 3.16 shows the variation of radiation peak amplitude with $K_o a$ varied in the allowed limits (for excitation of TEM mode in co-axial line $K_o a < 1$)

3.4 EXCITATION BY WAVEGUIDE EXCITED IN CIRCULAR SYMMETRIC MODE (TM_{01} AND TE_{01} MODE):

3.4.1 INTRODUCTION:

In case of magnetic ring source excitation (section 3.1) and in case of electric ring source excitation (section 3.2), it is found that the diameter of the ring source does not affect the directions of radiation peaks but affects their amplitudes. In case of co-axial line excitation (section 3.3) it is found that the amplitude of the radiation peak increases with the increase in the inner diameter of the outer conductor. But the consideration for the proper excitation of TEM in co-axial line puts limits on the inner diameter (a_3) of the outer conductor

($K_o a_3 \angle 1$ for TEM mode excitation in coaxial line). Circular waveguide provides higher values of $K_o a_3$ (for TM_{01} mode $2.4 \angle K_o a_3 \angle 3.5$ and for TE_{01} mode $3.83 \angle K_o a_3 \angle 5.13$ where a_3 is the inner diameter of the outer conductor of the waveguide at the open end). This fact inspired to look for practically feasible and promising case of waveguide excitation.

This section is concerned with the study of the radiation pattern of an open ended circular waveguide in the air core having central conductor along its axis and surrounded by an annular plasma column. The field distribution at the open end cross-section of the circular waveguide excited in TM_{01} and TE_{01} mode is assumed to be equivalent to the vector sum of current rings of various radii ranging from the outer radius of the central conductor to the inner radius of the circular waveguide at the open end. The radiation pattern is obtained as a vector sum of field components due to individual rings of current.

In both the cases (waveguide excited in TM_{01} and TE_{01} mode) this type of geometry gives rise to well enhanced and narrow radiation peaks beyond the critical angle.

3.4.2 ANALYSIS:

An infinitely long air core of radius a_2 having a central conductor of radius a_1 along its axis and surrounded by an annular plasma column of inner radius a_2 and outer radius b is oriented with its axis along the Z axis of the cylindrical coordinate system (r, Ø, Z) shown in fig. 3.17. The source of electromagnetic radiation is an open ended waveguide (excited in TM_{01} and TE_{01} mode) with open end at Z = 0 plane.

<u>Waveguide Excitation (Waveguide Excited in TM_{01} Mode):</u>

The expression for the radiation pattern of magnetic ring source in an air core having central conductor and surrounded by an annular plasma column is given in equation (3.8). After some simplification it can be put as

$$H_\phi (R, \theta) = - \frac{j w \epsilon}{\pi} \; F_{\text{magnetic ring}}(\theta) \frac{e^{jK_oR}}{R}$$

$$F_{\text{magnetic ring}}(\theta) = F_1(\theta) \, F_2(\theta)$$

$$F_1(\theta) = \frac{(v_2b)\left\{I_1(v_2b)K_o(v_2b)+I_o(v_2b)K_1(v_2b)\right\}}{a_{67}\left\{a_{12}(a_{76} X_1-a_{75} X_2)-a_{11}(a_{76} X_3-a_{75} X_4)\right\} - a_{77}\left\{a_{12}(a_{66} X_1-a_{65} X_2)-a_{11}(a_{66} X_3-a_{65} X_4)\right\}}$$

$$F_2(\theta) = a\left\{J_o(v_1a_1)Y_1(v_1a)- Y_o(v_1a_1)J_1(v_1a)\right\}$$

The expressions for a_{11}, a_{12}, a_{65}, a_{66}, a_{67}, a_{75}, a_{76}, a_{77} X_1, X_2, X_3 and X_4 are given in section(3.1.2). The field in the excitation aperture (cross- section of open ended waveguide at Z = 0 plane) is assumed to be same as that of incident wave in the waveguide at Z = 0 plane. Under these conditions the field distribution at the open end of the waveguide can be considered to be equivalent to the vector sum of magnetic current rings with various radii ranging from the outer radius of the central conductor to the inner radius of the circular waveguide. The magnitude of the magnetic current in each ring is assumed to be proportional to the value of H_ϕ at that particular location in the waveguide. In the waveguide for circular symmetric TM_{01} mode, H_ϕ is proportional to $J_1(h r)$ where h, in the case of circular symmetric TM_{01} mode is given by the first root of $J_o(ha_3) = 0$, a_3 is the inner radius of the waveguide at Z = 0 plane. The total radiation pattern of open ended waveguide excited in TM_{01} mode with open end at Z = 0 plane is obtained as a vector sum of the field components due to individual rings of magnetic current. So in the case of waveguide TM_{01} mode excitation $F(\theta)$ is modified to

$$F(\theta) = \int_{a_1}^{a_3} F(\theta)_{\text{magnetic ring}} \; J_1(ha)\, da$$

$$= F_1(\theta) \int_{a_1}^{a_3} F_2(\theta)\, J_1\,(ha)\, da$$

$$=F_1(\theta)\int_{a_1}^{a_3}\left\{J_o(v_1a_1)Y_1(v_1a)-Y_o(v_1a_1)J_1(v_1a)\right\}\ a\ J_1(ha)da$$

$$=\frac{F_1(\theta)}{v_1^2-h^2}\left[(v_1a_3)J_1(ha_3)\left\{Y_o(v_1a_1)J_o(v_1a_3)-J_o(v_1a_1)Y_o(v_1a_3)\right\}\right.$$

$$\left.+\frac{2}{\pi}J_o(h\ a_1)\left(\frac{h}{v_1}\right)\right],\ \text{for } h\neq v_1. \quad (3.27)$$

$$=.5F_1(\theta)\left[A\ a_3^2\ J_1(ha_3)\left\{-Y_o(ha_1)J_1(ha_3)+J_o(ha_1)Y_1(ha_3)\right\}-\right.$$

$$-\frac{1}{h^2}\left(\frac{2}{\pi}\right)J_o(ha_1)+\left(\frac{a_1}{h}\right)\left(\frac{2}{\pi}\right)J_1(ha_1)$$

$$\left.-\frac{a_3}{h}\ J_o(ha_1)Y_o(ha_3)J_1(ha_3)\right],\ \text{for } h=v_1. \quad (3.28$$

<u>Waveguide Excitation (Waveguide Excited in TE_{01} Mode):</u>

The expression for the radiation pattern of electric ring source in air core having central conductor and surrounded by an annular plasma column is given in equation (3.24). After some simplification it can be put in the form

$$E_\phi(R,\theta) = -\frac{jw\mu}{\pi}\ \underset{\text{Electric ring}}{F'(\theta)}\ \frac{e^{jK_oR}}{R} \quad (3.29)$$

$$\underset{\text{Electric ring}}{F'(\theta)} = F_1'(\theta)\ F_2'(\theta)$$

$$F_1'(\theta)=\frac{(v_2b)\left\{I_1(v_2b)K_o(v_2b)+I_o(v_2b)K_1(v_2b)\right\}}{a_{67}\left\{a_{12}(a_{76}X_1-a_{75}X_2)-a_{11}(a_{76}X_3-a_{75}X_4)\right\}-a_{77}\left\{a_{12}(a_{66}X_1-a_{65}X_2)-a_{11}(a_{66}X_3-a_{65}X_4)\right\}}$$

$$F_2^1(\theta) = a \left\{ J_1(v_1a_1)Y_1(v_1a) - Y_1(v_1a_1)J_1(v_1a) \right\}$$

The corresponding expressions for a_{11}, a_{12}, a_{65}, a_{66}, a_{75}, a_{76}, a_{67}, a_{77}, X_1, X_2, X_3 and X_4 are given in section (3.2.2).

The field in the excitation aperture (i.e. at the cross-section of the open ended waveguide at Z = 0 plane) is assumed to be same as that of the incident wave in the waveguide at Z = 0 plane. The field distribution at the excitation aperture can be considered to be equivalent to the vector sum of electric current rings with various radii ranging from the outer radius of the central conductor to the inner radius of the circular waveguide at the open end cross-section of the circular waveguide. The magnitude of electric current in each ring is considered to be proportional to the value of E_ϕ at that particular location in the waveguide. For circular symmetric TE_{01} mode, E_ϕ is proportional to J_1 (hr), where h, in case of circular symmetric, TE_{01} mode, is given by the first root of J_0' $(ha_3) = 0$, a_3 is the inner radius of the circular waveguide at the open end. The total radiation pattern of open ended waveguide excited in TE_{01} mode with its open end at Z = 0 plane can be obtained as a vector sum of the field components due to individual rings of electric current. In the case of wave guide (TE_{01} mode excitation) F' (θ) is modified to

$$F'(\theta) = \int_{a_1}^{a_3} F'(\theta)_{\text{Electric ring}} \, J_1 \, (ha) \, da$$

$$= F_1'(\theta) \int_{a_1}^{a_3} F_2'(\theta)\, J_1(ha)\, da$$

$$= F_1'(\theta) \int_{a_1}^{a_3} \left\{ J_1(v_1a_1)Y_1(v_1a) - Y_1(v_1a_1)J_1(v_1a) \right\} a\, J_1(ha)\, da$$

$$= \frac{F_1'(\theta)}{v_1^2 - h^2} \Big[(a_3h) J_0(ha_3) \left\{ J_1(v_1a_1)Y_1(v_1a_3) - J_1(v_1a_3)Y_1(v_1a_1) \right\} + \frac{2}{\pi} J_0(ha_1) \Big], \text{ for } h \neq v_1. \quad (3.30)$$

$$F'(\theta) = .5\, F_1'(\theta) \Big[a_3^2 J_0(ha_3) \left\{ Y_0(ha_3)J_1(ha_1) - Y_1(ha_1)J_0(ha_3) \right\} + \frac{a_1}{h}\frac{2}{\pi} J_1(ha_1) - \left(\frac{a_1}{h}\frac{2}{\pi}\right) J_0(ha_1) - \frac{a_3}{h} J_1(ha_1)Y_1(ha_3)J_0(ha_3) \Big],$$

$$\text{for } h = v_1. \quad (3.31)$$

3.4.3 CHARACTERISTICS OF THE RADIATION FIELD:

The radiation patterns (variation of $F(\theta)$ with θ) have been computed with the help of IBM-1130 computer for the waveguide excited in TM_{01} mode with parametric values $K_o b = 6\pi$ $K_o a_1 = .09$, $K_o a_3 = 2.4$, $K_o a_2 = \pi$, $\epsilon_p = .1$, $\epsilon_p = .5$ (see fig. 3.18) and for the waveguide excited in TE_{01} mode with parameteric values $K_o b = 6\pi$, $K_o a_1 = .09$, $K_o a_3 = 3.83$, $K_o a_2 = 1.5\pi$, $\epsilon_p = .1$, $\epsilon_p = .5$ (see fig. 3.23). In all these cases well enhanced and narrow radiation peaks beyond the critical angle ($\sin^2 \theta_c = \epsilon_p$) are formed. The detailed structure of these peaks is shown in fig. (3.19) and fig. (3.24). The effect of different parameters on the shape of the radiation pattern near the radiation peaks is discussed below.

Effect of $K_o b$:

In both the cases (waveguide excited in TM_{o1} mode and TE_{o1} mode) with the increase in the value of $K_o b$ the amplitude of the radiation peaks increases. This behaviour is shown in fig. (3.20) and fig. (3.25).

Effect of $K_o a_3$:

In both the cases (waveguide excited in TM_{o1} and TE_{o1} mode) $K_o a_3$ does not affect the directions of the radiation peaks but affects their amplitudes. Consideration for proper excitation of TM_{o1} mode in circular waveguide limits the value of $K_o a_3$. In circular cylindrical waveguide for TM_{o1} mode the passband extends from $K_o a_3 = 2.4$ to $K_o a_3 = 3.5$ and for TE_{o1} mode the passband extends from $K_o a_3 = 3.83$ to $K_o a_3 = 5.13$. The variation of peak amplitude with $K_o a_3$ ($K_o a_3$ varied only in the passband) is shown in fig. (3.21) and fig. (3.26).

Effect of Plasma density:

Directions of the radiation peaks depend upon the plasma denwity. The location of radiation peaks for different values of ϵ_p (which for constant source frequency, corresponds to different plasma densities) is shown in fig. (3.18) and fig. (3.23).

Effect of $K_o a_2$:

With the increase in the value of $K_o a_2$ (i.e. for thiner annular plasma column) the number of radiation peaks formed beyond the critical angle increases. This is shown in Table (3.4).

***

CHAPTER 4.

EXCITATION OF THREE ANNULAR PLASMA LAYERS OF DIFFERENT PLASMA DENSITIES HAVING CENTRAL CONDUCTOR ALONG ITS AXIS.

CHAPTER 4.

EXCITATION OF THREE ANNULAR PLASMA LAYERS OF DIFFERENT PLASMA DENSITIES HAVING CENTRAL CONDUCTOR ALONG ITS AXIS.

4.1 INTRODUCTION:

Chapter 2 is concerned with the radiation pattern of different circular symmetric sources of electromagnetic waves in plasma column having central conductor along its axis. In these cases enhanced radiation peaks near and before the critical angle are formed. Chapter 3 is concerned with the radiation pattern of different sources in air core having central conductor along its axis and surrounded by an annular plasma column. In this case well enhanced and quite sharp radiation peaks are formed beyond the critical angle. In this geometry, the importance of an air core has been stressed and it is pointed out that air core is mainly responsible for the formation of radiation peaks beyond the critical angle.

In chapter 2, the plasma is assumed to be an isotropic incompressible and homogeneous medium. Practical realization of homogeneous plasma is very difficult. In actual practice the plasma column of radius b having central conductor of radius a_1 will have maximum plasma density near $r = \frac{b}{2}$ and minimum near $r = b$ and $r = a_1$ due to diffusion effects. A practically feasible geometry which is approximately comparable to that of discussed in chapter 2 is a plasma column of three annular layers of different plasma densities having central conductor (shown in fig. 4.1). The relative dielectric constant of 1st layer is higher than that of 2nd layer. Comparing this geometry with that of discussed in chapter 3, we find that first layer corresponds to air core, 2nd layer to annular plasma layer and there is an extra third annular layer surrounding the 2nd layer.

The present study is concerned with the open ended co-axial line excitation and open ended waveguide excitation in 1st layer having central conductor and surrounded by two more annular plasma layers. Following the same lines, as discussed in chapter 2 and 3, the expressions for the radiation pattern of open ended co-axial line excited in TEM mode and open ended waveguide excited in TM_{01} mode in 1st layer having central conductor along its axis and surrounded by two more annular plasma layers have been derived. In both the cases, well enhanced radiation peaks beyond the critical angle corresponding to the plasma layer having least relative dielectric constant, are formed.

4.2 EXCITATION BY OPEN ENDED CO-AXIAL LINE EXCITED IN TEM MODE :

4.2.1 ANALYSIS:

The configuration of the geometry analysed is shown in fig. 4.1. An infinitely long plasma column of radius a_2 and relative dielectric constant ϵ_1 having central conductor of radius a_1 along its axis and surrounded by two more annular plasma layers is located such that its longitudinal axis corresponds to the Z axis of circular cylindrical coordinate system (r, Ø, Z). The second annular plasma layer extends from $r = a_2$ to $r = a_3$ and has its relative dielectric constant as ϵ_2 . The third annular plasma layer extends from $r = a_3$ to $r = b$ and has its relative dielectric constant as ϵ_3 . The source of excitation is an open ended co-axial line excited in TEM mode in 1st plasma column with its open end at Z = 0 plane. The expression for the radiation pattern of magnetic ring source of radius a' in the first plasma column, following the same guide lines as discussed in chapter 2 and 3 can be put in the form:

$$H_\phi (R, \theta) = \frac{j\, w\, \epsilon_1}{\pi} \quad F(\theta) \quad \frac{e^{jK_oR}}{R} \tag{4.1}$$

$$F(\theta) = F_1(\theta)\, F_2(\theta)$$

$$F_1(\theta) = a' \left\{ J_o(v_1 a_1)\, Y_1(v_1 a') - Y_o(v_1 a_1)\, J_1(v_1 a') \right\}$$

$$F_2(\theta) = \frac{(a_{76}\, a_{65} - a_{66}\, a_{55})(a_{87}\, a_{98} - a_{88}\, a_{97})}{a_{11}\left\{(a_{55}\, a_{44} - a_{45}\, a_{54})X_1 - (a_{56}\, a_{44} - a_{46}\, a_{54})\, X_2\right\} - a_{12}\left\{(a_{55}\, a_{43} - a_{45}\, a_{53})X_1 - (a_{56}\, a_{43} - a_{46}\, a_{53})X_2\right\}}$$

$$X_1 = (a_{77}\,a_{66} - a_{67}\,a_{76})(a_{88}\,a_{99} - a_{98}\,a_{89}) -$$
$$-(a_{78}\,a_{66} - a_{68}\,a_{76})\,(a_{87}\,a_{99} - a_{97}\,a_{89}),$$

$$X_2 = (a_{77}\,a_{65} - a_{67}\,a_{75})(a_{88}\,a_{99} - a_{98}\,a_{89}) -$$
$$-(a_{78}\,a_{65} - a_{68}\,a_{75})\,(a_{87}\,a_{99} - a_{89}\,a_{97}),$$

$a_{11} = J_o(v_1 a_1)$, $a_{12} = Y_o(v_1 a_1)$, $a_{43} = J_1(v_1 a_2)$, $a_{44} = Y_1(v_1 a_2)$,

$a_{45} = -J_1(v_2 a_2)$, $a_{46} = -Y_1(v_2 a_2)$, $a_{53} = (v_1 a_2) J_o(v_1 a_2) - J_1(v_1 a_2)$,

$a_{54} = (v_1 a_2) Y_o(v_1 a_2) - Y_1(v_1 a_2)$, $a_{55} = -\left\{\frac{\epsilon_1}{\epsilon_2}(v_2 a_2) J_o(v_2 a_2) - J_1(v_2 a_2)\right\}$,

$a_{56} = -\left\{\frac{\epsilon_1}{\epsilon_2}(v_2 a_2) Y_o(v_2 a_2) - Y_1(v_2 a_2)\right\}$, $a_{65} = J_1(v_2 a_3)$, $a_{66} = Y_1(v_2 a_3)$,

$a_{67} = -J_1(v_2 a_3)$, $a_{68} = -Y_1(v_2 a_3)$, $a_{75} = (v_2 a_3) J_o(v_2 a_3) - J_1(v_2 a_3)$,

$a_{76} = (v_2 a_3) Y_o(v_2 a_3) - Y_1(v_2 a_3)$, $a_{77} = -\left\{\frac{\epsilon_2}{\epsilon_3}(v_3 a_3) J_o(v_3 a_3) - J_1(v_3 a_3)\right\}$,

$a_{78} = -\left\{\frac{\epsilon_2}{\epsilon_3}(v_3 a_3) Y_o(v_3 a_3) - Y_1(v_3 a_3)\right\}$, $a_{87} = J_1(v_3 b)$, $a_{88} = Y_1(v_3 b)$,

$a_{89} = -H_1(v_o b)$, $a_{97} = (v_3 b) J_o(v_3 b) - J_1(v_3 b)$,

$a_{98} = (v_3 b) Y_o(v_3 b) - Y_1(v_3 b)$, $a_{99} = -\left\{\frac{\epsilon_3}{\epsilon_o}(v_3 b) H_o(v_o b) - H_1(v_o b)\right\}$,

$v_o = K_o \cos\theta$, $v_1 = K_o\sqrt{\epsilon_1 - \sin^2\theta}$, $v_2 = K_o\sqrt{\epsilon_2 - \sin^2\theta}$,

$v_3 = K_o\sqrt{\epsilon_3 - \sin^2\theta}$, $K_o^2 = w^2 \mu_o \epsilon_o$.

$F(\theta)$ is a factor which determines the variation of radiation field with θ. $F_1(\theta)$ is independent of the source parameter and $F_1(\theta)$ contains source parameter. The field distribution of an open ended co-axial line at Z = 0 plane can be considered to be equivalent to the vector sum of the magnetic current rings with various radii ranging from the outer radius of the inner conductor to the inner radius of the outer conductor of the co-axial line. The magnitude of the magnetic current in each ring is considered to be proportional to the value of H_ϕ at that particular location in the co-axial line. For the co-axial line, excited in TEM mode, H_ϕ is proportional to $\frac{I_o}{2\pi a'}$ where I_o is the total current in the line. The total radiation pattern of open ended co-axial line with its open end at Z = 0 plane can be obtained as a vector sum of the field components due to individual rings of magnetic current. F(θ) in this case is modified as

$$F(\theta) = \int_1^2 F(\theta)_{\text{Magnetic ring source}} \frac{I_o}{2\pi a'} \, da'$$

where a_1 is the outer radius of the inner conductor, a is the inner radius of the outer conductor of the open ended co-axial line at Z = 0 plane.

It reduces to

$$F(\theta) = \frac{F_2(\theta)\, I_o}{2\, v_1 \pi} \left\{ Y_o(v_1 a_1) J_o(v_1 a) - J_o(v_1 a_1) Y_o(v_1 a) \right\} \qquad (4.2)$$

4.2.2 CHARACTERISTICS OF THE RADIATION FIELD:

Radiation pattern (variation of F(θ) with θ) for different parameters has been computed with the help of IBM-1130 computer. In these computed results the plasma layers are taken to be of equal radial thickness i.e. $K_o a_2 = K_o b/3$, $K_o a_3 = (\frac{2}{3}) K_o b$. The radiation pattern for $K_o b = 6\pi$, $K_o a_1 = .09$, $K_o a = .9$, $\epsilon_1 = .5$, $\epsilon_2 = .1$ and $\epsilon_3 = .5$ is shown in fig. 4.2. In this case we get sharp radiation peaks beyond the critical angle of the layer having least relative dielectric constant.

The detailed structure of these radiation peaks is shown in fig. 4.3. The half power beam width for these radiation peaks is $.06^\circ$ and $.0001^\circ$ respectively. It is expected that with the increase in plasma densities in different layers, the directions of the radiation peaks will change. The effect of different parameters on the shape of the radiation pattern is discussed below.

Effect of $K_o b$:

With the increase in the value of $K_o b$, the amplitudes of the radiation peaks increase. For the sharper radiation peak, formed approximately at 44.2585°, the behaviour is shown in fig. 4.4.

Effect of $K_o a$:

Directions of the radiation peaks do not depend upon $K_o a$. The variation of radiation peak amplitude, formed at

44.2585° with $K_o a$ varied in the allowed limits (for excitation of TEM mode in co-axial line $K_o a < 1$) is shown in fig. 4.5.

4.3 EXCITATION BY OPEN ENDED CIRCULAR WAVEGUIDE EXCITED IN TM_{01} AND TE_{01} MODE:

4.3.1. ANALYSIS:

The configuration of the geometry analysed is shown in figs 4.6. and 4.11 The only difference between the present geometry and the one discussed in section 4.2 is that of the source of excitation. Here, the source of excitation is an open ended circular cylindrical waveguide excited in circular symmetric modes (TM_{01} and TE_{01} mode). The expression for the radiation pattern of magnetic ring source of radius a' in place of open ended waveguide is given in equation 4.1.

Following on the similar lines the expression for the radiation pattern of electric ring source in place of open ended waveguide can be put in the form

$$E_{\phi}(R, \theta) = \frac{jw\mu}{\pi} \quad F'(\theta) \quad \frac{e^{jK_oR}}{R}$$

$$F'(\theta) = F_1'(\theta)\, F_2'(\theta)$$

$$F_1'(\theta) = a' \left\{ J_1(v_1 a_1) Y_1(v_1 a') - Y_1(v_1 a_1)\, J_1(v_1 a') \right\}$$

$$F_2'(\theta) = \frac{(a_{76}\, a_{65} - a_{66}\, a_{55})\,(a_{87}\, a_{98} - a_{88}\, a_{97})}{a_{11} \left\{ (a_{55}\, a_{44} - a_{45}\, a_{54}) X_1 - (a_{56}\, a_{44} - a_{46}\, a_{54}) X_2 \right\} - a_{12} \left\{ (a_{55}\, a_{43} - a_{45}\, a_{53}) X_1 - (a_{56}\, a_{43} - a_{46}\, a_{53}) X_2 \right\}}$$

$$X_1 = (a_{77}\, a_{66} - a_{67}\, a_{76})(a_{88}\, a_{99} - a_{98}\, a_{89}) - (a_{78}\, a_{66} - a_{68}\, a_{76})(a_{87}\, a_{99} - a_{97}\, a_{89}),$$

$$X_2 = (a_{77}\, a_{65} - a_{67}\, a_{75})(a_{88}\, a_{99} - a_{98}\, a_{89}) - (a_{78}\, a_{65} - a_{68}\, a_{75})(a_{87}\, a_{99} - a_{97}\, a_{89}),$$

$a_{11} = J_1(v_1 a_1)$, $a_{12} = Y_1(v_1 a_1)$, $a_{43} = J_1(v_1 a_2)$, $a_{44} = Y_1(v_1 a_2)$,
$a_{45} = -J_1(v_2 a_2)$, $a_{46} = -Y_1(v_2 a_2)$, $a_{53} = (v_1 a_2) J_o(v_1 a_2) - J_1(v_1 a_2)$,
$a_{54} = (v_1 a_2) Y_o(v_1 a_2) - Y_1(v_1 a_2)$, $a_{55} = -\left\{(v_2 a_2) J_o(v_2 a_2) - J_1(v_2 a_2)\right\}$,
$a_{56} = -\left\{(v_2 a_2) Y_o(v_2 a_2) - Y_1(v_2 a_2)\right\}$, $a_{65} = J_1(v_2 a_3)$, $a_{66} = Y_1(v_2 a_3)$,
$a_{67} = -J_1(v2 a_3)$, $a_{68} = -Y_1(v_2 a_3)$, $a_{75} = (v_2 a_3) J_o(v_2 a_3) - J_1(v_2 a_3)$,
$a_{76} = (v_2 a_3) Y_o(v_2 a_3) - Y_1(v_2 a_3)$, $a_{77} = -\left\{(v_3 a_3) J_o(v_3 a_3) - J_1(v_3 a_3)\right\}$,
$a_{78} = -\left\{(v_3 a_3) Y_o(v_3 a_3) - Y_1(v_3 a_3)\right\}$, $a_{87} = J_1(v_3 b)$, $a_{88} = Y_1(v_3 b)$,
$a_{89} = -H_1(v_o b)$, $a_{97} = (v_3 b) J_o(v_3 b) - J_1(v_3 b)$, $a_{98} = (v_3 b) Y_o(v_3 b) - Y_1(v_3 b)$

$a_{99} = -\{(v_3 b) H_0 (v_0 b) - H_1 (v_0 b)\}$, $v_0 = K_0 \cos\theta$, $v_1 = K_0 \sqrt{\epsilon_1 - \sin^2\theta}$,

$v_2 = K_0 \sqrt{\epsilon_2 - \sin^2\theta}$, $v_3 = K_0 \sqrt{\epsilon_3 - \sin^2\theta}$, $K_0^2 = w^2 \mu_0 \epsilon_0$

$F'(\theta)$ is a factor which determines the variation of radiation field with θ. $F_2'(\theta)$ is independent of the source parameter $k_0 a'$ and $F_1'(\theta)$ contains source parameter.

Wave guide Excitation (waveguide excited in TM_{01} mode) :-

The field in the excitation aperture (cross-section of the open ended waveguide at Z = 0 plane) is assumed to be same as that of incident wave in the waveguide at Z = 0 plane. Under these conditions the field distribution at the open end of the waveguide can be considered to be equivalent to the vector sum of magnetic current rings with various radii ranging from the outer radius of the central conductor to the inner radius of the circular waveguide. The magnitude of the magnetic current in each ring is assumed to be proportional to the value of H_ϕ at that particular location in the waveguide. The total radiation pattern of open ended waveguide excited in TM_{01} mode can be obtained as vector sum of field components due to individual rings of magnetic current. In the waveguide for circular symmetric TM_{01} mode, H_ϕ is proportional to $J_1(h\,r)$, where h in the case of circular symmetric TM_{01} mode is given by the first root of $J_0(h\,a) = 0$, a is the inner radius of the waveguide at Z = 0 plane. So in the case of waveguide TM_{01} mode excitation

F(θ) is modified to

$$F(\theta) = \int_{a_1}^{a} F(\theta)_{\text{Magnetic ring}} \; J_1(ha')\, da'$$

$$= \frac{F_2(\theta)}{v_1^2 - h^2} \left[(v_1 a) J_1(ha) \left\{ Y_o(v_1 a_1) J_o(v_1 a) - J_o(v_1 a_1) Y_o(v_1 a) \right\} + \right.$$

$$\left. + \frac{2}{\pi} \left(\frac{h}{v_1} \right) J_o(ha_1) \right] \text{ for } h \neq v_1$$

$$= .5\, F_2(\theta) \left[a^2 J_1(ha) \left\{ J_o(ha_1) Y_1(ha) - Y_o(ha_1) J_1(ha) \right\} - \right.$$

$$- \frac{1}{h^2} \left(\frac{2}{\pi} \right) J_o(ha_1) + \frac{a_1}{h} \frac{2}{\pi} J_1(ha_1) -$$

$$\left. - \frac{a}{h} J_o(ha_1) Y_o(ha) J_1(ha) \right], \text{ for } h = v_1.$$

Waveguide excitation (waveguide excited in TE_{01} mode):

The field in the excitation aperture (i.e. at the cross-section of the open ended waveguide at Z = 0 plane) is assumed to be same as that of the incident wave in the waveguide at Z = 0 plane. The field distribution at the excitation aperture can be considered to be equivalent to the vector sum of electric current rings with various radii ranging from the outer radius of the central conductor to the inner radius of the circular waveguide at the open end cross-section of the circular waveguide. The magnitude of electric current in each ring is considered to be proportional to the value of E_ϕ at that particular location in the waveguide. For circular symmetric TE_{01} mode, E_ϕ is proportional to $J_1(hr)$

where h in case of circular symmetric TE_{01} mode is given by the first root of $J_0'(ha) = 0$, a is the inner radius of the circular waveguide at the open end. The total radiation pattern of open ended waveguide excited in TE_{01} mode with open end at Z = 0 plane is obtained as a vector sum of the field components due to individual rings of electric current. In this case of waveguide in TE_{01} mode excitation F'(θ) is modified to

$$F'(\theta) = \int_{a_1}^{a} F'(\theta)_{\text{Electric ring}} \quad J_1(ha')\,da'$$

$$= \frac{F'_2(\theta)}{v_1^2 - h^2}\left[(ha)J_0(ha)\left\{J_1(v_1a_1)Y_1(v_1a) - J_1(v_1a)Y_1(v_1a_1)\right\} + \left(\frac{2}{\pi}\right) J_1(ha_1)\right], \quad \text{for } h \neq v_1$$

$$= .5\,F'_2(\theta)\left[a^2 J_0(ha)\left\{Y_0(ha)J_1(ha_1) - Y_1(ha_1)J_0(ha)\right\} - \frac{2}{\pi}J_0(ha_1)\left(\frac{a_1}{h}\right) + \left(\frac{2}{\pi}\right)\left(\frac{a_1}{h}\right)J_1(ha_1) - \frac{a}{h}J_1(ha_1)Y_1(ha)J_0(ha)\right], \quad \text{for } h = v_1.$$

4.3.2 CHARACTERISTICS OF THE RADIATION FIELD:

Radiation patterns (variation of F(θ) with θ) have been computed with the help of IBM-1130 computer for the waveguide excited in TM_{01} mode with parametric values $K_0b = 6\pi$, $K_0a_2 = \frac{K_0b}{3}$, $K_0a_3 = K_0b\left(\frac{2}{3}\right)$, $K_0a_1 = .09$,

$K_o a = 2.4$, $\epsilon_1 = .5$, $\epsilon_2 = .1$, $\epsilon_3 = .5$ (see fig. 4.7) and for the waveguide excited in TE_{01} mode with parametric values $K_o b = 6\pi$, $K_o a_2 = \frac{K_o b}{3}$, $K_o a_3 = \frac{2}{3} K_o b$, $K_o a_1 = .09$, $K_o a = 3.83$, $\epsilon_1 = .5$, $\epsilon_2 = .1$, $\epsilon_3 = .5$ (see fig. 4.12). In case of waveguide excited in TM_{01} mode we get two radiation peaks beyond the critical angle corresponding to the layer having least relative dielectric constant. But in case of waveguide excited in TE_{01} mode, only one radiation peak beyond the critical angle corresponding to the layer having least relative dielectric constant is formed. The detailed structure of these radiation peaks is shown is fig. 4.8 and fig. 4.13. Effect of different parameters on the shape of the radiation pattern is discussed below.

Effect of $K_o b$:

In both cases, with the increase in the value of $K_o b$ the amplitude of the radiation peaks increases. This behaviour is shown in fig. 4.3 and in fig. 4.14.

Effect of $K_o a$:

In both the cases (waveguide excited in TM_{01} and TE_{01} mode) $K_o a$ does not affect the directions of the radiation peaks but affects their amplitudes. Consideration for proper excitation of TM_{01} and TE_{01} mode in circular waveguide limits the value of $K_o a$. In circular cylindrical waveguide for TM_{01} mode, the passband extends from K_oa =2.4 to K_oa = 3.5 and for TE_{01} mode the passband extends from K_oa = 3.83 to K_oa = 5.13. The variation of peaks amplitude with K_oa (K_oa varied only in the passband) is shown in fig. 4.10 and fig. 4.15.

***

CHAPTER NO. 5.

Radiation from magnetic ring source in compressible plasma column having central conductor along its axis.

CHAPTER NO. 5.

Radiation from Magnetic Ring Source in Compressible Plasma Column.

5.1 INTRODUCTION:-

The interaction of radiation from an antenna surrounded by a plasma is one of the important recent topics in Physics and Engineering. It is because of its application to satellite-borne antennas used to make measurements within the earth's atmosphere. The radiation pattern of an antenna in free space is entirely different from that of an antenna immersed in plasma environments. The distortion in the radiation pattern of an antenna immersed in plasma due to plasma environment has been widely investigated, but larger number of published work on the studies has been based on the assumption that the plasma is an incompressible isotropic and dielectric medium characterised by the relative dielectric constant $\epsilon_p = \epsilon_0 \left(1 - \frac{w_p^2}{w^2}\right)$. This type of medium does not predict the possibility of excitation of acoustic waves and their coupling with electromagnetic waves.

Now it is well recognised that the finite compressibility of the plasma plays an important role in determining the resultant shape of the radiation pattern of the antenna immersed in plasma. Cohen[24-25] (1962) and other workers (Hessel and Shmoys[26] (1962), Chen[27] (1964), Wait[28] (1964)) have shown that electromagnetic sources placed in a compressible plasma can excite an electroacoustic wave in addition to an electromagnetic (EM) wave. Much work[29-38] has been done in the field of sources immersed in compressible plasma. These studies are mainly concerned with the characteristic performance of antennas and the excitation of acoustic waves along with electromagnetic waves in the plasma itself. Comparitively less work has been done in the direction of excitation of leaky waves or surface waves on compressible plasma geometries. Chen[39] (1965) has given a good discussion on basic equations with source terms in compressible and incompressible plasmas.

Samaddar[5] (1964) discussed the excitation of electro-acoustic and electromagnetic waves on compressible plasma column excited by magnetic ring source in plasma. He hinted the excitation of leaky waves on such a geometry. Chen[40] (1970) found out the radiation pattern of magnetic ring source placed co-axially out side the compressible plasma column.

In this chapter the electromagnetic and plasma waves excited by magnetic ring source in plasma column having central conductor along its axis are discussed. To simplify the mathematics involved, rigid boundary conditions instead of absorptive boundary conditions are used. Source form of Maxwell's equations and linearized hydrodynamic equations of motion for electron are used. It is shown that in this case also, it is possible to separate electromagnetic and electroacoustic modes. Using Fourier transformation and the standard method (saddle point integration) for calculating the far field , it is concluded that the compressibilty of plasma affects the radiation pattern of the magnetic ring source in plasma column having central conductor in a complicated way.

5.2 ANALYSIS:-

The geometry of the configuration analysed is shown in fig. 5.1. An infinitely long plasma column of radius b having infinitely long central conductor of radius a_1 along its longitudinal axis, is oriented with its axis along z- axis of the (r, ∅ , z) cylindrical coordinate system. Source of excitation of electromagnetic waves is a magnetic ring source of radius a ($a_1 < a < b$) and is situated co-axially inside the plasma column at Z = 0 plane. Such a magnetic ring source can mathematically be represented by the relation,

$$\bar{K} = \bar{\varnothing} M \delta (r - a) \delta (z)$$

Where δ represents Kronecker's delta function, $\bar{\varnothing}$ is a unit vector in ∅ direction and M is the amplitude factor.

Assumptions made here are:

(1) Plasma is a continuous neutral fluid of electrons and ions.

(2) Ions are stationary.

(3) Losses due to collisions are negligible.

(4) The plasma obeys the ideal gas laws.

(5) It has adiabatic motion and is stationary as a whole.

(6) Plasma is a compressible fluid and its compressibility is characterised by the nonvanishing perturbed (deviation from the mean) pressure P of the electrons.

(7) Plasma is homogeneous having n_o as electron density and average electron velocity V.

Under these assumptions, on the basis of single- fluid linearized theory (Oster[45] (1960)) for small signals. The following set of linearized equations in the plasma region can be written,

$$\nabla \times E = j\, w\, \mu_o H - \bar{K} \qquad (5.1)$$

$$\nabla \times H = -j\, w \epsilon\, E - e\, n_o\, V \qquad (5.2)$$

$$j\, w\, m\, n_o\, V = n_o\, e\, E + \nabla P \qquad (5.3)$$

$$u^2 m\, n_o \nabla V = j\, w\, P \qquad (5.4)$$

In the above equations e^{-jwt} is assumed as time dependent factor and is ommitted. First two equations are source forms of Maxwell's equations, third one is the linearized hydrodynamic equation of motion of electrons and the fourth one is a linearized combined equation of continuity and the equation of state. Equation from (5.1) to (5.4) can be combined to have the following two homogeneous Helmholtz equations in H and P

$$\nabla^2 \times H + w^2 \mu_o \epsilon_o \epsilon_p H = - j\, w\, \epsilon_o \epsilon_p \bar{K} \qquad (5.5)$$

$$\nabla^2 P + \frac{w^2}{u^2} P = 0 \qquad (5.6)$$

The total electric field E can be written as a sum of a solenoidal vector E_e and an irrotational vector E_p (Cohen 1965) as,

$$E = E_e + E_p \tag{5.7}$$

$$E_e = \frac{j}{w\, \epsilon_o \epsilon_p} \nabla \times H \tag{5.8}$$

$$E_p = \frac{e}{w^2 m\, \epsilon_o \epsilon_p} \nabla P \tag{5.9}$$

here, E_e corresponds to electromagnetic modes and E_p corresponds to plasma modes (acoustic modes).

So we have,

(a) In plasma region;

(i) Electromagnetic mode

$$\frac{d^2 H_\phi}{d r^2} + \frac{1}{r} \frac{d H_\phi}{d r} + \frac{d^2 H_\phi}{d z^2} + \left(w^2 \mu_o \epsilon_o \epsilon_p - \frac{1}{r^2} \right) H_\phi$$

$$= - j\, w \epsilon_o \epsilon_p K \tag{5.10}$$

$$E_{ez} = \frac{j}{w\, \epsilon_o\, \epsilon_p} \left(\frac{d H_\phi}{d r} + \frac{H_\phi}{r} \right) \tag{5.11}$$

(ii) Plasma mode

$$\frac{d^2 P}{d r^2} + \frac{1}{r} \frac{d P}{d r} + \frac{d^2 P}{d z^2} + \frac{w^2}{u^2} \epsilon_p \quad P = 0 \tag{5.12}$$

$$E_{pz} = \frac{e}{w^2\, m\, \epsilon_o \epsilon_p} \frac{dP}{dz} \tag{5.13}$$

(b) In free region

$$\frac{d^2 H_\phi}{d r^2} + \frac{1}{r} \frac{d H_\phi}{d r} + \frac{d^2 H_\phi}{d z^2} \left(w^2 \mu_o \epsilon_o - \frac{1}{r^2} \right) H_\phi = 0 \qquad (5.14)$$

$$E_z = \frac{j}{w \epsilon_o} \left(\frac{d H_\phi}{d r} + \frac{H_\phi}{r} \right) \qquad (5.15)$$

Equations (5.10), (5.12) and (5.14) can be solved with the help of integral transforms. Let the Fourier transform of G (r, Z) be defined as,

$$\bar{G} (r, \xi) = \int_{-\infty}^{\infty} G (r, Z) e^{-j \xi Z} dZ \qquad (5.16)$$

and its inverse transform be given by the relation

$$G (r, Z) = \frac{1}{2 \pi} \int_{-\infty}^{\infty} \bar{G} (r, \xi) e^{j \xi Z} dZ \qquad (5.17)$$

Applying Fourier transformation to equation (5.10) to (5.15) we get

(a) In plasma region;

(i) Electromagnetic mode

$$\frac{d^2 \bar{H}_\phi}{d r^2} + \frac{1}{r} \frac{d \bar{H}_\phi}{d r} + \left(v_1^2 - \frac{1}{r^2} \right) \bar{H}_\phi = -j w \epsilon_o \epsilon_p \bar{M} \delta (r-a) \qquad (5.18)$$

the source variation δ (z) vanishes because

$$\int_{-\infty}^{\infty} \delta(z) e^{-j \xi Z} d Z = 1$$

$$\bar{E}_{ez} = \frac{j}{w \epsilon_o \epsilon_p} \left[\frac{d \bar{H}_\phi}{d P} + \frac{\bar{H}_\phi}{P} \right] \qquad (5.19)$$

Where $v_1^2 = w^2 \mu_o \epsilon_o \epsilon_p - \xi^2$ (5.20)

(ii) Plasma mode

$$\frac{d^2\bar{P}}{d\,r^2} + \frac{1}{r}\,\frac{d\,\bar{P}}{d\,r} + v_p^2\,\bar{P} = 0 \qquad (5.21)$$

$$\bar{E}_{pz} = \frac{j\,e\,\xi}{w^2\epsilon_o\epsilon_p m_o}\,\bar{P} \qquad (5.22)$$

$$\text{where } v_p^2 = \frac{w^2}{u^2}\,\epsilon_p - \xi^2 \qquad (5.23)$$

(b) In free space

$$\frac{d^2\bar{H}_\phi}{d\,r^2} + \frac{1}{r}\,\frac{d\,\bar{H}_\phi}{d\,r} + \left(v_o^2 - \frac{1}{r^2} \right) \bar{H}_\phi = 0 \qquad (5.24)$$

$$\bar{E}_z = \frac{j}{w\,\epsilon_o}\left[\frac{d\,\bar{H}_\phi}{d\,r} + \frac{\bar{H}_\phi}{r} \right] \qquad (5.25)$$

$$\text{where } v_o^2 = w^2\,\mu_o\epsilon_o - \xi^2 \qquad (5.26)$$

These equations are considered to be ordinary differential equations with ξ as a parameter constant. The important equations are (5.18), (5.21) and (5.24). All other vectors of the waves can be easily derived from $\bar{H}_\phi$ and $\bar{P}$. The boundary conditions on $\bar{H}_\phi$ and $\bar{P}$ follow from the boundary conditions on their respective inverse Fourier transforms. Taking into account the proper boundary conditions on H_ϕ and its derivative with respect to r, the solution for $\bar{H}_\phi$ in free space is obtained. Its inverse Fourier transform H_ϕ gives the radiation field in free space.

Computation of Boundary Value Problem:-

Consider the inhomogeneous differential equation (5.18). The delta function is related by the relation

$$\delta (r - a) = 0 \text{ for } r \neq a$$
$$= 1 \text{ for } r = a$$

For all values of r other than r = a the equation (5.18) reduces to a homogeneous differential equation

$$\frac{d^2 \bar{H}_\phi}{d r^2} + \frac{1}{r} \frac{d \bar{H}_\phi}{d r} + (v_1^2 - \frac{1}{r^2}) \bar{H}_\phi = 0 \qquad (5.27)$$

The delta function $\delta (r - a)$ imposes boundary condition on $\bar{H}_\phi$ which must be satisfied at r = a. Multiplying equation (5.18) by dr, integrating over the interval 2Δ from $a - \Delta$ to $a + \Delta$, assuming the continuation of $\bar{H}_\phi$ at r = a and taking limit as $\Delta \rightarrow 0$ we have

$$\left. \frac{d \bar{H}_\phi}{d r} \right|_{a - \Delta}^{a + \Delta} = - j w \epsilon_0 \bar{M} \qquad (5.28)$$

The remaining boundary conditions on $\bar{H}_\phi$ follow from the boundary conditions imposed on H_ϕ and its derivative by Maxwell's equations, Hydrodynamic equation of motion, equation of comtinuity and the equation of state. As shown in fig.(5.1), the whole region is devided into three regions, the region between $r = a_1$ to r = a is denoted as region I, between r = a to r = b as region II and the region for r > b as region III.

The solutions of equation (5.27) and (5.21) in the region I are given as,

$$\bar{H}_\phi = A_1 J_1 (v_1 r) + B_1 Y_1 (v_1 r) \qquad (5.29)$$

$$\bar{P} = A_1^I J_0 (v_p r) + B_1^I Y_0 (v_p r) \qquad (5.30)$$

In the region II as,

$$\bar{H}_\phi = A_2 J_1 (v_1 r) + B_2 Y_1 (v_1 r) \tag{5.31}$$

$$\bar{P} = A_1^I J_o (v_p r) + B_1^1 Y_o (v_p r) \tag{5.32}$$

In the region III also taking into account the radiation condition on $\bar{H}_\phi$, the solutions for $\bar{H}_\phi$ and $\bar{P}$ can be written as

$$\bar{H}_\phi = A_3 H_1 (v_o r) \tag{5.33}$$

$$\bar{P} = 0 \tag{5.34}$$

At the boundaries of these three regions the transformed quantities obey the following conditions:

(1) (a) At $r = a_1$ (conductor surface), the tangential component of the electric field is continuous

$$\bar{E}_{ez}(a_1^+) + \frac{j e \xi}{w^2 m \epsilon_o \epsilon_p} \bar{P} (a_1^+) = 0 \tag{5.35}$$

(b) At $r = a_1$ (conductor surface) the normal component of the electron velocity is zero (because of the rigid boundary condition assumed)

$$\frac{d \bar{P} (a_1^+)}{dr} + \frac{n_o e \xi}{w \epsilon_o \epsilon_p} \bar{H}_\phi (a_1^+) = 0 \tag{5.36}$$

2. (a) At $r = a$ (magnetic ring source), one is already mentioned boundary condition (equation No. 5.28), namely.

$$\left. \frac{d \bar{H}_\phi}{d r} \right|_{a - \Delta}^{a + \Delta} = - j w \epsilon_o \bar{M} \tag{5.37}$$

(b) $\bar{H}_{\phi}$ is continuous at r = a

which gives

$$\bar{H}_{\phi}(a^-) = \bar{H}_{\phi}(a^+) \tag{5.38}$$

3. (a) At r = b (Boundary of plasma column), continuation of the tengential components of the electric and magnetic fields gives,

$$\bar{E}_{ez}(b^-) + \frac{i\, e\, \xi}{w^2 m\, \epsilon_o \epsilon_p}\, \bar{P}(b^-) = \bar{E}_z(b^+) \tag{5.39}$$

$$\bar{H}_{\phi}(b^-) = \bar{H}_{\phi}(b^+) \tag{5.40}$$

(b) At r = b (Boundary of plasma column), the normal component of the electron velocity is zero (because of the rigid boundary conditions assumed) giving

$$\frac{d\, P(b^-)}{d\, r} + \frac{n_o\, e\, \xi}{w\, \epsilon_o}\, \bar{H}_{\phi}(b^-) = 0$$

Applying all these boundary conditions on the solution for different regions we have,

$$\frac{v_1 a_1}{w\, \epsilon_o \epsilon_p}\left(A_1 J_o(v_1 a_1) + B_1 Y_o(v_1 a_1)\right) + \frac{e\, \xi\, a_1}{w^2 m\, \epsilon_o \epsilon_p}$$

$$\left(A_1' J_o(v_p a_1) + B_1^1 Y_o(v_p a_1)\right) = 0 \tag{5.41}$$

$$\frac{a_1 n_o e \xi}{w\, \epsilon_o}\left(A_1 J_1(v_1 a_1) + B_1 Y_1(v_1 a_1)\right) -$$

$$(v_p a_1)\left(A_1^1 J_1(v_p a_1) - B_1^1 Y_1(v_p a_1)\right) = 0 \tag{5.42}$$

$$A_1 J_1(v_1 a) + B_1 Y_1(v_1 a) - A_2 J_1(v_1 a) -$$

$$- B_2 Y_1(v_1 a) = 0 \qquad (5.43)$$

$$A_1((v_1 a) J_0(v_1 a) - J_1(v_1 a)) + B_1((v_1 a) Y_0(v_1 a) -$$

$$- Y_1(v_1 a)) - C_2((v_1 a) J_0(v_1 a) - J_1(v_1 a)) -$$

$$- D_2((v_1 a) Y_0(v_1 a) - Y_1(v_1 a)) = j\, w \epsilon_0 \xi \bar{M}\, a \qquad (5.44)$$

$$- A_1^1 (v_p b) J_1(v_p b) - B_1^1 (v_p b) Y_1(v_p b) +$$

$$+ \frac{n_0 e \xi b}{w \epsilon_0} (C_2 J_1(v_1 b) + D_2 Y_1(v_1 b)) = 0 \qquad (5.45)$$

$$\frac{1}{w \epsilon_0 \epsilon_p} (A_2 (v_1 b) J_0(v_1 b) + B_2 (v_1 b) *$$

$$* Y_1(v_1 b)) + \frac{e \xi b}{w^2 m \epsilon_0 \epsilon_p} (A_1^1 J_0(v_p b) + B_1^1 Y_0(v_p b)) -$$

$$- \frac{1}{w \epsilon_0} A_3 (v_0 b) H_0(v_0 b) = 0 \qquad (5.46)$$

$$A_2 J_1(v_1 b) + B_2 Y_1(v_1 b) - A_3 H_1(v_0 b) = 0 \qquad (5.47)$$

There are seven equations involving seven constants. Solving these equations for A_3 we have:

$$A_3 = \frac{N}{D}$$

$$N = \frac{j\,2\,w\epsilon_0 M e \xi a_1 n_o}{\pi \epsilon_0^2 \epsilon_p W^2} \Big[Y_1(v_1 b)\Big\{\big((v_1 a)J_o(v_1 a) - J_1(v_1 a)\big)X_7 - $$

$$- \frac{n_o e \xi b}{w \epsilon_o} J_1(v_1 b)X_8 + \frac{e \xi b}{w^2 m \epsilon_o \epsilon_p} *$$

$$* J_o(v_p b)X_9\Big\} - J_1(v_1 b) *$$

$$* \Big\{-\big((v_1 a) Y_o(v_1 a) - Y_1(v_1 a)\big)X_7 -$$

$$- \frac{n_o e \xi b}{w \epsilon_o} Y_1(v_1 b)X_8 + \frac{e \xi b}{w^2 m \epsilon_o \epsilon_p} Y_o(v_p b)X_9\Big\}\Big]$$

$$D = \frac{w^4 \pi \epsilon_o^4 \epsilon_p^3}{2 n_o e \xi a_1 (v_1 a_1)^2 J_o^2(v_1 a) X_1} \Big[\frac{1}{w\epsilon_o}(v_o b) H_o(v_o b)\Big\{Y_1(v_1 b)X_{10} -$$

$$- J_1(v_1 b)X_{11}\Big\} + H_1(v_o b) *$$

$$* \Big\{X_{10} X_{12} - \frac{X_{13} X_{11}}{X_1(X_4 X_1 - X_3 X_2)}\Big\}\Big]$$

$$X_1 = \frac{2 a_1^2 \xi^2 e^2 n_o}{\pi w^4 m \epsilon_o^3 \epsilon_p^2} \quad J_o(v_p a_1) J_1(v_1 a) + \left(\frac{v_1 a_1}{w \epsilon_o \epsilon_p}\right) *$$

$$* \Big\{Y_1(v_1 a) J_o(v_1 a_1) - Y_o(v_1 a_1) J_1(v_1 a)\Big\} * \Big\{\left(\frac{(v_p a_1)(v_1 a_1)}{w \epsilon_o \epsilon_p}\right) *$$

$$* J_1(v_p a_1) J_o(v_1 a_1) + \frac{e^2 \xi^2 a_1^2 n_o}{w^3 m \epsilon_o^2 \epsilon_p} J_o(v_p a_1) J_1(v_1 a)\Big\}$$

$$X_2 = \frac{2\, a_1^2\, \xi^2\, e^2\, n_o}{\pi\, w^4\, m\, \epsilon_o^3\, \epsilon_p^2}\; J_o(v_p a_1) \left\{(v_1 a)\, J_o(v_1 a) - J_1(v_1\, a)\right\} -$$

$$-\left(\frac{v_1\, a_1}{w\, \epsilon_o\, \epsilon_p}\right)\left\{J_o(v_1 a_1)\left((v_1 a)\, Y_o(v_1 a) - Y_1(v_1 a)\right) - Y_o(v_1 a_1) *\right.$$

$$\left. *\left((v_1\, a) J_o(v_1 a) - J_1(v_1\, a)\right)\right\} * \left\{\left(\frac{(v_p\, a_1)\;(v_1\, a_1)}{w\;\; \epsilon_o\, \epsilon_p}\right) *\right.$$

$$\left. * J_1(v_p\, a_1)\, J_o(v_1 a_1) + \frac{e^2\, \xi^2\, a_1^2\, n_o}{w^3\, m\, \epsilon_o^2\, \epsilon_p}\; J_o(v_p\, a_1)\, J_1(v_1\, a_1)\right\}$$

$$X_3 = \frac{2\, a_1^2\, \xi^2\, e^2\, n_o}{\pi\, w^4\, m\, \epsilon_o^3\, \epsilon_p^2}\; Y_o\,(v_p\, a_1)\, J_1(v_1\, a) - \left(\frac{v_1\, a_1}{w\, \epsilon_o \epsilon_p}\right) *$$

$$* \left\{J_o(v_1 a_1)\, Y_1(v_1 a) - Y_o(v_1 a_1) J_1(v_1 a)\right\} * \left\{\left(\frac{(v_p a_1)\;(v_1\, a_1)}{w\;\; \epsilon_o\, \epsilon_p}\right) *\right.$$

$$\left. * J_o(v_1 a_1)\, Y_1(v_p a_1) - \frac{e^2\, \xi^2\, a_1^2\, n_o}{w^3\, m\, \epsilon_o^2 \epsilon_p}\; J_1(v_1 a_1)\, Y_o(v_p a_1)\right\}$$

$$X_4 = -\, \frac{e\, \xi\, a_1}{w^2\, m \epsilon_o \epsilon_p}\, Y_o(v_p a_1) \left\{(v_1 a)\, J_o(v_1 a) - J_1(v_1\, a)\right\} *$$

$$* \left(\frac{-2\, a_1\, n_o\, \epsilon\, \xi}{\pi\, w^2\, \epsilon_o^2\, \epsilon_p}\right) - \left(\frac{v_1\, a_1}{w \epsilon_o \epsilon_p}\right) * \left\{J_o(v_1 a_1)\left((v_1 a)\;\; Y_o(v_1\, a) -\right.\right.$$

$$\left.\left. - Y_1(v_1 a)\right) - Y_o(v_1 a_1)\left((v_1 a)\, J_o(v_1 a) - J_1(v_1\, a)\right)\right\} *$$

$$* \left\{\frac{(v_p a_1)\;(v_1 a_1)}{w\, \epsilon_o\, \epsilon_p}\;\; J_o(v_1 a_1)\, Y_1(v_p a_1) - \left(\frac{e^2\;\; \xi^2 a_1^2\;\; n_o}{w^3\, m\;\; \epsilon_o^2\;\; \epsilon_p}\right) *\right.$$

$$\left. * J_1(v_1 a_1)\, Y_o(v_p\, a_1)\right\}$$

$$X_5 = \frac{2 e^2 a_1^2 \xi^2 n_o}{w^4 m \epsilon_o^3 \epsilon_p^2 \pi} J_o(v_p a_1)\left((v_1 a) J_o(v_1 a) - J_1(v_1 a)\right) +$$

$$+ \frac{v_1 v_p a_1^2}{w \epsilon_o \epsilon_p} J_1(v_p a_1) J_o(v_1 a_1) + \frac{e^2 \xi^2 a_1^2 n_o}{w^3 m \epsilon_o^2 \epsilon_p} *$$

$$* J_o(v_p a_1) J_1(v_1 a_1)\left(\frac{v_1 a_1}{w \epsilon_o \epsilon_p}\right) * \Big(J_o(v_1 a_1)\big((v_1 a) Y_o(v_1 a) -$$

$$- Y_1(v_1 a)\big) - Y_1(v_1 a_1)\big((v_1 a) J_o(v_1 a) - J_1(v_1 a)\big)\Big)$$

$$X_6 = \frac{2 e^2 a_1^2 \xi^3 n_o}{w^4 m \epsilon_o^3 \epsilon_p^2 \pi} Y_o(v_p a_1)\left((v_1 a) J_o(v_1 a) - J_1(v_1 a)\right) -$$

$$- \Big\{ \frac{v_1 v_p a_1^2}{w \epsilon_o \epsilon_p} Y_1(v_p a_1) J_o(v_1 a) - \frac{e^2 \xi^2 a_1^2 n_o}{w^2 m \epsilon_o^2 \epsilon_p} Y_o(v_p a_1) J_1(v_1 a_1)$$

$$* \left(\frac{v_1 a_1}{w \epsilon_o \epsilon_p}\right) * \big\{ J_o(v_1 a_1)\big((v_1 a) Y_o(v_1 a) - Y_1(v_1 a)\big) -$$

$$- Y_o(v_1 a_1)\big((v_1 a) J_o(v_1 a) - J_1(v_1 a)\big)\big\}$$

$$X_7 = \frac{(v_p b)(v_1 b)}{w \epsilon_o \epsilon_p} \left\{ J_o(v_1 b) Y_1(v_p b) - J_1(v_p b) Y_o(v_1 b) \right\}$$

$$X_8 = \frac{v_1 b}{w \epsilon_o \epsilon_p} \left\{ J_o(v_1 b) X_5 - J_o(v_1 b) X_6 \right\}$$

$$X_9 = \frac{w^3 \epsilon_o^3 \epsilon_p^2 \pi}{2 a_1^2 v_1 n_o e \xi J_o(v_1 a_1)} \Big\{ (v_p b) J_1(v_p b) X_6 -$$

$$- (v_p b) Y_1(v_p b) X_5 \Big\}$$

$$X_{10} = (X_4 X_1 - X_3 X_2) \left\{ \frac{n_o e \xi b}{w \epsilon_o} \quad J_1 (v_1 b) X_1 + J_1(v_1 a)(v_p b) * \right.$$

$$\left. * J_1(v_p b) J_o (v_1 a_1) \left(\frac{-2v_1 a_1^2 n_o e \xi}{w^3 \pi \epsilon_o^3 \epsilon_p^3} \right) \right\} -$$

$$- \left\{ \left((v_1 a) J_o(v_1 a) - J_1 (v_1 a) \right) X_1 + J_1(v_1 a) X_2 \right\} *$$

$$* \left\{ - (v_p b) Y_1 (v_p b) X_1 + (v_p b) J_1 (v_p b) X_3 \right\} *$$

$$* J_o (v_1 a_1) \left(\frac{-2v_1 a_1^2 n_o e \xi}{w^3 \pi \epsilon_o^3 \epsilon_p^2} \right)$$

$$X_{11} = (X_4 X_1 - X_3 X_2) \left\{ \frac{n_o e \xi b}{w \epsilon_o} \quad Y_1(v_1 b) X_1 + Y_1(v_1 b) * \right.$$

$$\left. * (v_p b) J_1(v_p b) J_o (v_1 a_1) \left(\frac{-2 v_1 a_1^2 n_o e \xi}{w^3 \pi \epsilon_o^3 \epsilon_p^2} \right) \right\} -$$

$$- \left\{ \left((v_1 a) Y_o (v_1 a) - Y_1 (v_1 a) \right) X_1 + Y_1 (v_1 a) X_2 \right\} *$$

$$* \left\{ (-v_p b) Y_1 (v_p b) X_1 + (v_p b) (J_1(v_p b) X_3 \right\}$$

$$* J_o (v_1 a_1) \left(\frac{-2 v_1 a_1^2 n_o e \xi}{w^2 \pi \epsilon_o^3 \epsilon_p^2} \right)$$

$$X_{12} = \frac{1}{X_1(X_4 X_1 - X_3 X_2)} \Bigg[(X_4 X_1 - X_3 X_2) \Bigg\{ \frac{e\, \xi\, b}{w^2 m\, \epsilon_0 \epsilon_p} X_1 *$$

$$* Y_0(v_p b) + \frac{1}{w\, \epsilon_0 \epsilon_p} (v_1 b) J_0(v_1 b) Y_1(v_1 a) *$$

$$* \left(\frac{-2 v_1 a_1^2 n_0 e \xi}{w^2 \pi \epsilon_0^3 \epsilon_p^2} J_0(v_1 a_1) \right) \Bigg\} - \Bigg\{ \frac{1}{w\, \epsilon_0 \epsilon_p} (v_1 b) Y_0(v_1 b) X_1 -$$

$$- \frac{1}{w\, \epsilon_0 \epsilon_p} (v_1 b) J_0(v_1 b) X_3 \Bigg\} * \Bigg| \left(Y_1(v_1 a) - (v_1 a) Y_0(v_1 a) \right) X_1 +$$

$$+ Y_1(v_1 a) X_2 \Bigg\} \left(\frac{-2 v_1 a_1^2 n_0 e \xi}{w^2 \pi \epsilon_0^3 \epsilon_p^2} J_0(v_1 a_1) \right) \Bigg]$$

$$X_{13} = (X_4 X_1 - X_3 X_2) \Bigg\{ \frac{e\, \xi\, b}{w^2 m\, \epsilon_0 \epsilon_p} J_0(v_p b) X_1 + J_1(v_1 a)(v_p b) *$$

$$* J_1(v_1 a_1) \left(\frac{-2 v_1 a_1^2 n_0 e \xi}{w^3 \pi \epsilon_0^3 \epsilon_p^2} \right) \Bigg\} - \Big\{ \big((v_1 a) J_0(v_1 a) - J_1(v_1 a) \big) X_1 + J_1(v_1 a) X_2 \Big\} *$$

$$* \Bigg\{ \frac{v_1 b}{w\, \epsilon_0 \epsilon_p} Y_0(v_1 b) X_1 - \frac{v_1 b}{w\, \epsilon_0 \epsilon_p} J_0(v_1 b) X_2 \Bigg\} *$$

$$* J_0(v_1 a_1) \left(\frac{-2 v_1 a_1^2 n_0 e \xi}{w^2 \pi \epsilon_0^3 \epsilon_p^2} \right)$$

Therefore the solution in free space is given as

$$\bar{H}_\phi (r, \xi) = A_3 H_1 (v_0 r) \tag{5.48}$$

The radiation field in free space can be found out by taking the inverse Fourier Transform of $\bar{H}_\phi$ as shown

$$H_\phi (r, Z) = \frac{1}{2\pi} \int_{-\infty}^{\infty} A_3 H_1(v_0 r) e^{j \xi Z} d\xi \tag{5.49}$$

5.3 SURFACE WAVE AND RADIATION FIELD:-

To evaluate the integral of equation (5.49), it is first necessary to examine the nature and location of the singularities of the integrand in the complex ξ plane. The variables v_1 and v_p which appear in the integrand of equation (5.49), are multiple valued functions in the neighbourhood of $\xi = \pm k_0\sqrt{\epsilon_p}$ and $\xi = \pm \omega\sqrt{\epsilon_p}\, U^{-1}$.

It can be shown by expanding the integrand about $\xi = \pm k_0\sqrt{\epsilon_p}$ and $\xi = \pm \omega\sqrt{\epsilon_p}\, U^{-1}$ that it is an even function of v_1 and v_p. However, since Hankel functions have a logarithmic singularity at the origin $\xi = \pm k_0$. $\xi = \pm k_0$ are branch points of the integrand contributing to the radiation field. Poles of the integrand are those values of ξ (hence the value of v_1, v_p and v_0) for which the denominator D (ξ) vanishes. The residues at these poles contribute to the surface waves which can be guided by the plasma column. The general expression for the surface- wave fields, H_ϕ (r, Z) which propagate in the positive Z direction in the region $r \geq b$ is given by

$$H_\phi (r, Z) = \sum_{s} \frac{N(\xi_s)\, H_1(v_{0s} r)\, e^{j\xi_s z}}{\left.\frac{\partial D(\xi)}{\partial \xi}\right|_{\xi = \xi_s}} \qquad \text{for } r \geq b,\ z > 0.$$

Leaky wave is faster than light wave in free space. It continuously radiates energy. It corresponds to a complex transverse wave number even if the medium is lossless. For leaky wave, the wave number ξ which is a root of equation $D(\xi) = 0$ is also complex. If one can compute the location of these leaky poles with the help of equation $D(\xi) = 0$ then leaky wave field can be computed just like that of surface waves.

For leaky wave poles, it is difficult to solve equation $D(\xi) = 0$ which involves Bessel and Hankel functions with complex arguments. Numerical methods may be helpful in solving equation $D(\xi) = 0$ for leaky wave poles.

Let us focus our attention again on integral of equation (5.49). Consider this integral as contour integral in ξ plane. Introduce the transformation,

$$\xi = k_o \sin\psi$$
$$\psi = \tau + j\lambda \qquad (5.50)$$

This transformation transforms the region of integration in ξ plane into a strip in the ψ plane, which is bounded by two curved lines corresponding to the branch cuts in the ξ plane. The branch cuts in ψ plane are given by,

$$\sin\tau \, \cosh\lambda = \pm 1$$

This transformation yields,

$$v_o = K_o \cos\psi$$
$$v_1 = K_o\sqrt{\epsilon_p - \sin^2\psi}$$

In order to shift from cylindrical coordinate system (r, ϕ , Z) to spherical coordinate system (R, θ, ϕ) introduce the transformation

$$r = R \cos \theta$$
$$Z = R \sin \theta \tag{5.51}$$

Taking appropriate value of Hankel function in the integrand of equation (5.49) for large value of R, namely,

$$H_1(v_o R \cos \theta)\, e^{j \xi Z} \simeq e^{-j\left(\frac{3\pi}{4}\right)} \left[\frac{2}{\pi K_o R \cos\theta \cos\psi}\right]^{1/2} e^{jK_o R \cos(\psi - \theta)} \tag{5.52}$$

we have

$$H_{\phi} = \left(\frac{2 K}{R \cos \theta}\right)^{1/2} e^{-j(3\pi/4)} \int_c \cos \psi \; A_3 \, e^{jK_o R \cos(\psi - \theta)} d\psi \tag{5.53}$$

The saddle point of integral of equation (5.53) is given by

$$\frac{d}{d \psi} \cos (\psi - \theta) = 0$$

Which gives $\psi = \theta$ as a saddle point. The steepest descent path (S. D. P.) is given by the constant phase of the exponential factor of the integrand of equation (5.53) and is to pass through the saddle point. So we have

$\mathrm{Im} \left[j \cos (\psi - \theta)\right]$ = constant and is to pass through $\psi = \theta$ which gives

$$\cos (\tau - \theta) = 0$$

part contributed by leaky wave poles on the path of integration and a radiation part arising from the branch points of the integrand. In the near field the contribution due to surface wave and leaky waves is dominant and in the far field radiation part is dominant. Compa-ring equation(5.54) with equation (2.16), it follows that the compressibility of the plasma affects the radiation pattern in a complicated way.

Applying the standard method of saddle point integration (see Appendix A), the lowest order approximation of the integral is given as

$$(R, \theta) \approx \frac{2 A_3^1}{\pi} \frac{e^{ikR}}{R} \tag{5.54}$$

...med value of A_3 , i. e. , to say ... of A_3 at $\psi = \theta$.

This gives the radiation field in free space. In this analysis it has been assumed that leaky wave poles are not very close to the saddle point. In case they are very close to the saddle point, special care must be taken to include their effect on the asymptotic evaluation.

5.4 DISCUSSION:-

Inside the plasma column both electromagnetic and electroacoustic modes can be excited and they are mutually coupled. Compressibility of the plasma gives rise to acoustic waves and the boundary conditions tries to couple electromagnetic and electroacoustic waves. In this analysis regid boundary conditions are assumed which is a special case of more appropriate absorptive boundary conditions. Outside the plasma column the field consists of three parts, a surface wave part, contributed by the surface wave poles on the path of integration, leaky wave part contributed by leaky wave poles on the path of integration and a radiation part arising from the branch points of the integrand. In the near field the contribution due to surface wave and leaky waves is dominant and in the far field radiation part is dominant. Compa-ring equation(5.54) with equation (2.16), it follows that the compressibility of the plasma affects the radiation pattern in a complicated way.

CHAPTER NO. 6.

Summary, concluding remarks and suggestions for further work.

6.1 Summary.

6.2 Concluding remarks.

6.3 Suggestions for further work.

CHAPTER 6.

SUMMARY, CONCLUDING REMARKS AND SUGGESTIONS FOR FURTHER WORK.

6.1 SUMMARY:

The radiation pattern of a magnetic ring source in a plasma column having central conductor along its axis has been studied. Plasma is considered to be an isotropic, Incompressible and homogeneous medium characterised by a relative dielectric constant given by the relation $\epsilon_r = 1 - \frac{w_p^2}{w^2}$, where w is the source frequency and w_p is the plasma frequency. Source form of the Maxwell's equations is used. Differential equation is solved by applying the method of integral transforms yielding the solution for the field in the form of a definite integral. The radiation pattern is obtained by the usual method of saddle point integration. In this case the radiation peak before and near the critical angle is formed. The effect of different parameters on the radiation pattern of a magnetic ring source in a plasma column having central conductor along its axis is discussed in section 2.1 of chapter 2. On the same guide lines the radiation pattern of an electric ring source in a plasma column having central conductor along its axis has been studied in section 2.2 of the second chapter. Here, more than one radiation peaks before the critical angle are formed. Beyond the critical angle the radiation field falls off rapidly. In the magnetic ring source excitation as well as in electric ring source excitation the importance of the central conductor has been emphasized. In both the cases of ring source excitation, it is found that the decrease in the value of the radius of the central conductor for constant source frequency gives rise to stronger radiation peaks before the critical angle. The speculation that the absence of the central conductor in plasma column may give rise to strongest radiation peak before the critical angle is not correct. The expression for the radiation pattern of a ring source in a plasma column can not be deduced from that of the ring source in a plasma column having central conductor along its axis simply by putting zero in place of a_1 (radius of central conductor) in the latter expression. The very presence of the central conductor changes the form of boundary conditions to be satisfied at the surface of the central conductor. In both the cases of the ring source excitation it is also found that the radius of the ring source does not affect the directions of the radiation peaks but affects their amplitude. The more practically feasible case of co-axial line excitation has also been discussed in section 2.3 of chapter 2. The field distribution at the excitation aperture (at the open end of the co-axial line in the plasma column having central conductor and excited in TEM mode) is considered to be equivalent to the vector sum of magnetic current rings with various radii ranging from the outer radius of the central conductor to the inner radius of the outer conductor of the co-axial line at its open end. The magnitude of magnetic current in each ring is considered to be equivalent to the value of H_{ϕ} at that particular location in the co-axial line. The total radiation pattern is obtained as a vector sum of field components due to individual rings of magnetic curre-nt. In this study of the radiation pattern of open ended co-axial line excited in TEM mode in plasma column having central conductor along its axis, it is found that a radiation peak near and before the critical angle is formed. The amplitude of this radiation peak increases with the increase in the inner radius of the outer conductor of co-axial line at the open end. Another practically convenient case of waveguide excitation (waveguide excited in circular symmetric mode i.e. TM_{01} and TE_{01} mode in a plasma column having central conductor along its axis) has also been studied in section 2.4 of chapter 2. Here also it is found that radiation peak near and before the critical angle is formed. Its amplitude increases with the increase in the inner radius of the waveguide at the open end. In all these cases (magne-tic ring source excitation, electric ring source excitation, co-axial line excitation in TEM mode and waveguide excitation in TM_{01} and TE_{01} mode in plasma column having central conductor), it is found that the direction of the radiation peak formed near and before the critical angle can be changed by changing the plasma density.

The radiation pattern of a magnetic ring source in air core having central conductor along its axis and surrounded by an annular plasma column has been discussed in section 3.1 of chapter 3. In this case well enhanced radiation peaks beyond the critical angle are formed. Number of radiation peaks formed depends upon $K_o b$, $K_o a_2$ and $K_o a_1$. $K_o a$ does not affect the directions of the radiation peaks but affects their amplitude. On the similar lines the expression for the radiation pattern of a electric ring source in air core having central conductor and surrounded by an annular plasma column has been derived. In this case also well enhanced radiation peaks beyond the critical angle are formed. The number of radiation peaks depends upon $K_o b$, $K_o a_1$ and $K_o a_2$. $K_o a$ does not affect the directions of the radiation peaks but affects their amplitude. This is discussed in section 3.2 of chapter 3. In both of these cases (magnetic ring source excitation and electric ring source axcitation), the directions of the radiation peaks can be changed by changing the plasma density of the plasma column. The importance of the central conductor and air core has been emphasized. It is pointed out that the air core is mainly responsible for the formation of well enhanced radiation peaks beyond the critical angle. The more practically convenient cases of co-axial line (excited in TEM mode) excitation and waveguide (excited in circular symmetric modes i.e. TM_{01} and TE_{01} mode) excitation has also been discussed.

The expression for the radiation pattern of the magnetic ring source in a plasma column having central conductor and surrounded by two more annular plasma columns has been derived in chapter 4. On the similar lines the expression for the radiation pattern of electric ring source in plasma column having central conductor and surrounded by two more annular plasma column has also been derived. Practically convenient cases of co-axial line (excited in TEM mode) excitation and waveguide (excited in circular symmetric modes i.e. TM_{01} and TE_{01} mode) excitation have been discussed. In case of co-axial line excitation and waveguide excitation, radiation peaks beyond the critical angle, corresponding to the layer having lest relative dielectric constant, are formed.

The expression for the radiation pattern of the magnetic ring source in a compressible plasma column having central conductor along its axis has been derived in chapter 5. It is shown that the finite compressibility of the plasma gives rise to the excitation of acoustic waves in the plasma. The compressibility of the plasma affects the radiation pattern of the magnetic ring in plasma column having central conductor along its axis in a complicated way.

6.2 CONCLUDING REMARKS:

The work reported in this thesis is mainly concerned with the radiation pattern characteristics of different sources in different plasma geometries. Attempt has been made in the direction of selecting practically feasible geometries with proper parametric values, excited by practically convenient sources of electromagnetic waves so as to give well enhanced radiation peaks in their radiation pattern. The study of the radiation patterns of circular symmetric sources (magnetic ring source, electric ring source, co-axial line excited in TEM mode, waveguide excited in TM_{01} and TE_{01} mode) in air core having central conductor and surrounded by an annular plasma column reveals the emergence of well enhanced and quite sharp radiation peaks beyond the critical angle corresponding to the annular plasma layer. But the angle through which the directions of these radiation peaks can be changed by changing the plasma density is quite small as compared to that of the case discussed in chapter 2. The most promising case from practical point of view with an eye on having larger scanning angle seems to be that of co-axial line excitation in a plasma column having central conductor along its axis. Based upon these results it is suggested to develop an electronically scannable narrow beam plasma antenna system. The direction of the radiation peak can be changed by changing the plasma density. A d.c. discharge can be used to generate the plasma column and its density can be changed by changing the plasma current. Different circular symmetric sources (magnetic current ring, electric current ring, open ended co-axial line excited in TEM, open ended circular waveguide excited in TM_{01} and TE_{01} modes) of electromagnetic waves can be used as source of excitation. The field distribution ($\delta(r-a)\,\delta(z)$) of a magnetic ring source can physically be approximated by a co-axial line excited in the TEM mode and tapered to a narrow annular aperture. In case of an open ended co-axial line excitation the inner conductor of the co-axial line can be extended to serve as a central conductor. Special care should be taken in the case of waveguide excitation. The central conductor should be introduced in such a way so as not to disturb the field configuration at the open end of the open ended waveguide. It is suggested that the central conductor should be tapered, small portion of the tapered pin should go inside the waveguide and it should attain its required dimensions near the open end of the open ended waveguide. The experimental results may not axactly agree with the corresponding theoretical results. It is because, the radial variation of plasma density, and the effect of plasma container (glass insulation) have not been taken into account in the theoretical analysis. The plasma state can also be simulated with the help of the artificial dielectrics[41].

In solids[42], the plasma state can be achieved by an injection process and the plasma density can be varied by varying the injection current.

6.3 SUGGESTIONS FOR FURTHER WORK:

In all the geometries considered, the radiation peaks formed in the radiation patterns of corresponding sources are expected to be due to the excitation of leaky waves on the plasma surfaces. It is proposed to do theoretical analysis of calculating radiation field from the near field consideration of properly excited leaky waves by Kirchoff Huygen integration method. For this purpose, first the location of leaky wave poles is to be calculated. Analytical calculation for the location of leaky wave poles is difficult because of the involvement of Bessel functions with complex agruments. Numerical methods may be helpful in calculating the location of leaky wave poles.

In all the cases considered, plasma is assumed to be a homogeneous medium. In practice it is not possible to achieve a homogeneous plasma medium. The radial variation of plasma density should be taken into account. The plasma density is minimum near the walls of the container. It is suggested to calculate the radiation pattern of circular symmetric source in n annular plasma layers of different densities.

Then the limiting case (with $n \to \infty$ and thickness of different annular layers $\to 0$) will be the expression for the radiation pattern of the circular symmetric source in continuous plasma column having central conductor along its axis.

The temperature effect (compressibility) of plasma state should also be taken into account in all geometries. In chapter 5, rigid boundary conditions have been assumed. It is suggested to do the analysis with actual absorptive boundary conditions.

Throughout this present study plasma is assumed to be an isotropic medium, An-isotropy introduced due to the earth's magnetic field in the plasma formed around space vehicle should also be taken into account.

The theoretical analysis of the waveguide having holes on its surface and containing plasma should be done. This geometry is expected to give rise to leaky wave radiation peaks, and the directions of these radiation peaks may be changed by changing the plasma density. For obtaining a radiation pattern with a limited extent in a-Zimuthal plane, it is necessary to excite a dipolar or multipolar mode on the plasma column. Excitation of these higher order modes on the plasma column could be studied both theoretically and experimentally.

On the basis of presented theoretical results and guidelines it is suggested to do experimental work. In order to observe experimentally the excitation of leaky waves on the surfaces of already discussed configurations it is suggested to simulate ideal plasma medium[44] (i.e. an incompressible isotropic medium having uniform plasma density).

REFERENCES

1. Harris, J. H. (1963), "RADIATION THROUGH CYLINDRICAL PLASMA SHEATHS", J. Res. NBS 67D(Radio Prop.), No. 6, 717.

2. Harris, J. H., A. T. Villeneuve, and L. A. Bsoca (1965), "RADIATION FROM PLASMA ENCLOSED CYLINDRICAL HYPERSONIC VEHICLES", Radio Sci., J. Res. NBS 69D, No. 10, 1335.

3. Tamir, T., and A. A. Oliner (1962), "THE INFLUENCE OF COMPLEX WAVES ON THE RADIATION FIELD OF A SLOT EXCITED PLASMA LAYER", IRE Trans. Ant. Prop. AP-10, No. 1, 55.

4. Gupta, K. C. (1970), "A MULTIPLE NARROW BEAM ANTENNA SYSTEM USING A COLUMN OF ISOTROPIC PLASMA", Int. J. Electronics, 29, 45.

5. Samaddar, S. N. and M. Yildiz (1964), "EXCITATION OF COUPLED ELECTRO-ACOUSTICAL WAVES BY A RING SOURCE IN A COMPRESSIBLE PLASMA CYLINDER", Canadian Journal of Physics , Vol. 42, 638.

6. Bachynski, M. P. (1967), "SOURCES IN PLASMA" R.C. A., Review, 28, 111.

7. Seshadri, S. R. (1965), "RADIATION FROM AN ELECTRIC DIPOLE IN A PLASMA COLUMN", Proc. I.E.E., 112, 249.

8. Seshadri, S. R. (1965), "RADIATION FROM AN ELECTRIC DIPOLE IN AN INFINITE COLUMN OF WARM PLASMA", Proc. I.E.E., 112, 1279.

9. Yip, G. L. and S. R. Seshadri (1967), "SURFACE WAVES ALONG AN AXIALLY MAGNETIZED PLASMA COLUMNS", Canadian Journal of Physics, Vol. 45, 2889.

10. Tamir, T. and A. A. Oliner (1963), "THE SPECTRUM OF ELECTROMAGNETIC WAVES GUIDED BY A PLASMA LAYER", Proc. I.E.E.E., 51, 317.

11. Harris , J. H. (1968), "LEAKY WAVE BEAMS OF MULTIPLY LAYERED PLASMA MEDIA", Radio Sci. Vol. 3, 181.

12. Zucker, F. J. (1954), "THE GUIDING AND RADIATION OF SURFACE WAVES", Proc. Symp. on Modern Advances in Microwave Techniques, Polytechnic Institute of Brookly, New York, 403.

13. Rumsey, V. H. (1953), "THEORY OF TRAVELLING WAVE SLOT ANTENNAS", J. Appl. Phys., 24, 1358.

14. Goldstone, L. O. and A. A. Oliner (1959), "LEAKY WAVE ANTENNA PART 1- RECTANGULAR WAVEGUIDES", I.R.E. Ant. and Prop. Trans. AP-7, 307.

15. Goldstone, L.O. and A. A. Oliner (1961), "LEAKY WAVE ANTENNAS PART II- CIRCULAR WAVEGUIDE", I.R.E. Trans. Ant. Prop. AP-9, 280.

16. Marcuvitz, N. (1959), "ON FIELD REPRESTATIONS IN TERMS OF LEAKY MODES OR EIGEN MODES", I.R.E. Trans. Ant. Prop. AP-4, 192.

17. Collin, R. E. (1962), "ANALYTICAL SOLUTION FOR A LEAKY WAVE ANTENNA", I.R.E. Trans. Ant. Prop. AP-10, 561.

18. Hessel, A. (1962), "ON THE INFLUENCE OF COMPLEX POLES ON THE RADIATION PATTERN OF LEAKY WAVE ANTENNAS", I.R.E. Trans. Ant. Prop. AP-10, 646.

19. Jasik, H. (1961), "ANTENNA ENGINEERING HAND BOOK", McGraw-Hill Book Co; Inc., New York, N.Y. 16.

20. Meltz, G. and R. A. Shore (1965), "LEAKY WAVES SUPPORTED BY UNIAXIAL PLASMA LAYERS", I.E.E.E. Trans. Ant. Prop. AP-13, 94.

21. Honey, R. C. (1959), "A FLUSH MOUNTED LEAKY WAVE ANTENNA WITH PREDICTABLE PATTERNS", I.R.E. Trans. Ant. Prop. AP-7, 320.

22. Laxpati, S. R. (1965), "ENERGY CONSIDERATIONS IN OPEN AND CLOSED WAVEGUIDES", I.E.E.E. Trans. Ant. Prop. AP-13, 883.

23. Gupta, K. C. and R. K. Garg (1971), "ANTENNA USING CYLINDRICAL COLUMNS OF ISOTROPIC PLASMA", Research Report I.I.T., Kanpur/E E/71.

24. M. H. Cohen (1962) "RADIATION IN A PLASMA II", Phys. Rev., Vol. 126, p. 389.

25. M. H. Cohen, (1962), "RADIATION IN A PLASMA III," METAL BOUNDARIES, Phys. Rev. Vol. 126, p. 398.

26. Hessel, A., and J. Shmoys (1962), "EXCITATION OF PLASMA WAVES IN A HOMOGENEOUS ISOTROPIC PLASMA BY A DIPOLE", Proceedings of the symposium on electromagnetics and fluid dynamics of gases plasma, 173-184 (Polytechnic Press, Brooklyn, N. Y.).

27. Chen, K. M. (1964), "INTERACTION OF A RADIATING SOURCE WITH A PLASMA", Proc. I.E.E. Vol. 111, p. 1668.

28. Wait, J. R. (1964), "THEORY OF A SLOTTED SPHERE ANTENNA IMMERSED IN A COMPRESSIBLE PLASMA PART I AND PART II", Radio Sci. J. Research N.B.S. Vol. 68D, p. 127.

29. J. R. Wait, (1964-1965), "ON RADIATION OF ELECTROMAGNETIC AND ELECTROACOUSTIC WAVES IN A PLASMA", Appl. Sci. Research, Sec B, Vol. 11, p. 423.

30. J. R. Wait (1965), "ON RADIATION OF ELECTROMAGNETIC AND ELECTROACOUSTIC WAVES IN PLASMA PART II", Appl. Sec. Research Sec B Val. 12, p. 130.

31. J. R. Wait, and K. P. Spies (1966), "THEORY OF A SLOTTED SPHERE ANTENNA IMMERSED IN A COMPRESSIBLE PLASMA PART III", Radio Science, Vol. 1, p. 21.

32. J. R. Wait, (1966), "RADIATION FROM A SPHERICAL APERTURE ANTENNA IMMERSED IN A COMPRESSIBLE PLASMA", I.E.E.E. Trans. Ant. Prop. AP- 14, p. 360.

33. Wait, J. R. (1965), "WAVES CIRCULATING AROUND A RIGID CYLINDRICAL OBSTACLE IN A COMPRESSIBLE PLASMA", Radio Sci., J. Research NBS, Vol. 69D, p. 567.

34. Cook, K. R. and B. C. Edgar, (1966), "CURRENT DISTRIBUTION AND IMPEDANCE OF A CYLINDRICAL ANTENNA IN AN ISOTROPIC COMPRESSIBLE PLASMA", Radio Sci. Vol. 1, p. 13.

35. Langeliar, R. M. and F. V. Schultz, (1966), "RADIATION FROM A VERTICAL DIPOLE IN A WARM PLASMA PARTS I AND II", I.E.E.E. Trans. Ant. Prop. Vol. AP-14, p. 207.

36. Kuehl, H. H. (1966), "RESISTANCE OF A SHORT ANTENNA IN A WARM PLASMA", Radio Sci. Vol. 1, p. 971-

37. Lin, S. H. and K. K. Mei, (1968), "NUMERICAL SOLUTIONS OF DIPOLE RADIATION IN A COMPRESSIBLE PLASMA", I.E.E.E. Trans. Ant. Prop. Vol. 1 , p. 235.

38. Lin, S. H. and K. K. Mei (1970), "ON THE EFFECT OF SHEATH COLLISION AND ABSORPTIVE SURFACE ON THE PERFORMANCE OF A LINEAR ANTENNA IN A COMPRESSIBLE PLASMA", I.E.E.E. Trans. Ant. Prop. Vol. AP- 18, p. 672.

39. Chen, K. M. (1965), "DISCUSSION ON BASIC EQUATIONS WITH SOURCE TERMS IN COMPRESSIVE AND INCOMPRESSIBLE PLASMA", Radio Sci. J. Research , NBS, Vol. 69D, No. 2.

40. Cheng, D. K. and H. C. Chen (1970), "RADIATION FROM A RING SOURCE AROUND A COMPRESSIBLE PLASMA COLUMN", App. Sci. Res. 22, 259.

41. Rotman, W. (1962), "PLASMA SIMULATION BY ARTIFICIAL DIELECTRICS AND PARALLEL- PLATE MEDIA", I.R.E. Trans. Ant. Prop. AP- 10, 82.

42. Chynoweth, A. G. and S. J. Bachsbaum (1965), "SOLID STATE PLASMA", Physics Today 18, No. 11, 26.

43. Brekhovskikh, L. M. (1960), "WAVES IN LAYERED MEDIA", Academic Press Inc. 264.

44. Tyras, G., P.C. Bargeliotes., J.M. Hamm., R.R. Schell. (1965), " AN EXPERIMENTAL STUDY OF PLASMA SHEATH EFFECTS ON ANTENNAS." Radio Science J. Res. NBS/USNC-URSI Vol. 69 D, No. 6, 839.

45. Oster, L. (1960), " LINEARIZED THEORY OF PLASMA OSCILLATIONS." Rev. Mod. Phys. 32, 141.

APPENDIX A.

STEEPEST DESCENT METHOD:

Representation in the steepest descent plane involves a transformation

$$\xi = K_o \operatorname{Sin} \psi \qquad (A.1)$$

with

$$\psi = \tau + j\lambda \qquad (A.2)$$

This transformation will map the two-sheeted ξ-plane into a connected strip of the ψ-plane as shown in fig. A.2. The path of integration about the branch-cut in ξ-plane then maps into the path P in the ψ-plane. The path of integration is next deformed into the path of steepest descent, shown as SDP in fig. A.2, its equation is given by

$$\operatorname{Re} \operatorname{Cos} (\psi - \theta) = \operatorname{Cos} (\tau - \theta) \operatorname{Cosh} \lambda = 1 \qquad (A.3)$$

The latter path goes through the 'saddle point' at $\psi = \theta$, θ being a polar angle. For integration over the SDP, the integral may be written as

$$G_s(R, \theta) = F(\psi) \exp jK_oR \operatorname{Cos} (\psi - \theta) \; d\psi \qquad (A.4)$$

To evaluate this integral we choose a transformation

$$\operatorname{Cos} (\psi - \theta) = 1 + ju^2 \qquad (A.5)$$

where u is purely real. The integration will now run along the real values of u ($-\infty < u < \infty$) and Eq. (A.4) is transformed as

$$G_s(R, \theta) = \int_{-\infty}^{\infty} L(u) \exp (-K_o R u^2) du \qquad (A.6)$$

where

$$L(u) = F (\psi) \exp (jK_o R) d\psi /du$$

For $K_o R \gg 1$ assuming that L(u) is a well-behaved and slowly-varying function, the integral is given by the asymplotic approximation as,

$$G_s(R, \theta) \sim (\pi /K_o R)^{1/2} L(u) \Big|_{u = 0}$$

At u = 0, $\psi = \theta$, we have

$$\frac{d\psi}{du}\Big|_{u=0} = - \frac{2ju}{\sin(\psi - \theta)}\Big|_{u=0} = - \frac{2j}{\frac{d\psi}{du}\Big|_{u = 0}}$$

Hence

$$\frac{d\psi}{du}\Big|_{u = 0} = (-2j)^{1/2}$$

Making these substitutions,

$$G_s(R, \theta) \sim (2\pi/K_oR)^{1/2} F(\theta) \exp\{j(K_oR - \pi/4)\}, \quad F(\theta) \neq 0 \tag{A.7}$$

If however, $F(\theta) = 0$ at $\theta = \theta_o$, $L(u)$ is expanded first in a Taylor's series in the neighbourhood of $u = 0$.

$$L(u) = u\, L'(0) + \frac{u^2}{2} L''(0)$$

$$G_s(R, \theta) = \frac{L''(0)}{4}\left\{\pi/(K_oR)^3\right\}^{1/2} + O(K_oR)^{-5/2}$$

Evaluating the second derivative of $L(u)$

$$L''(u) = \exp(jK_oR)\left[F''(\psi)\left(\frac{d\psi}{du}\right)^3 + 3F'(\psi)\frac{d\psi}{du}\frac{d^2\psi}{du^2} + F(\psi)\frac{d^3\psi}{du^3}\right]$$

At $u = 0$, $\psi = \theta_o$, $F(\theta_o) = 0$ and $\frac{d^2\psi}{du^2} = 0$, only the first terms remains. Substituting of $\frac{d\psi}{du} = (-2j)^{1/2}$ yields,

$$G_s(R, \theta) \sim \tfrac{1}{2}\left\{2\pi/(K_oR)^3\right\}^{1/2} F''(\theta_o) \exp\{j(K_oR + \pi/4)\}, \quad F(\theta_o) = 0 \tag{A.8}$$

This analysis is valid when the leaky wave poles are not very close to the saddle point. If leaky wave poles are located very close to the saddle point then the saddle point integration method is to be modified to include their effect[43].

LIST OF PUBLICATIONS

1. Dhani Ram, J. S. Verma, "Electronically Scannable Narrow Beam Plasma Antenna System", accepted for publication in International Journal of Electronic (U.K.) 28th August,'71.

2. Dhani Ram, J. S. Verma, "Electronically Scannable Plasma Leaky Wave Antenna System", Journal of the Institution of Telecommunication Engineers, April, 1972.

3. Dhani Ram, J. S. Verma, "An Antenna System Using a Plasma Column having a Central Conductor & Excited by a Co-axial Line", accepted for publication in International Journal of Electronic (U.K.) 11th Jan., 1972.

4. Dhani Ram, J. S. Verma, "Electronically Scannable Narrow Beam Antenna System Using Isotropic Plasma Column having Central Conductor along the axis and Excited by Magnetic Ring Source", accepted for publication in Indian Journal of Pure and Applied Physics, 6th March, 1972.

5. Dhani Ram, J. S. Verma, "An Antenna System Using a Plasma Column Having a Central Conductor and Excited by W Wave Guide", Communicated the revised version of the manuscript for publication in Radio Science Journal of Research (U.S.A.) Nov., 1972.

6. Dhani Ram, J. S. Verma, "Multiple Narrow Beam Plasma Antenna System", presented in the Symposium on Sattellite and Space Communication on 11th Nov., 1971 at Poon and to be published in the Journal of Telecommunication Engineers (Special issue).

7. Dhani Ram, J. S. Verma, "An Antenna System Using a Plasma Column having a Central Conductor Excited by a Wave-guide (TM_{01} mode) to be presented in 60th Session of Indian Science Congress, 3 Jan. 1972 at Punjab University, Chandigarh.

8. Dhani Ram, J. S. Verma,"Electronically Scannable Narrow Beam Antenna System Using Isotropic Plasma Column having Central Conductor along the Axis and Excited by Electric Ring Source" Communicated for publication in Journal of Telecommunication Engineers, Dec., 1972.

9. Dhani Ram, J. S. Verma, "Radiation Pattern of Magnetic Ring Source in Compressible Plasma Column having Central Conductor along its axis, Accepted for presentation in the Symposium on Aeronomy and Radio Propagation to be held at N.P.L. Delhi on Feb., 19-23, 1973.

***

TABLE - 3.1

ϵ_b	$K_o b$	$K_o a_1$	$K_o a$	$K_o a_2$	Directions of Radiation peaks θ_p
.5	6π	.09	1.5714	5.8927	52.51687 83.51868
,,	,,	,,	,,	10.2141	49.55429 67.28225 36.302662
,,	,,	,,	,,	12.1783	55.56629 70.87025 86.91994

TABLE - 3.2

$K_o b$	$K_o a_1$	$K_o a$	$K_o a_2$	Direction of Radiation peaks θ_p
6π	.09	1.5714	5.8927	58.0528 86.10072
,,	,,	,,	10.2141	53.04579 72.43154 87.84455
,,	,,	,,	14.5354	50.58629 65.15399 77.84514 88.52340

TABLE - 3.3

ϵ_r	$K_o b$	$K_o a_z$	Direction of Radiation peaks
.1	5	2.54 3.36 4.18	71.1899 76.365 79.4791
5	5	2.54 3.36 4.18	75.9079 79.2919 82.0159
.1	10	4.54	27.0929 80.2622
		6.36	48.3451 83.3269
		8.18	28.9099 58.8921 54.9609
.5	10	4.54	81.6177
		6.36	54.8849 84.0044
		8.18	62.3914 85.4172
.1	15	6.54	49.6937 83.5312
		9.36	37.9899 63.1334 85.6550
		12.18	30.9829 52.5169 69.7399 86.7489
.5	15	6.54	55.5718 84.1631
		9.36	65.2831 85.9535
		12.18	55.7259 70.9313 86.9272

.1	20	8.54	31.0075 60.2879 85.1912
		12.36	31.9101 53.1366 70.0481 86.8005
		16.18	32.5443 49.2139 62.7378 74.9400 87.6158
.5	20	8.54	63.0100 85.5527
		12.36	56.0554 71.1459 86.9669
		16.18	62.7379 75.5490 87.7113

TABLE - 3.4

For waveguide excited in TM_{01} mode.

	$K_0 b$	$K_0 a_3$	$K_0 a_2$	Direction of radiation peaks θ_p
.5	6	2.4	6.5142	55.4539 84.1399
			10.6284	50.9099 68.1449 86.4181
			14.7426	48.5639 62.4678 74.1569 87.4789

Waveguide excited in TE_{01} mode

.5	6	3.83	7.5867	69.0911
			11.3434	59.9277 76.1022
			15.1001	54.5569 67.8743 79.5745

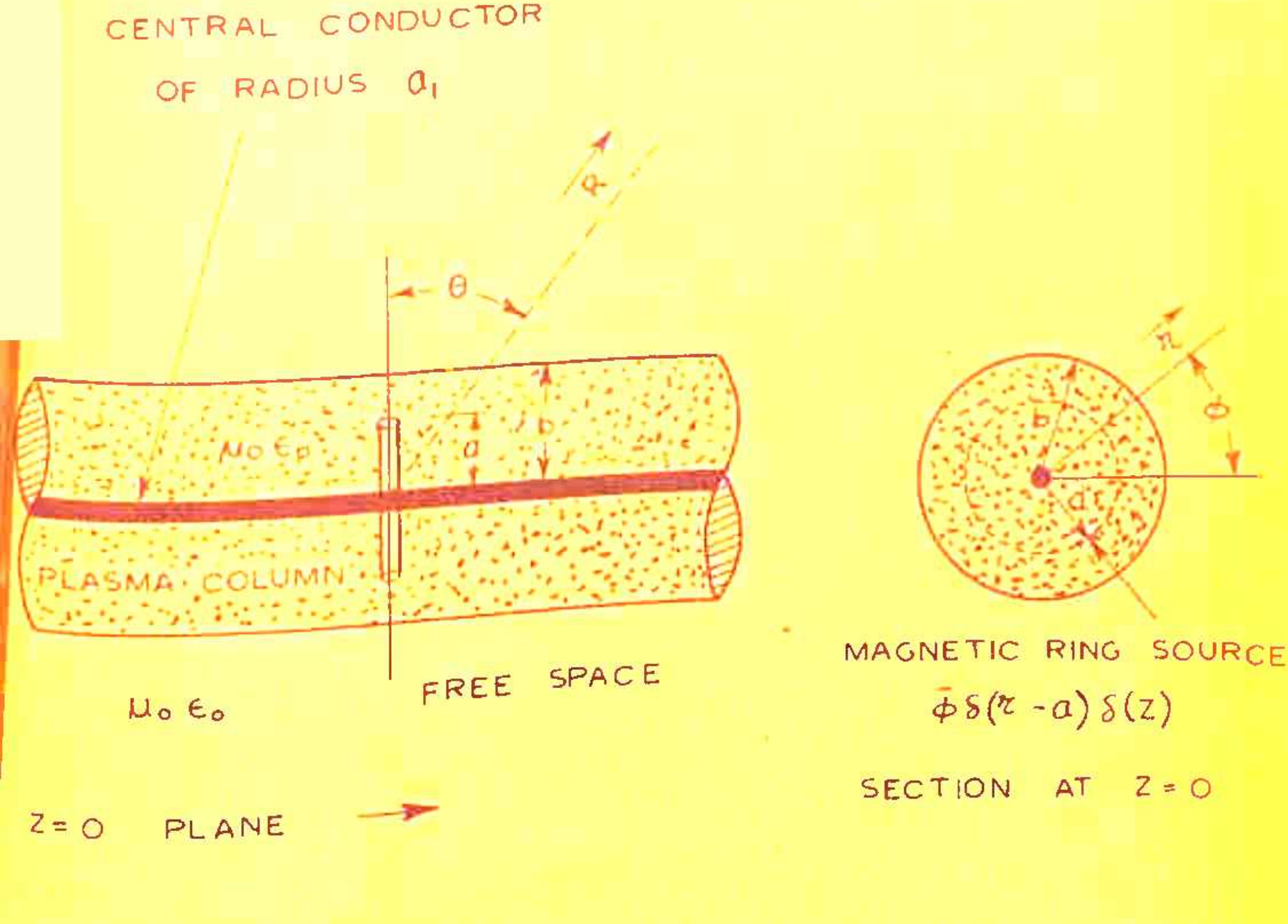
CENTRAL CONDUCTOR
OF RADIUS a_1
$\mu_0 \epsilon_p$
PLASMA COLUMN
FREE SPACE
$\mu_0 \epsilon_0$
Z = 0 PLANE
MAGNETIC RING SOURCE
$\bar{\phi}\delta(r-a)\delta(z)$
SECTION AT Z = 0

FIG. - 2·1

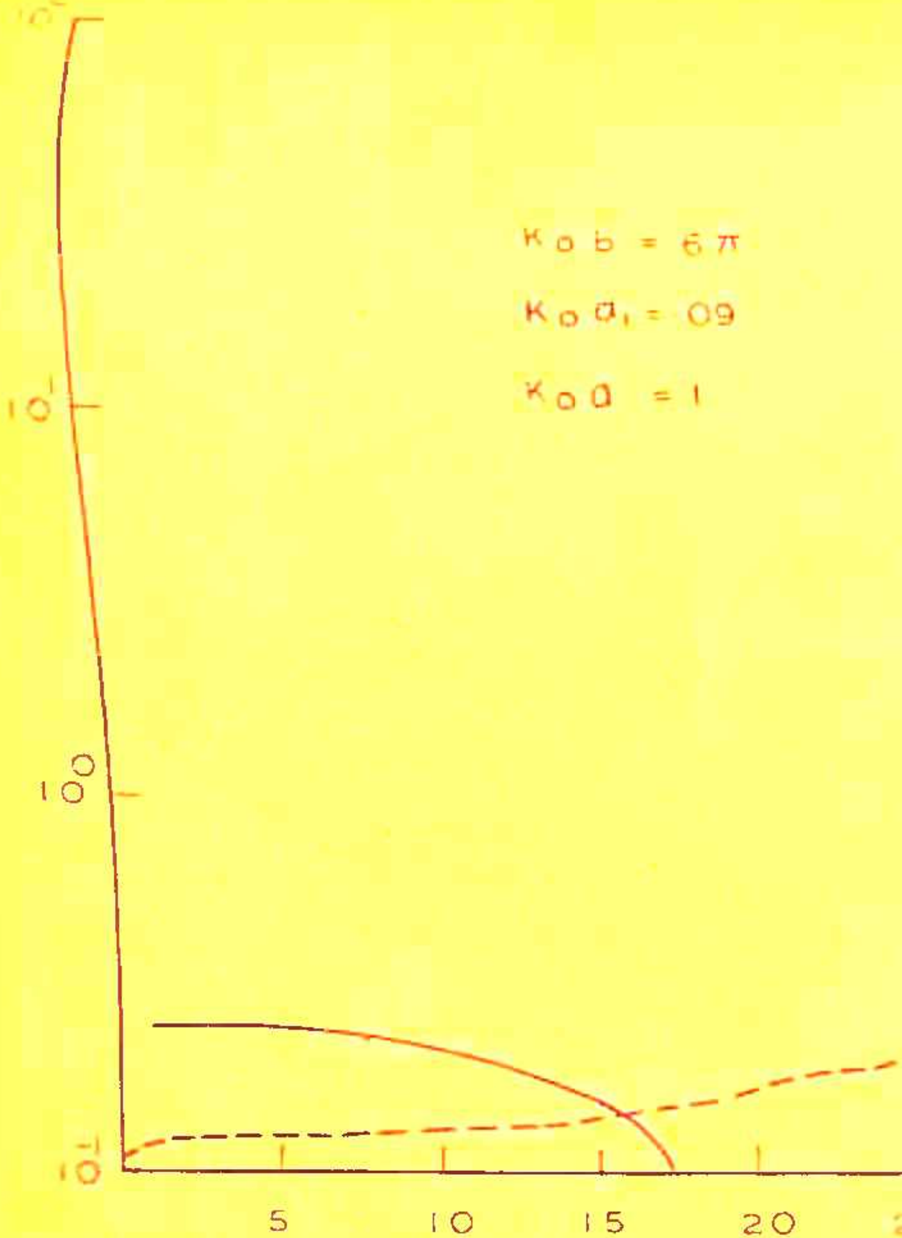

10^2
10^1
10^0
10^{-1}
$K_0 b = 6\pi$
$K_0 a_1 = .09$
$K_0 a = 1$
5
10
15
20

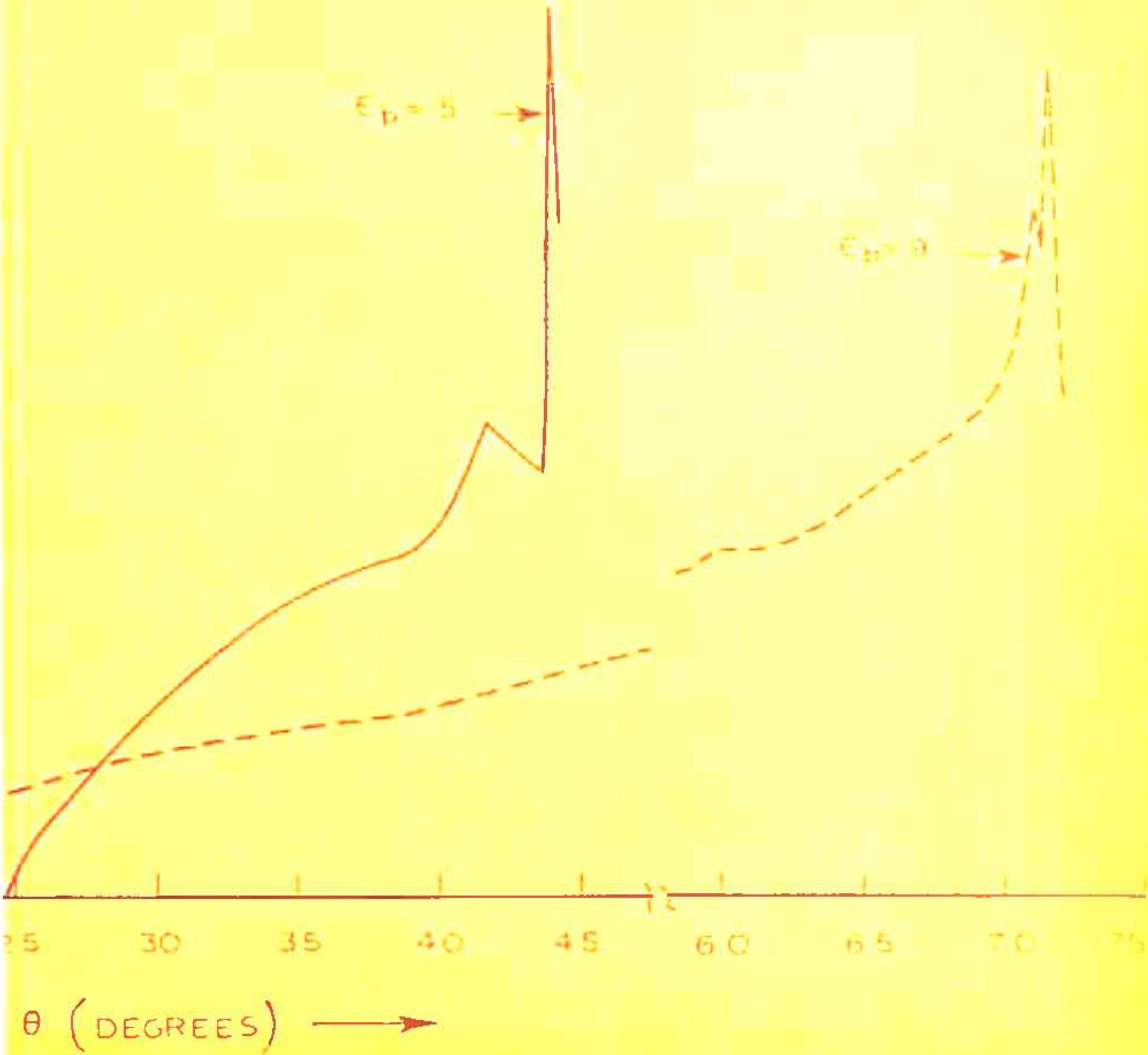

FIG.-2·2

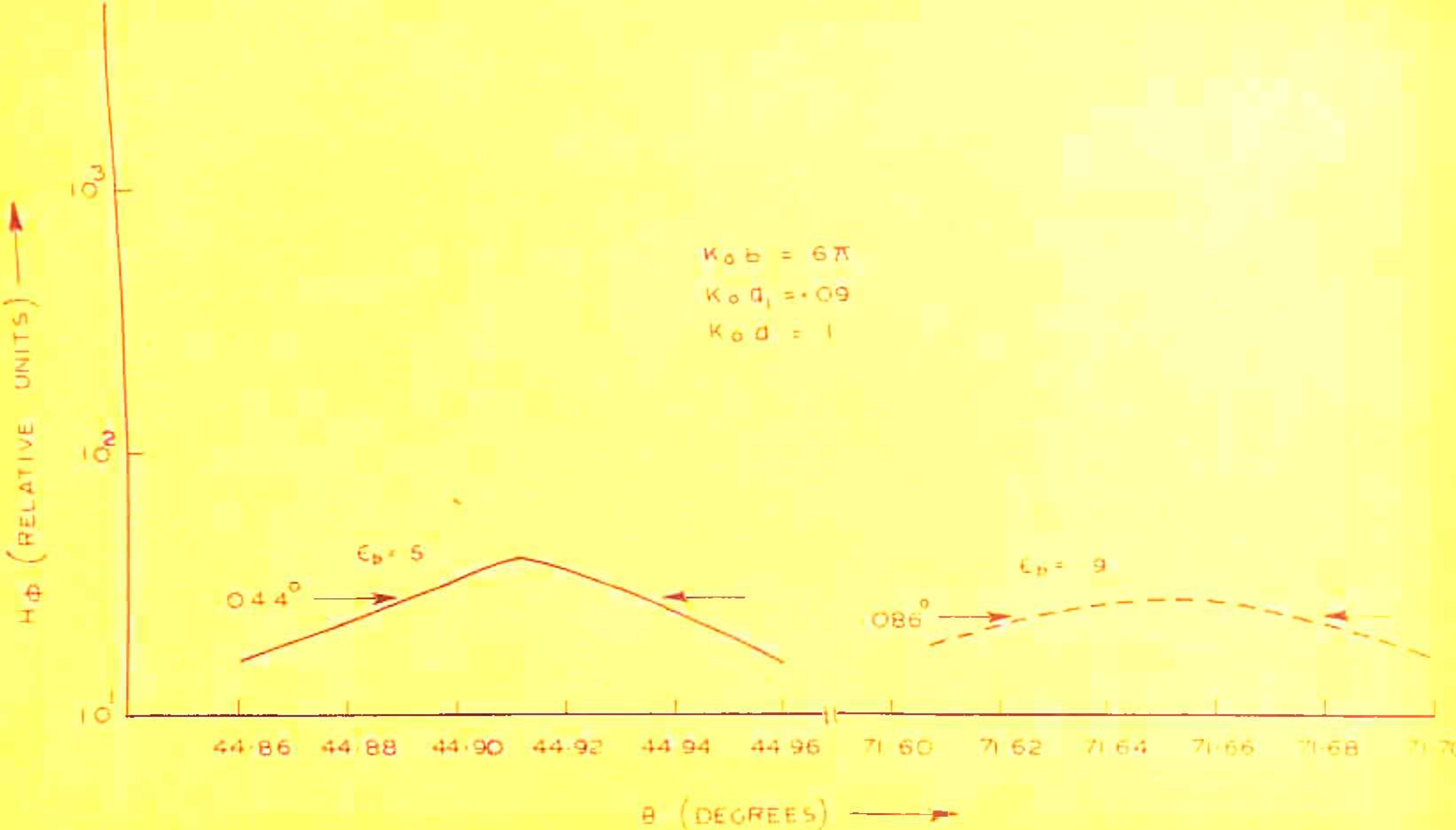

Hφ (RELATIVE UNITS)
10^3
10^2
10^1
$K_o b = 6\pi$
$K_o a_1 = .09$
$K_o a = 1$
$\epsilon_b = 5$
0.44°
$\epsilon_b = 9$
0.86°
44·86
44·88
44·90
44·92
44·94
44·96
71·60
71·62
71·64
71·66
71·68
71·70
θ (DEGREES)

FIG. - 2·3

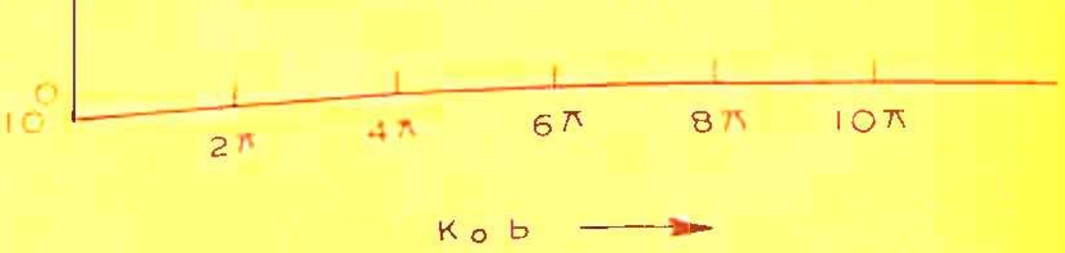

FIG.-2.4

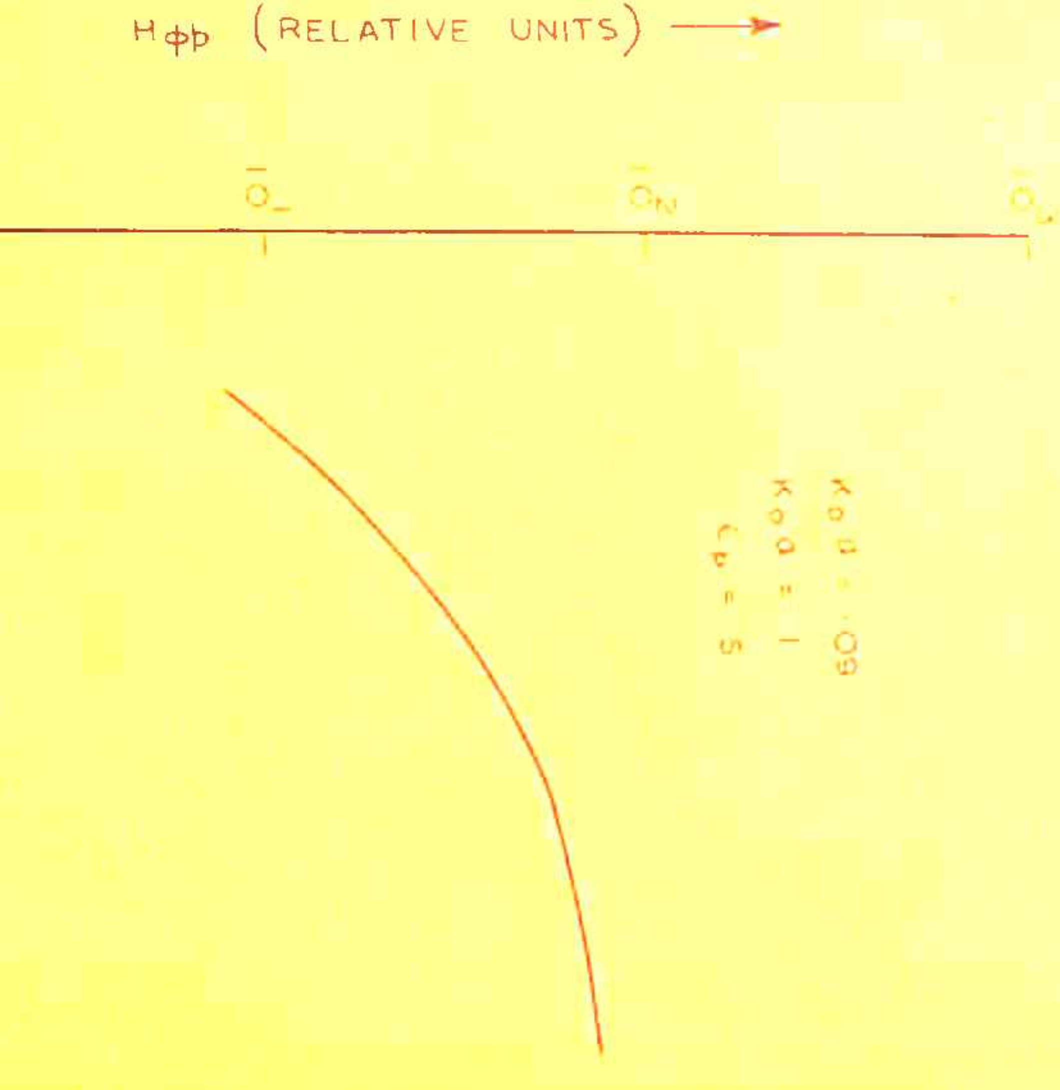

Hφp (RELATIVE UNITS)
Kp a = .09
Kp d = 1
Cp = 5

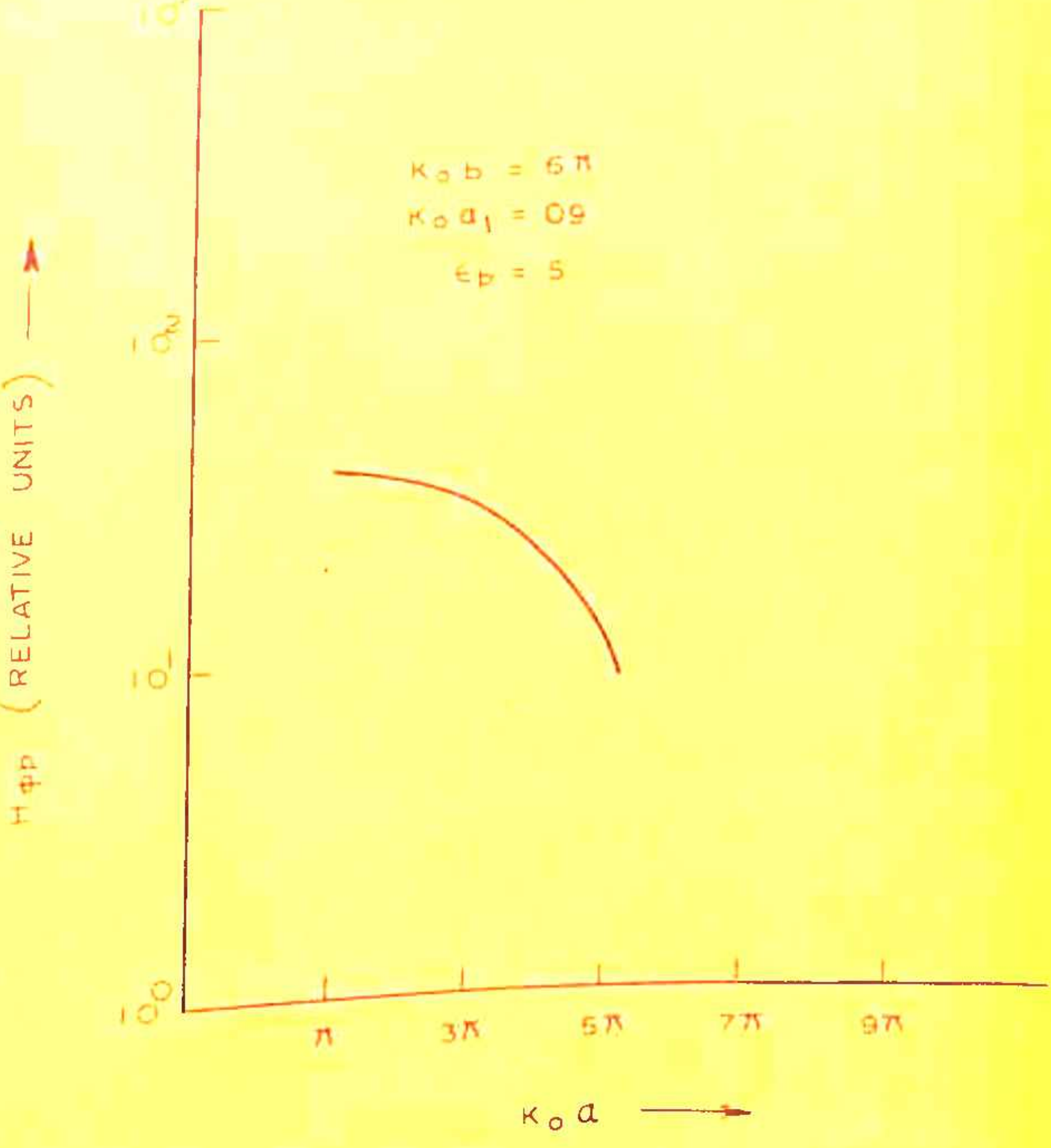
$K_o b = 6\pi$
$K_o a_1 = 09$
$\epsilon_p = 5$
$H_{\phi p}$ (RELATIVE UNITS)
10^3
10^2
10^1
10^0
π
3π
5π
7π
9π
$K_o a$

FIG. – 2·5

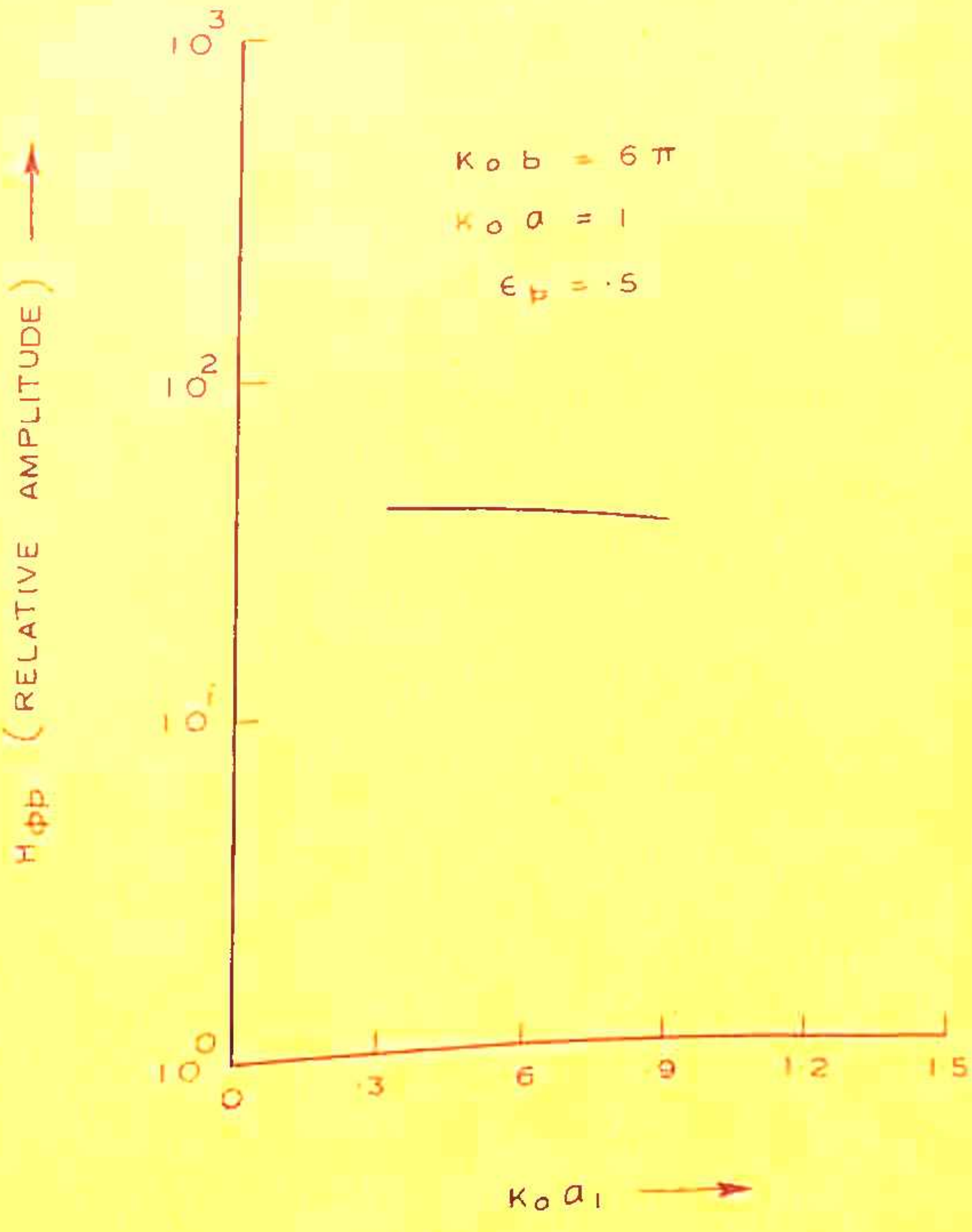
10^3
10^2
10^1
10^0
$K_0 b = 6\pi$
$K_0 a = 1$
$\epsilon_p = \cdot 5$
$H_{\phi p}$ (RELATIVE AMPLITUDE)
0
·3
·6
·9
1·2
1·5
$K_0 a_1$

FIG. - 2·6

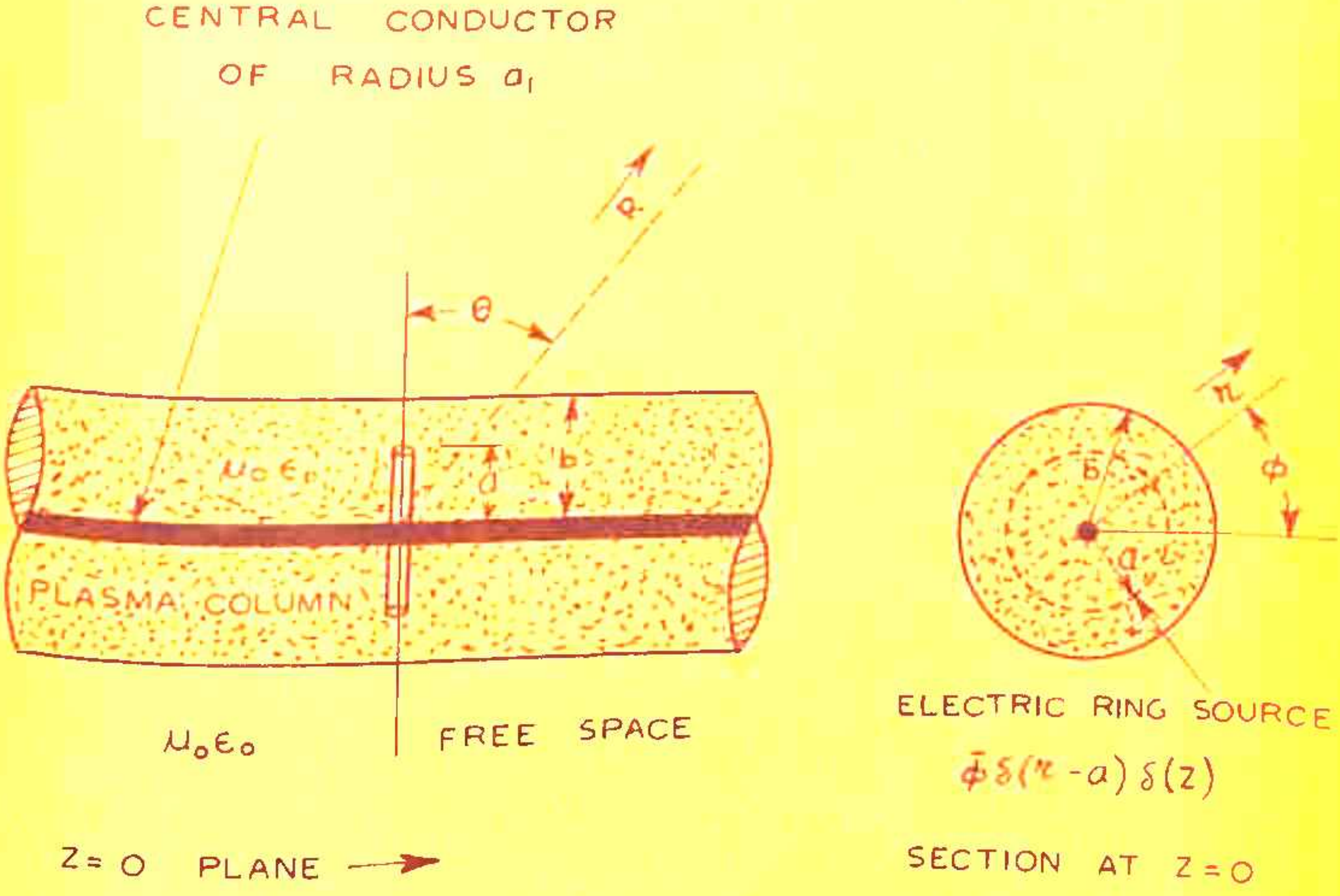
CENTRAL CONDUCTOR
OF RADIUS a_1
θ
R
$\mu_0 \epsilon_0$
a
b
PLASMA COLUMN
$\mu_0 \epsilon_0$
FREE SPACE
Z= O PLANE
b
r
φ
a
ELECTRIC RING SOURCE
$\bar{\Phi}\,\delta(r-a)\,\delta(z)$
SECTION AT Z=O

FIG. - 2.7

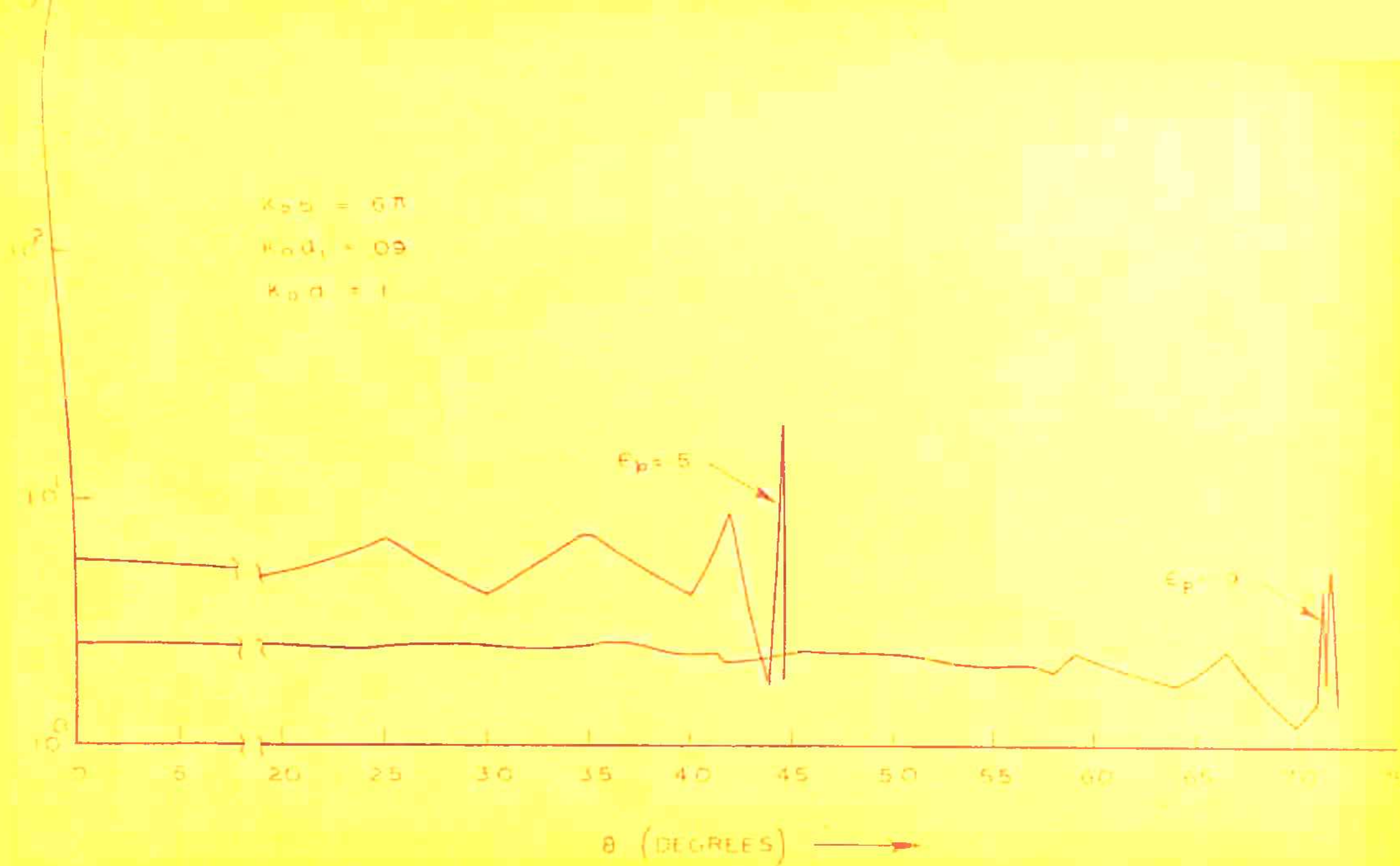

$K_0 b = 6\pi$
$K_0 d_1 = 0.9$
$K_0 d = 1$
$\epsilon_p = 5$
10^2
10^1
10^0
0
5
20
25
30
35
40
45
50
55
60
65
70
θ (DEGREES)

FIG. – 2.8

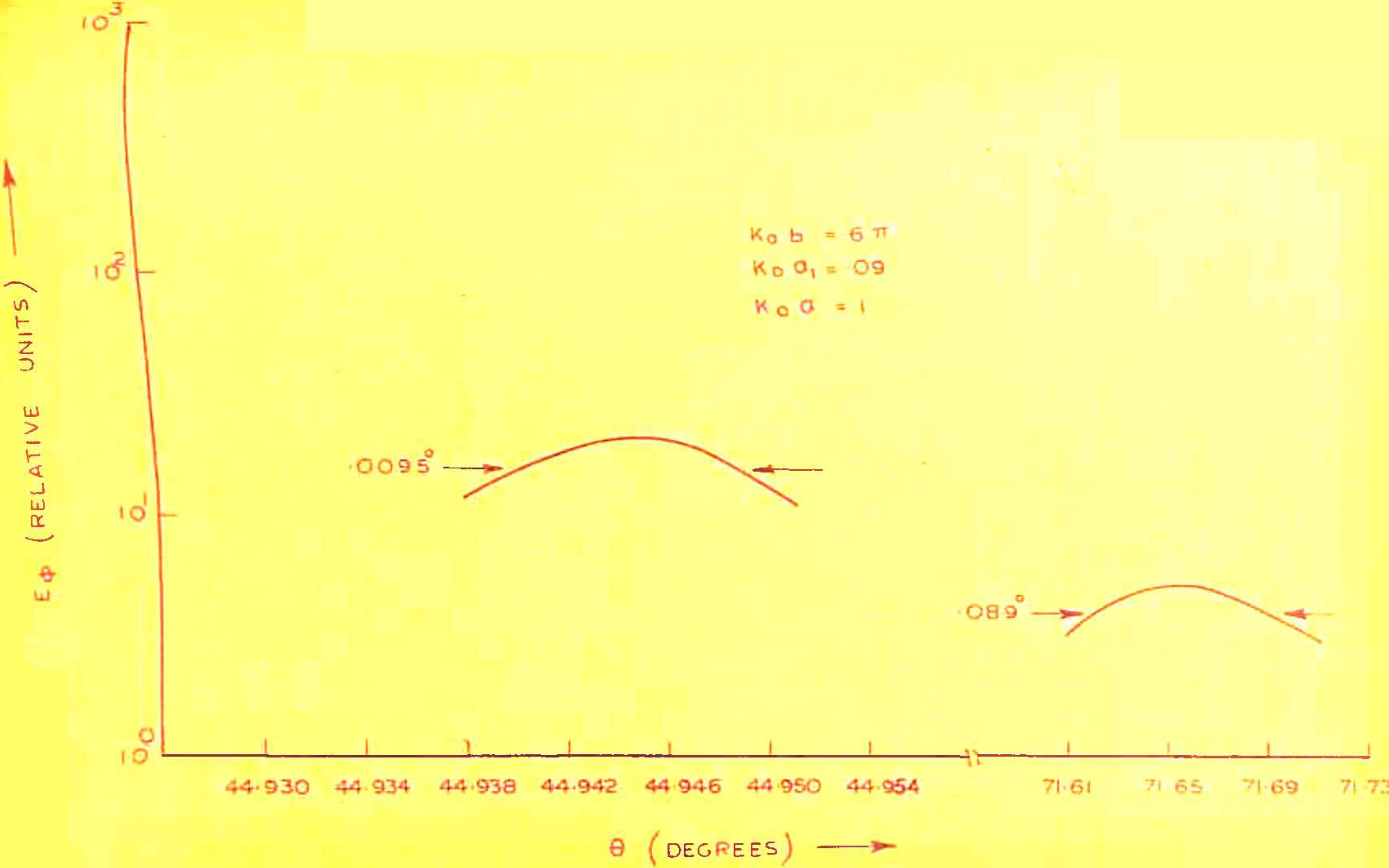
10^3
10^2
10^1
10^0
E_ϕ (RELATIVE UNITS)
$K_0 b = 6\pi$
$K_0 a_1 = \cdot 09$
$K_0 a = 1$
·0095°
·089°
44·930
44·934
44·938
44·942
44·946
44·950
44·954
71·61
71·65
71·69
71·73
θ (DEGREES)

FIG. - 2·9

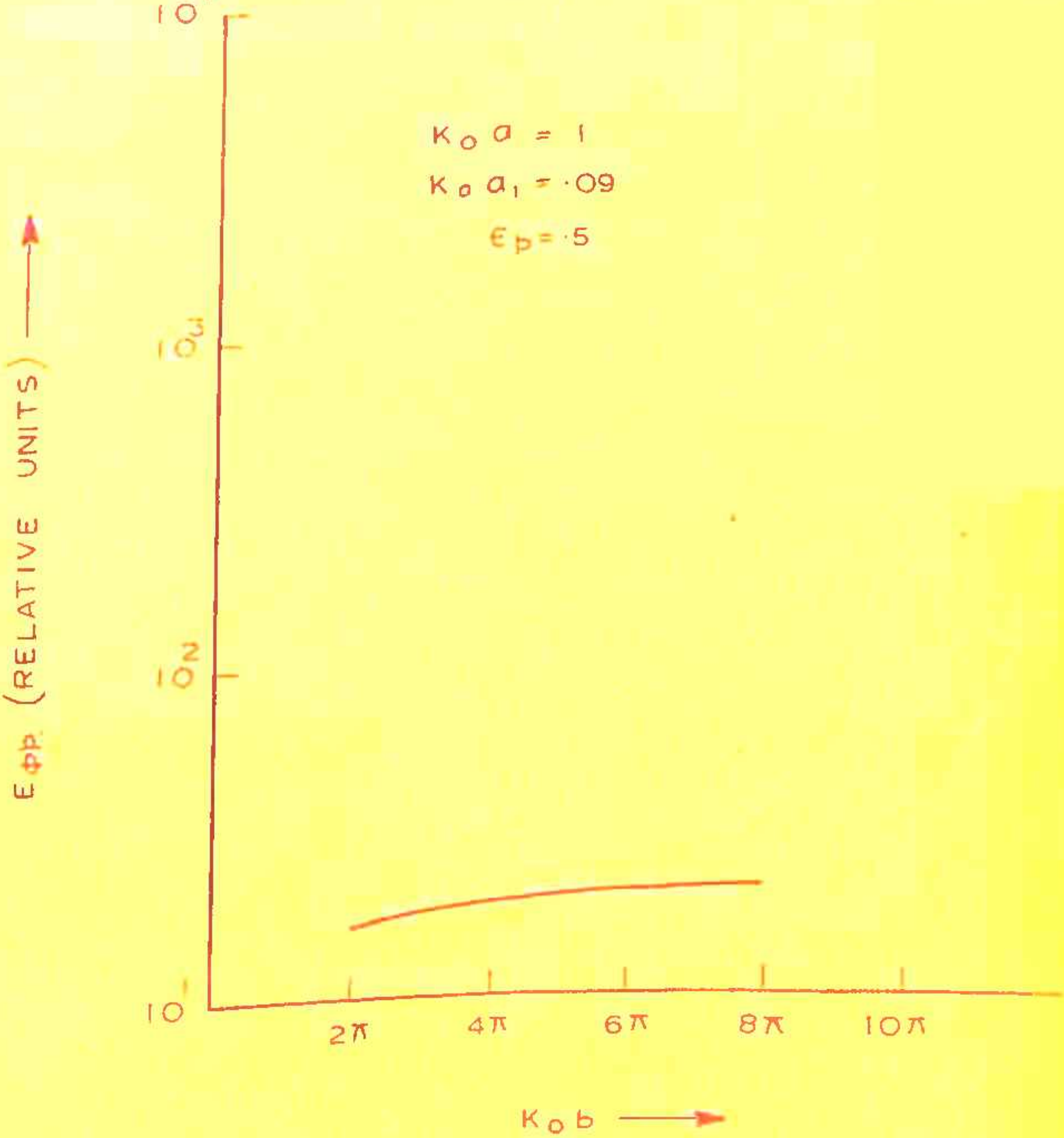

10^4
10^3
10^2
10^1
$K_o a = 1$
$K_o a_1 = \cdot 09$
$\epsilon_p = \cdot 5$
$E_{\phi p}$ (RELATIVE UNITS)
2π
4π
6π
8π
10π
$K_o b$

FIG. - 2·10

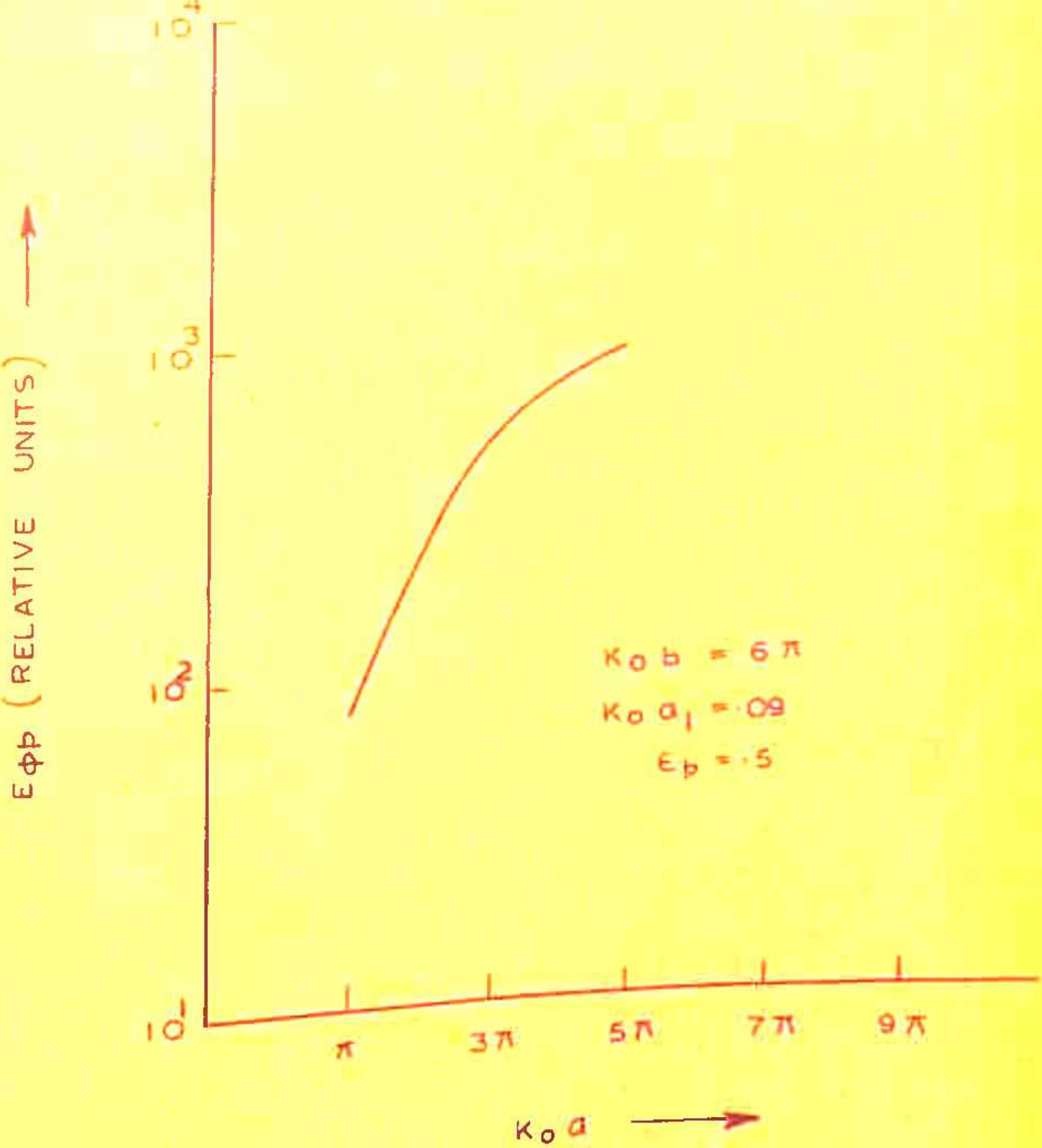

10^4
10^3
10^2
10^1
$E_{\phi p}$ (RELATIVE UNITS)
$K_0 b = 6\pi$
$K_0 a_1 = \cdot 09$
$\epsilon_p = \cdot 5$
π
3π
5π
7π
9π
$K_0 a$

FIG. – 2·11

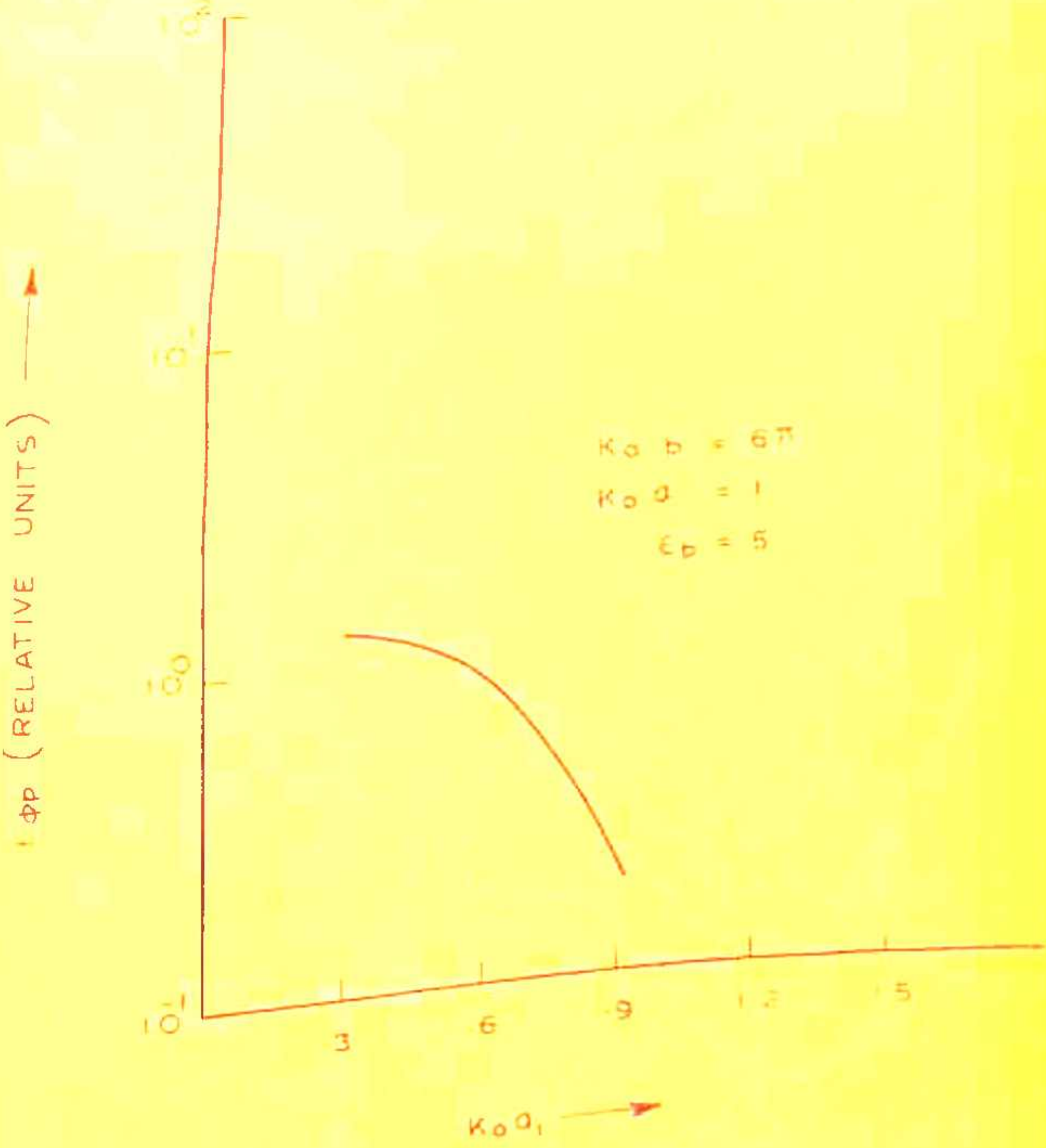
10^{2}
10^{1}
10^{0}
10^{-1}
Φ_P (RELATIVE UNITS)
$K_0 b = 6\pi$
$K_0 d = 1$
$\epsilon_b = 5$
3
6
9
1.2
1.5
$K_0 a_1$

FIG. – 2.12

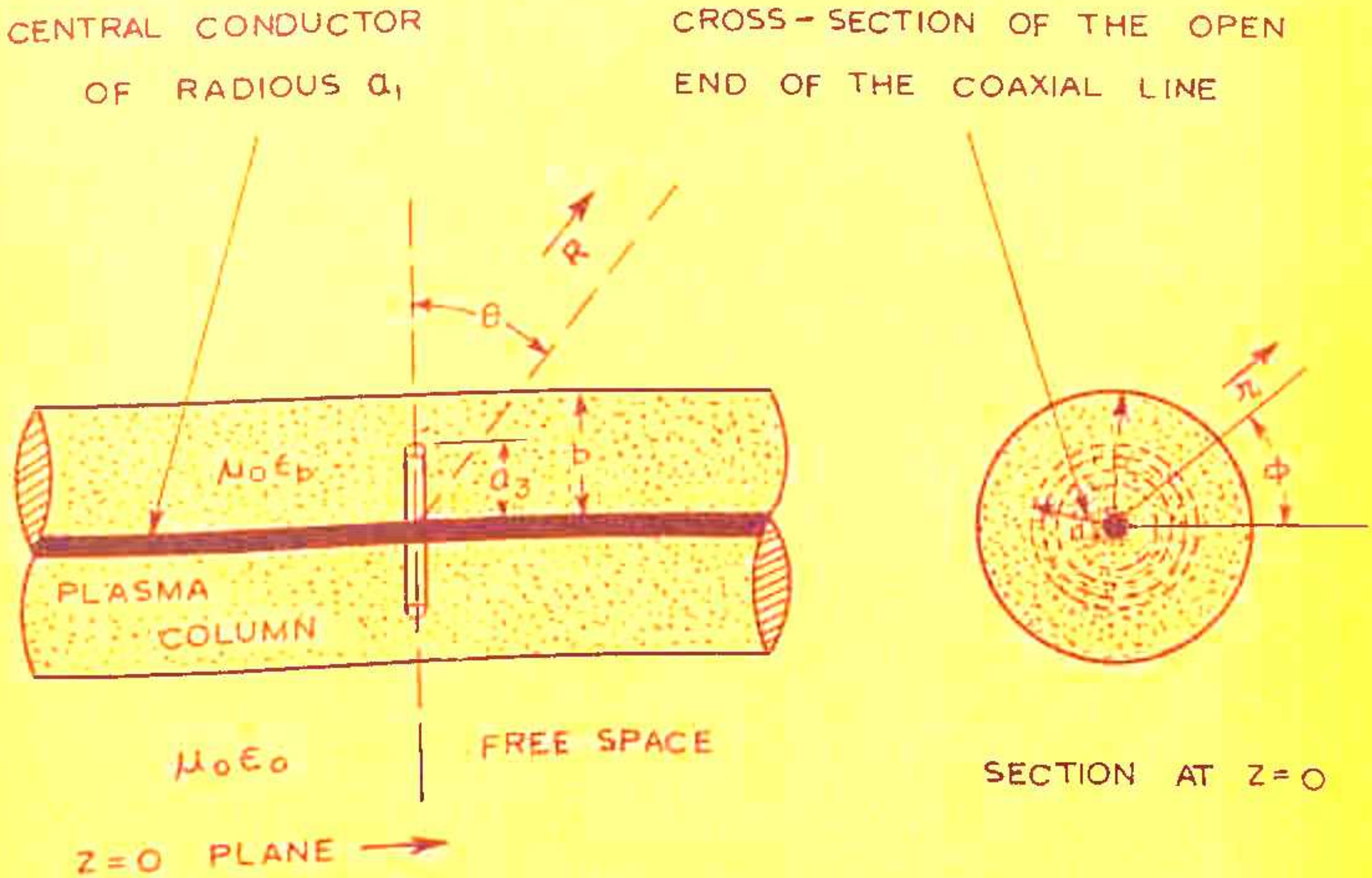
CENTRAL CONDUCTOR
OF RADIOUS a_1
CROSS - SECTION OF THE OPEN
END OF THE COAXIAL LINE
R
θ
$\mu_0 \epsilon_p$
a_3
b
PLASMA
COLUMN
$\mu_0 \epsilon_0$
FREE SPACE
Z = O PLANE
r
ϕ
SECTION AT Z = O

FIG. 2·13

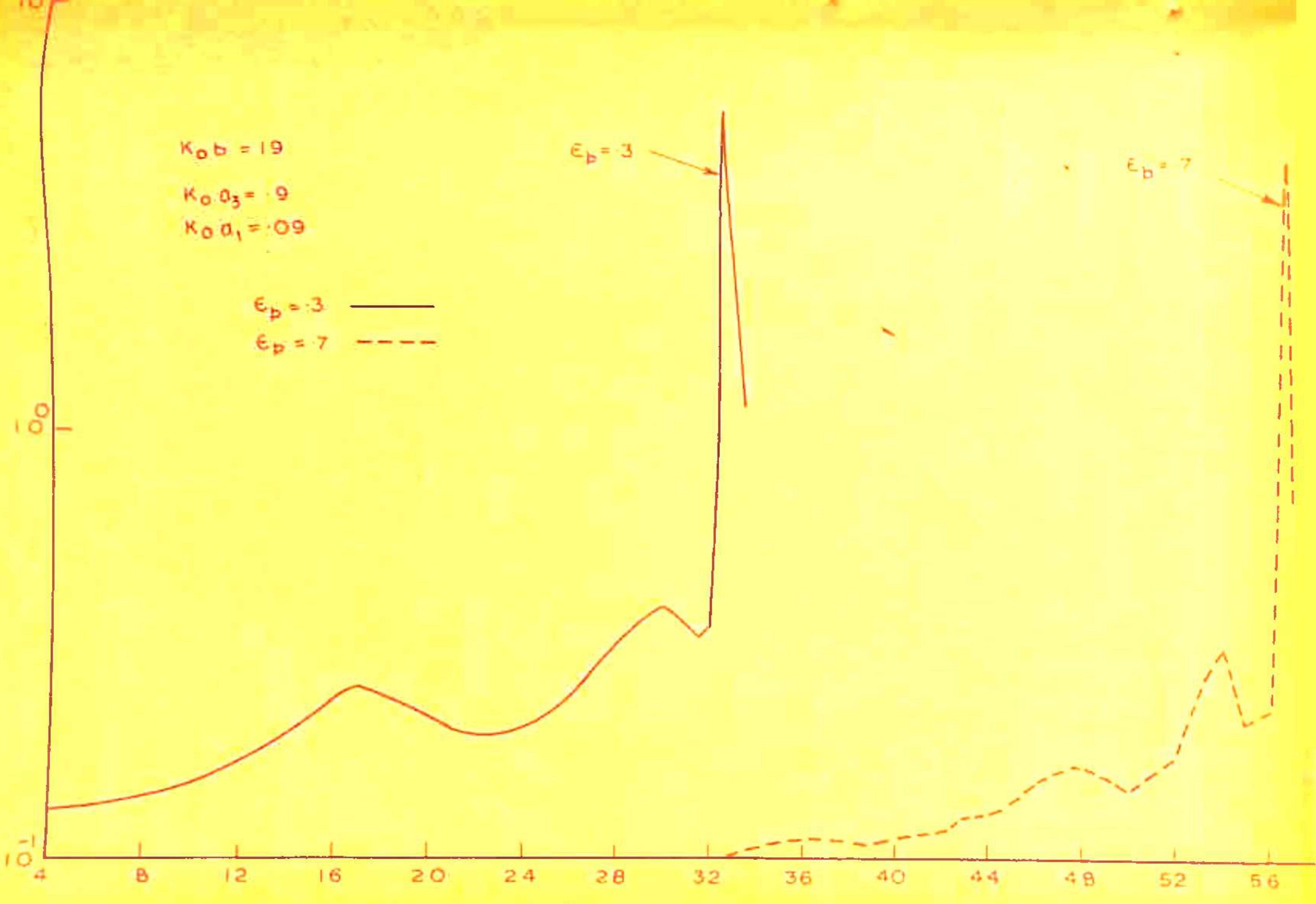
$K_0 b = 19$
$K_0 a_3 = \cdot 9$
$K_0 a_1 = \cdot 09$
$\epsilon_p = 3$
$\epsilon_p = 7$
$\epsilon_b = 3$
$\epsilon_b = 7$
10^0
10^{-1}
4
8
12
16
20
24
28
32
36
40
44
48
52
56
ANGLE (DEGREES)

FIG 2.14

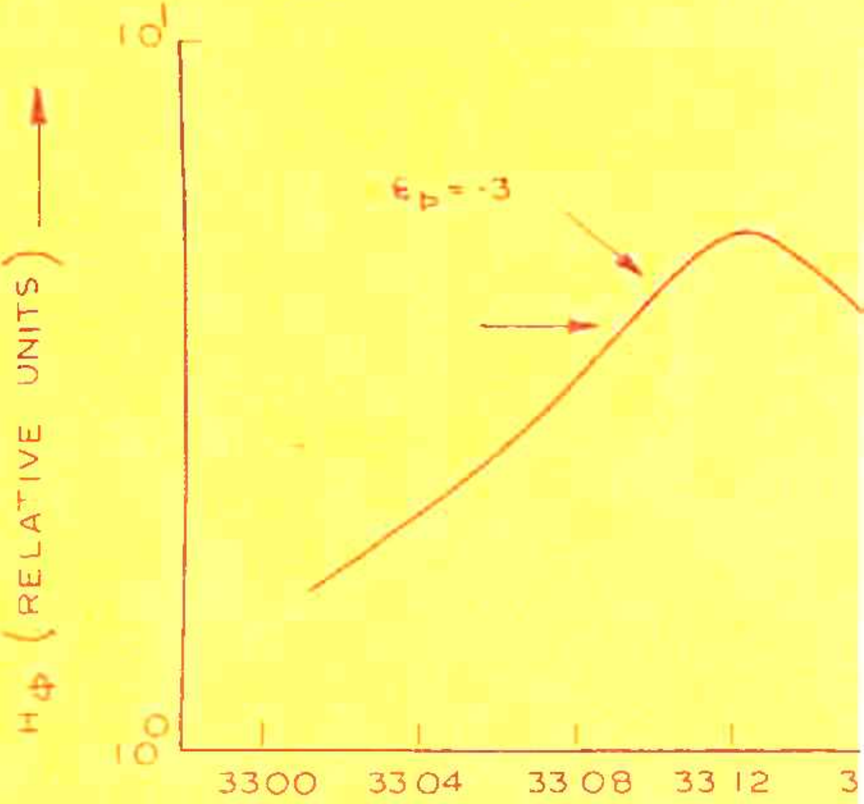

10¹
10⁰
Hφ (RELATIVE UNITS)
εp = ·3
3300
3304
3308
3312
3

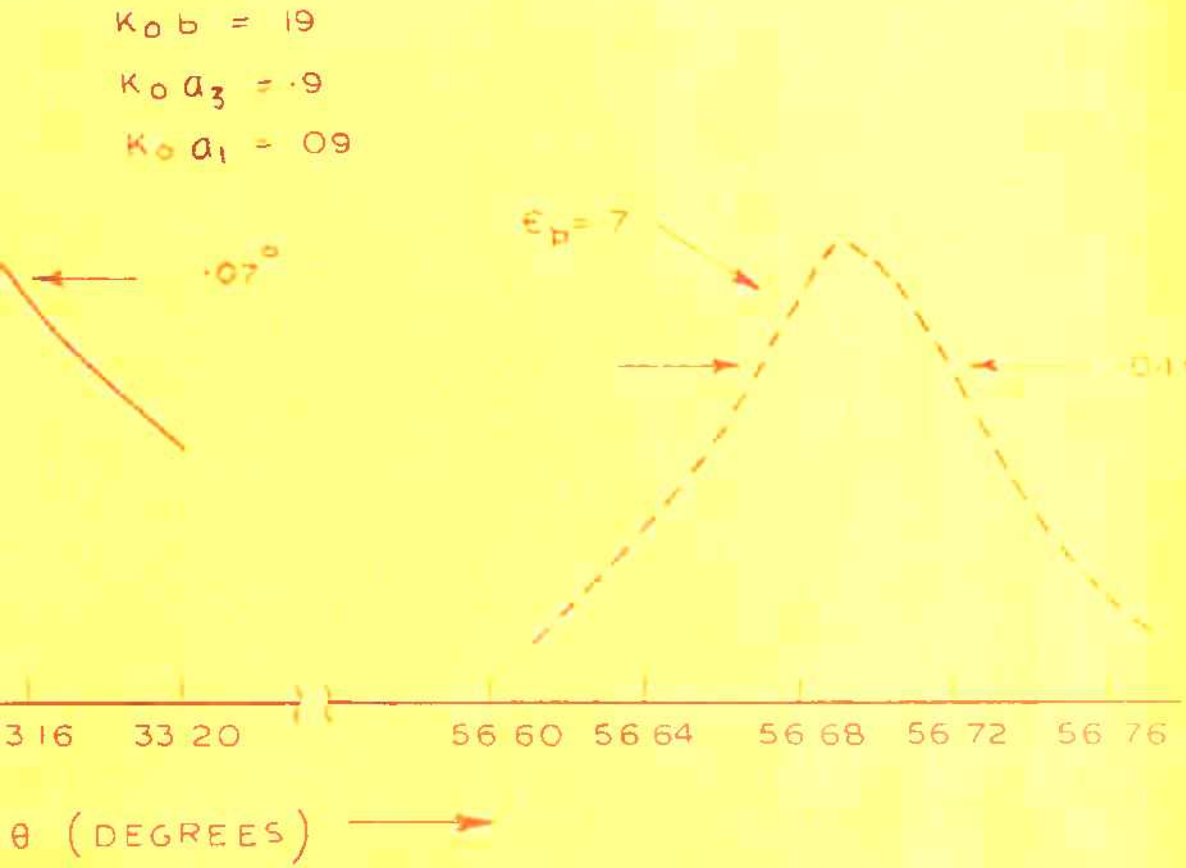

Ko b = 19
Ko a3 = ·9
Ko a1 = 09
εp = 7
·07°
3 16
33 20
56 60
56 64
56 68
56 72
56 76
θ (DEGREES)

FIG. - 2·15

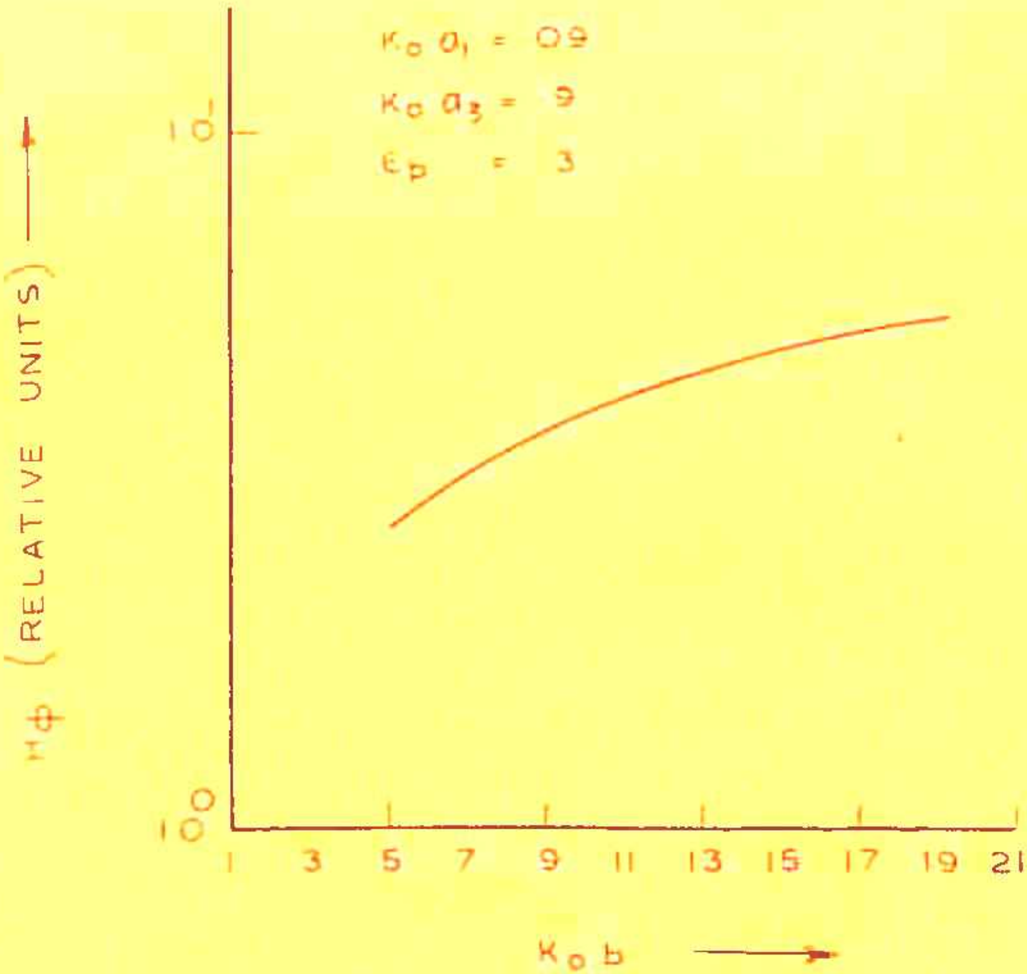

$K_o a_1$ = 09
$K_o a_3$ = 9
ϵ_p = 3
10^1
10^0
H_ϕ (RELATIVE UNITS)
1 3 5 7 9 11 13 15 17 19 21
$K_o b$

FIG. 2·16

Ko b = 19
Ko a1 = 09
εp = 3
Hφ (RELATIVE UNITS)
10¹
10⁰
10⁻¹
0
0·2
0·4
0·6
0·8
1·0
Ko d3

FIG. 2·17

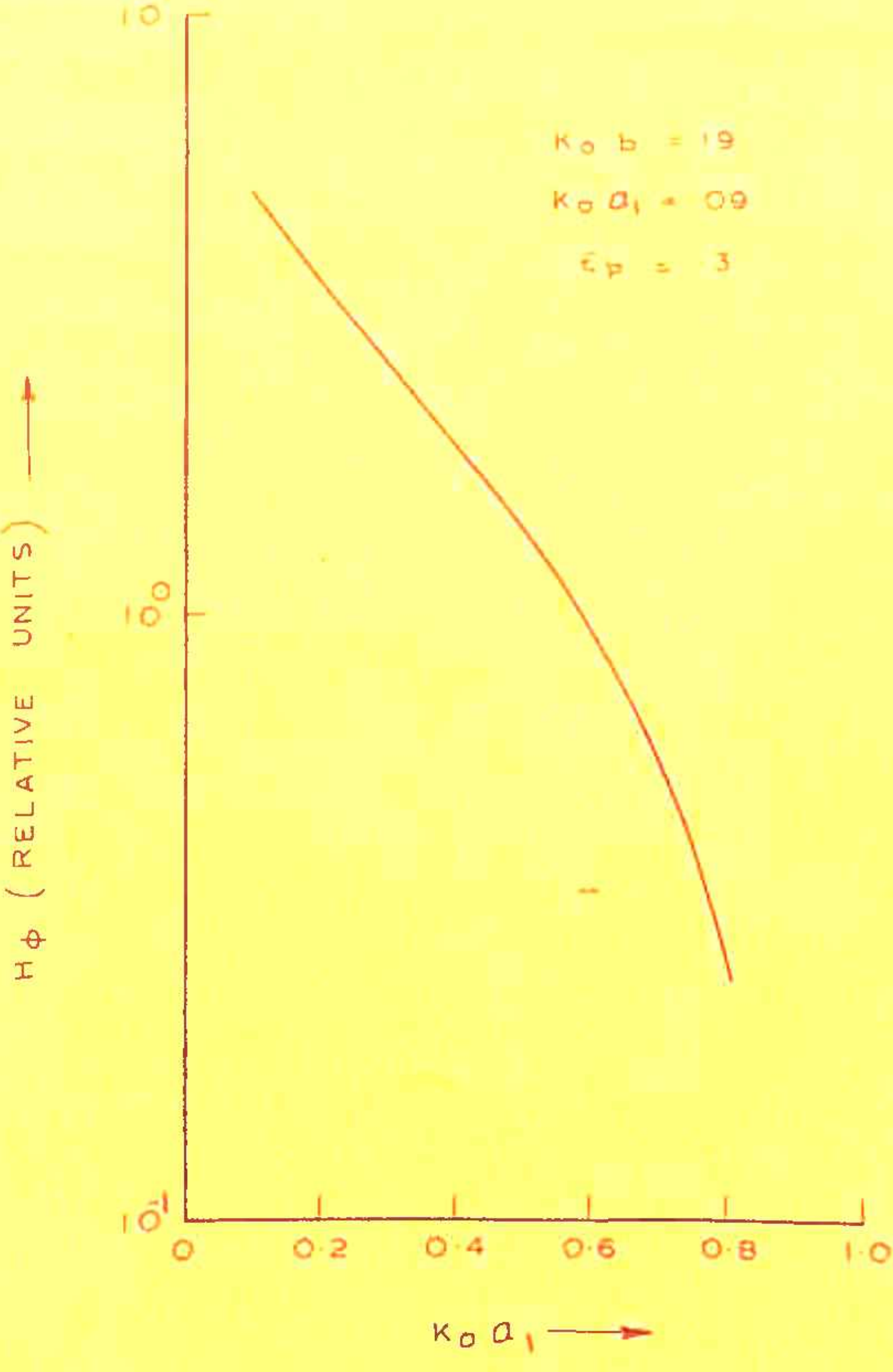

$K_o b = 19$
$K_o a_1 = 09$
$\epsilon_p = 3$
H_ϕ (RELATIVE UNITS)
10^1
10^0
10^{-1}
0
0·2
0·4
0·6
0·8
1·0
$K_o a_1$

FIG. -2·18

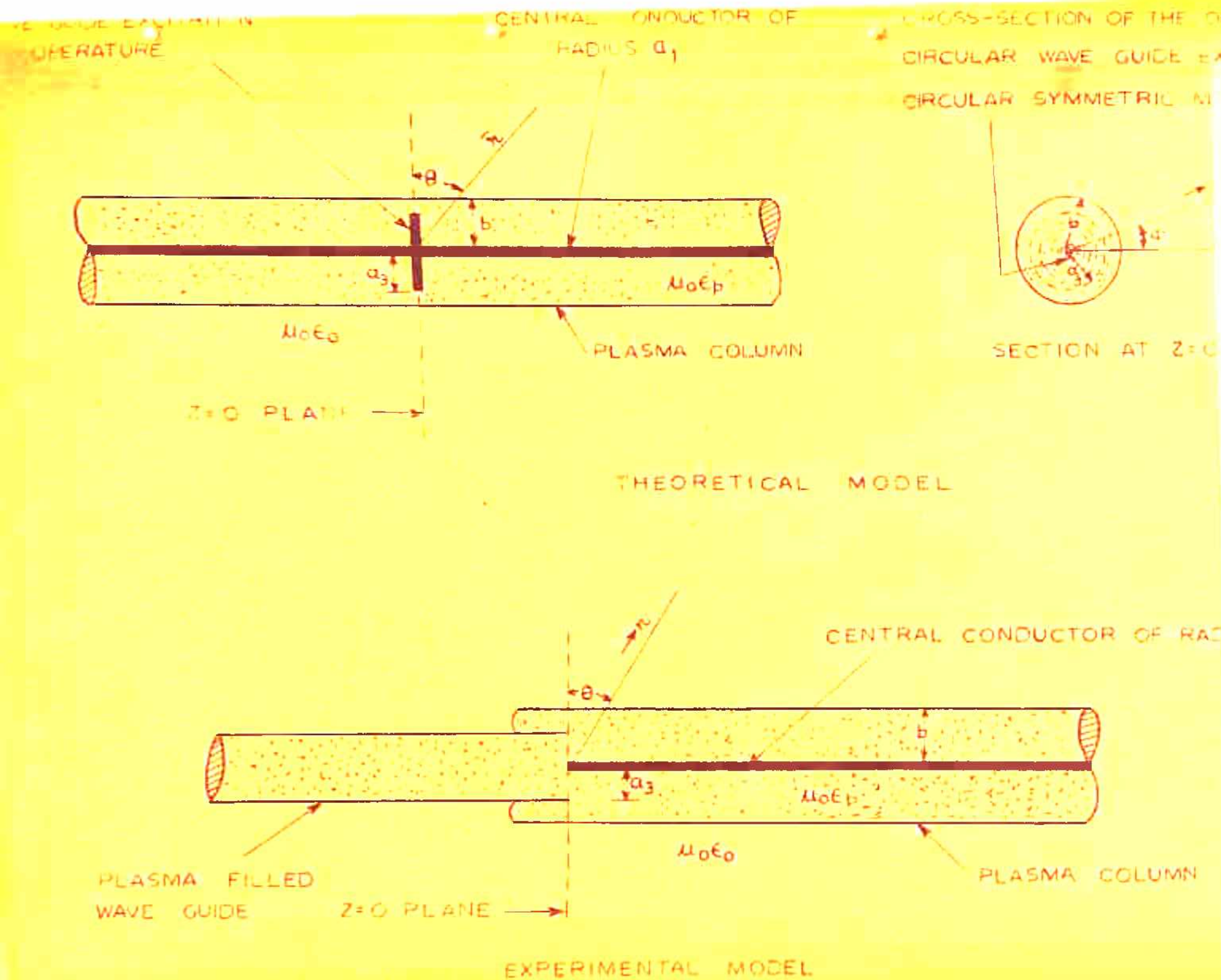
APERTURE
CENTRAL CONDUCTOR OF
RADIUS a_1
CROSS-SECTION OF THE OPEN
CIRCULAR WAVE GUIDE
CIRCULAR SYMMETRIC
θ
b
a_3
$\mu_0\epsilon_p$
$\mu_0\epsilon_0$
PLASMA COLUMN
SECTION AT Z=
Z=O PLANE
THEORETICAL MODEL
CENTRAL CONDUCTOR OF RA
θ
b
a_3
$\mu_0\epsilon_p$
$\mu_0\epsilon_0$
PLASMA FILLED
WAVE GUIDE
Z=O PLANE
PLASMA COLUMN
EXPERIMENTAL MODEL

FIG.2.19

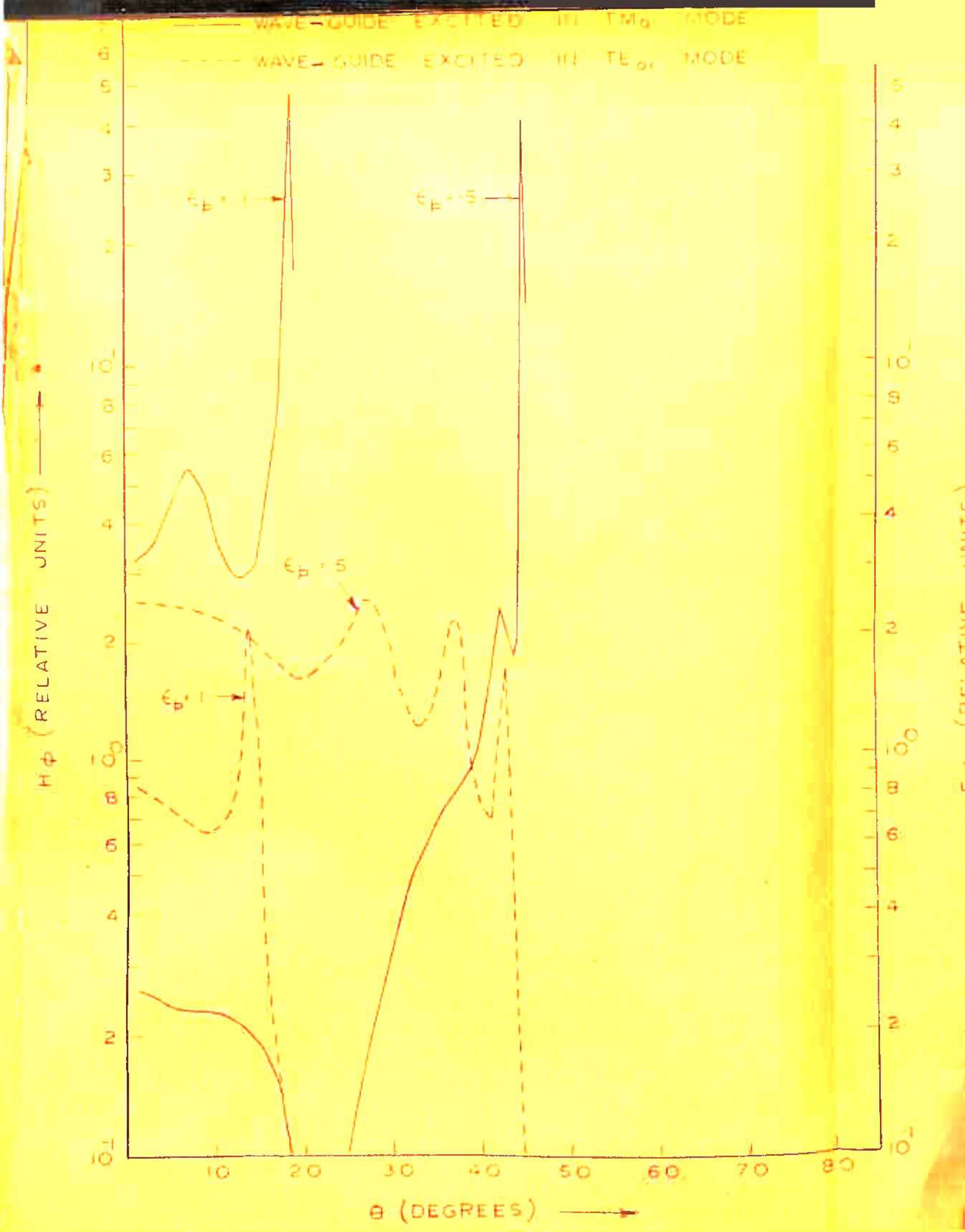
WAVE-GUIDE EXCITED IN TM MODE
WAVE-GUIDE EXCITED IN TE MODE
θ (DEGREES)
Hφ (RELATIVE UNITS)

FIG 2·20

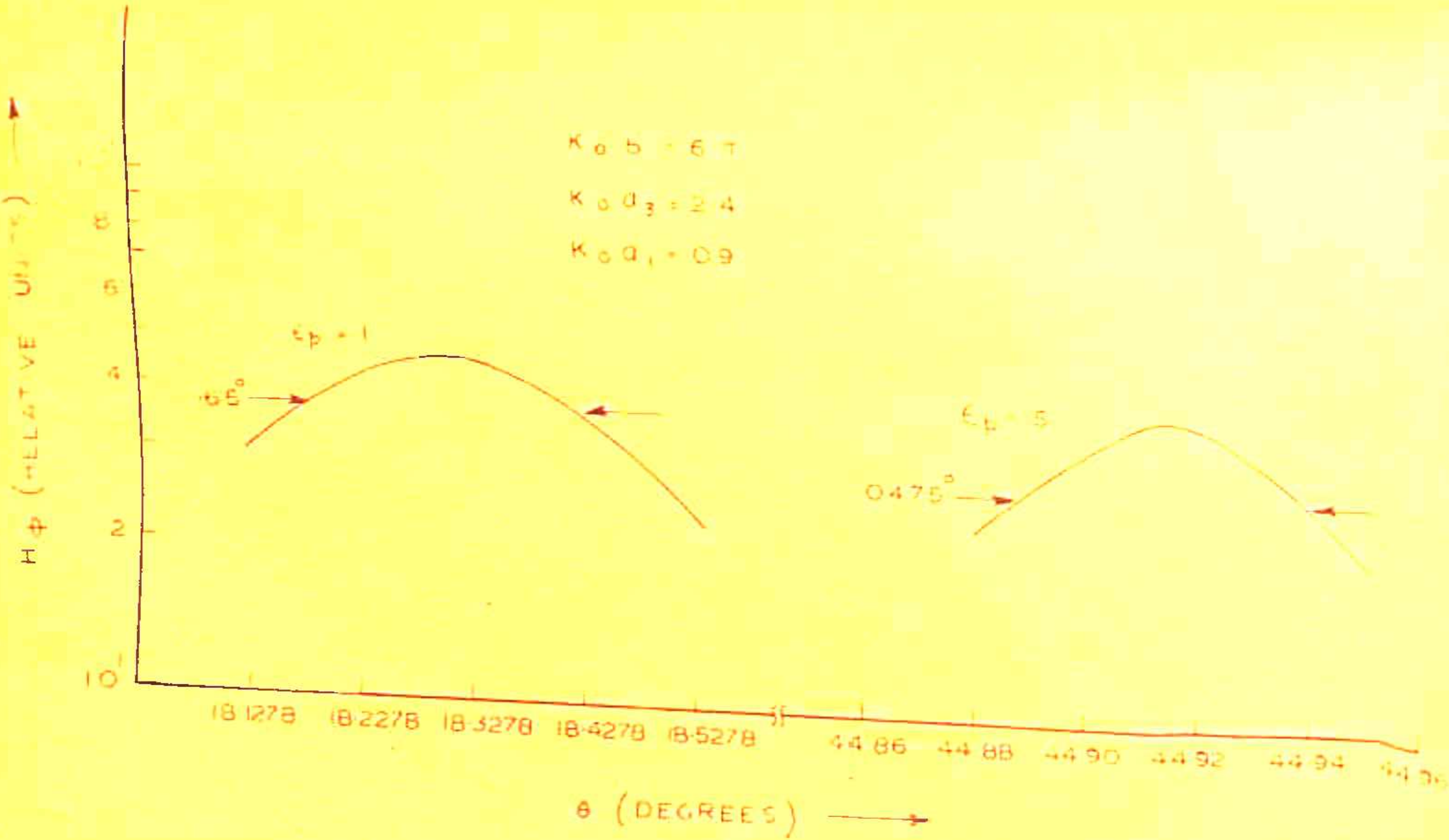
Hφ (RELATIVE UNITS)
2
4
6
8
10
$K_0 b = 6.7$
$K_0 a_3 = 2.4$
$K_0 a_1 = 0.9$
$\epsilon_p = 1$
·65°
$\epsilon_p = 5$
0.475°
18.1278
18.2278
18.3278
18.4278
18.5278
44.86
44.88
44.90
44.92
44.94
θ (DEGREES)

FIG. 2.21a

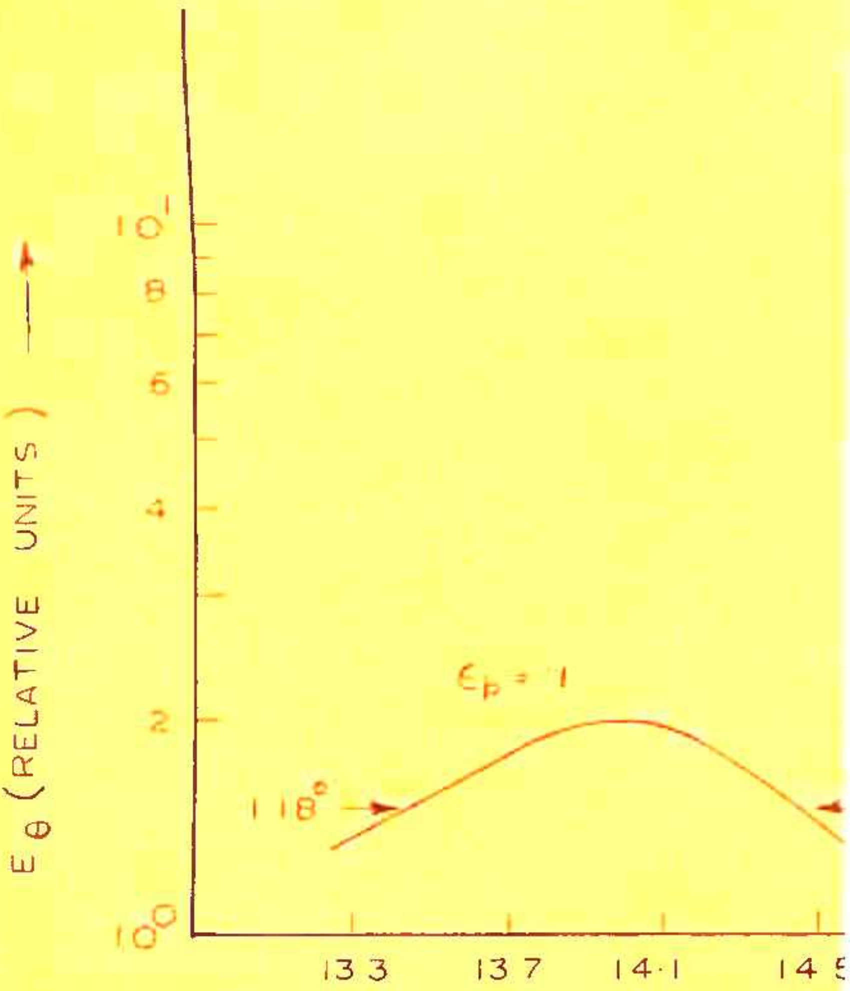
E θ (RELATIVE UNITS)
10^1
8
6
4
2
10^0
εp = 1
118°
13 3
13 7
14·1

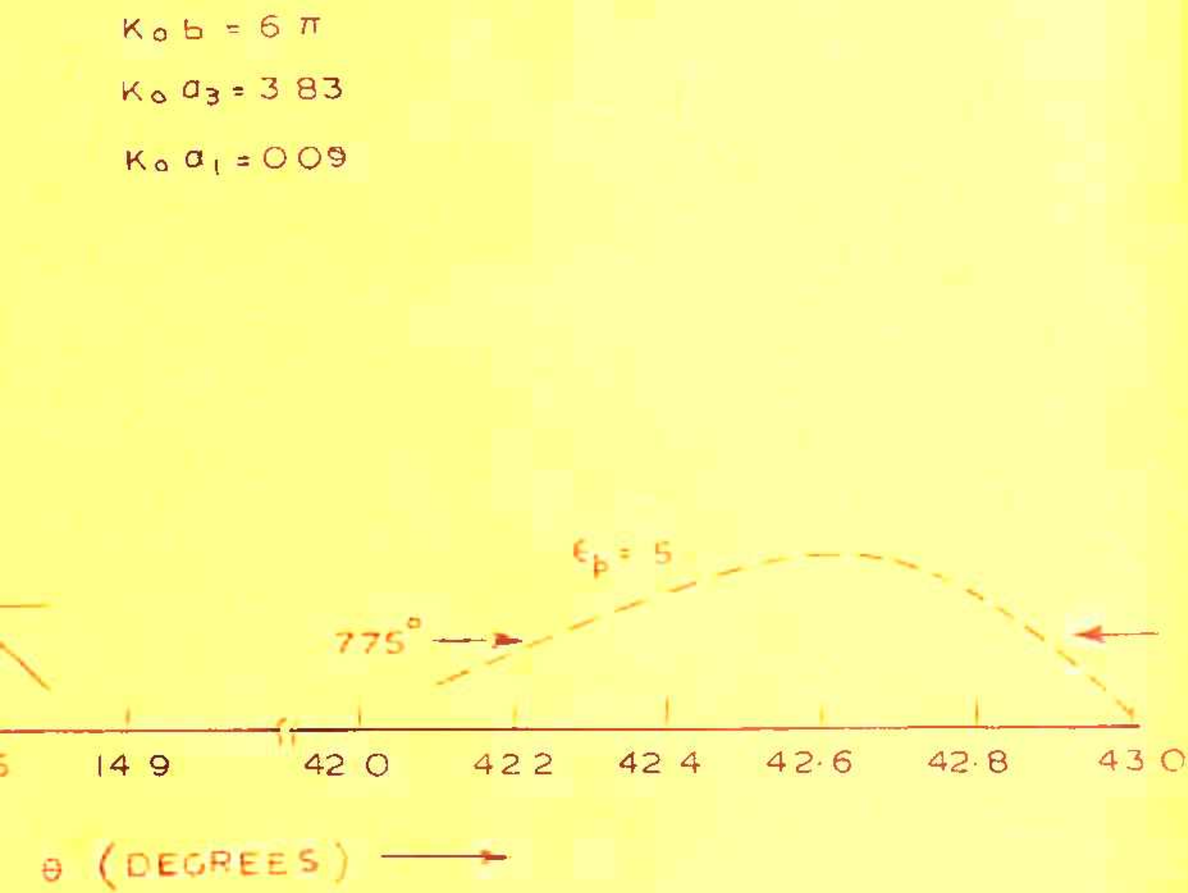
K₀b = 6π
K₀a₃ = 3 83
K₀a₁ = 0 09
εₚ = 5
775°
14 9
42 0
42 2
42 4
42·6
42·8
43 0
θ (DEGREES)

FIG. 2.21 b

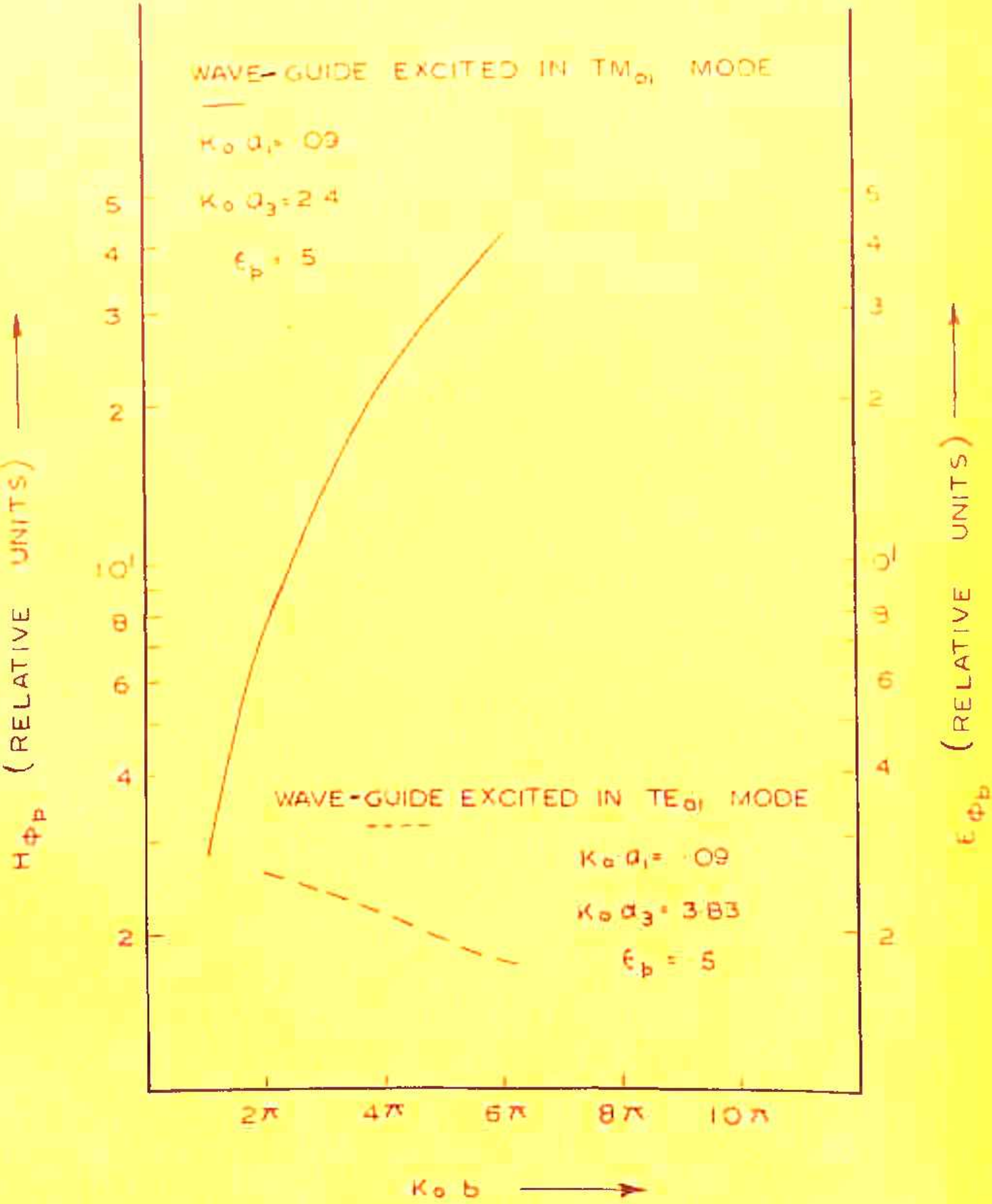

WAVE-GUIDE EXCITED IN TM01 MODE
Ko a1 = ·09
Ko a3 = 2·4
εp = 5
WAVE-GUIDE EXCITED IN TE01 MODE
Ko a1 = ·09
Ko a3 = 3·83
εp = 5
Hφp (RELATIVE UNITS)
Eφp (RELATIVE UNITS)
5
4
3
2
10¹
8
6
4
2
2π
4π
6π
8π
10π
Ko b

FIG. 2·22

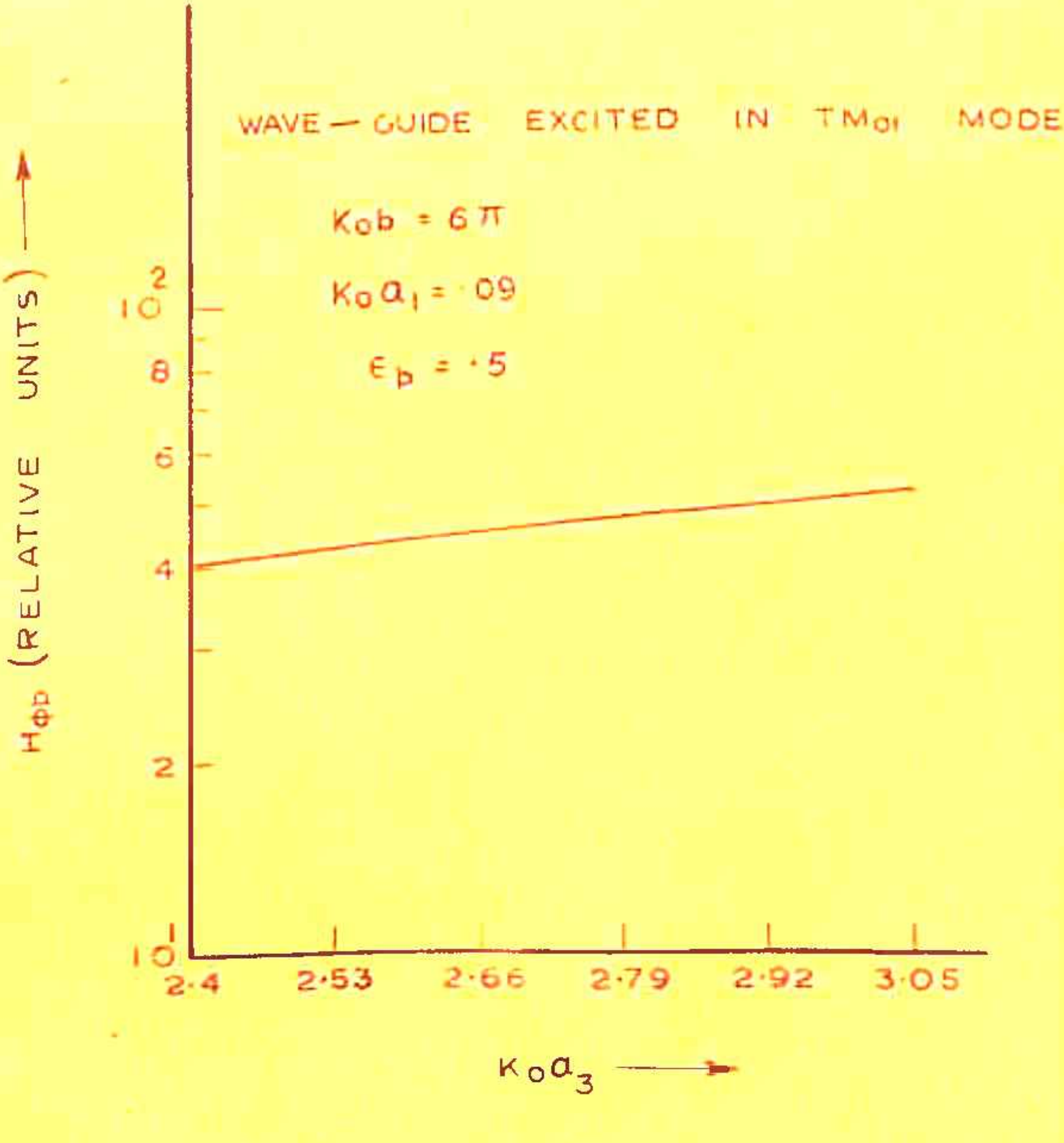
WAVE — GUIDE EXCITED IN TM01 MODE
Kob = 6π
Koa1 = ·09
εb = ·5
Hφb (RELATIVE UNITS)
10^2
8
6
4
2
10^1
2·4
2·53
2·66
2·79
2·92
3·05
Koa3

FIG. 223 a

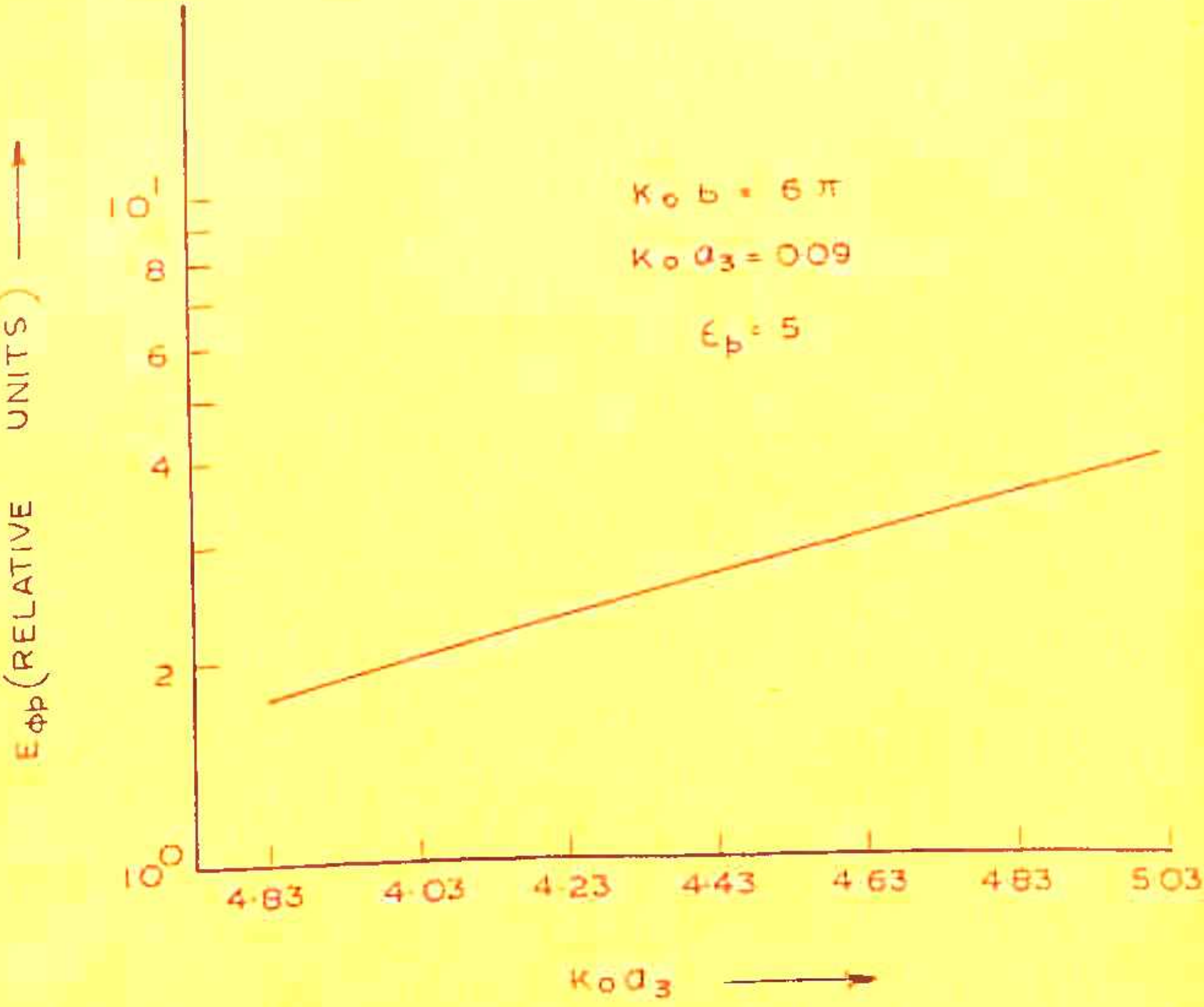

$K_o b = 6\pi$
$K_o a_3 = 0.09$
$\epsilon_b = 5$
$E_{\phi p}$ (RELATIVE UNITS)
10^1
8
6
4
2
10^0
4.83
4.03
4.23
4.43
4.63
4.83
5.03
$K_o a_3$

FIG 2.25b

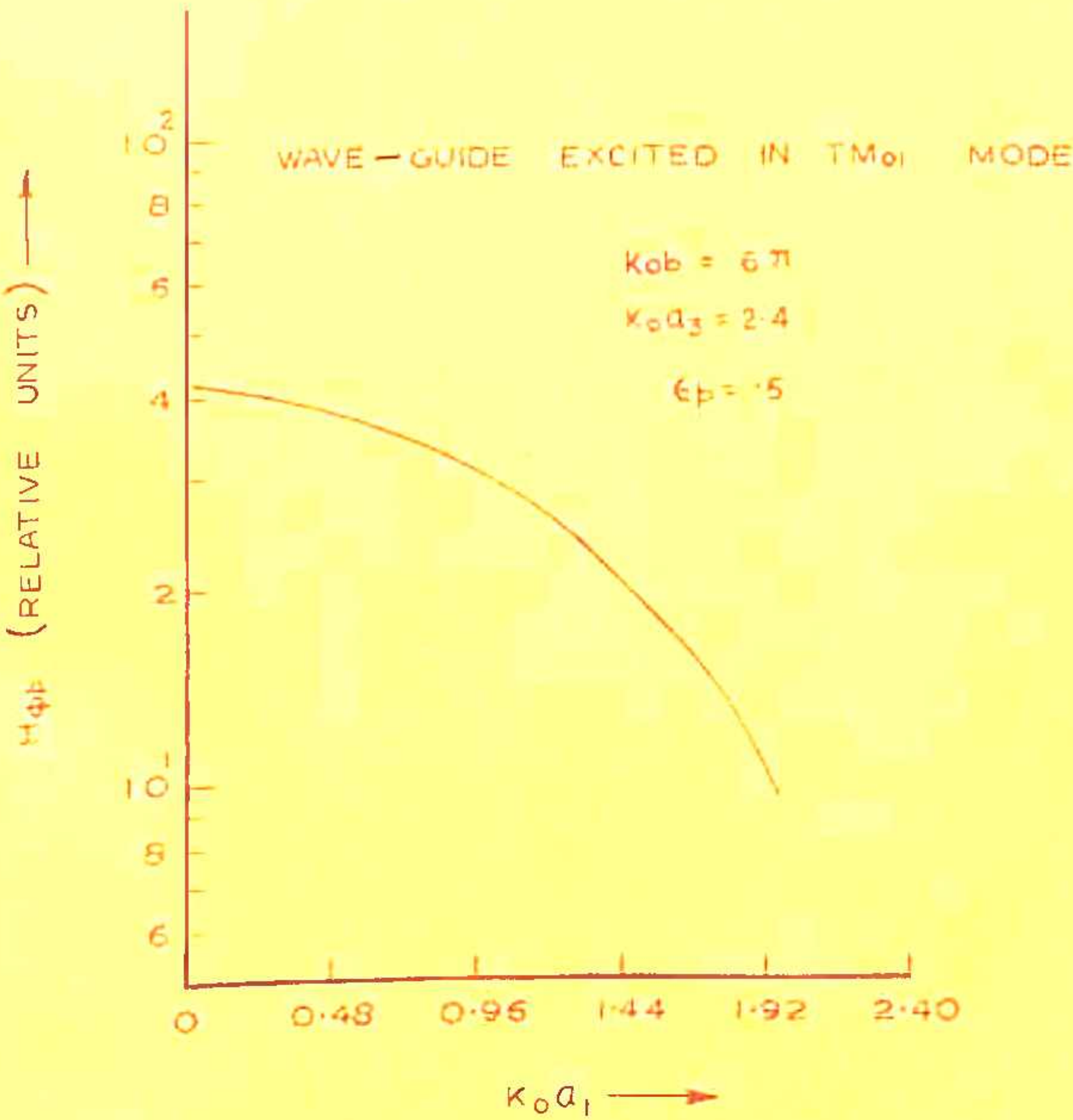

WAVE — GUIDE EXCITED IN TM01 MODE
Kob = 6 π
Koa3 = 2·4
εp = ·5
Hφb (RELATIVE UNITS)
10²
8
6
4
2
10¹
8
6
0
0·48
0·96
1·44
1·92
2·40
Koa1

FIG. 224 a

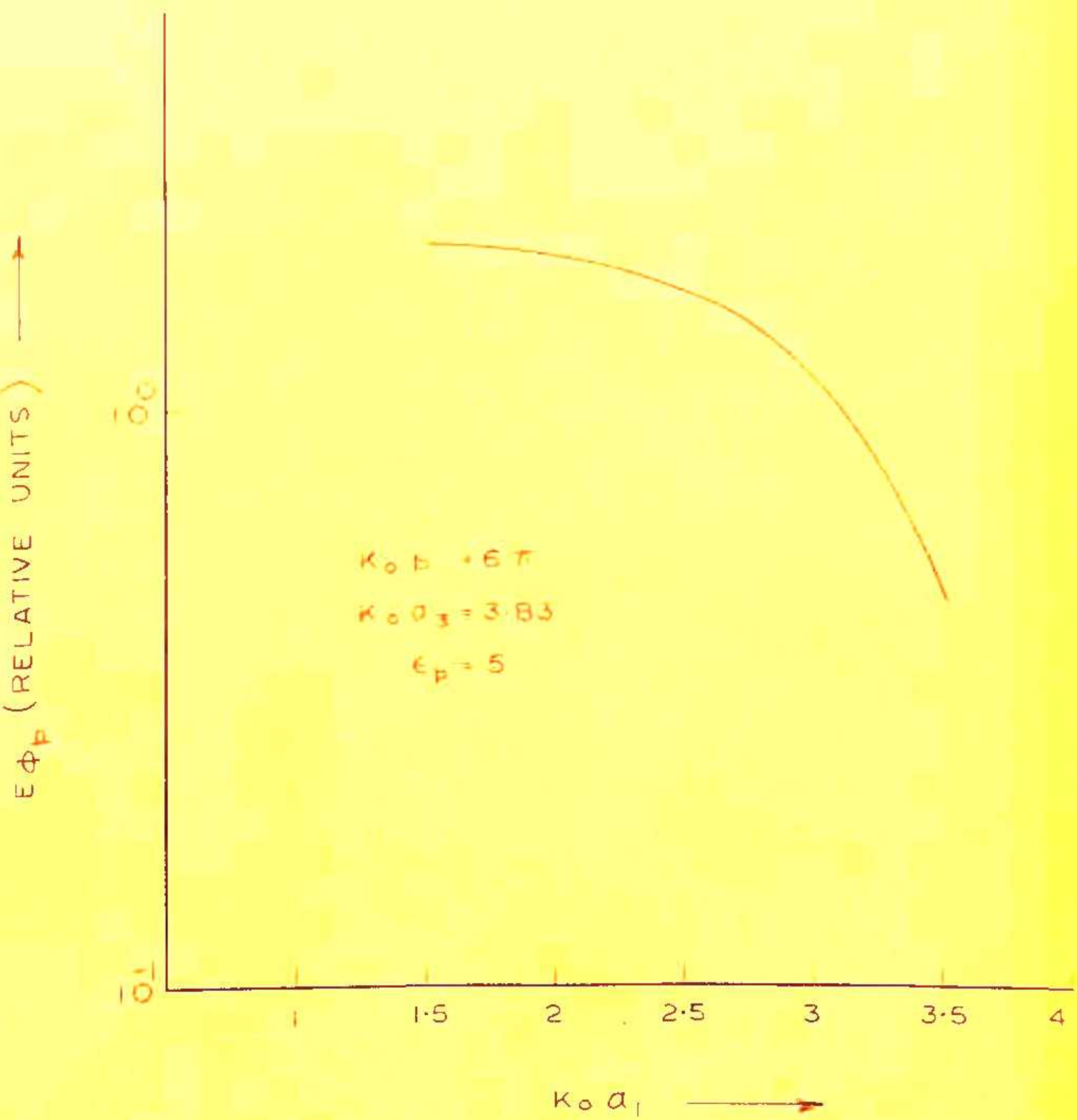

$E\Phi_p$ (RELATIVE UNITS)
10^0
10^{-1}
$K_o b = 6\pi$
$K_o a_3 = 3.83$
$\epsilon_p = 5$
1
1·5
2
2·5
3
3·5
4
$K_o a_1$

FIG. 2·24 b

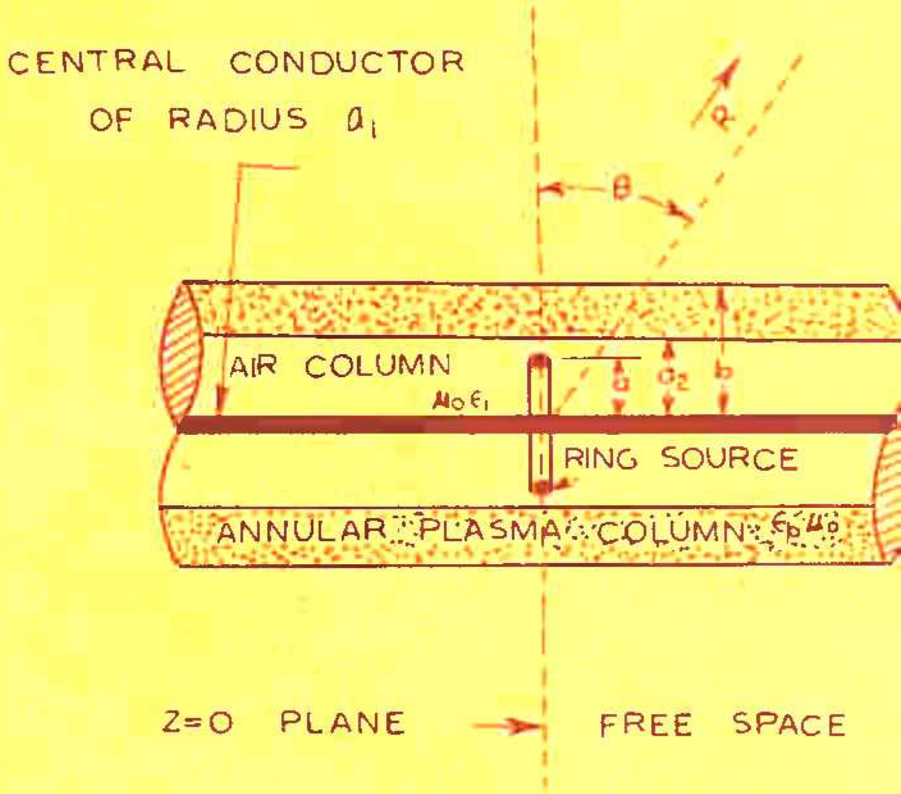
CENTRAL CONDUCTOR
OF RADIUS a_1
θ
R
AIR COLUMN
$\mu_0 \epsilon_1$
a
a_2
b
RING SOURCE
ANNULAR PLASMA COLUMN $\epsilon_p \mu_0$
Z=0 PLANE
FREE SPACE

FIG. 3

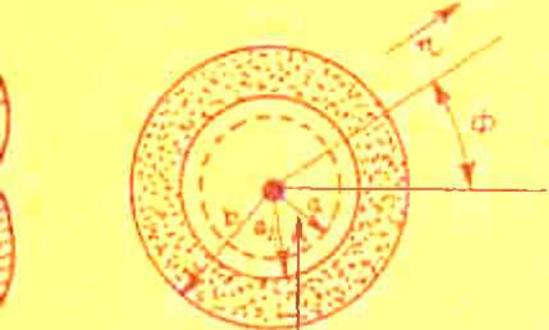

MAGNETIC RING SOURCE

$\delta(r-a)\,\delta(z)$

SECTION AT Z=0

-1

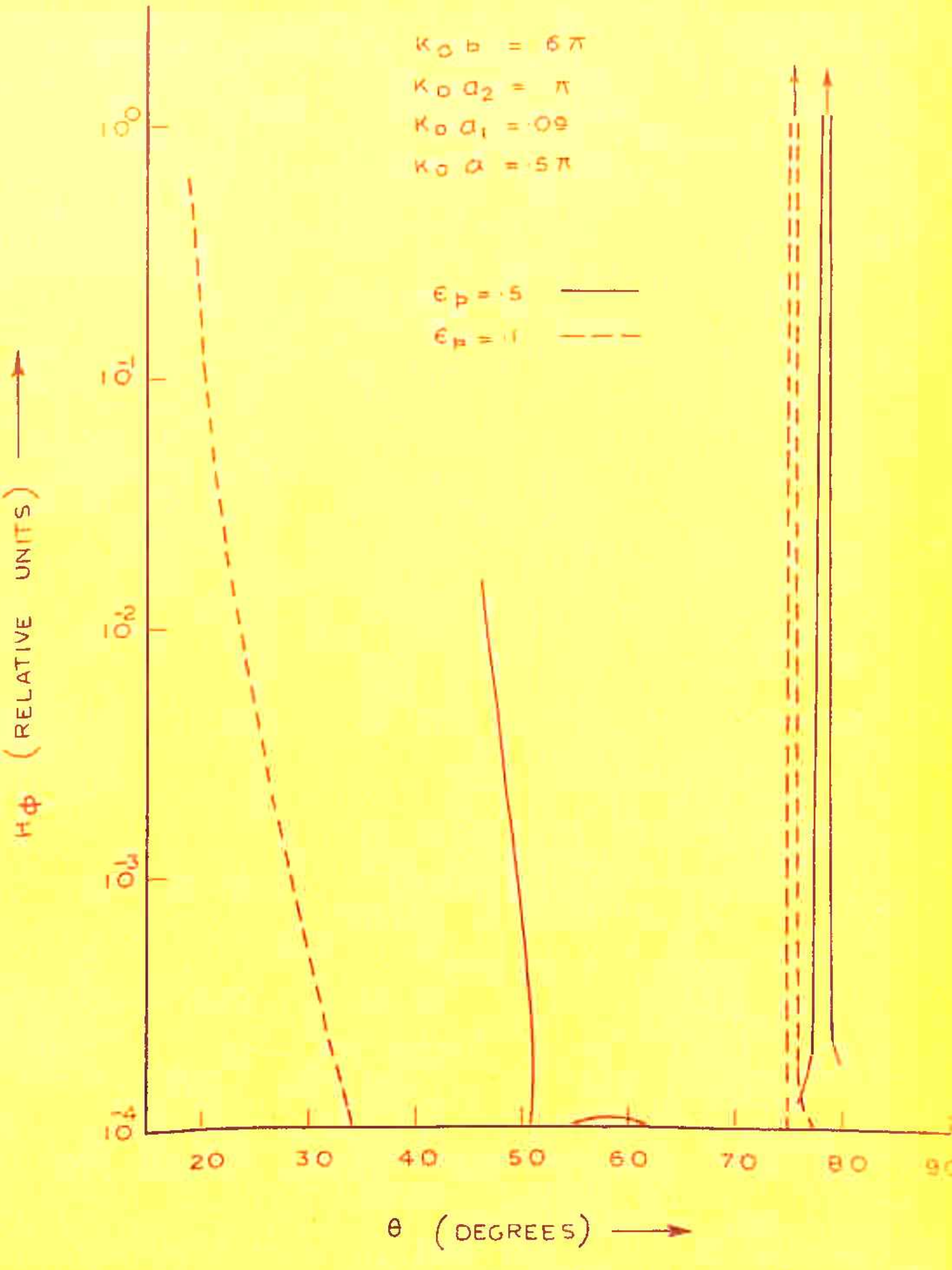

$K_o b = 6\pi$
$K_o a_2 = \pi$
$K_o a_1 = \cdot 09$
$K_o a = \cdot 5\pi$
$\epsilon_p = \cdot 5$
$\epsilon_p = 1$
$1 \cdot 0$
10^{-1}
10^{-2}
10^{-3}
10^{-4}
H_ϕ (RELATIVE UNITS)
20
30
40
50
60
70
80
90
θ (DEGREES)

FIG. – 3·2

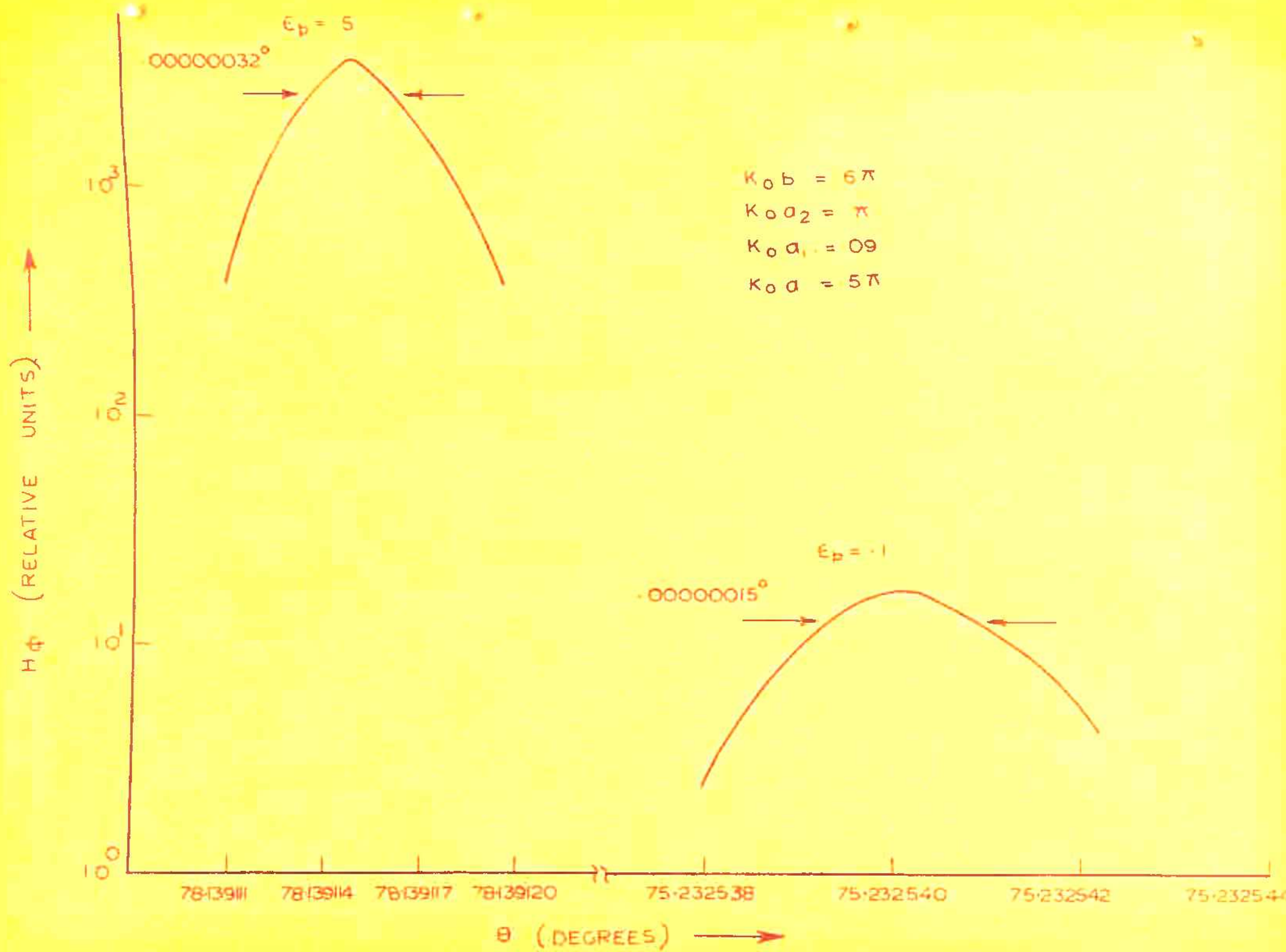

Hφ (RELATIVE UNITS)
10^3
10^2
10^1
10^0
εp = 5
.00000032°
εp = .1
.00000015°
Ko b = 6π
Ko a2 = π
Ko a1 = 09
Ko a = 5π
78.139111
78.139114
78.139117
78.139120
75.232538
75.232540
75.232542
75.232544
θ (DEGREES)

FIG.-3.3

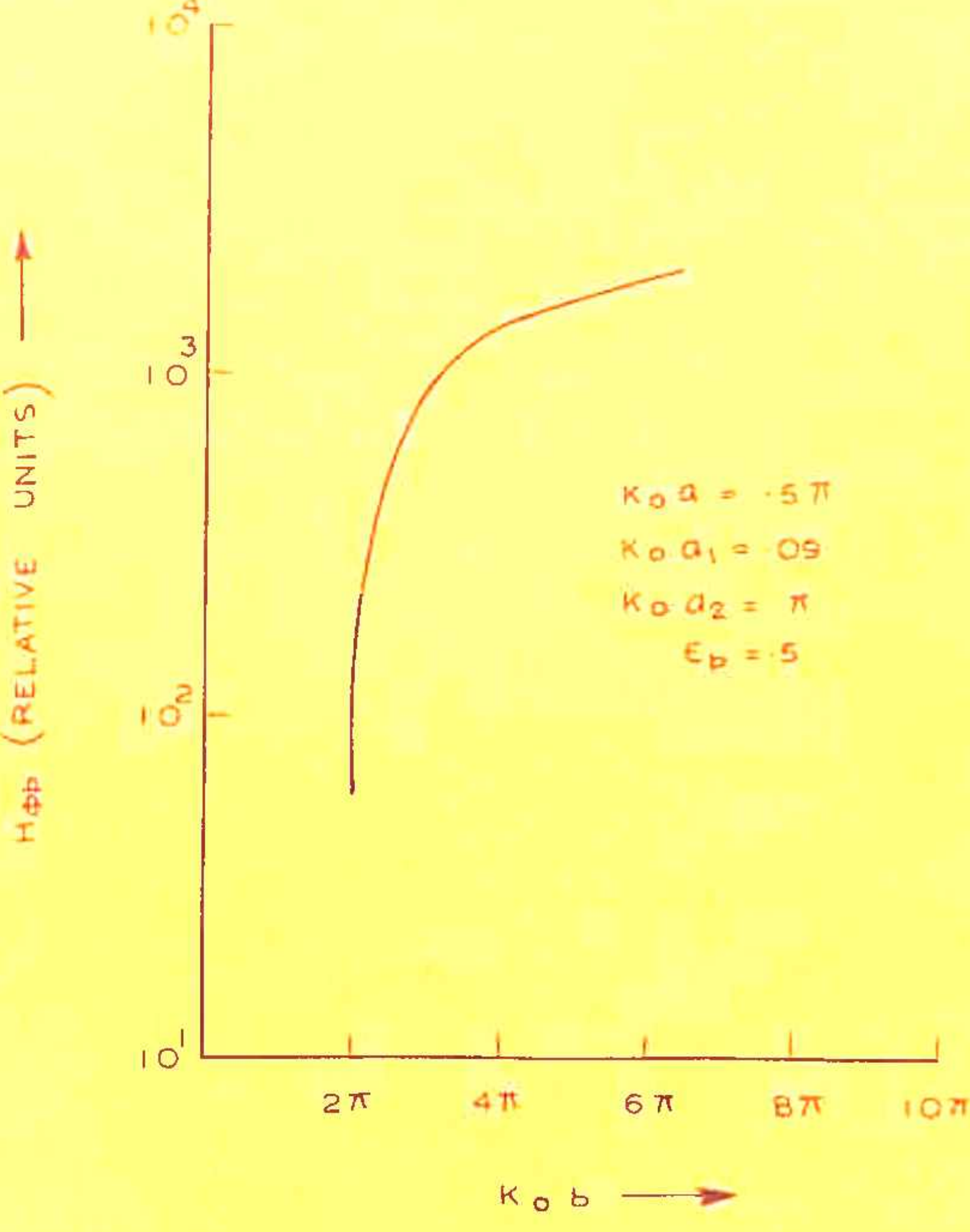

10^4
10^3
10^2
10^1
$H_{\phi p}$ (RELATIVE UNITS)
$K_0 a = \cdot 5\pi$
$K_0 a_1 = \cdot 09$
$K_0 a_2 = \pi$
$\epsilon_p = \cdot 5$
2π
4π
6π
8π
10π
$K_0 b$

FIG. – 3·4

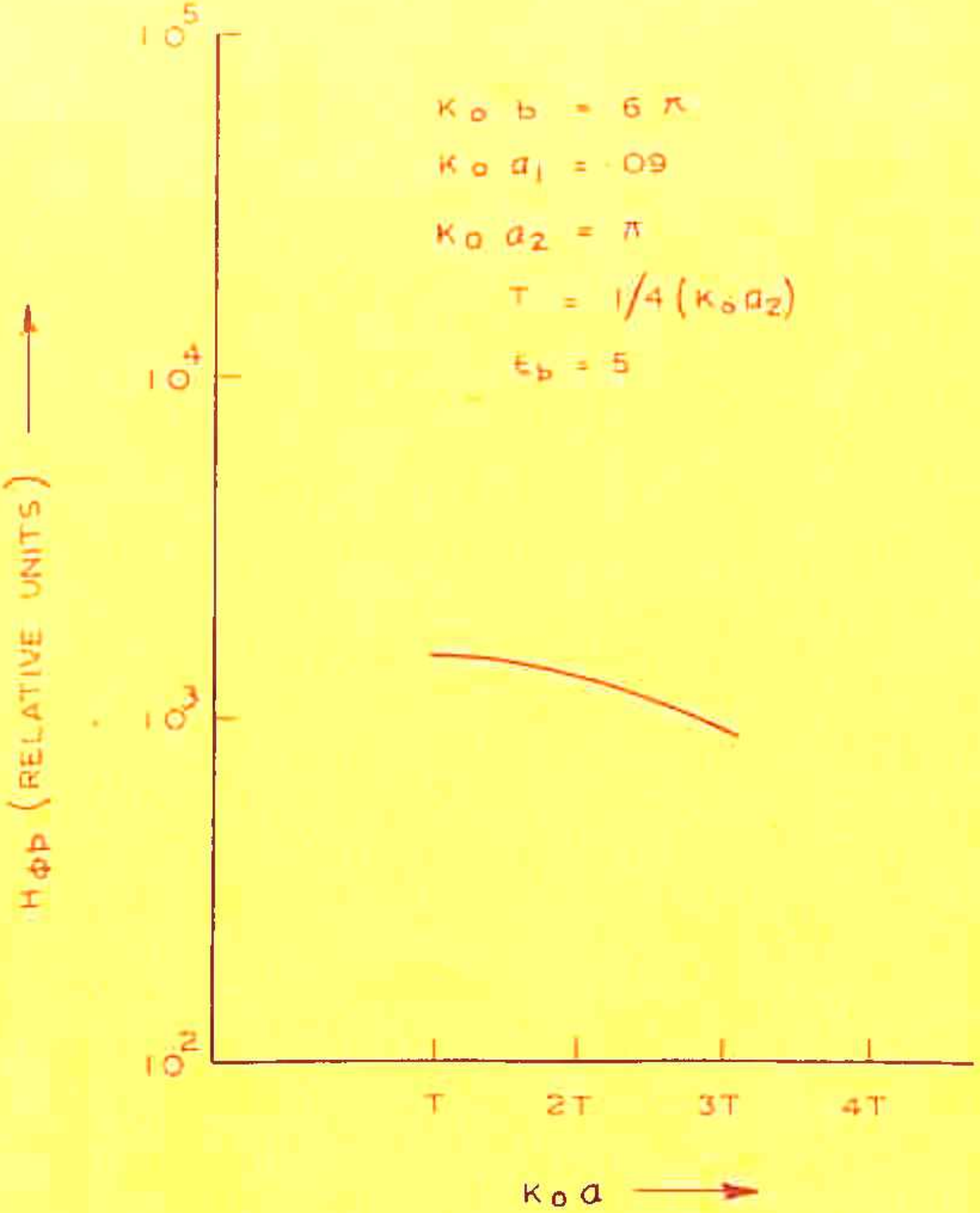

10^5
10^4
10^3
10^2
$K_0 b = 6\pi$
$K_0 a_1 = \cdot 09$
$K_0 a_2 = \pi$
$T = 1/4 (K_0 a_2)$
$\epsilon_b = 5$
$H_{\phi b}$ (RELATIVE UNITS)
T
2T
3T
4T
$K_0 a$

FIG.-3·5

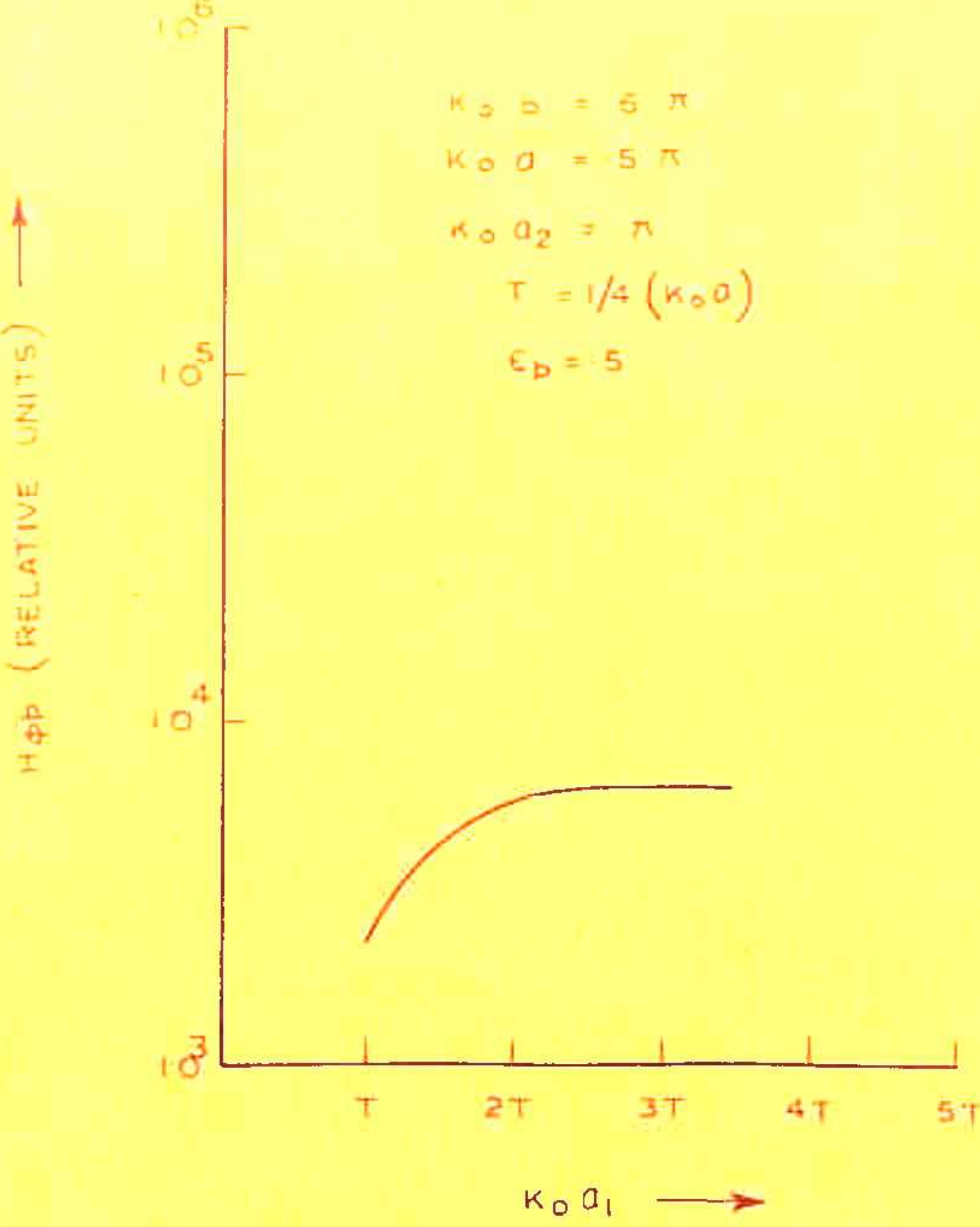

$K_0 b = 6\pi$
$K_0 a = 5\pi$
$K_0 a_2 = \pi$
$T = 1/4 (K_0 a)$
$\epsilon_b = 5$
$H_{\phi b}$ (RELATIVE UNITS)
10^6
10^5
10^4
10^3
T
2T
3T
4T
5T
$K_0 a_1$

FIG.-3·6

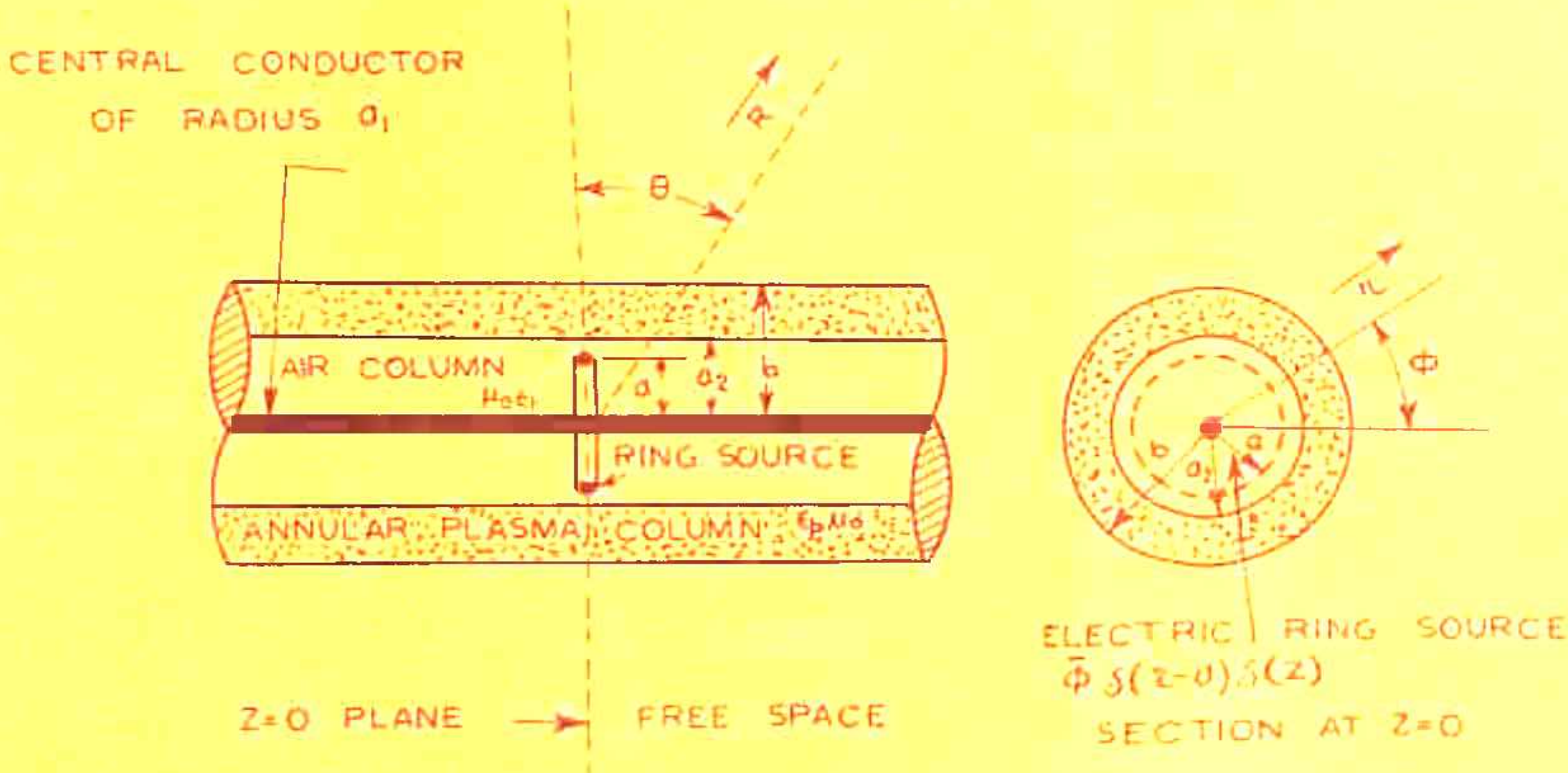
CENTRAL CONDUCTOR
OF RADIUS a_1
AIR COLUMN
$\mu_0\epsilon_1$
RING SOURCE
ANNULAR PLASMA COLUMN $\epsilon_p\mu_0$
θ
R
a
a_2
b
Z=0 PLANE
FREE SPACE
Φ
ELECTRIC RING SOURCE
$\bar{\Phi}\,\delta(r-a)\,\delta(z)$
SECTION AT Z=0

FIG. - 37

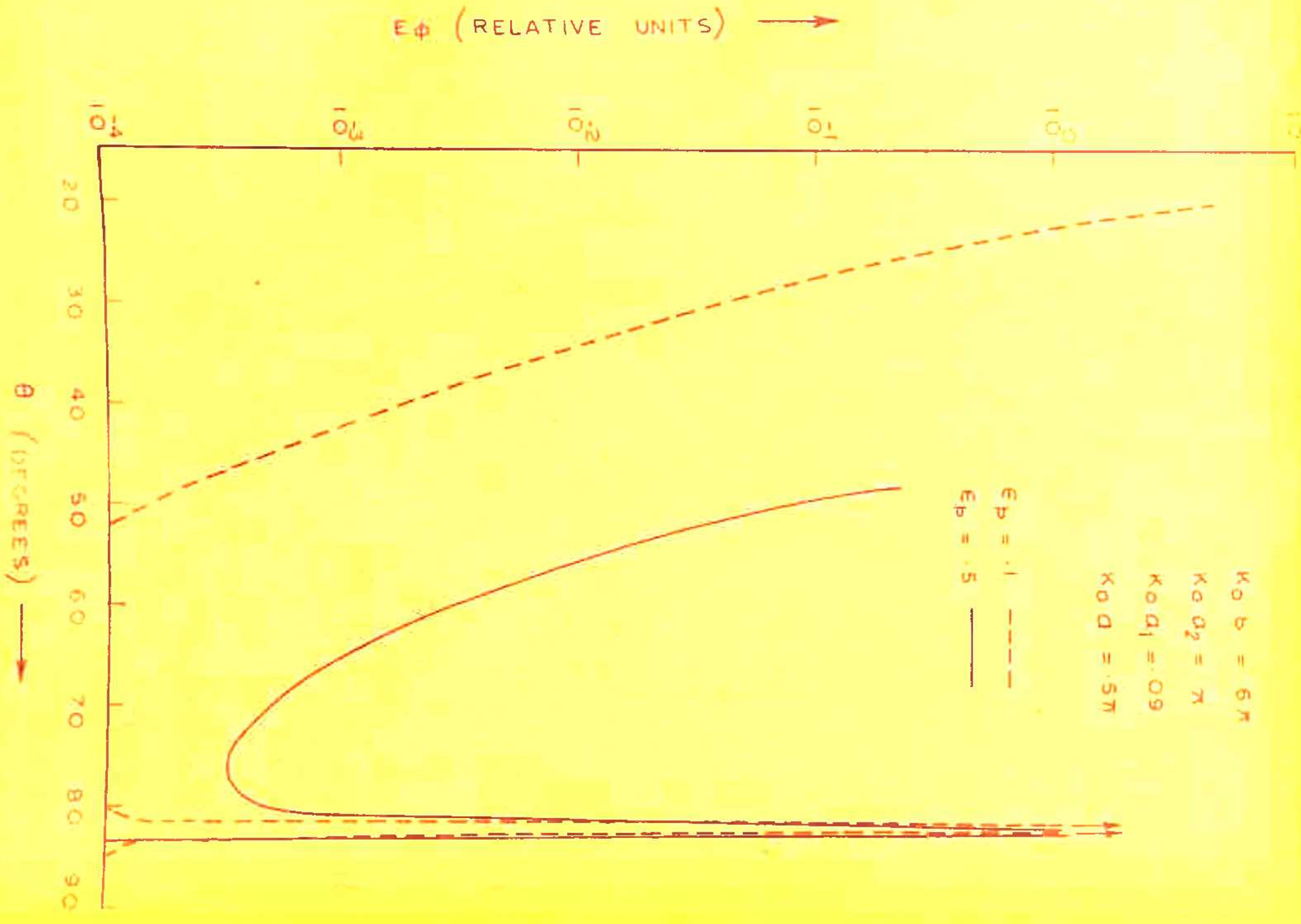
Eφ (RELATIVE UNITS)
θ (DEGREES)
20
30
40
50
60
70
80
90
10^{-4}
10^{-3}
10^{-2}
10^{-1}
10^{0}
10^{1}
Ep = .1
Ep = .5
Ko b = 6π
Ko a2 = π
Ko a1 = .09
Ko a = .5π

FIG. 8

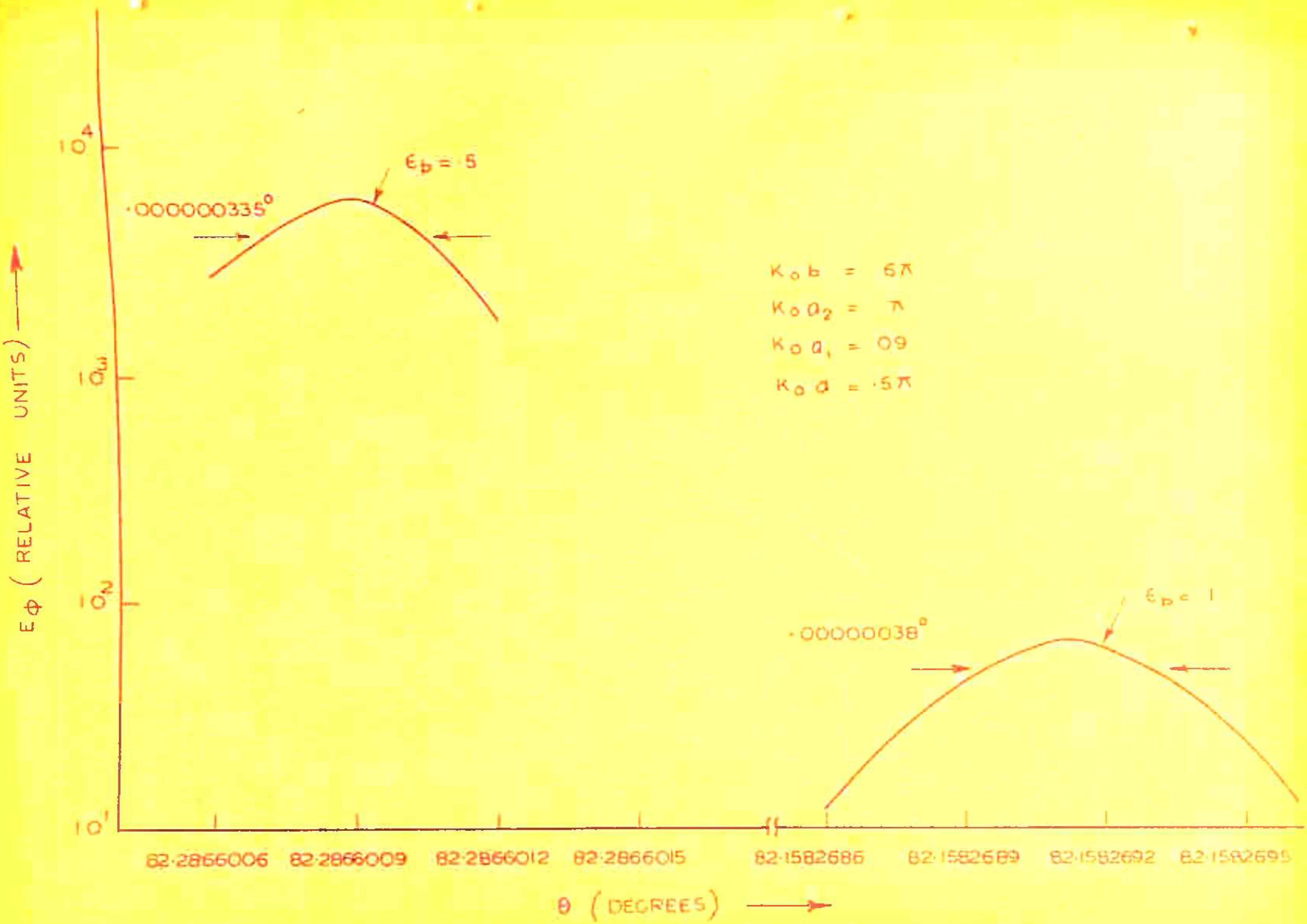

Eφ (RELATIVE UNITS)
10⁴
10³
10²
10¹
·000000335°
εb = 5
·00000038°
εb = 1
K₀b = 6π
K₀a₂ = π
K₀a₁ = 09
K₀a = ·5π
82·2866006
82·2866009
82·2866012
82·2866015
82·1582686
82·1582689
82·1582692
82·1582695
θ (DEGREES)

FIG. - 3·9

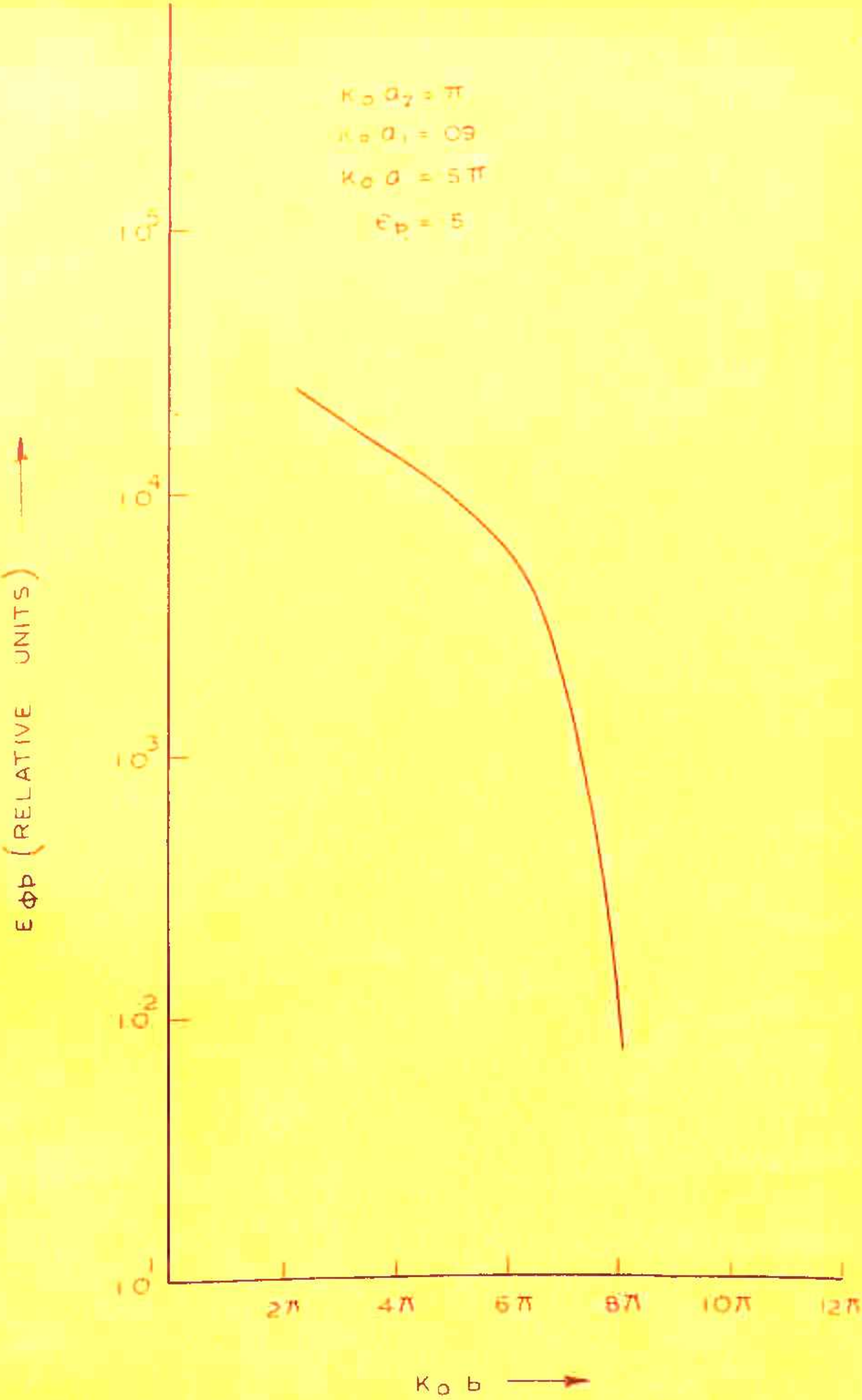

K₀ a₂ = π
K₀ a₁ = 0.9
K₀ a = 5π
εp = 5
10^5
10^4
10^3
10^2
10^1
EΦp (RELATIVE UNITS)
2π
4π
6π
8π
10π
12π
K₀ b

FIG. - 3·10

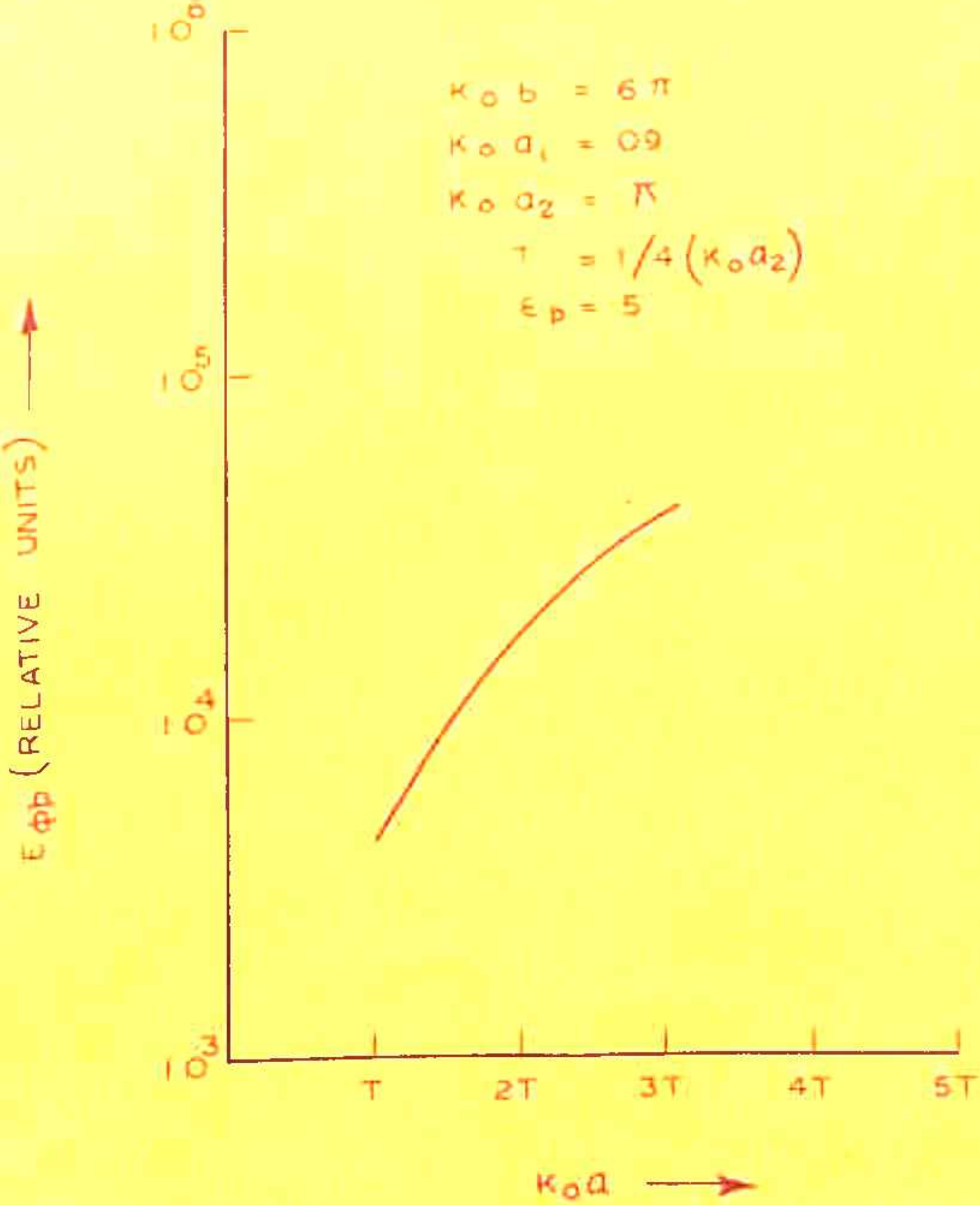

10^6
10^5
10^4
10^3
$K_0 b = 6\pi$
$K_0 a_1 = 0.9$
$K_0 a_2 = \pi$
$T = 1/4 (K_0 a_2)$
$\epsilon_p = 5$
$E_{\phi p}$ (RELATIVE UNITS)
T
2T
3T
4T
5T
$K_0 a$

FIG.-3.11

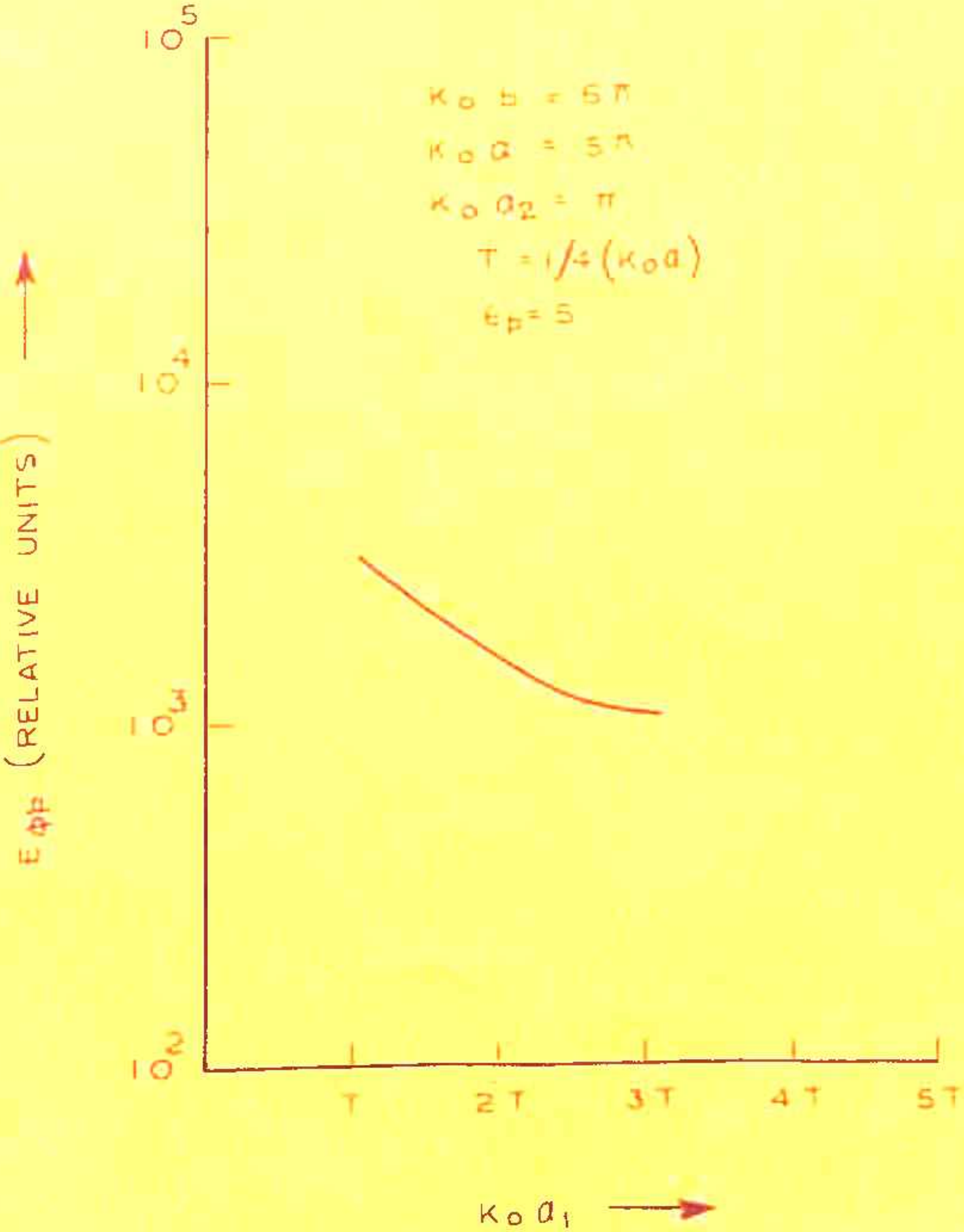

10^5
10^4
10^3
10^2
$K_o b = 5\pi$
$K_o a = 5\pi$
$K_o a_2 = \pi$
$T = 1/4 (K_o a)$
$\epsilon_p = 5$
$E_{\phi p}$ (RELATIVE UNITS)
T
2T
3T
4T
5T
$K_o a_1$

FIG. - 3·12

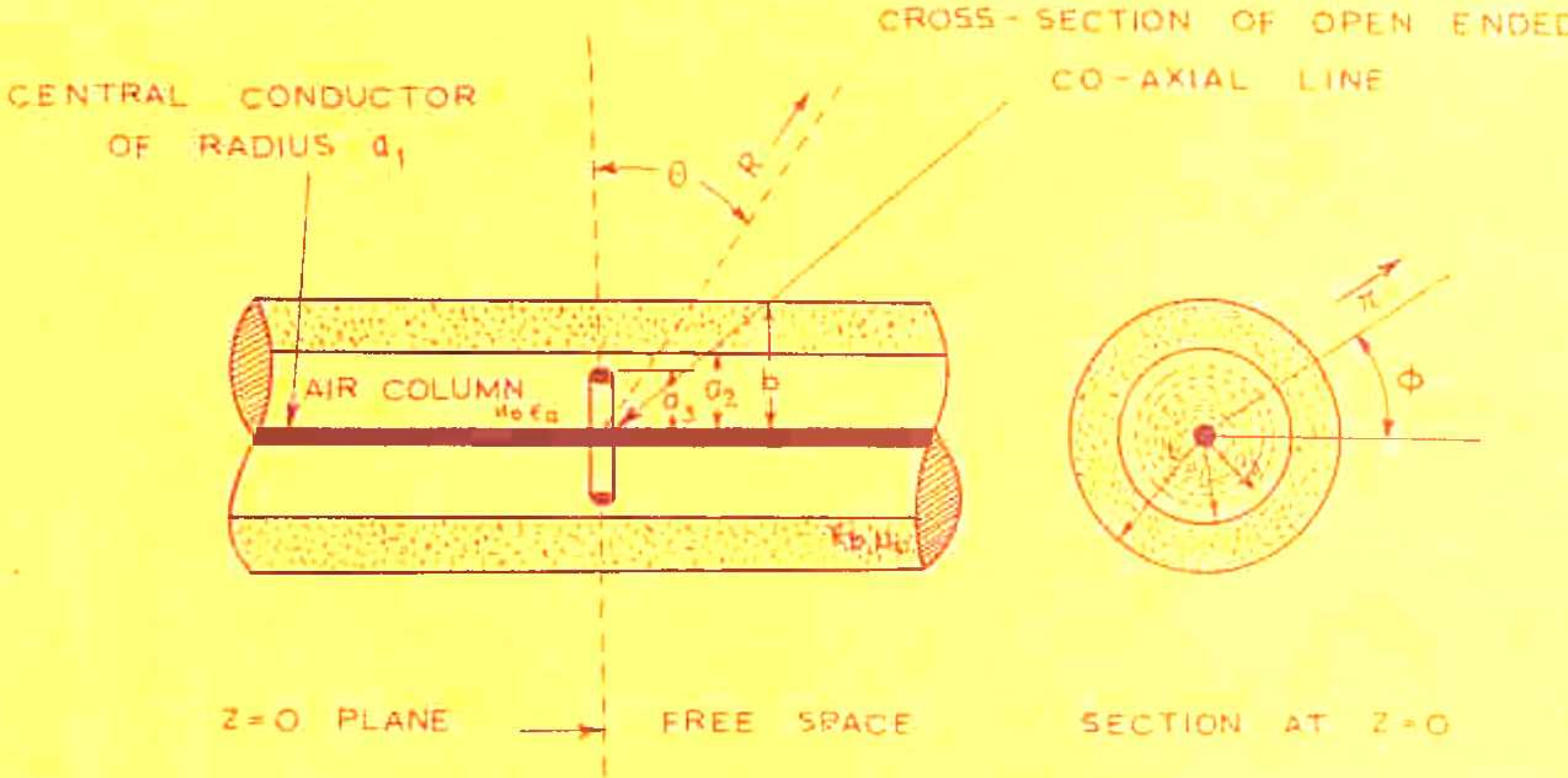
CROSS-SECTION OF OPEN ENDED
CO-AXIAL LINE
CENTRAL CONDUCTOR
OF RADIUS a_1
θ
R
AIR COLUMN
a_3
a_2
b
ϕ
Z=O PLANE
FREE SPACE
SECTION AT Z=O

FIG. -3.13

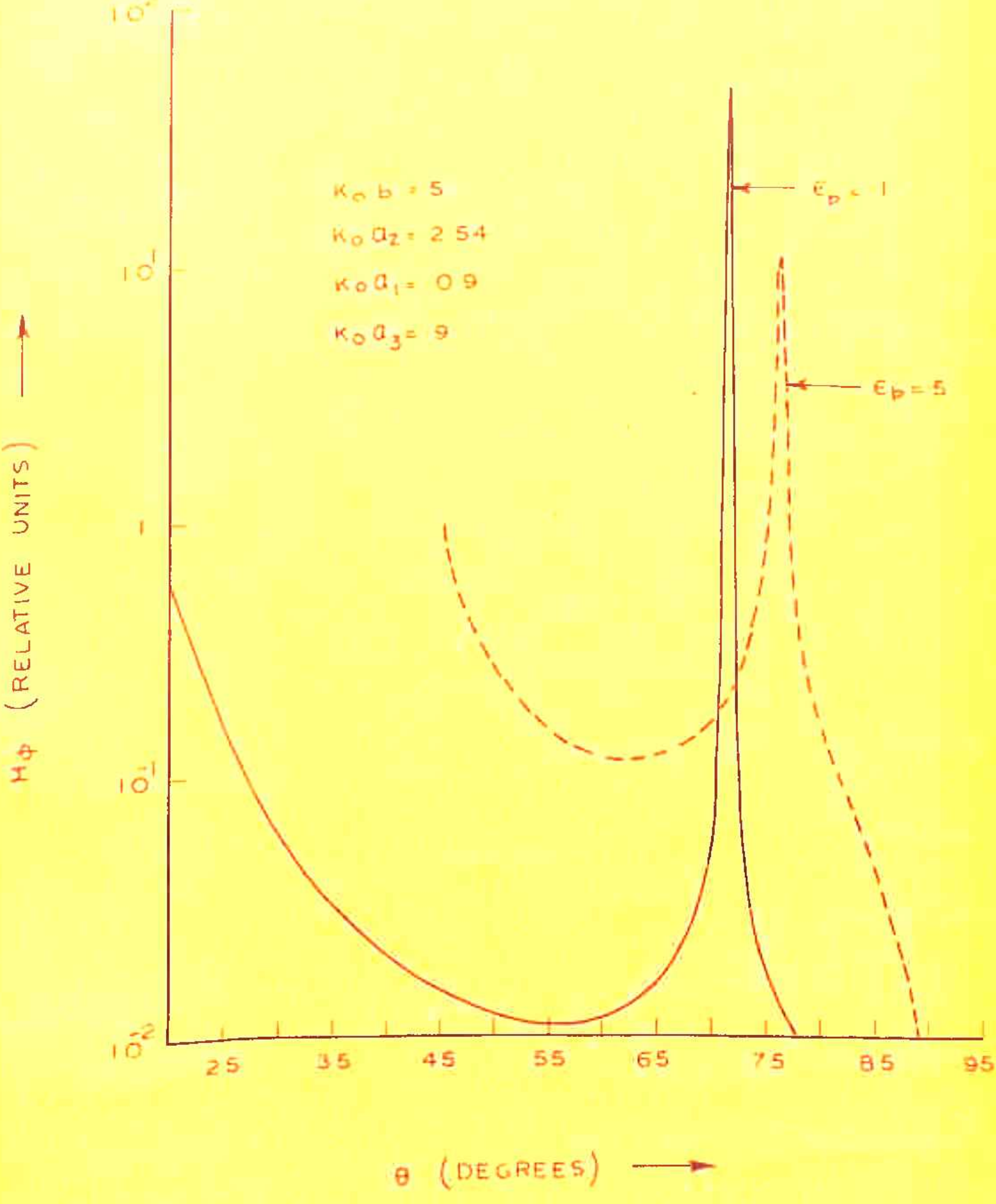
10^2
10^1
1
10^{-1}
10^{-2}
$K_0 b = 5$
$K_0 a_2 = 2.54$
$K_0 a_1 = 0.9$
$K_0 a_3 = 9$
$\epsilon_p = 1$
$\epsilon_p = 5$
H_ϕ (RELATIVE UNITS)
25
35
45
55
65
75
85
95
θ (DEGREES)

FIG. -3·14

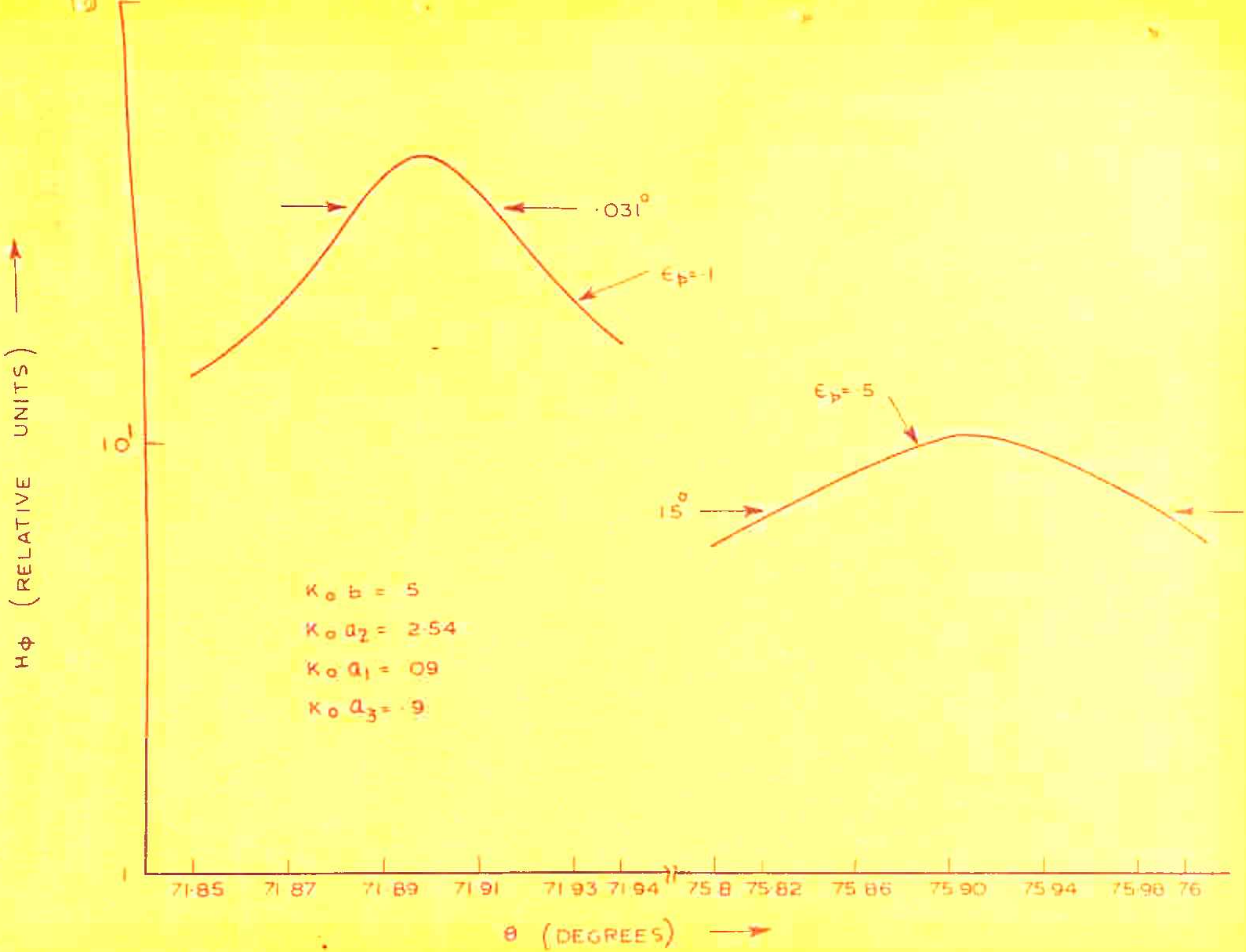
·031°
εp=·1
εp=·5
15°
Ko b = 5
Ko a2 = 2·54
Ko a1 = ·09
Ko a3 = ·9
10¹
1
71·85
71·87
71·89
71·91
71·93
71·94
75·8
75·82
75·86
75·90
75·94
75·98
76
Hφ (RELATIVE UNITS)
θ (DEGREES)

FIG -3·15

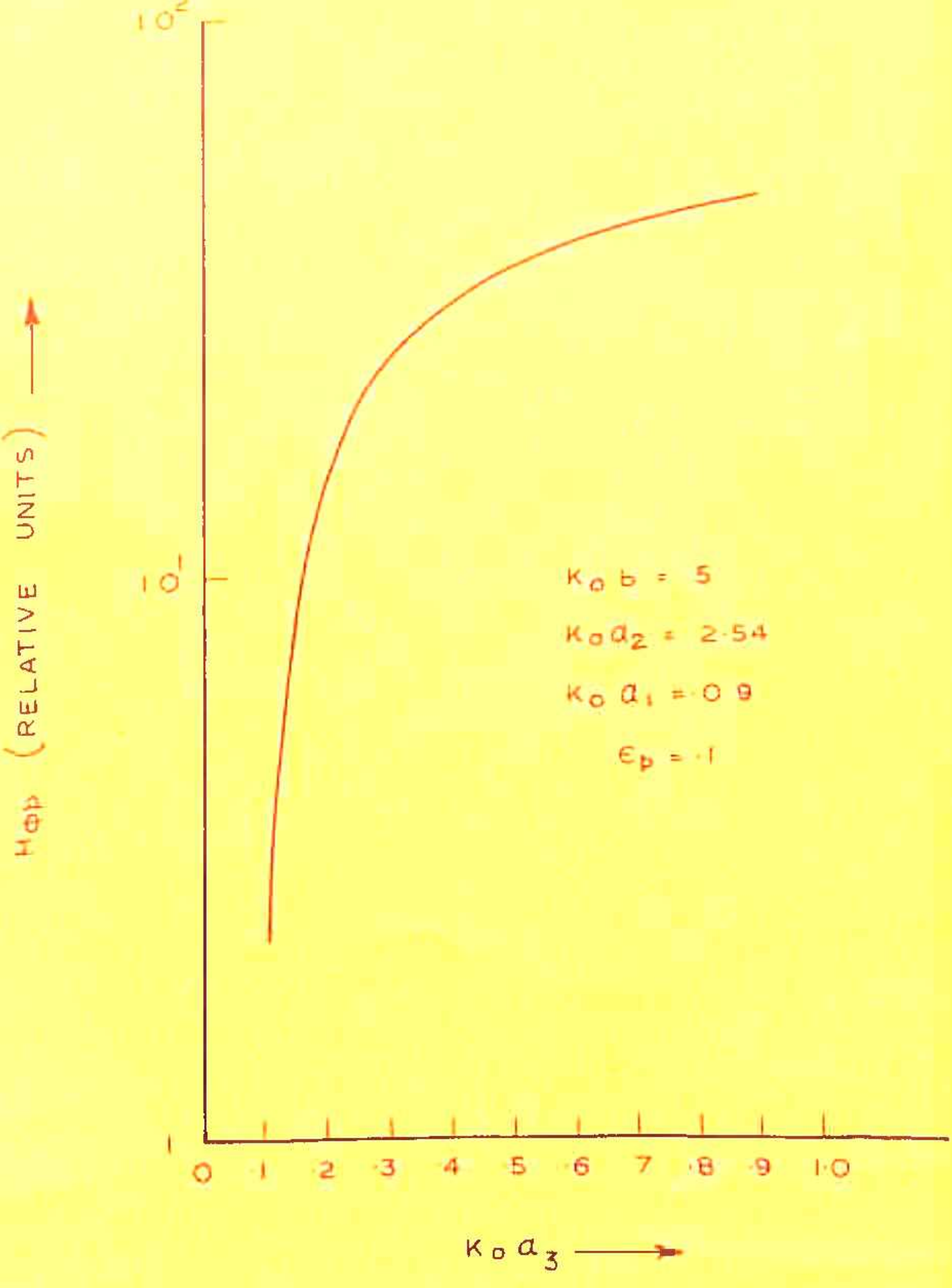
10^2
10^1
1
$H_{\phi p}$ (RELATIVE UNITS)
$K_0 b = 5$
$K_0 a_2 = 2{\cdot}54$
$K_0 a_1 = 0{\cdot}9$
$\epsilon_p = {\cdot}1$
0 ·1 ·2 ·3 ·4 ·5 ·6 ·7 ·8 ·9 1·0
$K_0 a_3$

FIG. 3·16

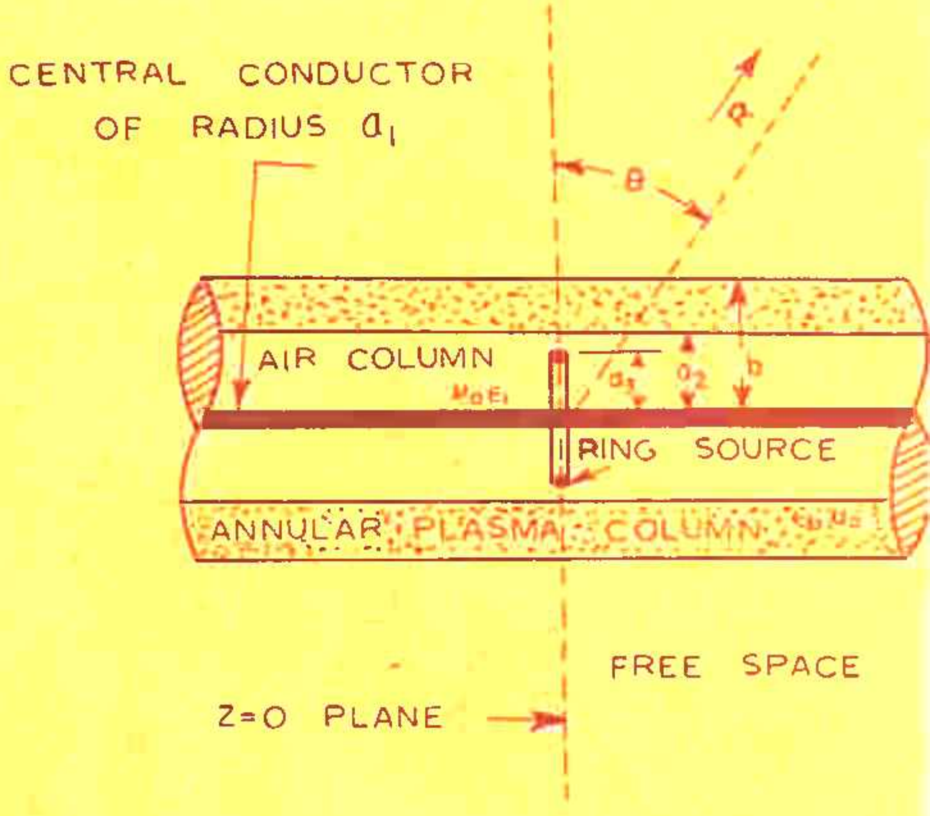

CENTRAL CONDUCTOR
OF RADIUS a_1
θ
AIR COLUMN
a_1
a_2
b
RING SOURCE
ANNULAR PLASMA COLUMN
FREE SPACE
Z=O PLANE

FIG - 3

CROSS SECTION OF OPEN ENDED CO-AXIAL LINE

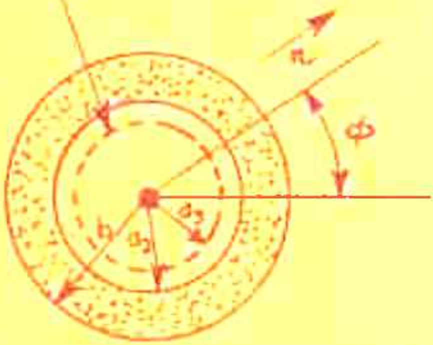

SECTION AT Z=0

-17

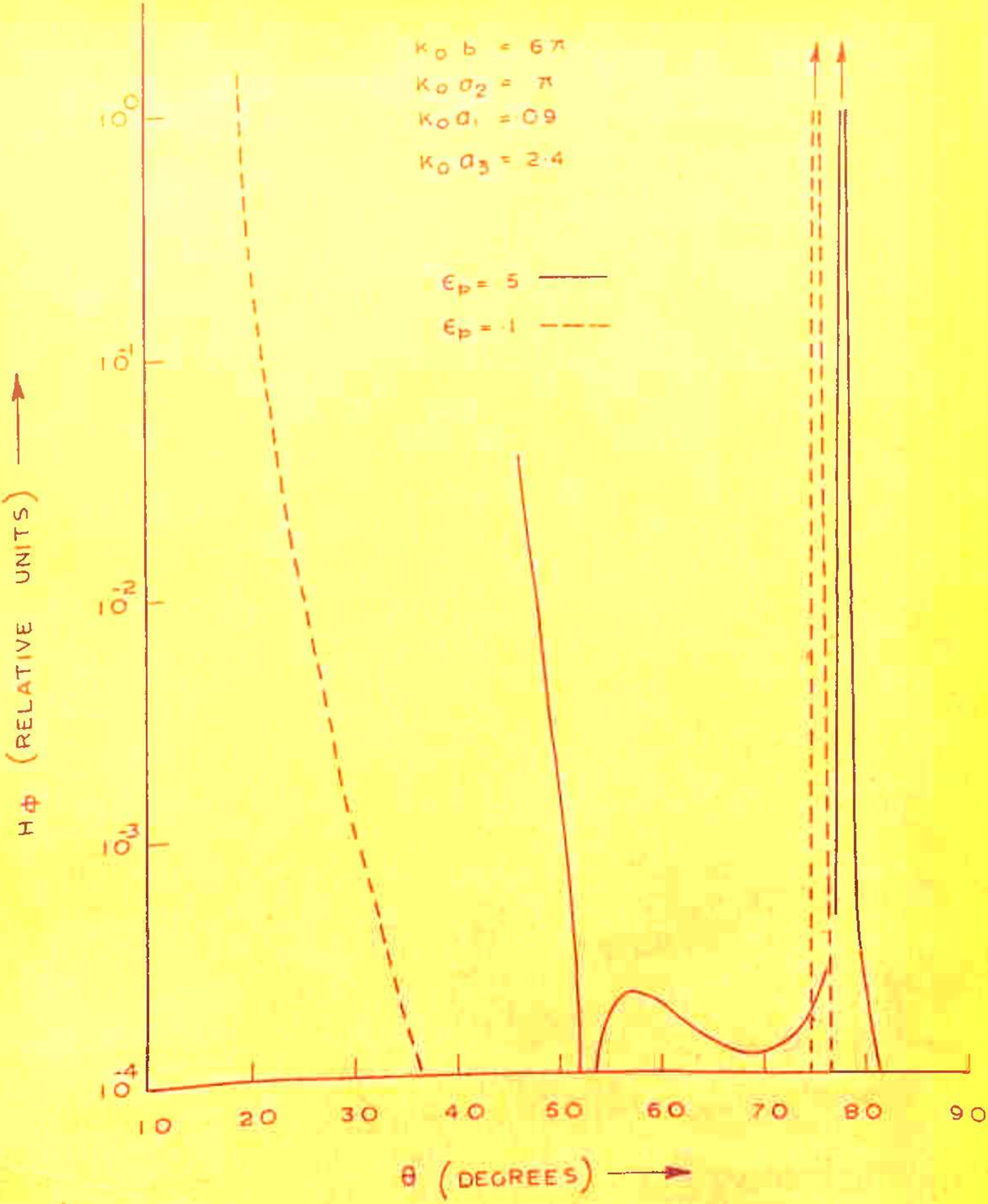

$K_0 b = 6\pi$
$K_0 a_2 = \pi$
$K_0 a_1 = 0.9$
$K_0 a_3 = 2.4$
$\epsilon_p = 5$
$\epsilon_p = 1$
10^0
10^{-1}
10^{-2}
10^{-3}
10^{-4}
H_ϕ (RELATIVE UNITS)
10
20
30
40
50
60
70
80
90
θ (DEGREES)

FIG.- 3.18

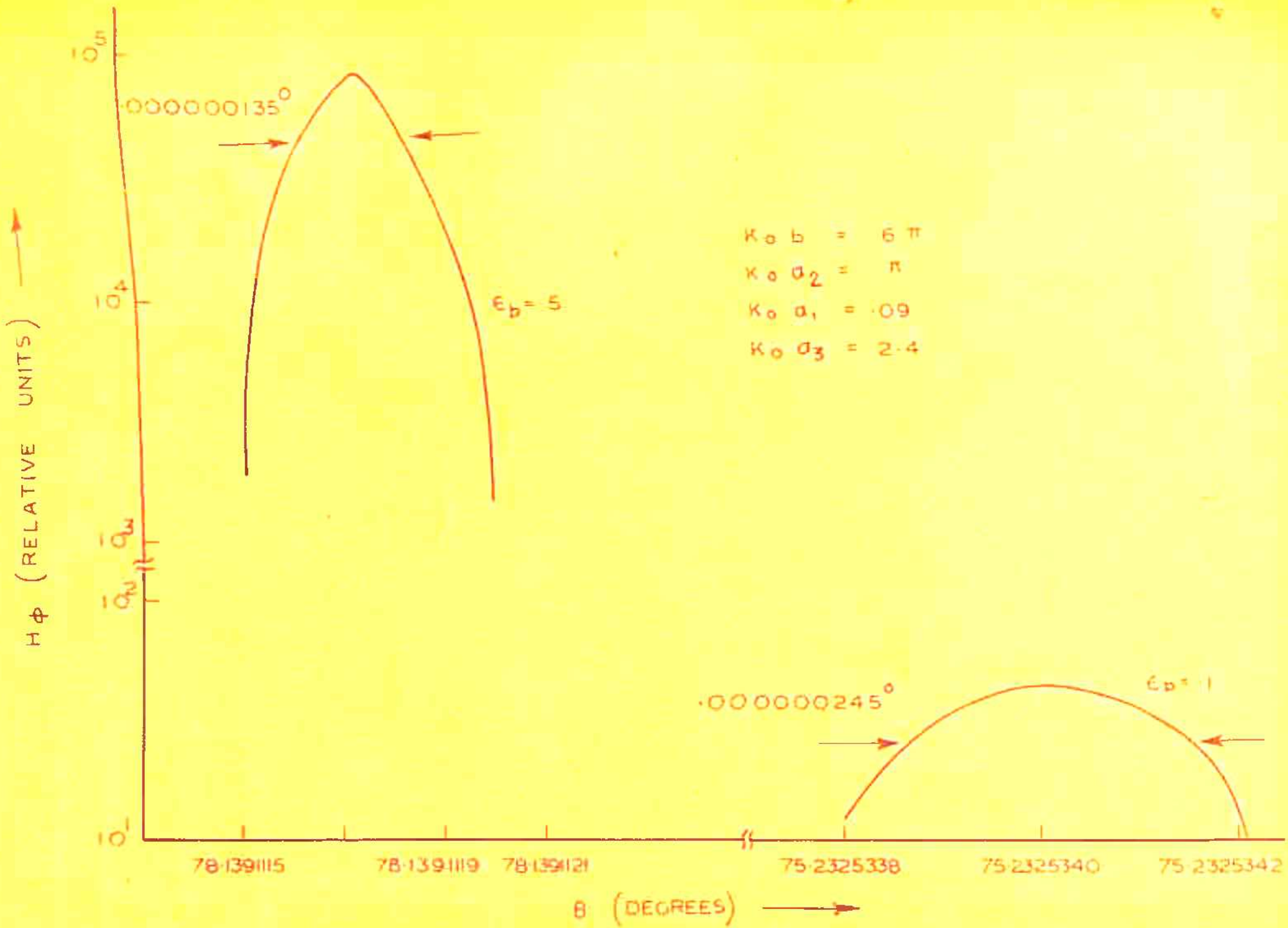

10^5
10^4
10^3
10^2
10^1
·000000135°
$\epsilon_b = 5$
$K_0 b = 6\pi$
$K_0 a_2 = \pi$
$K_0 a_1 = \cdot 09$
$K_0 a_3 = 2\cdot 4$
·000000245°
$\epsilon_b = 1$
78·139115
78·139119
78·139121
75·2325338
75·2325340
75·2325342
H φ (RELATIVE UNITS)
θ (DEGREES)

FIG. – 3·19

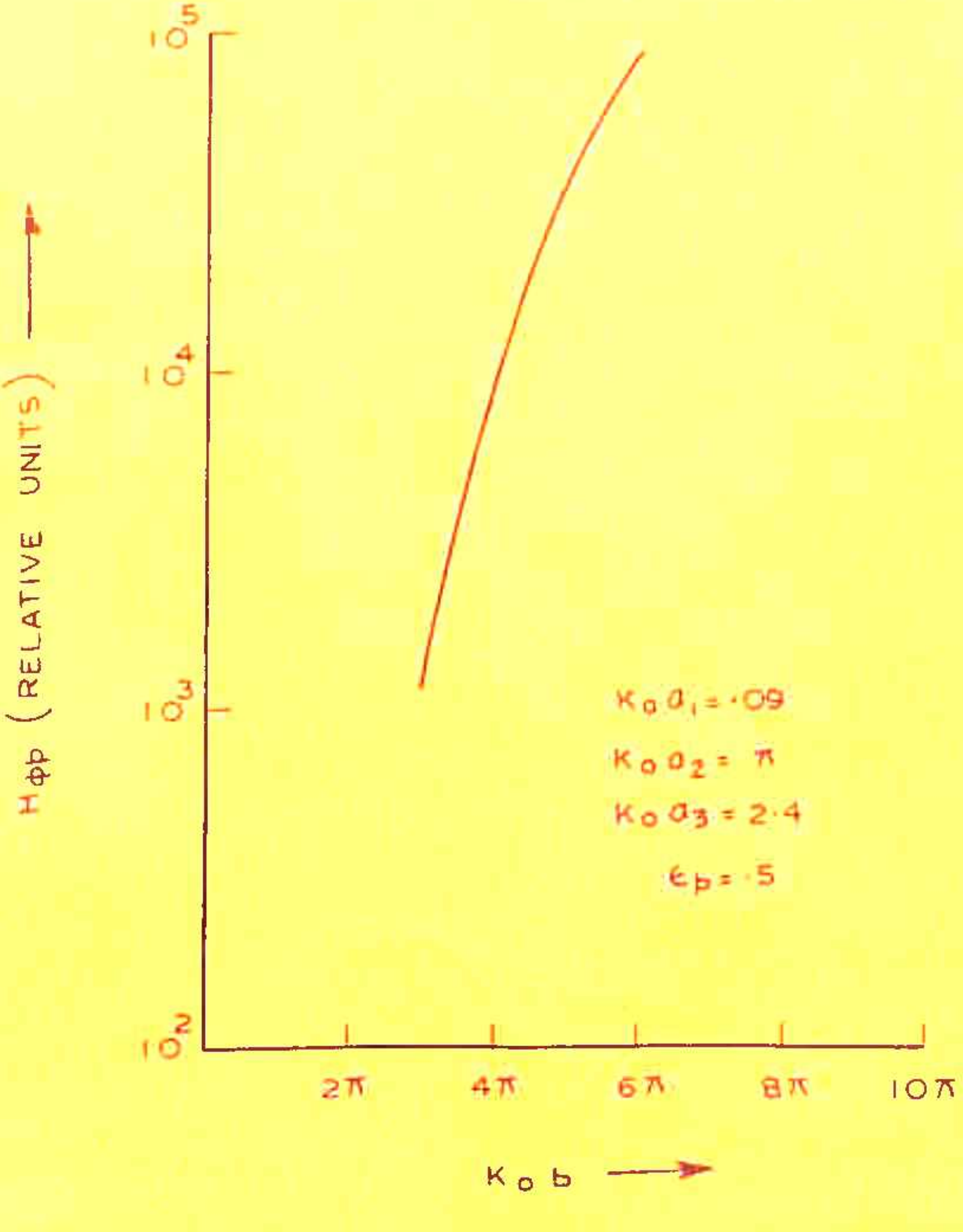

$H_{\phi p}$ (RELATIVE UNITS)
10^5
10^4
10^3
10^2
$K_0 a_1 = \cdot 09$
$K_0 a_2 = \pi$
$K_0 a_3 = 2 \cdot 4$
$\epsilon_p = \cdot 5$
2π
4π
6π
8π
10π
$K_0 b$

FIG. -3·20

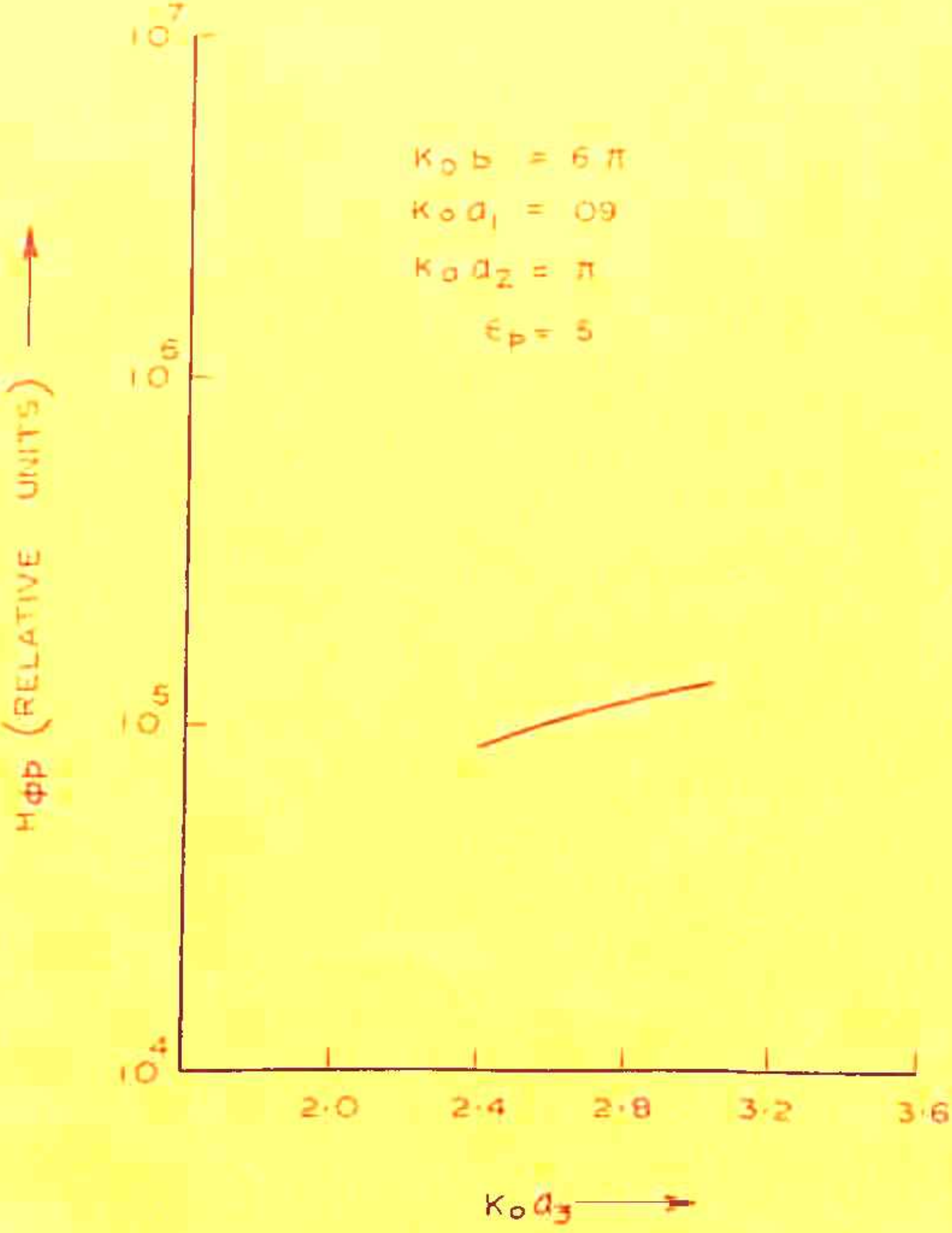

10^7
10^6
10^5
10^4
$H_{\phi P}$ (RELATIVE UNITS)
$K_0 b = 6\pi$
$K_0 a_1 = 09$
$K_0 a_2 = \pi$
$\epsilon_p = 5$
2.0
2.4
2.8
3.2
3.6
$K_0 a_3$

FIG. – 3·21

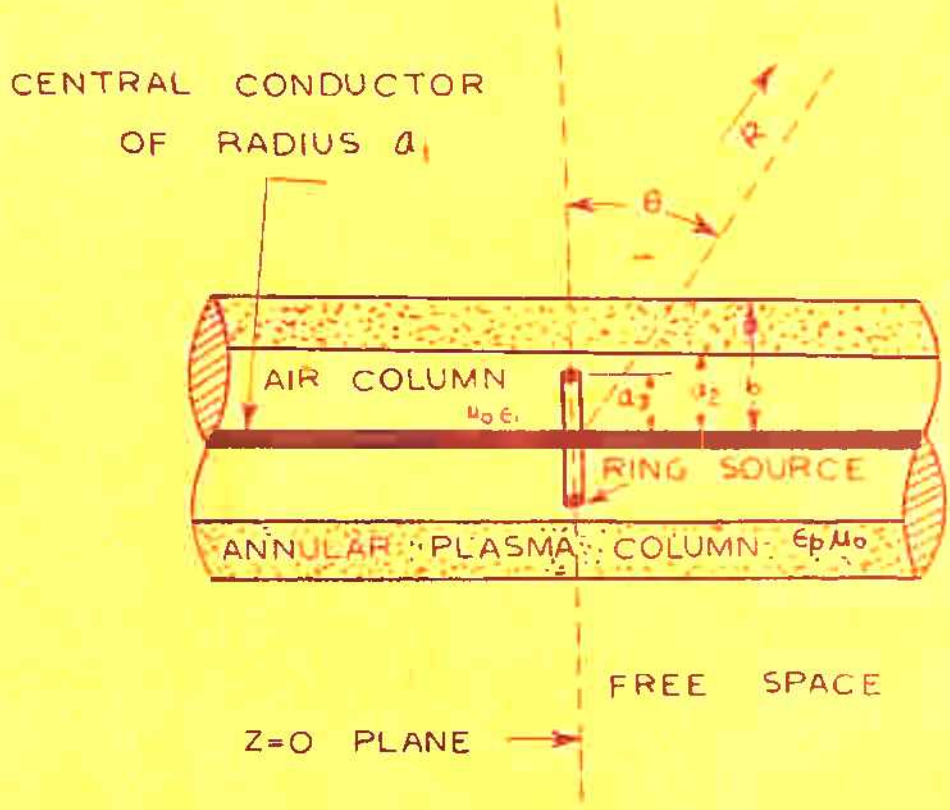
CENTRAL CONDUCTOR
OF RADIUS a_1
AIR COLUMN
$\mu_0 \epsilon_1$
RING SOURCE
ANNULAR PLASMA COLUMN $\epsilon_p \mu_0$
FREE SPACE
Z=O PLANE
θ
R
a_3
a_2
b

FIG. — 3·2

CROSS - SECTION OF OPEN EN

WAVE - GUIDE

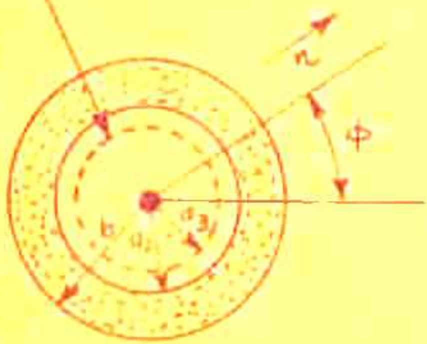

SECTION AT Z = O

22

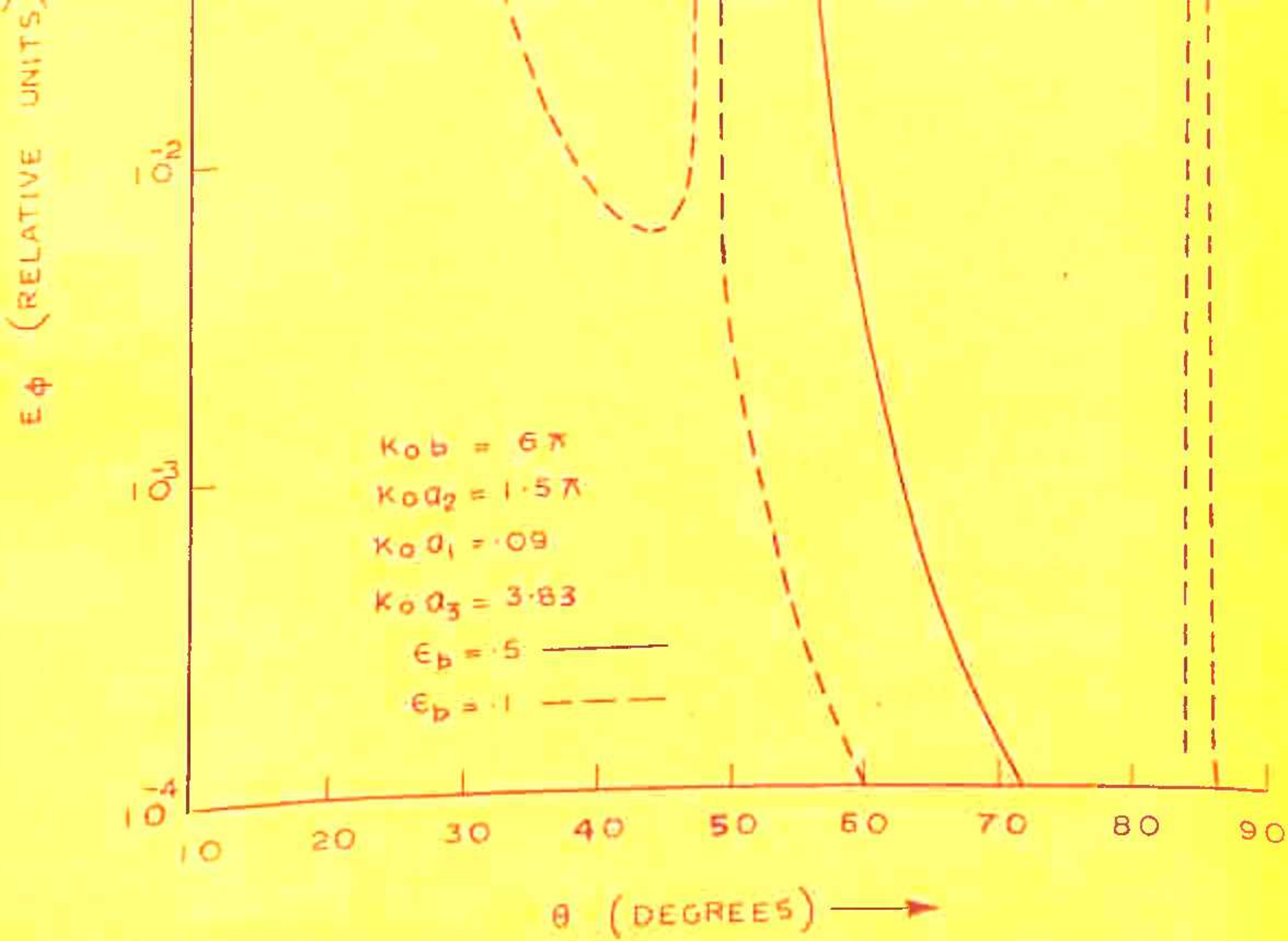
Eφ (RELATIVE UNITS)
10^{-2}
10^{-3}
10^{-4}
$K_0 b = 6\pi$
$K_0 a_2 = 1 \cdot 5\pi$
$K_0 a_1 = \cdot 09$
$K_0 a_3 = 3 \cdot 83$
$\epsilon_b = \cdot 5$
$\epsilon_b = \cdot 1$
10
20
30
40
50
60
70
80
90
θ (DEGREES)

FIG.-3·23

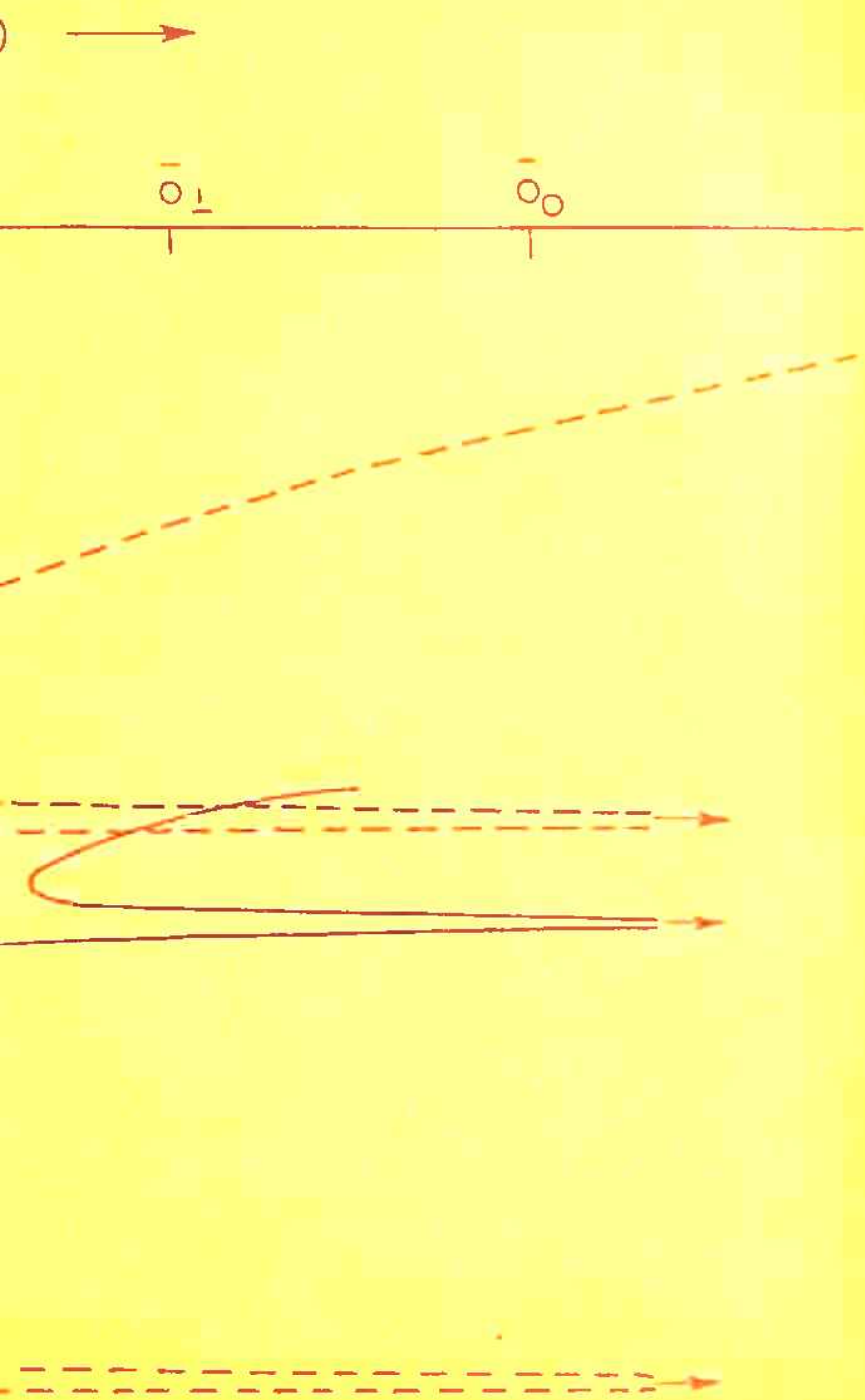

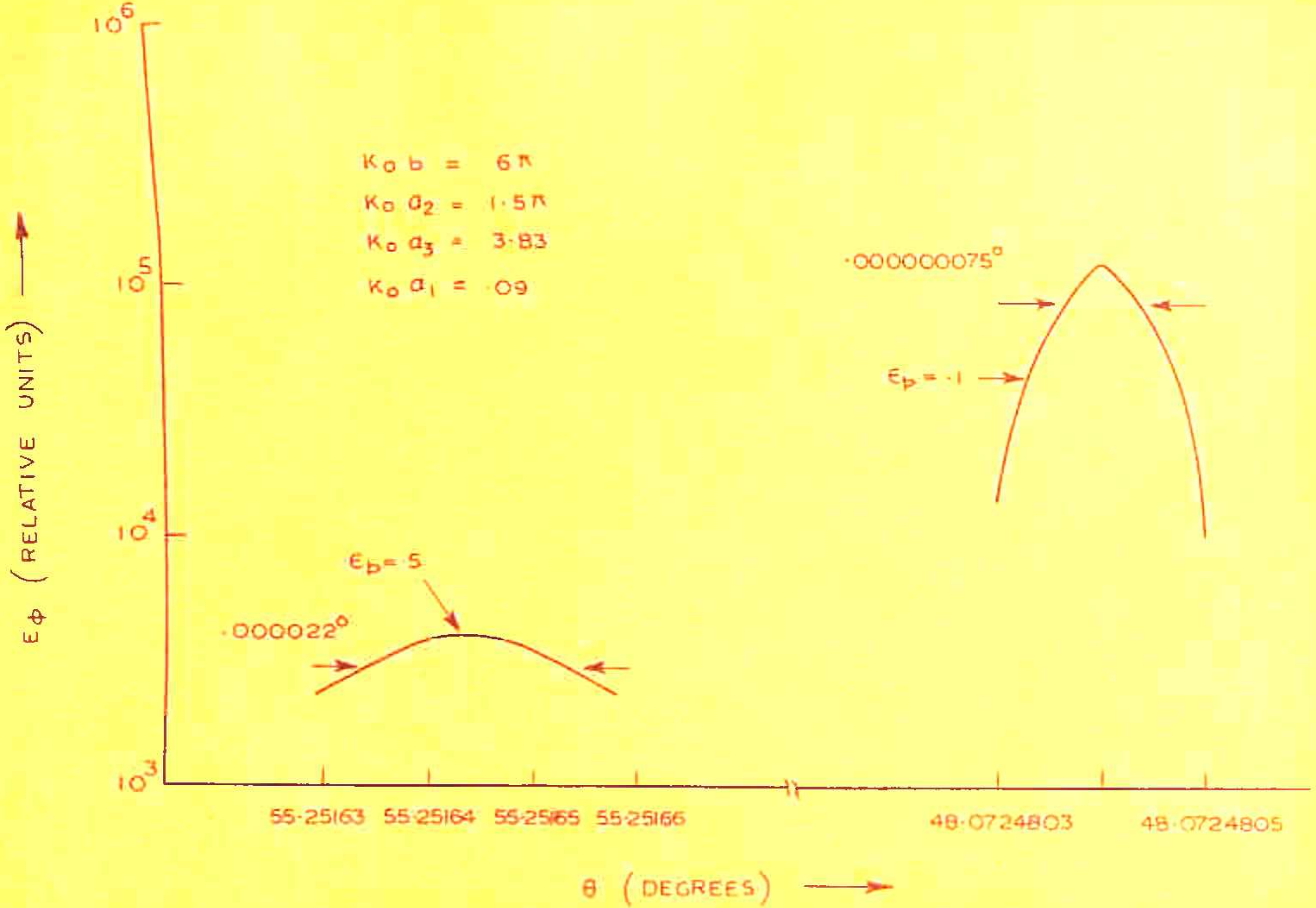

E_ϕ (RELATIVE UNITS)
10^6
10^5
10^4
10^3
$K_o b = 6\pi$
$K_o a_2 = 1.5\pi$
$K_o a_3 = 3.83$
$K_o a_1 = .09$
$\epsilon_b = .5$
$.000022^o$
$.000000075^o$
$\epsilon_b = .1$
55·25163
55·25164
55·25165
55·25166
48·0724803
48·0724805
θ (DEGREES)

FIG.-3.24

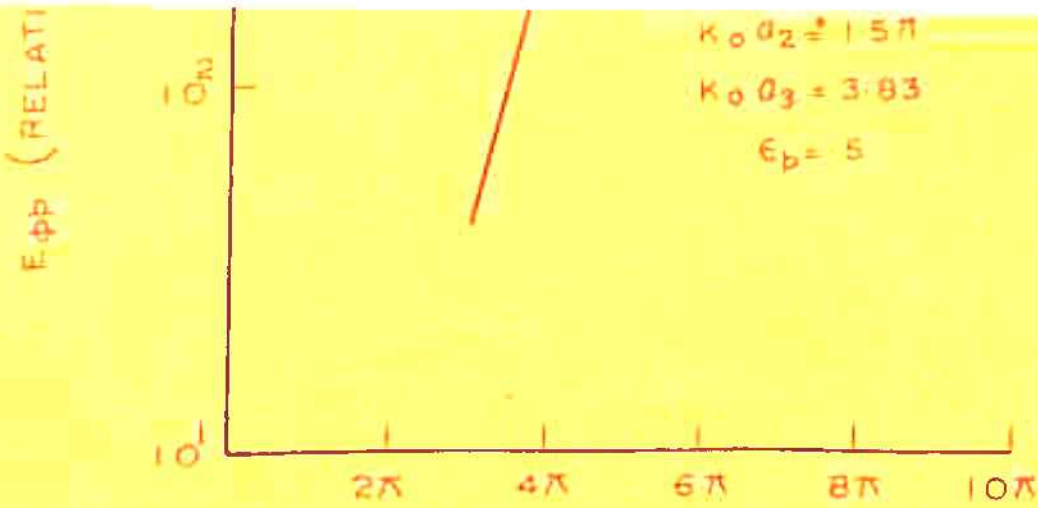

FIG. – 3.25

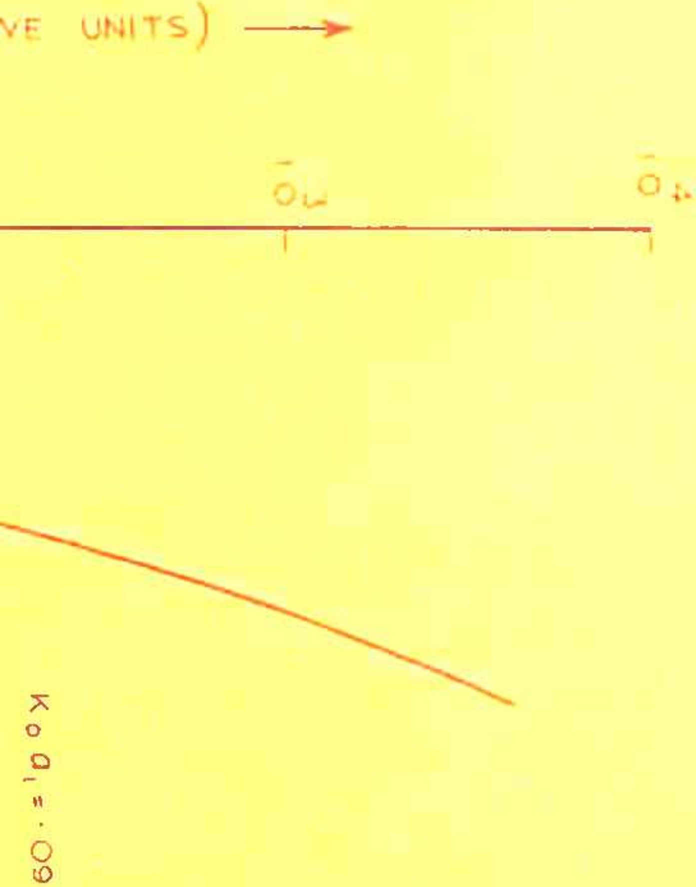
VE UNITS)

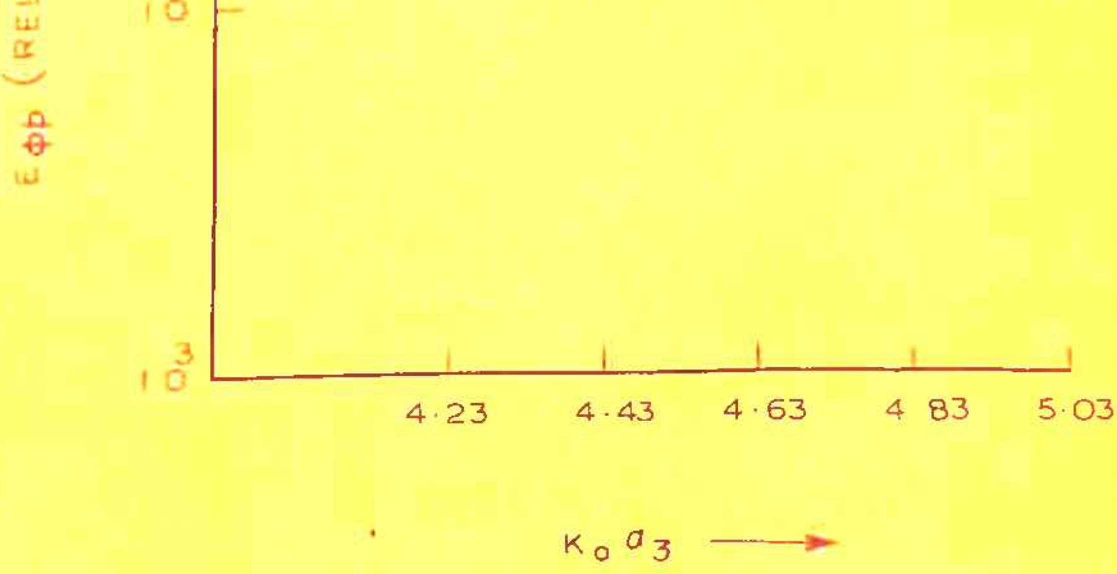

FIG. - 3·26

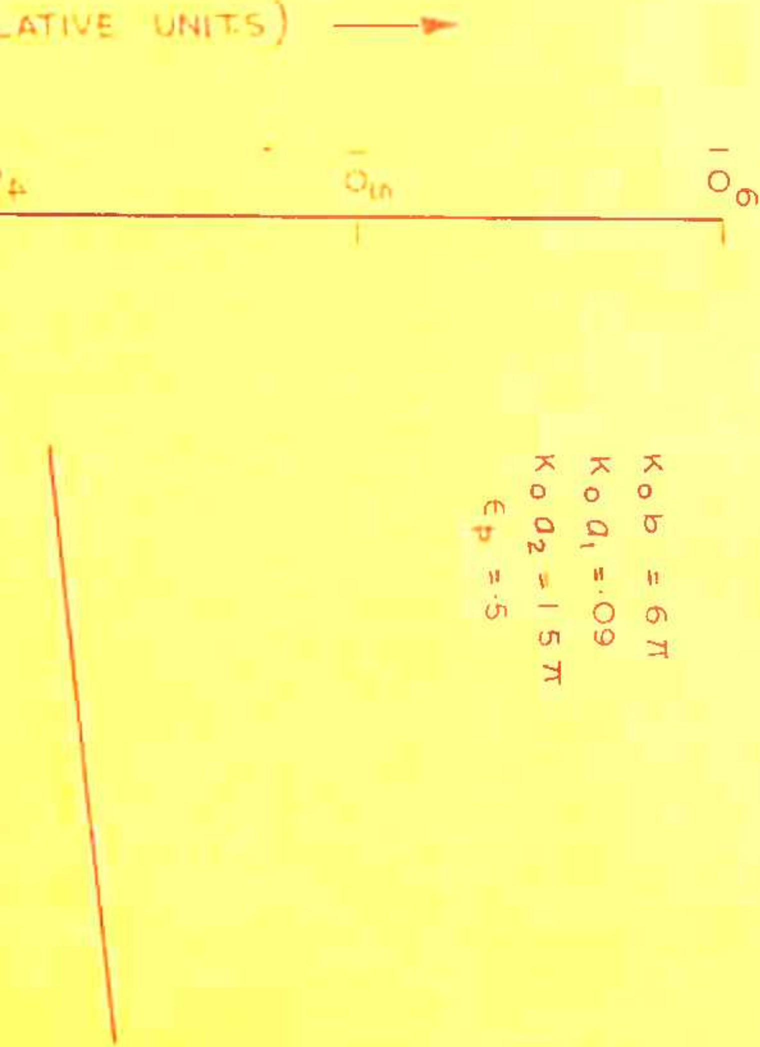

LATIVE UNITS)
$K_0 b = 6\pi$
$K_0 a_1 = .09$
$K_0 a_2 = 15\pi$
$\epsilon_p = .5$

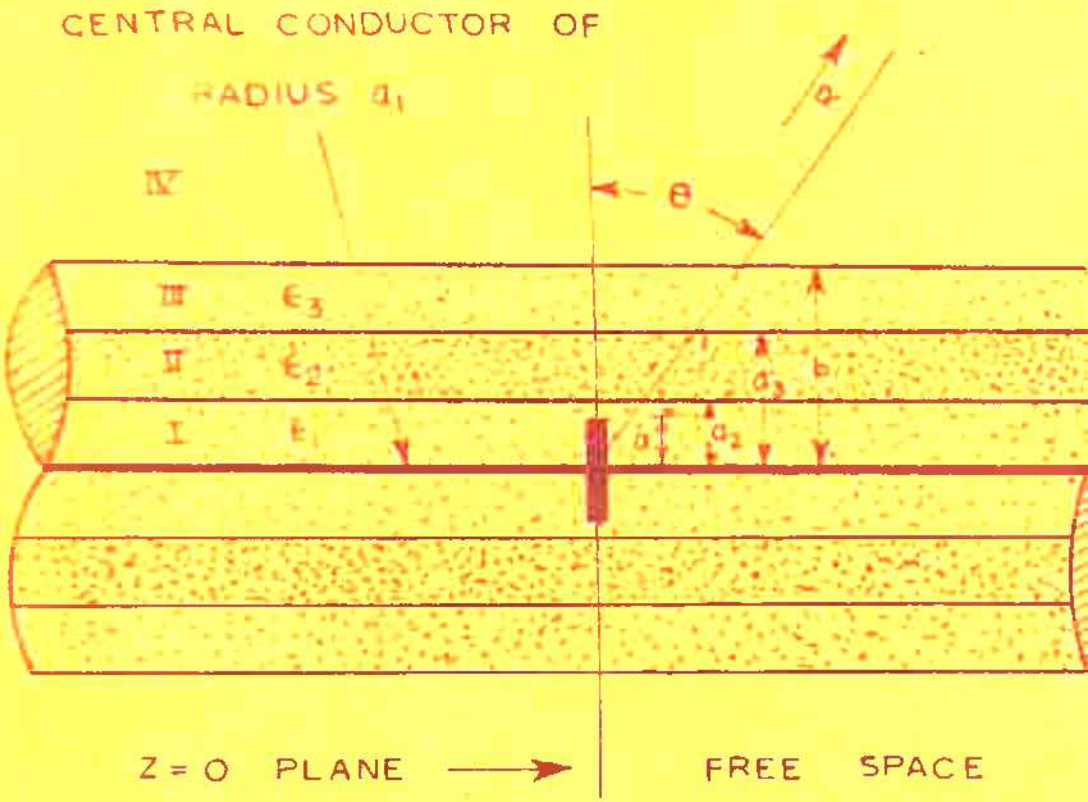
CENTRAL CONDUCTOR OF
RADIUS a_1
IV
θ
R
III ϵ_3
II ϵ_2
I ϵ_1
a
a_2
a_3
b
Z = O PLANE
FREE SPACE

FIG. -

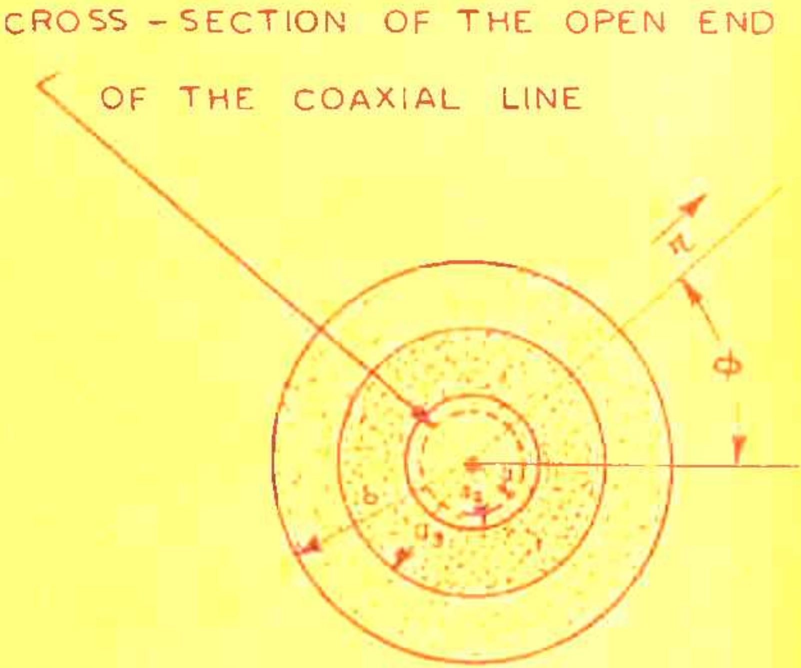

SECTION AT Z = O PLANE

4 · 1

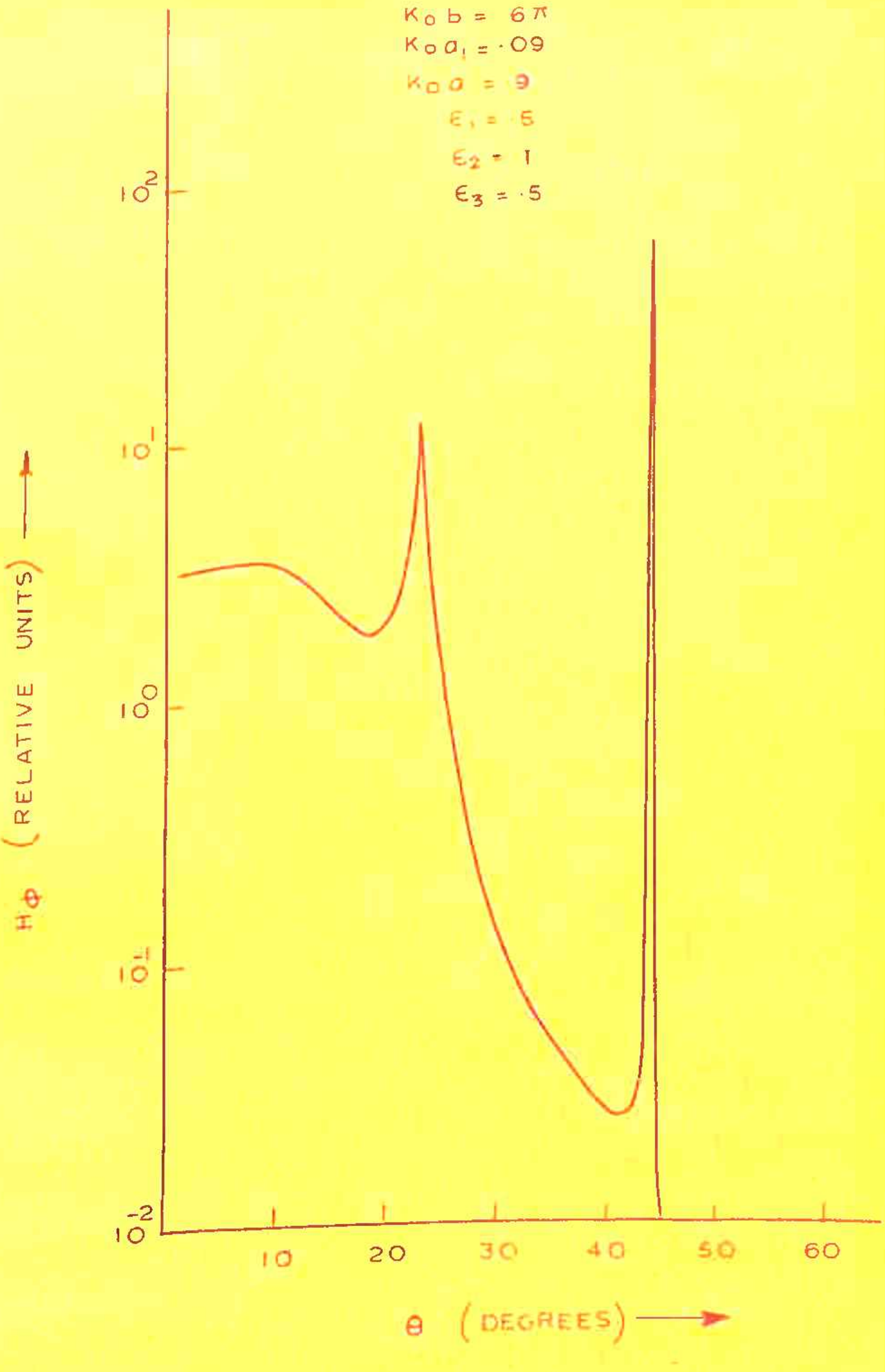

Ko b = 6π
Ko a1 = ·09
Ko a = 9
ε1 = ·5
ε2 = 1
ε3 = ·5
10^2
10^1
10^0
10^-1
10^-2
Hφ (RELATIVE UNITS)
10
20
30
40
50
60
θ (DEGREES)

FIG. - 4·2

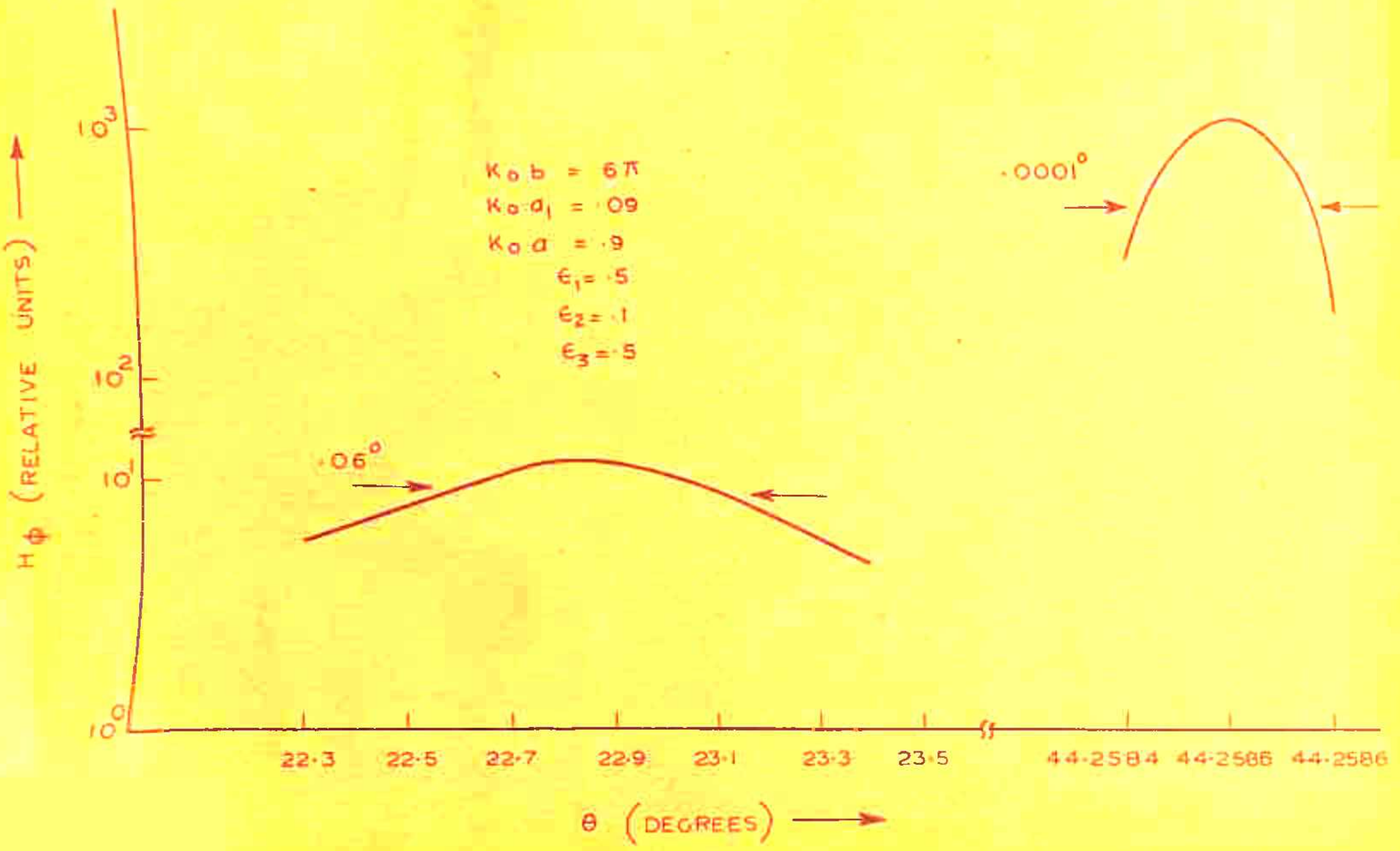
Hφ (RELATIVE UNITS)
10^3
10^2
10^1
10^0
Ko b = 6π
Ko a1 = ·09
Ko a = ·9
ϵ1 = ·5
ϵ2 = ·1
ϵ3 = ·5
·06°
·0001°
22·3
22·5
22·7
22·9
23·1
23·3
23·5
44·2584
44·2586
44·2586
θ (DEGREES)

FIG.- 4·3

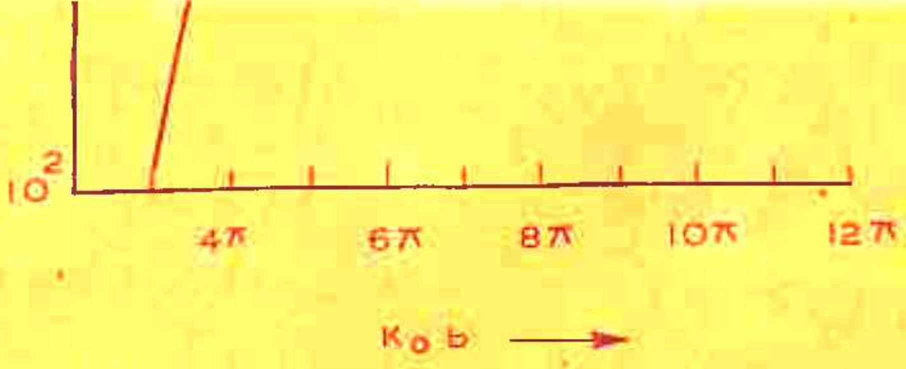

FIG.—4·4

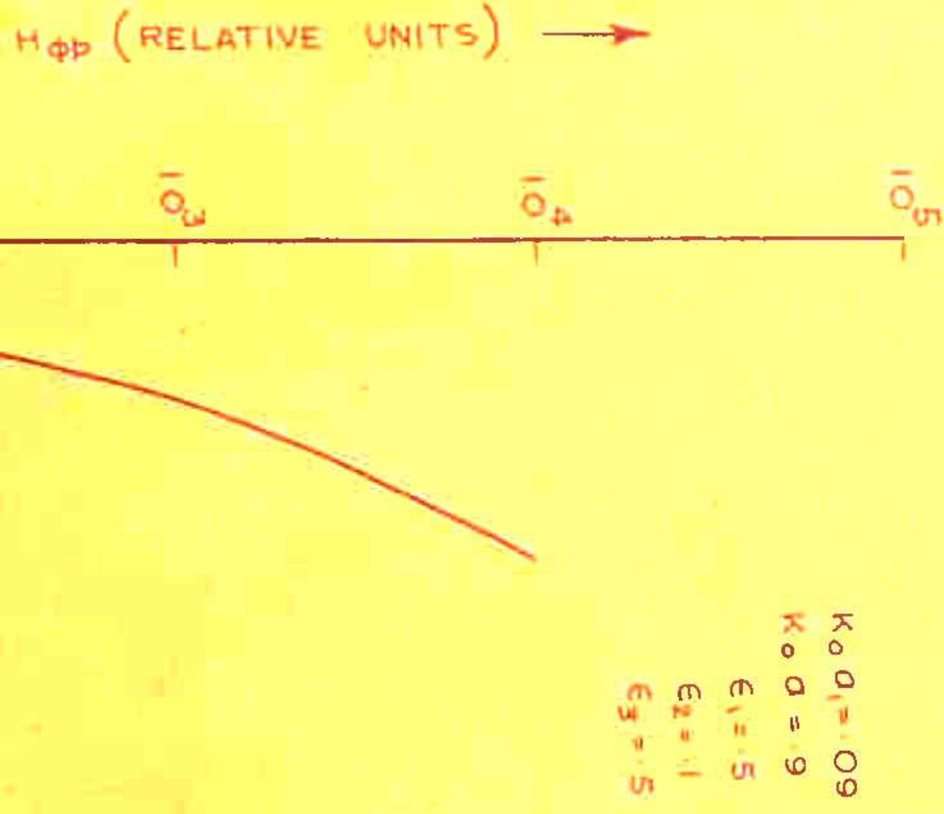

$H_{\phi b}$ (RELATIVE UNITS) →
10^3
10^4
10^5
$K_o a_1 = .09$
$K_o a = .9$
$\epsilon_1 = .5$
$\epsilon_2 = .1$
$\epsilon_3 = .5$

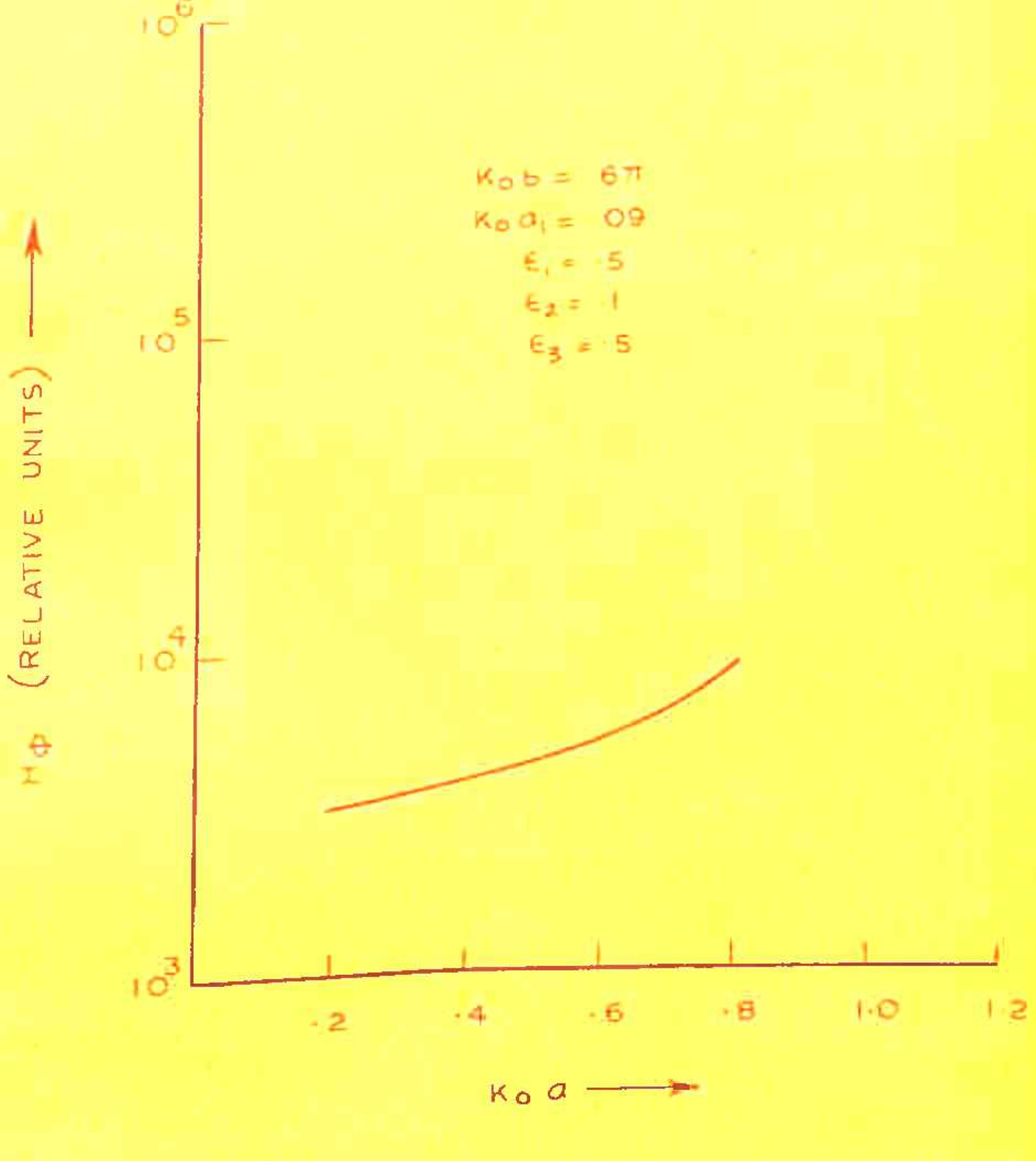

10^6
10^5
10^4
10^3
H_ϕ (RELATIVE UNITS)
$K_0 b = 6\pi$
$K_0 a_1 = .09$
$\epsilon_1 = .5$
$\epsilon_2 = .1$
$\epsilon_3 = .5$
·2
·4
·6
·8
1·0
1·2
$K_0 a$

FIG.- 4·5

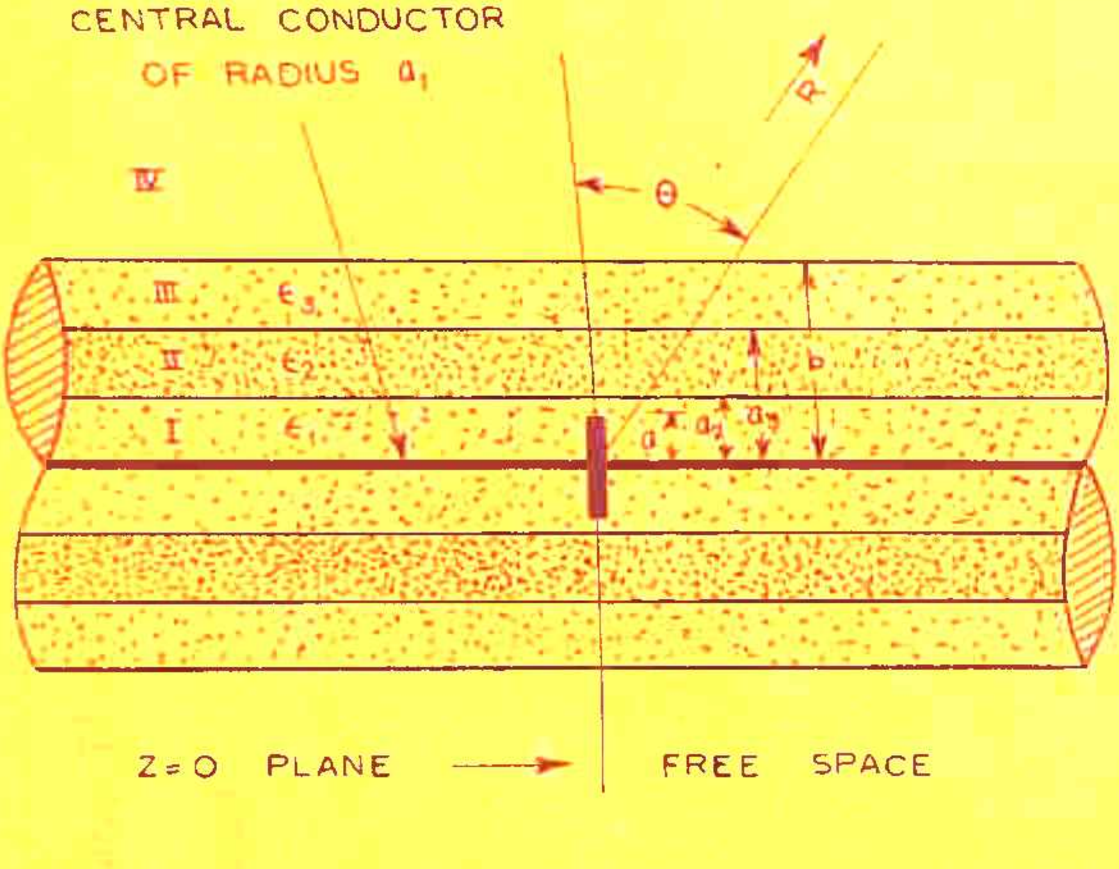
CENTRAL CONDUCTOR
OF RADIUS a_1
IV
θ
III ϵ_3
II ϵ_2
I ϵ_1
b
Z = O PLANE
FREE SPACE

FIG. - 4

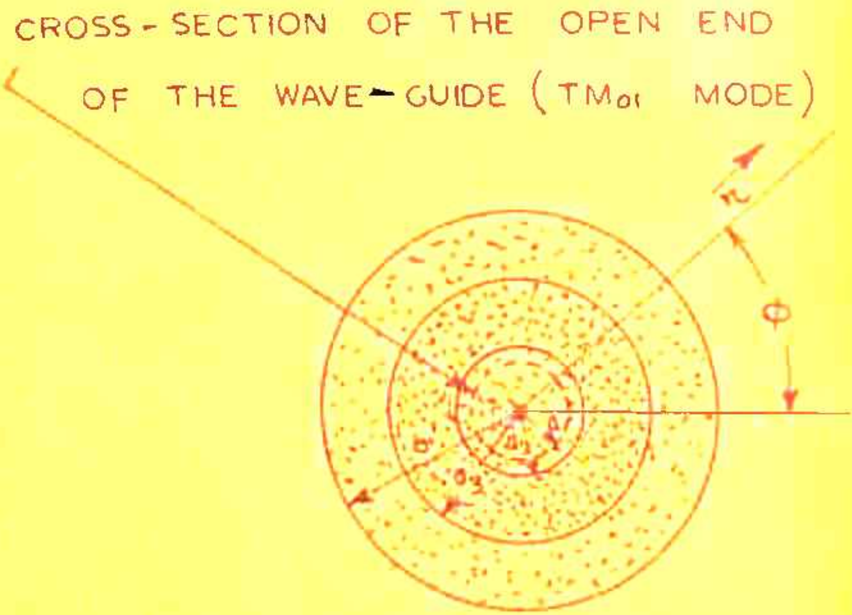

SECTION AT Z=0 PLANE

..6

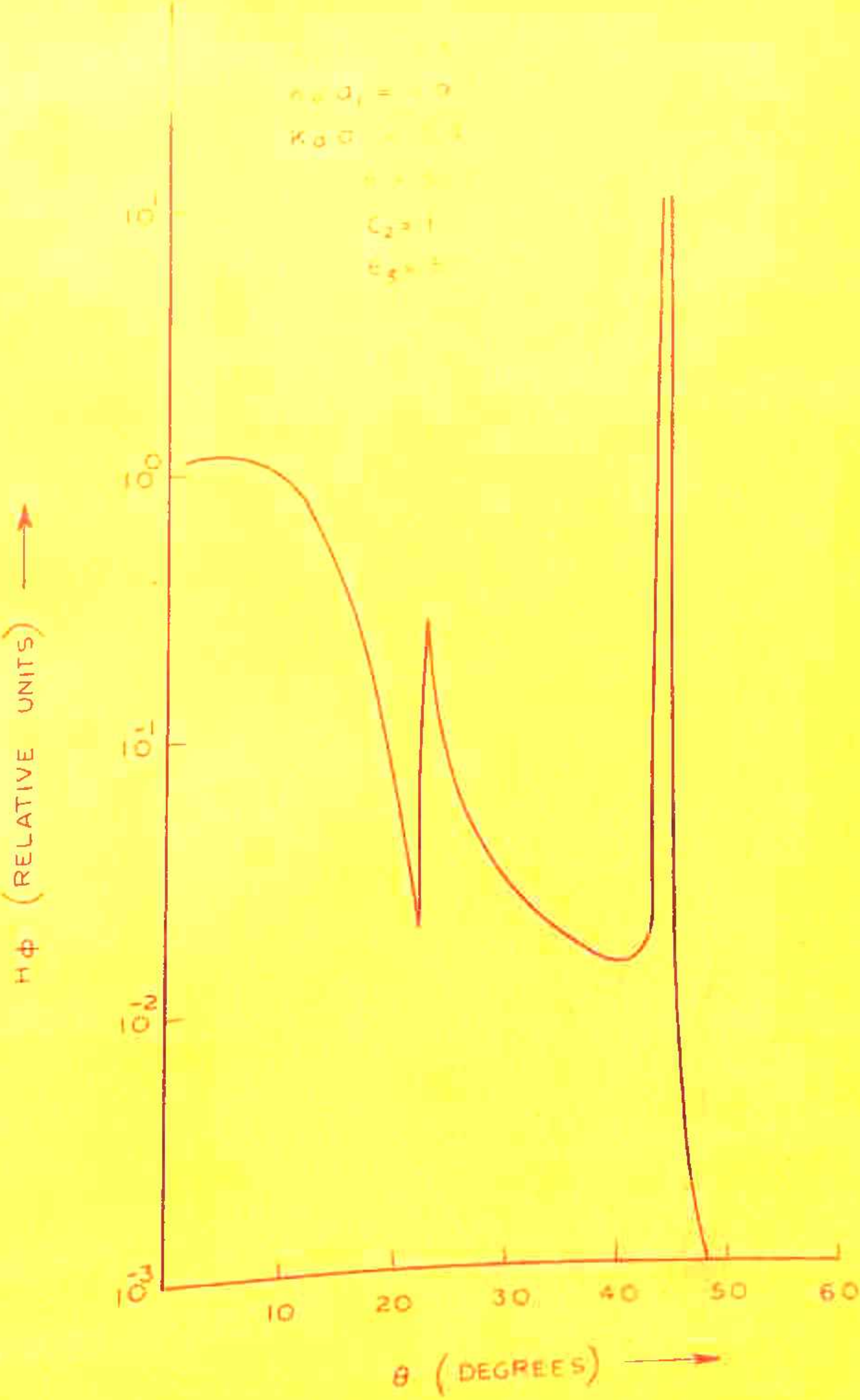

10^{1}
10^{0}
10^{-1}
10^{-2}
10^{-3}
10
20
30
40
50
60
Hφ (RELATIVE UNITS)
θ (DEGREES)

FIG. - 4·7

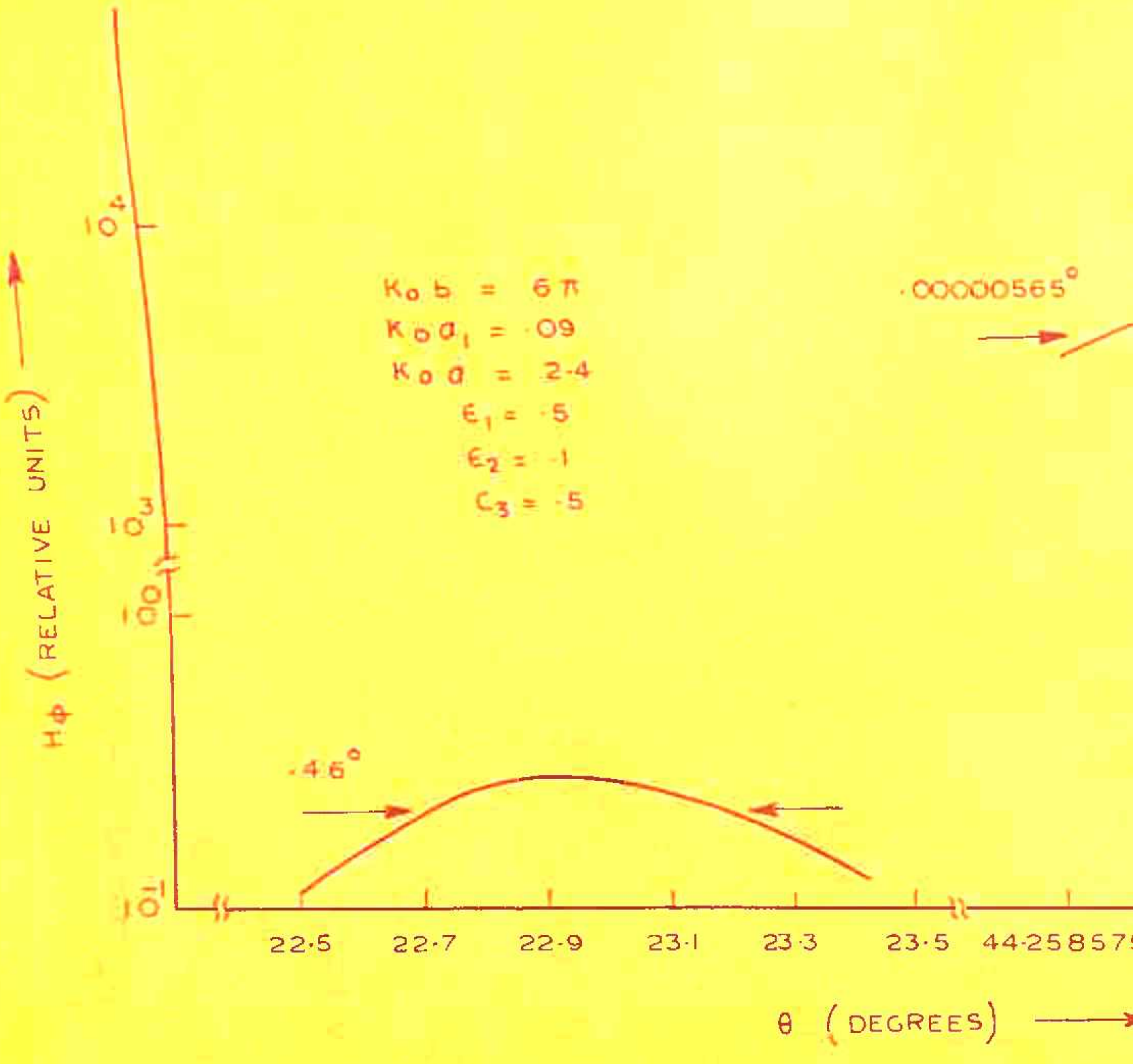

10^4
10^3
100
10^1
H_ϕ (RELATIVE UNITS)
$K_0 b = 6\pi$
$K_0 a_1 = \cdot 09$
$K_0 a = 2\cdot 4$
$\epsilon_1 = \cdot 5$
$\epsilon_2 = \cdot 1$
$\epsilon_3 = \cdot 5$
$\cdot 46^\circ$
$\cdot 00000565^\circ$
22·5
22·7
22·9
23·1
23·3
23·5
44·258575
θ (DEGREES)

FIG. - 4·8

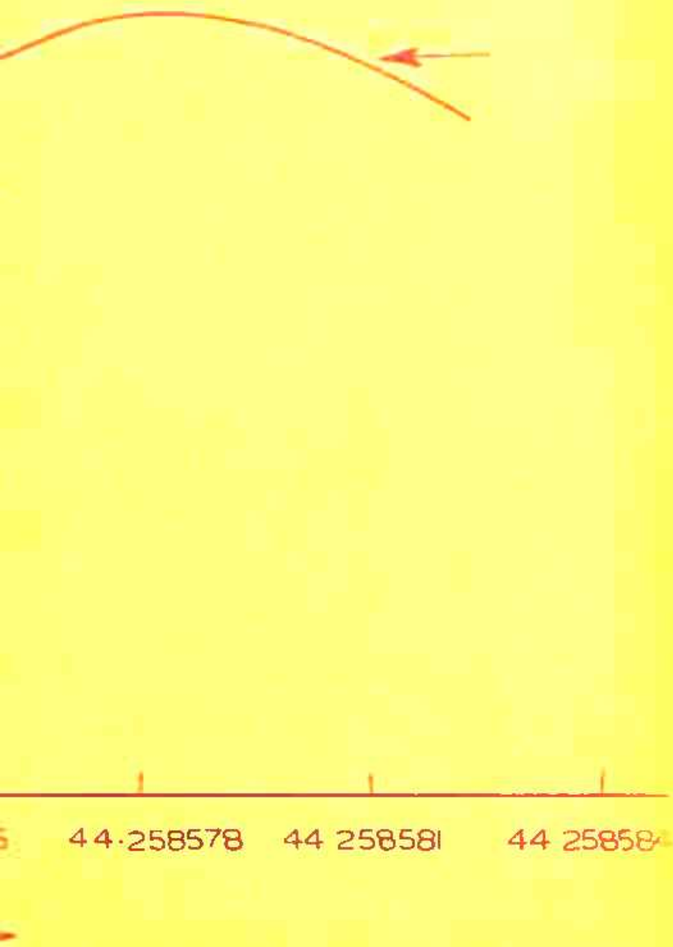

44·258578
44 258581
44 25858

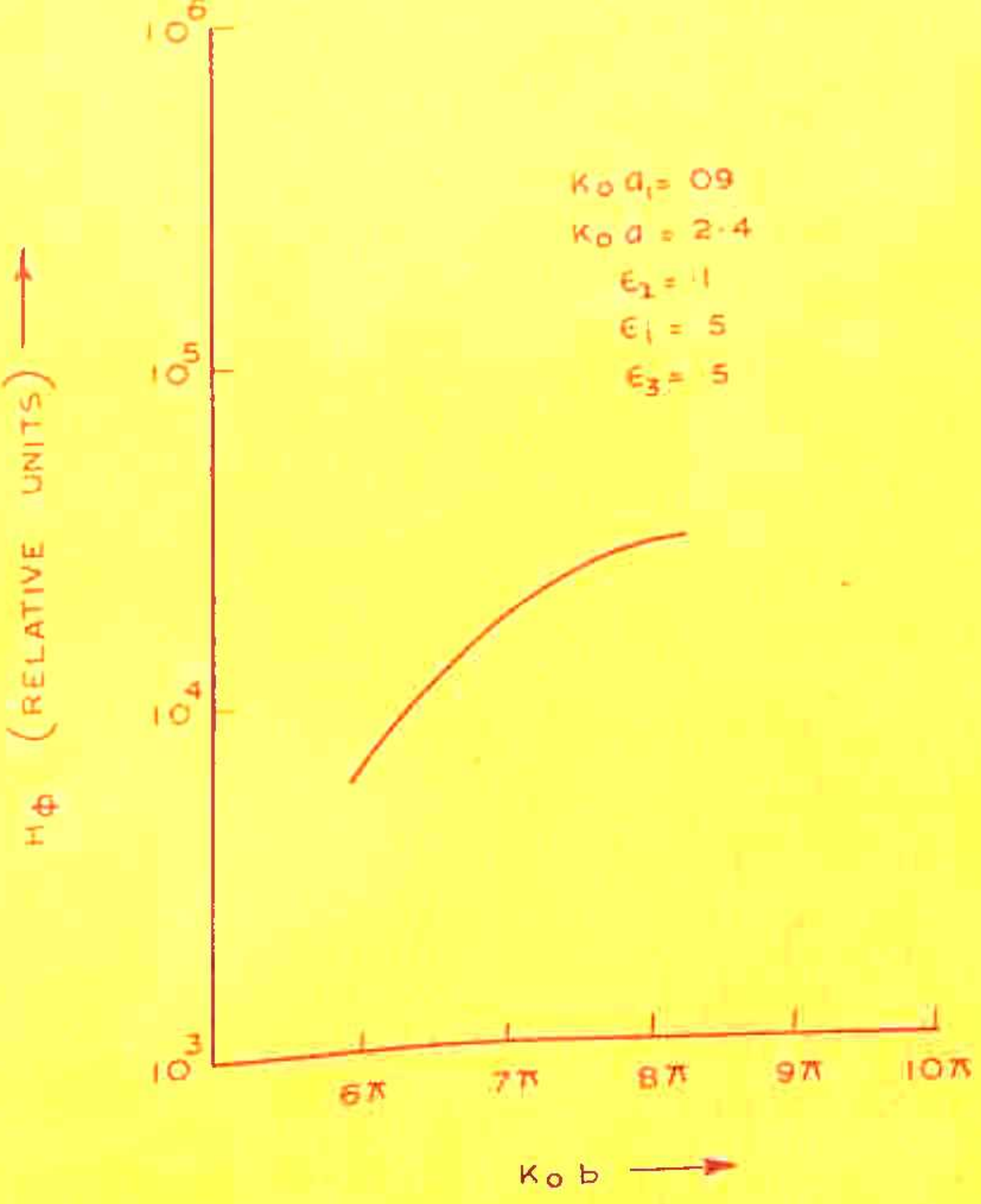

10^6
10^5
10^4
10^3
Hφ (RELATIVE UNITS)
Ko a1 = 09
Ko a = 2·4
ε2 = 1
ε1 = 5
ε3 = 5
6π
7π
8π
9π
10π
Ko b

FIG.-4·9

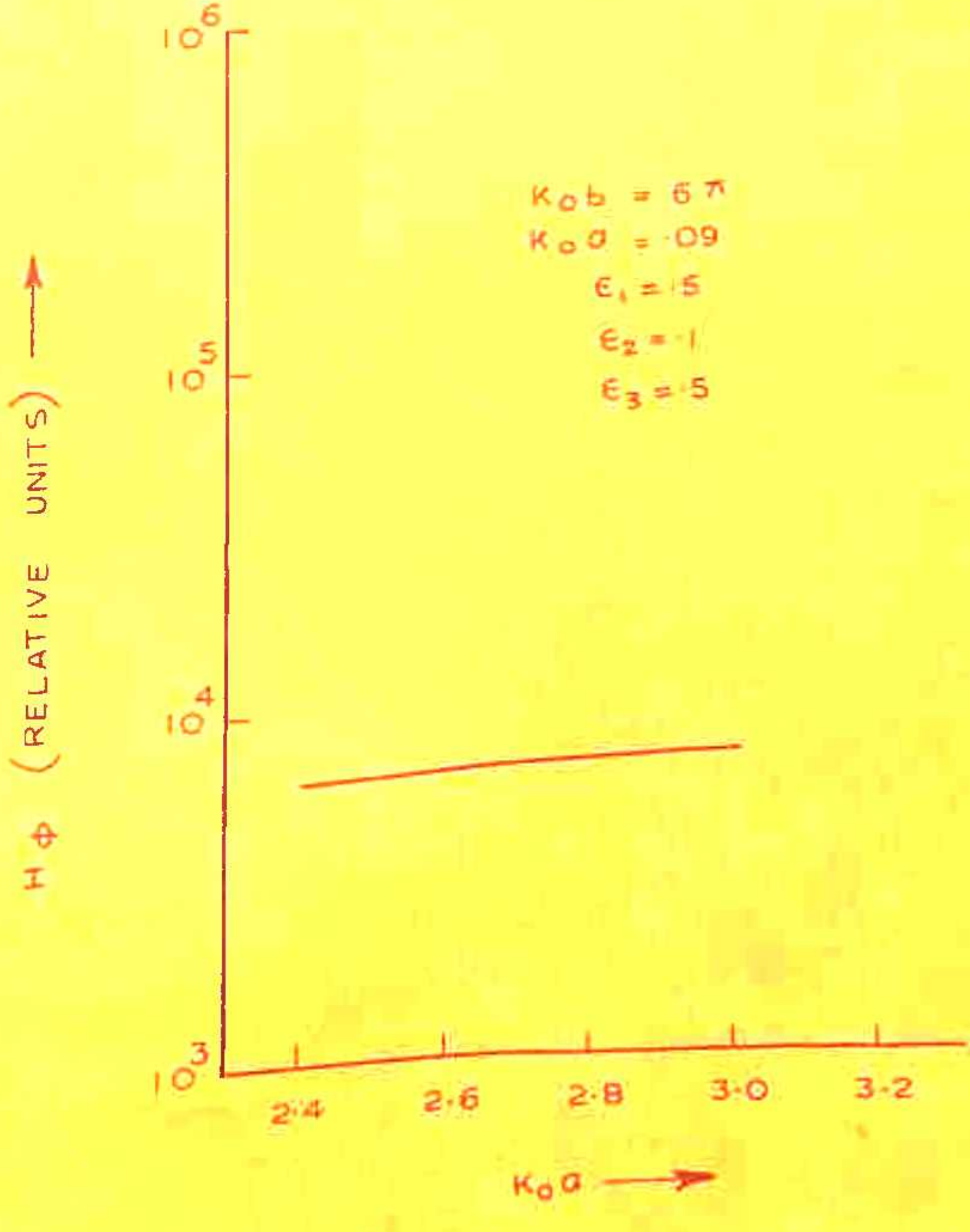

10^6
10^5
10^4
10^3
$K_o b = 6\pi$
$K_o a = \cdot 09$
$\epsilon_1 = \cdot 5$
$\epsilon_2 = \cdot 1$
$\epsilon_3 = \cdot 5$
$H\Phi$ (RELATIVE UNITS)
2·4
2·6
2·8
3·0
3·2
$K_o a$

FIG. – 4·10

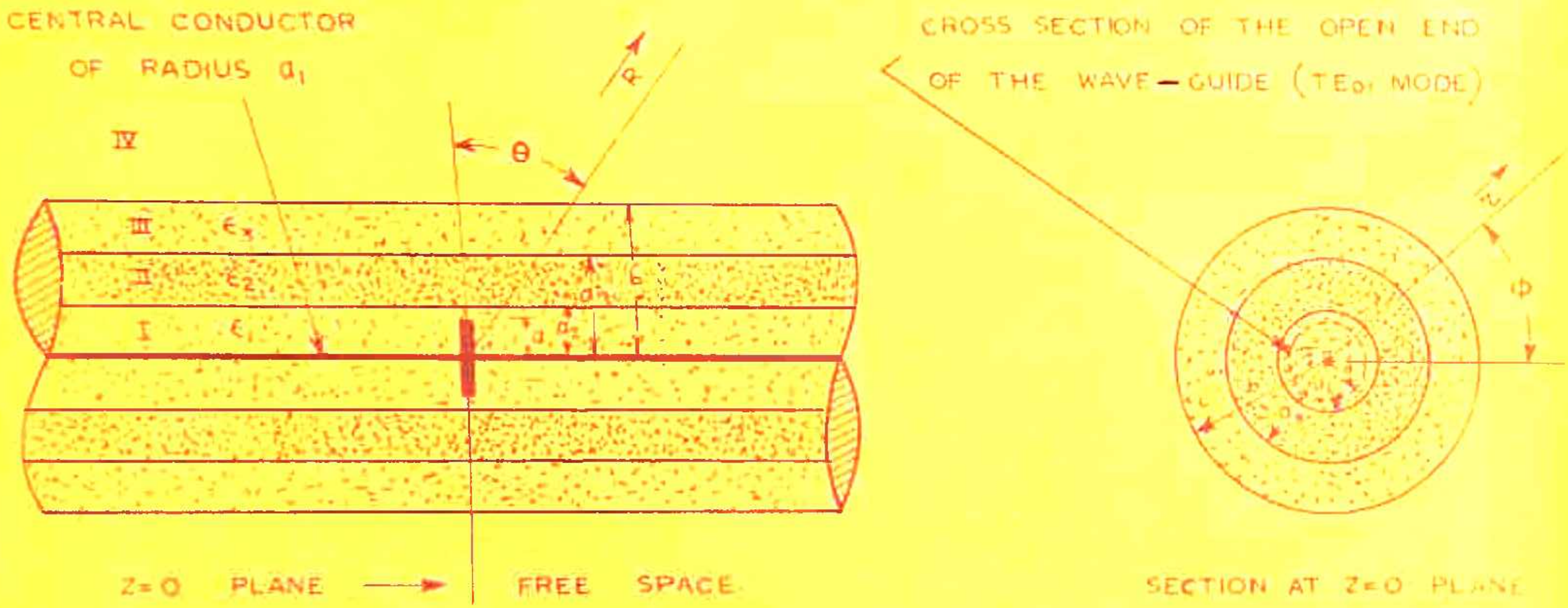
CENTRAL CONDUCTOR
OF RADIUS a_1
CROSS SECTION OF THE OPEN END
OF THE WAVE — GUIDE (TE_{01} MODE)
IV
III
II
I
θ
ϵ_3
ϵ_2
ϵ_1
b
φ
Z=0 PLANE
FREE SPACE
SECTION AT Z=0 PLANE

FIG. - 4.11

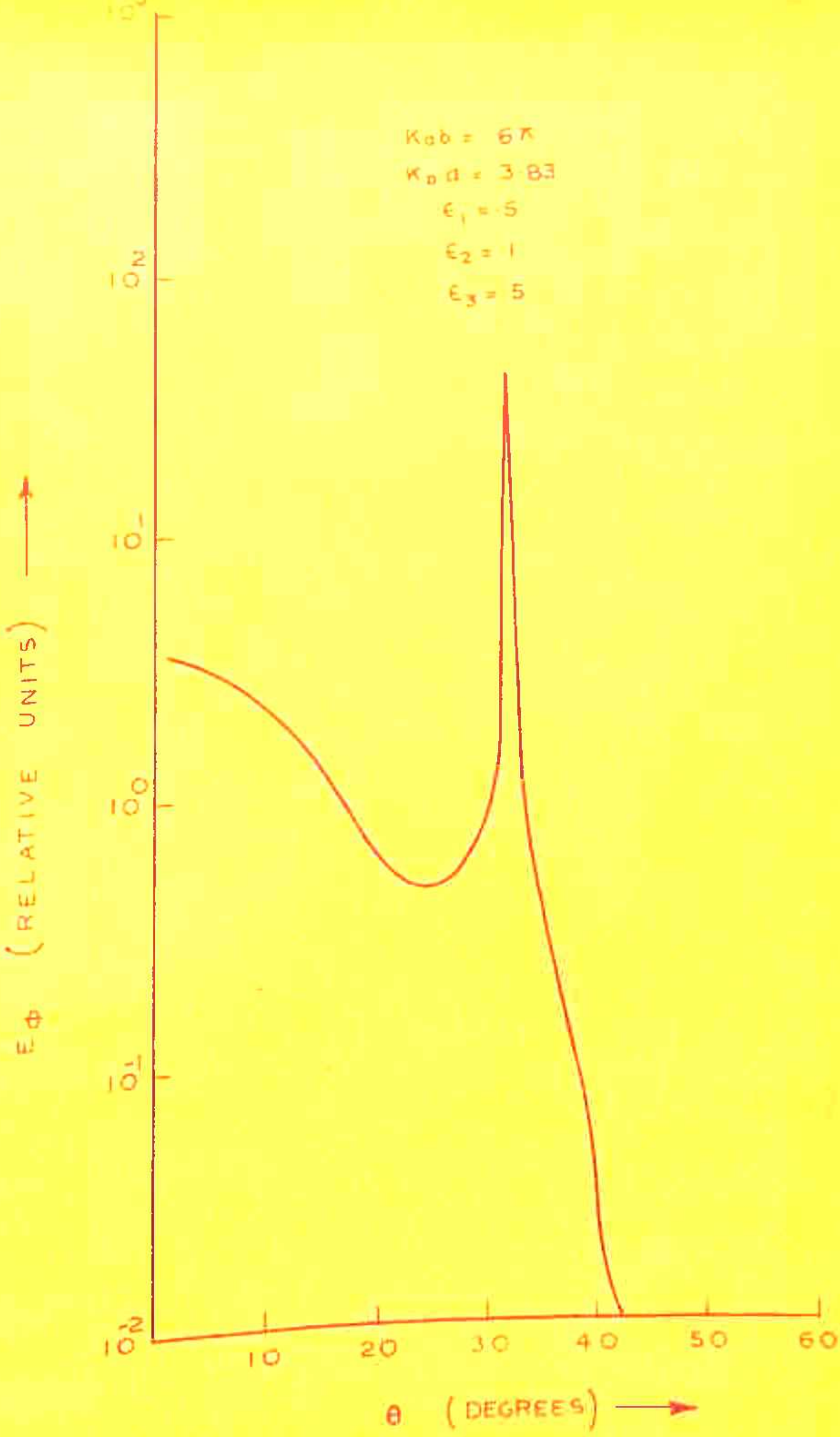
Kab = 6π
K₀ d = 3.83
ε₁ = .5
ε₂ = 1
ε₃ = 5
Eφ (RELATIVE UNITS)
θ (DEGREES)
10³
10²
10¹
10⁰
10⁻¹
10⁻²
10
20
30
40
50
60

FIG.-4.12

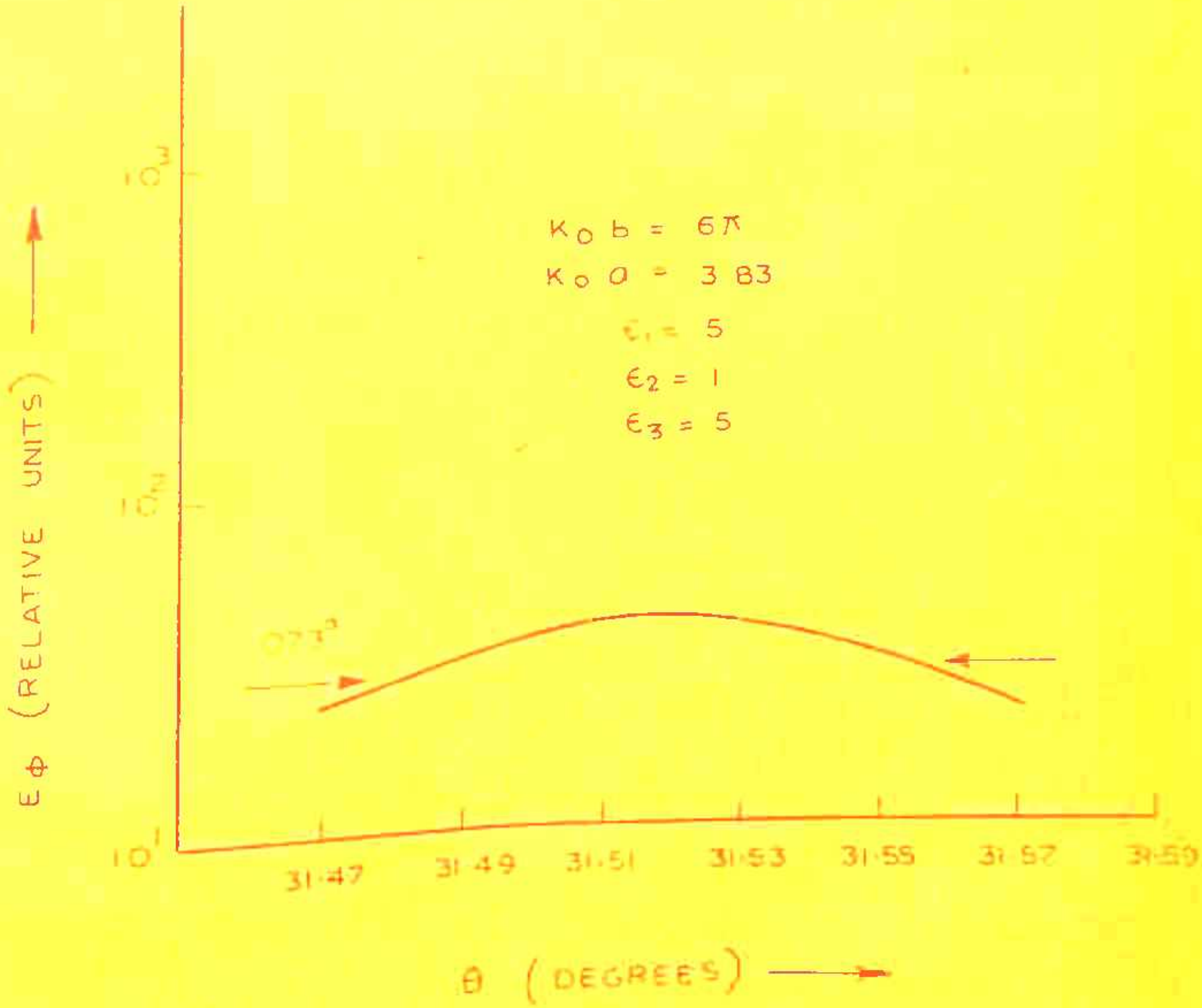

$K_0 b = 6\pi$
$K_0 a = 3.83$
$\epsilon_1 = 5$
$\epsilon_2 = 1$
$\epsilon_3 = 5$
E_ϕ (RELATIVE UNITS)
θ (DEGREES)
31·47
31·49
31·51
31·53
31·55
31·57
31·59

FIG - 4·13

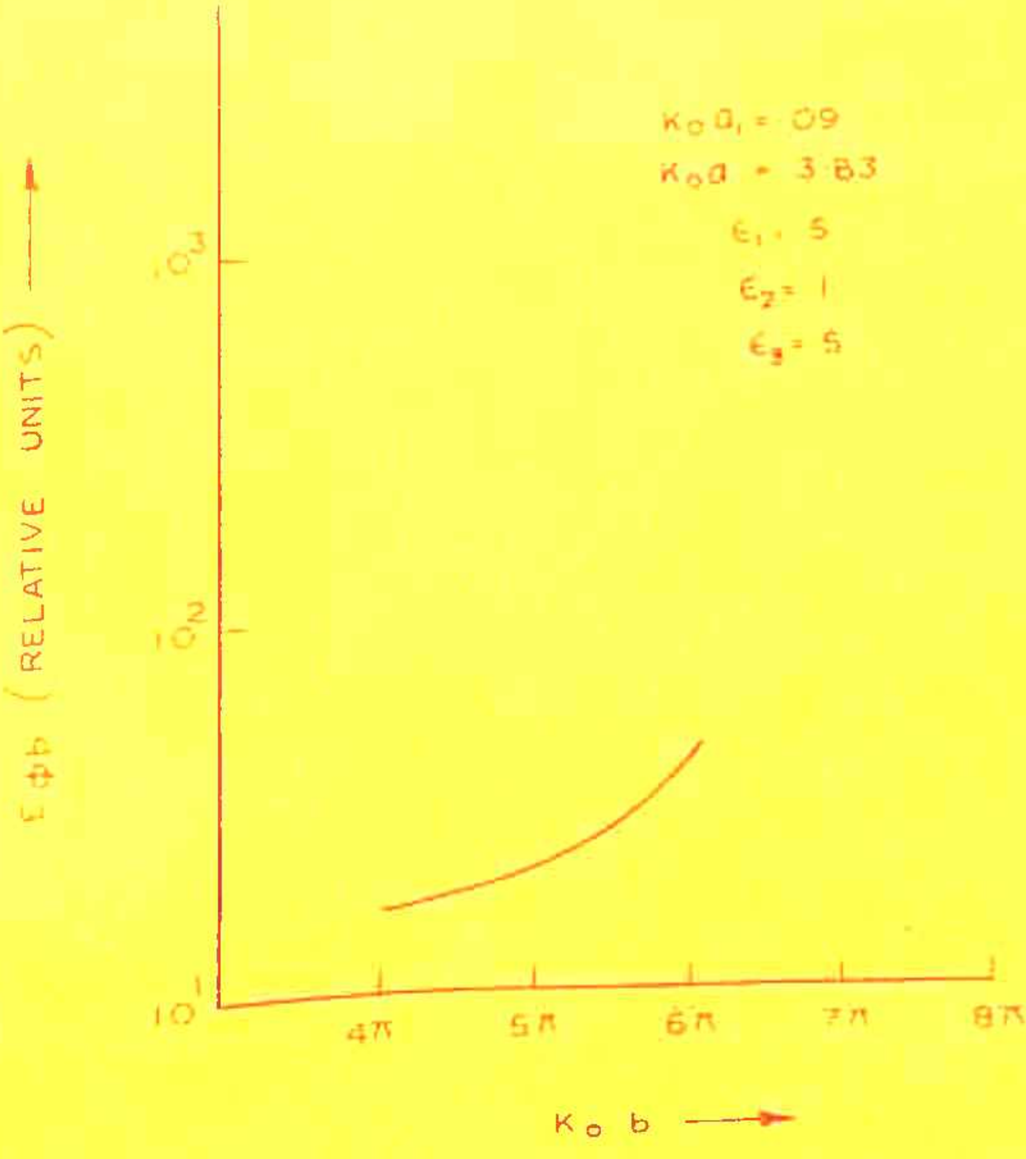

Ko a1 = ·09
Ko a = 3·83
ε1 = 5
ε2 = 1
ε3 = 5
10³
10²
10¹
Eφb (RELATIVE UNITS)
4π
5π
6π
7π
8π
Ko b

FIG. - 4·14

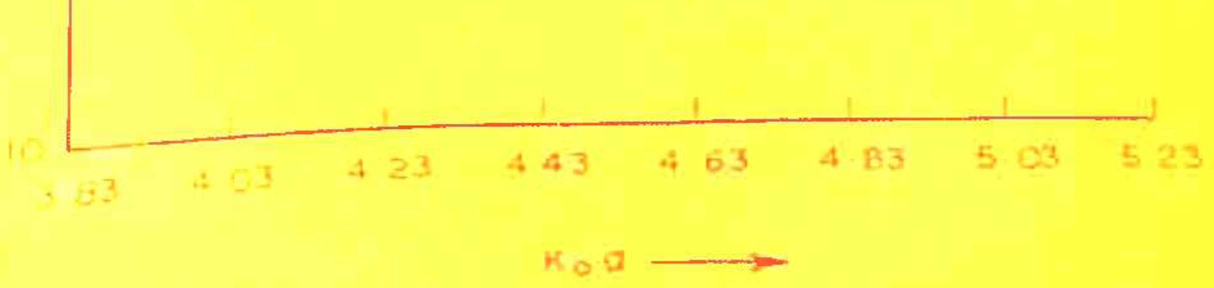

FIG – 4.15

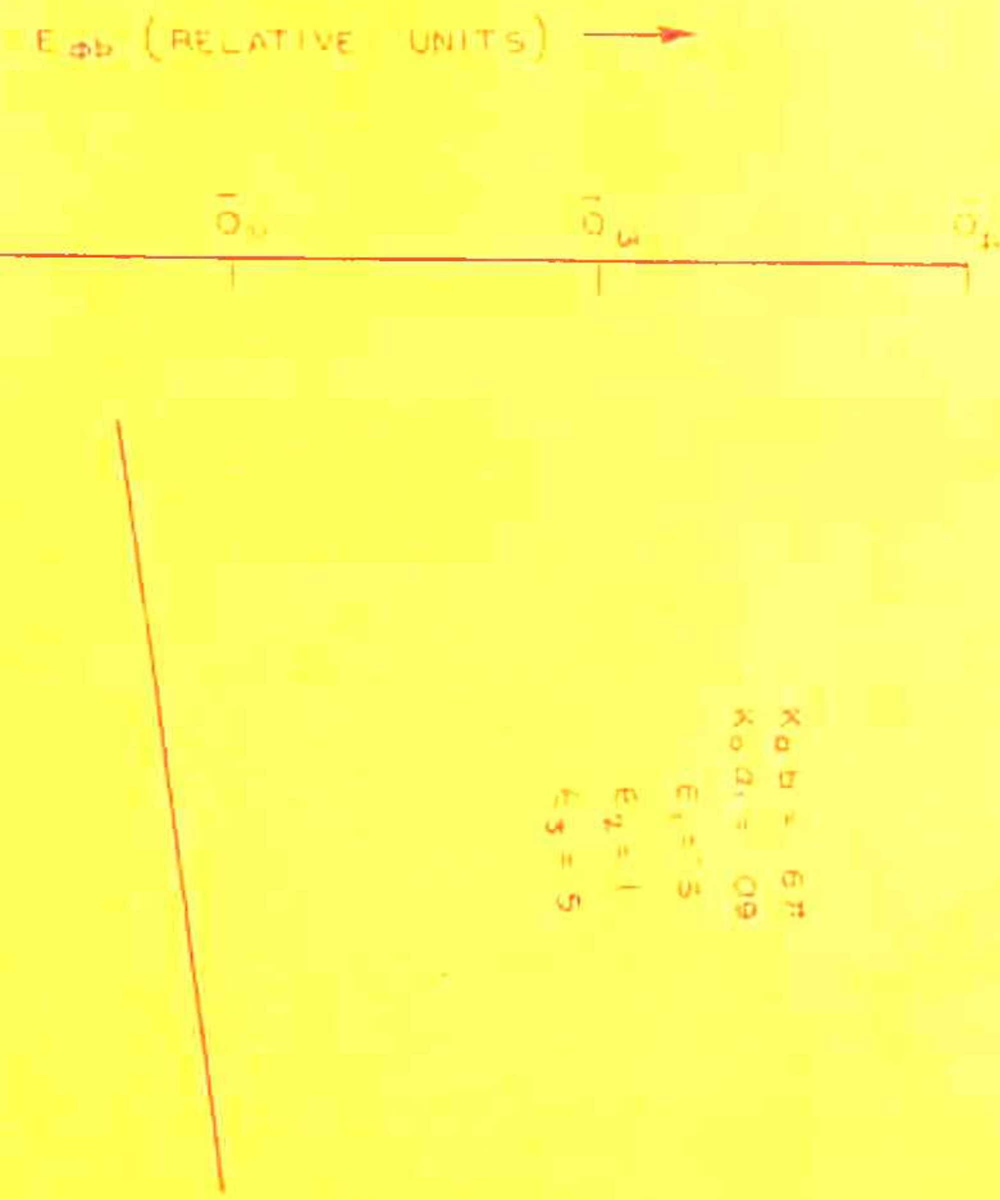
Eφb (RELATIVE UNITS)

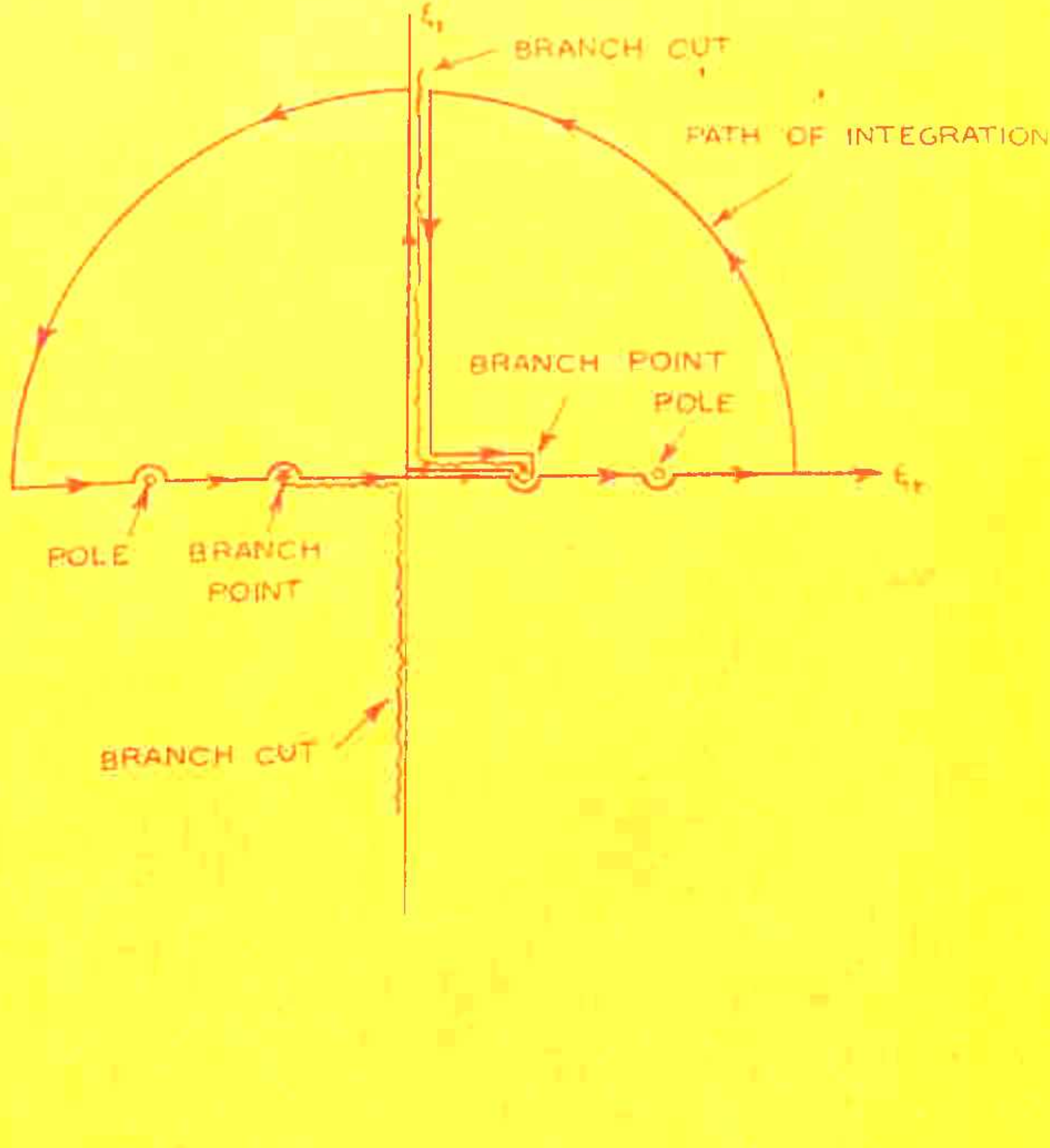
ξ_i
BRANCH CUT
PATH OF INTEGRATION
BRANCH POINT
POLE
ξ_r
POLE
BRANCH
POINT
BRANCH CUT

FIG. – A·1

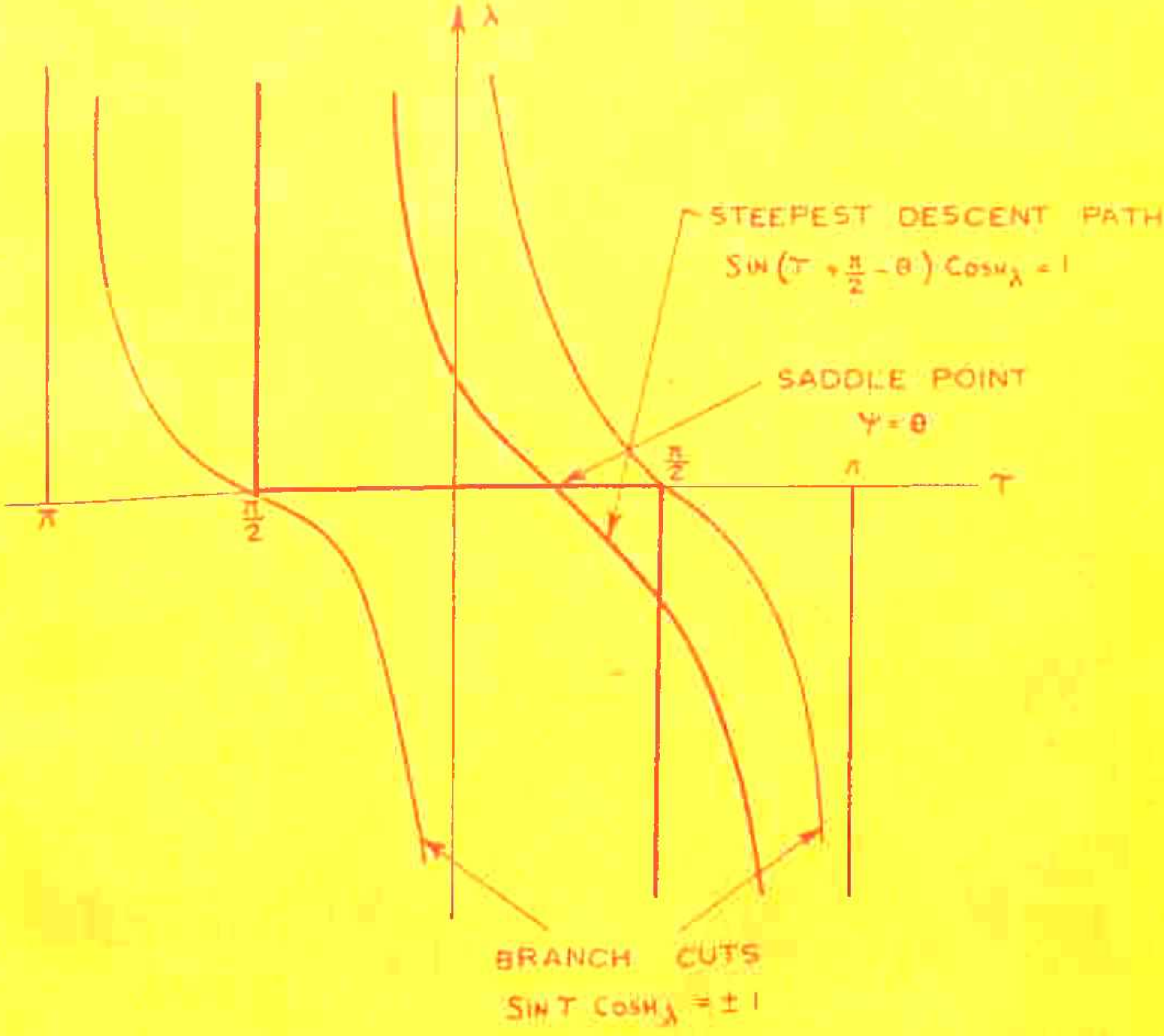
λ
STEEPEST DESCENT PATH
SIN (T + π/2 − θ) COSH λ = 1
SADDLE POINT
Ψ = θ
π/2
π
T
π
π/2
BRANCH CUTS
SIN T COSH λ = ± 1

FIG. – A·2